

Design of a Robotic Equine Forelimb for Testing Load-Bearing Rehabilitative Devices

David S. Ruppert

Thesis submitted to the faculty of the Virginia Polytechnic and State University in the partial fulfillment of the requirements of the degree

Master of Science
in
Mechanical Engineering

Graduate Committee Members:

Harry Dankowicz, Ph.D., Chair

Donald Leo, Ph.D.

Harry Robertshaw, Ph.D.

January 23, 2002
Blacksburg, Virginia

Keywords: Equine Robotic Replica, Equine Rehabilitation, Forelimb Injuries

*Design of a Robotic Equine Forelimb for Testing
Load-Bearing Rehabilitative Devices*

David S. Ruppert
Mechanical Engineering Department
Virginia Polytechnic and State University

(ABSTRACT)

Because horses are animals of flight, bone fractures in the horses' limbs are quite common. When foals fracture a bone in their leg, the healthy leg is often compromised. During convalescence, the animal tends to overstress the healthy leg in an attempt to relieve the stress on the injured leg. This results in angular limb deformities, lax tendons, laminitis, and similar problems. These problems could possibly be avoided through a load-bearing device that would relieve the additional weight from the foal's limbs.

In order to allow for in-vitro testing of such a load-bearing device, this thesis describes the design, analysis, and procedure of construction of a robotic replica of a foal's limb. In particular, the robotic replica has been designed to replicate all of the anticipated motion of a foal's limb, including walking, shifting weight from one leg to the other, and kicking, for example, using gait-analysis data from an actual horse's gait. From such data, the robotic replica has been designed in IDEAS and analyzed using multibody dynamics simulations code and the finite-element-analysis software ANSYS. To evaluate the function of the robotic replica, a control system was developed to reproduce observed gait characteristics. Comparison of the computer-simulated gait with the observed gait showed that a linear feedback control algorithm resulted in a response adequate for the proposed function.

The proposed robotic replica has the potential for aiding in the development of several other bioassistive devices. With minor modifications, the robotic replica could be used to test a device design to transfer load from the cannon bone to the ground for an animal inflicted with laminitis (founder). These possibilities should be investigated in the future.

Acknowledgments

First, I would like to thank the Department of Mechanical Engineering and Dr. Walter O'Brien for giving me the opportunity to continue my education at Virginia Tech.

Additionally, my thesis advisor Dr. Harry Dankowicz who provided me with extensive advice and assistance on my research warrants thanks.

Thanks, also goes to Dr. Elizabeth Dunnington and Dr. Rebecca Splan for the use of their foals for data collection and their equine knowledge.

For their engineering support and advice in the pursuit of a master's degree, I would like to thank Dr. Donald Leo and Dr. Harry Robertshaw.

Special thanks to Dr. Kenneth Sullins who provided me with invaluable advice relating to the final clinical application of the research topic and for his review of this work.

Finally, Petri Piironen, for his assistance in generating numerous computer codes used in this work.

Table of Contents

Abstract.....	ii
Acknowledgments.....	iii
List of Figures.....	vi
List of Tables.....	ix
1 Introduction.....	1
1.1 Motivation.....	1
1.2 Collateral, Load-Bearing Device.....	4
Cradle Design.....	5
Limb Frame Design.....	6
Actuation Design.....	8
1.3 Anatomic Forelimb Description.....	10
1.4 Approach to Robotic Replica.....	13
1.5 Scope.....	17
2 Equine Locomotion.....	18
2.1 Structural Size Data.....	19
2.2 Walk Data.....	21
2.3 Trot Data.....	25
3 Design of Robotic Replica.....	31
3.1 Mass Properties.....	31
3.2 Dynamics of Robot.....	35
Force calculations.....	35
Finite Element Analysis.....	42
3.3 Control System of Robot.....	44
Open Loop Control.....	44
Closed Loop Control.....	46
4 Results and Discussion.....	49
4.1 Structural Design.....	49
Mass and Geometry of Robotic Replica.....	50
Actuator Forces.....	51
FEA.....	54

4.2	<u>Comparison with Equine Gait</u>	60
	<u>Trot</u>	60
	<u>Walk</u>	63
5	<u>Construction of Robotic Replica</u>	65
5.1	<u>Assembly of Structural Members</u>	66
5.2	<u>Assembly of Hydraulic System</u>	75
6	<u>Conclusion and Recommendations</u>	83
6.1	<u>Alternative Application of Current Work</u>	84
6.2	<u>Future Work</u>	84
	<u>Glossary of Terms</u>	87
	<u>References</u>	90
	<u>Appendix A: Computer Codes</u>	92
	<u>Appendix B: Parts List</u>	110
	<u>Appendix C: Engineering Drawings</u>	112
	<u>Vita</u>	151

List of Figures

<u>Figure 1-1: Comparison of distal fractures that have little soft tissue surrounding them and proximal fractures that are obscured by soft tissue that is moving relative to the limb segment.</u>	2
<u>Figure 1-2: a. Carpal Valgus, b. Carpal Varus.</u>	3
<u>Figure 1-3: Schematics of the cradle of the sling of the <i>bioassistive</i> device.</u>	5
<u>Figure 1-4: Schematics of the <i>bioassistive</i> device in two positions.</u>	6
<u>Figure 1-5: A schematic of the shoe socket indicating its three rotational degrees of freedom.</u>	7
<u>Figure 1-6: The natural shifting of the body weight between the two forelimbs.</u>	9
<u>Figure 1-7: Skeletal structure of an equine forelimb.</u>	11
<u>Figure 1-8: Rotation of carpal joint through a sagittal plane (xy).</u>	12
<u>Figure 1-9: Muscular cradle supporting the scapula.</u>	13
<u>Figure 1-10: Reduction of number of joints in the fetlock region.</u>	14
<u>Figure 1-11: Sketch of the carpal design for the robotic replica.</u>	15
<u>Figure 1-12: Three actuators controlling the three degrees of freedom of the humerus.</u>	15
<u>Figure 1-13: Three actuators controlling the three degrees of freedom of the scapula.</u>	16
<u>Figure 2-1: Foot placement as a function of stride for walk.</u>	18
<u>Figure 2-2: Foot placement as a function of stride for trot.</u>	18
<u>Figure 2-3: Foot placement as a function of stride for a right lead canter.</u>	19
<u>Figure 2-4: Foot placement as a function of stride for a right lead transverse gallop.</u>	19
<u>Figure 2-5: Length of segments of the equine forelimb.</u>	20
<u>Figure 2-6: Definition of absolute angles for each limb section.</u>	22
<u>Figure 2-7: Joint angles relative to the ground as a function of stride for walking.</u> a. Scapula, b. Humerus.	22
<u>Figure 2-8: Joint angles relative to the ground as a function of stride for walking.</u> a. Radius, b. Carpus.	23
<u>Figure 2-9: Joint angles relative to the ground as a function of stride for walking.</u> a. Metacarpal, b. Fetlock.	23
<u>Figure 2-10: Angular velocities and accelerations per stride during walk, relative to the ground.</u> a. Scapula, b. Humerus.	24
<u>Figure 2-11: Angular velocities and accelerations per stride during walk, relative to the ground.</u> a. Radius, b. Carpus.	24

<u>Figure 2-12: Angular velocities and accelerations per stride during walk, relative to the ground. a. Metacarpal, b. Fetlock.</u>	25
<u>Figure 2-13: Joint angle relative to the ground as a function of stride for trotting. a. Scapula, b. Humerus, c. Radius, d. Carpus, e. Metacarpal, f. Fetlock.</u>	26
<u>Figure 2-14: Angular velocities and accelerations per stride during trot, relative to the ground. a. Scapula, b. Humerus.</u>	27
<u>Figure 2-15: Angular velocities and accelerations per stride during trot, relative to the ground. a. Radius, b. Carpus.</u>	27
<u>Figure 2-16: Angular velocities and accelerations per stride during trot, relative to the ground. a. Metacarpal, b. Fetlock.</u>	28
<u>Figure 2-17: Extension and flexion angles for fetlock.</u>	29
<u>Figure 2-18: Preliminary design of the robotic replica.</u>	30
<u>Figure 3-1: I-DEAS window displaying mass and associated properties.</u>	32
<u>Figure 3-2: Inertia properties as displayed by I-DEAS.</u>	33
<u>Figure 3-3: Orientation of xyz-triad to the scapula.</u>	34
<u>Figure 3-4: Vectors relative to the scapula.</u>	37
<u>Figure 3-5: Vector defining the caudal-dorsal scapula actuator.</u>	38
<u>Figure 3-6: Free-body-diagram.</u>	39
<u>Figure 3-7: Free-body-diagram.</u>	40
<u>Figure 3-8: Free-body-diagram.</u>	40
<u>Figure 3-9: Relocation of an actuator force to the center of mass.</u>	41
<u>Figure 3-10: Block diagram of design process.</u>	42
<u>Figure 3-11: Free-body-diagrams for FEA.</u>	43
<u>Figure 3-12: Block diagram of an open-loop control system.</u>	44
<u>Figure 3-13: Block diagram of a closed-loop control system.</u>	46
<u>Figure 4-1: Side view of replica and side view of foal's forelimb.</u>	50
<u>Figure 4-2: Actuator control forces at trot. A: Scapula-Humerus, B: Humerus-Radius, C: Radius-Carpus, D: Radius-Metacarpal, E: Metacarpal-Fetlock.</u>	52
<u>Figure 4-3: Shoulder actuator forces for trot. A: Caudal, Z1: Lateral, Z2: Medial.</u>	53
<u>Figure 4-4: Scapula hydraulic actuator forces at trot. O1: Caudal-Dorsal, O2: Cranial, O3: Caudal-Ventral.</u>	54
<u>Figure 4-5: Stress analysis of the fetlock during trot.</u>	55
<u>Figure 4-6: Stress analysis of metacarpal at trot.</u>	56
<u>Figure 4-7: Stress analysis of carpal joint at trot.</u>	57
<u>Figure 4-8: Stress analysis of radius at trot.</u>	58

<u>Figure 4-9: Stress analysis of humerus at trot.</u>	59
<u>Figure 4-10: Stress analysis of scapula at trot.</u>	60
<u>Figure 4-11: Open-loop response of radius angle for robotic replica.</u> a. starting at time=0sec, b. starting at time=0.2881sec	61
<u>Figure 4-12: Path of robotic replica (line) compared to collected data (points) for trot.</u> a. Scapula-Ground angle, b. Fetlock-Ground angle.....	62
<u>Figure 4-13: Comparison of closed-loop force (solid) to the open-loop force (dotted) for trot.</u> a. Cranial-Ventral actuator, b. Metacarpal-Fetlock actuator.....	63
<u>Figure 4-14: Path of robotic replica (line) compared to collected data (points) for walk.</u> a. Scapula-Ground angle, b. Fetlock-Ground angle.....	64
<u>Figure 4-15: Comparison of closed-loop force (solid) to the open-loop force (dotted) for walk.</u> a. Cranial-Ventral actuator, b. Metacarpal-Fetlock actuator.....	64
<u>Figure 5-1: Assembled robotic replica.</u>	65
<u>Figure 5-2: Assembly drawing of the phalangeal section.</u>	67
<u>Figure 5-3: Fetlock joint.</u>	68
<u>Figure 5-4: Knee joint (Carpus).</u>	69
<u>Figure 5-5: Elbow joint.</u>	70
<u>Figure 5-6: Shoulder joint.</u>	71
<u>Figure 5-7: Vertical actuation of cradle.</u>	72
<u>Figure 5-8: Horizontal control of cradle.</u>	73
<u>Figure 5-9: Secure shaft when in position.</u>	73
<u>Figure 5-10: Scapula to thorax connection.</u>	74
<u>Figure 5-11: Assembled robotic replica before installation of the actuators.</u>	75
<u>Figure 5-12: Installation of mounts for origins of scapula actuator.</u>	76
<u>Figure 5-13: Installation of scapula actuators.</u>	77
<u>Figure 5-14: Installation of actuators for controlling the humerus.</u>	78
<u>Figure 5-15: Installation of radius actuator.</u>	79
<u>Figure 5-16: Assembly of origins of carpal and metacarpal actuators on the radius.</u>	80
<u>Figure 5-17: Installation of insertion point of carpal actuator.</u>	80
<u>Figure 5-18: Installation of fetlock actuator and insertion point of metacarpal actuator.</u>	81
<u>Figure 5-19: Assembled robotic replica with hydraulic actuators.</u>	82

List of Tables

<u>Table 2-1: Forelimb length data</u>	21
<u>Table 2-2: Forelimb joint articulation range</u>	28

1 Introduction

The goal of this thesis is to present the design and development of a robotic replica of a foal's forelimb for use in the construction and testing of a rehabilitative, load-bearing device for treating limb fractures in young foals. This chapter gives an overview of the clinical motivation, some initial concept development of the proposed rehabilitative device, the approach for designing the robotic replica, and overall scope of the project.

1.1 Motivation

Because of the dynamic nature of a horse, its skeletal structure is vastly different from that of a human. The cross section of a horse's *distal*¹ limb bones is approximately 1/10 of those of a human after scaling for weight. Therefore, fractures of the bones in the limbs of these animals are common when the bones are subjected to excessive loads. Although young horses are more resilient than their parents, foals are still susceptible to fractures. These fractures may come about due to various reasons. These include the foal misplacing a hoof due to inexperience or panic, rough play with its peers, collision with a hard object, or rising hurriedly from the ground (Allen, 1996).

Although very little data has been collected on the injuries of foals, substantial records have been kept on racehorse injuries. These records suggest that as the horse ages it is less likely to injure itself during strenuous activities (Mohammed et al, 1991). While horses four years of age or older are more likely to experience breakdowns from the repetition of racing, horses three years of age or younger are at a significantly higher risk of sustaining hard-tissue injuries as observed by Haynes and Robinson (1988) and Kobluk (1998). In a study by Peloso et al (1994), it was estimated that 90.2 percent of such catastrophic injuries were related to the forelimbs. Moreover, in a seven-year study in the United Kingdom, it was shown that approximately 65 percent of the catastrophic injuries were fractures. Of these fractures, 59 percent were specified as limb fractures. However, 19 percent of the fractures went unspecified. Therefore, 84 percent of the specified fractures were associated with the limbs. (McKee, 1995) Hence, limb fractures have been documented as a common occurrence among young horses.

Due to the location and structure of the forelimb, distal fractures may be able to be stabilized in a cast. 'The principle of adequate immobilization of a fracture in a cast or any other device is that the joint proximal and distal to the fracture must be fixed by the cast. The cannon bone is the most proximal bone for which this is possible on the limb. However, for less stringent requirements, the carpus can be aided with a cast extending to the elbow' (Sullins). Some fractures warrant the use of internal fixation where plates and screws are used to keep the bones in place during convalescence. Regardless of the method use for repair, distal limb injuries generally heal with relatively fair success (Mueller, 1996).

More *proximal* fractures, on the other hand, are difficult and sometimes impossible to cast. This difficulty arises from the proximity to the *thorax* and the presence of muscles surrounding the proximal bones as seen in Figure 1-1. Surgery is often the only hope of

¹ All italicized words are defined in the glossary.

recovery. Even with surgery, proximal fractures generally do not heal properly (White, 2002). As a result, these proximal fractures result in the termination of the horse (cf. data on racehorse injuries in Peloso et al (1994) and Cohen et al (1997)).

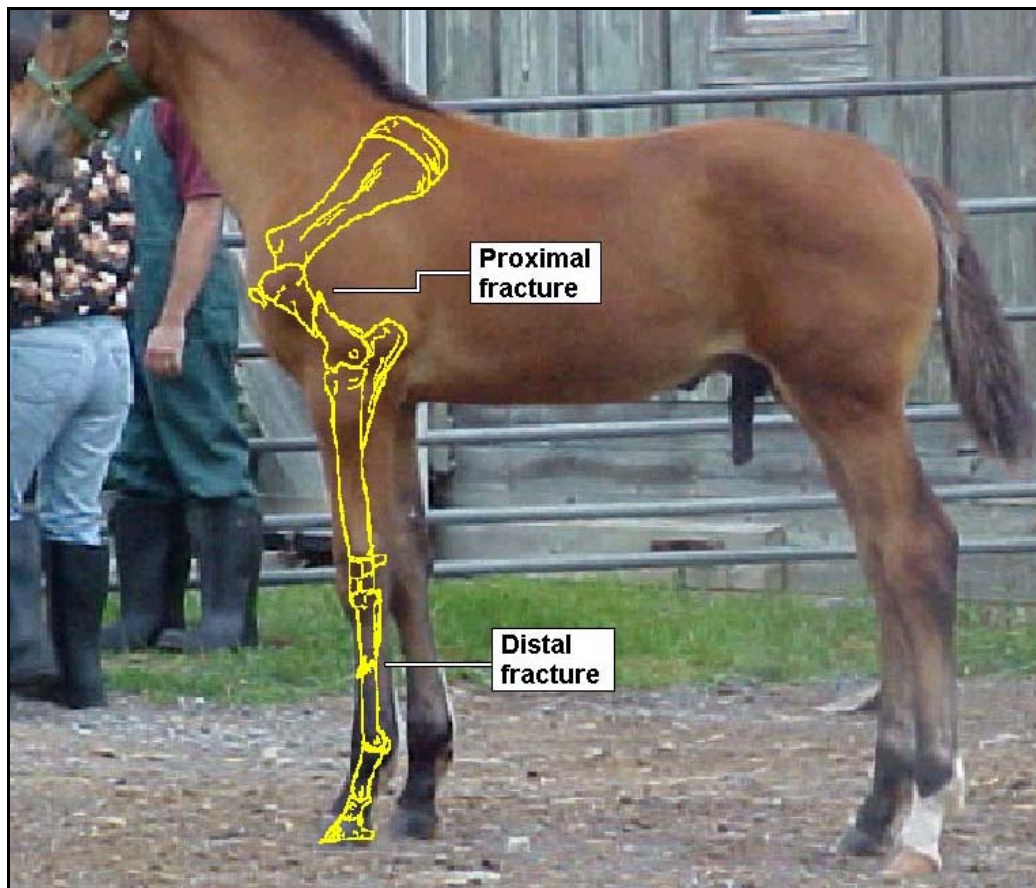


Figure 1-1: Comparison of distal fractures that have little soft tissue surrounding them and proximal fractures that are obscured by soft tissue that is moving relative to the limb segment.

As fractures—or any load-reducing injury—heal in foals, there is a tendency to offload the injured limb by shifting weight to the contralateral, healthy limb. Shifting weight to the healthy limb relieves stress from the injured limb. The reduction in stress reduces the experienced pain. However, maintaining continual stress on the healthy limb often results in the development of limb deformities. Some deformities occur due to the irregular *ossification* and maturation of *cartilage* to bone in the rapidly developing segments of the limb. The cartilage continues to grow and ossify with the limb in a non-natural position under load, resulting in a crooked bone. Two common such angular limb deformities (ALD's) are associated with the *carpus* and are referred to as *Carpal Valgus* and the more common *Carpal Varus* as shown in Figure 1-2 (King and Mansmann, 1997).

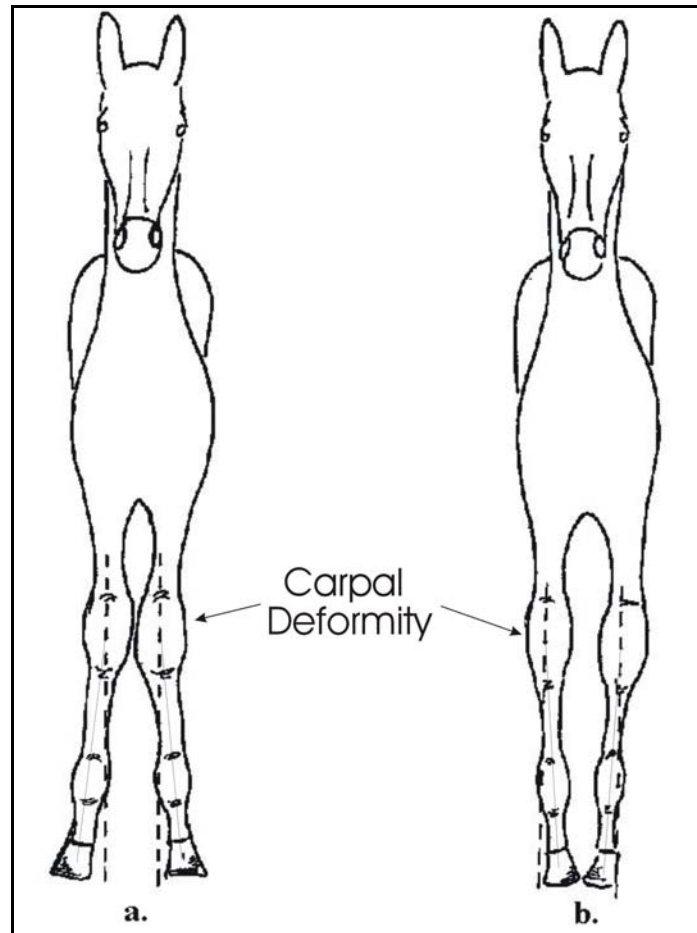


Figure 1-2: a. Carpal Valgus, b. Carpal Varus.

In addition to limb deformities, other problems arise from continual overloading of the limb. Overstressing of *tendons* and *laminitis* (inflammation and possible separation of the tissues at the junction of the sensitive and insensitive tissues along the inside of the hoof wall) are two common complications of excessive weight bearing in the healthy limb. Overstressing the tendons causes them to become lax and the horse to encounter joint problems (Allen, 1996).

In some situations, it is possible for the foal's injured limb to make a full recovery to health. Unfortunately, it isn't uncommon that, after the injured limb has healed, it supersedes the previously healthy limb in form and function (Auer, 1999).

To alleviate this condition, it appears desirable to partially or completely offload the additional weight that was transferred from the injured limb. Introducing a collateral load path guiding a portion of the weight of the trunk past the healthy limb and to the ground would reduce or eliminate the need for compensatory action of the healthy limb. Allowing a reasonable range of mobility and *articulation* of all joints while donning this load-bearing device would also support continued physical exercise and therapy. **It appears reasonable to expect that complications in the healthy limbs of foals, occurring as a result of functional compensation for lameness in injured limbs, could be reduced or eliminated using such adaptive, collateral, load-bearing devices supporting the healthy or injured limb.**

In addition, the use of a collateral load path on the injured limb would facilitate a controlled load through the injured limb that could be progressively increased through convalescence. Wolff's law states that bones modify their structure to cope with mechanical loads (Martin et al., 1998). Therefore, with a reduced load, the bone would reduce its structural stiffness deterring bone growth. Similarly, an increased load would stimulate bone growth to increase the stiffness of the bone. **Therefore, it seems reasonable to expect that healing of a stable fracture or injury to foals' limbs can be accelerated using adaptive, collateral, load-bearing devices supporting the injured limb that allow for a control of the load carried through the limb.**

This study will deal with only the *thoracic* limb (forelimb) of the foal. This selection was made because of the frequency of forelimb injuries relative to hind limb injuries. The horse supports 3/5ths to 2/3rds of its total weight through its forelimbs (Auer, 1999). In addition, the pelvic limbs are used for propulsion while the forelimbs are used primarily for shock absorption and support. Therefore, the frequency of injuries to the forelimb relative to the pelvic limb can be realized as more common as demonstrated through racehorse studies, as discussed above.

1.2 Collateral, Load-Bearing Device

In the previous section we proposed the design of an assistive, articulated, load-carrying device that will act to support a predetermined fraction of the load on a healthy or injured limb of a foal, while in no way restricting the limb's motion. Such a device would be used within a controlled environment, since the injured animal should be kept in isolation to avoid further injury.

Using a collateral, load-bearing device, significant gains are expected in reducing or eliminating the occurrence of deformities in healthy limbs due to compensatory load distribution, thus facilitating successful recovery from limb injuries. This section describes some initial design considerations as developed as part of funding proposals submitted to the Grayson Jockey Research Club.

The architecture of such a bioassistive device should be based on existing technology for control and actuation of multibody systems, taking full advantage of the mechanical principles underlying the horse anatomy. When applied to a healthy limb, the device should conform to the imposed action of the limb and trunk, reducing the horse's sensory awareness of the mechanism to a minimum. In contrast, it can be argued that a desirable goal for supporting an injured limb might include device-initiated movements (discussed later) to induce normal shifting of the body to eliminate the occurrence of tissue damage at the animal/device interface.

The structure of the load-bearing device should be unobtrusive in form, simple to operate, and cost-effective. Installation of auxiliary equipment should be kept to an absolute minimum, bundling any external components in a closed box that could be positioned out of the way of the animal, say in the ceiling of a stall. The fitting of the device to an individual horse should be simplified by a highly adaptable structure allowing a range of limb sizes and trunk widths.

Cradle Design

The forelimbs of the foal connect to the trunk only through muscles, in effect suspending the upper body in a muscle cradle between the two shoulders. As a result, the thorax can heave and roll without any reorientation of the limbs from their stance position.

It follows that to offload a forelimb and, consequently, the muscular cradle, the supporting structure must emanate from a similar cradle strapped to the animal's body. The connection between the cradle and the limb frame is effected by linear actuators serving both to guide the load path as well as to allow flexion, extension, and smaller amounts of *adduction* and *abduction*. The amount of load not carried by the supporting device is again transferred through the muscle cradle to the limb.

Consider the cradle design in Figure 1-3. Here, the foal's weight is transferred to the device through a set of nylon straps enclosing a solid piece of durable canvas padded with closed-cell foam to distribute the load evenly across the ribs and abdomen. Specifically, there should be two wide nylon straps around the abdomen and the thorax and a nylon strap of medium width running from the abdomen strap forward across the *sternum* and up to the *descending pectorals* where it divides into two straps forming a "Y". The latter two straps travel up, *cranial* to the *scapula*, to the rigid part of the supportive cradle. At the junction of the "Y", there should be a *ventrally* pointing triangular sheet of canvas padded with the closed-cell foam that would connect to the sternum padding to distribute a portion of the load across the chest.

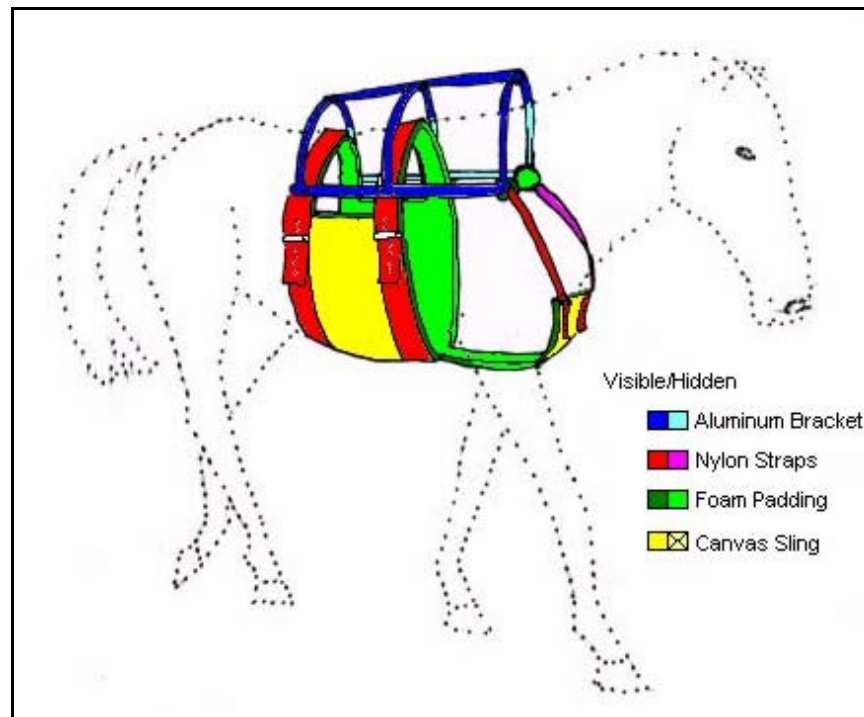


Figure 1-3: Schematics of the cradle of the sling of the *bioassistive* device.

The closed-cell foam would carry any relative motion between the body and the canvas and thereby significantly reduce the risk for abrasive damage to the skin. Similarly, openings in the cradle in the region surrounding the *scapula* and *humerus* would further reduce relative motion during ambulation and the risk for tissue damage. To reduce rotation

of the cradle about the longitudinal axis of the animal, the straps should completely encompass its trunk. There should be several adjustment buckles to provide a snug fit to the foal's body throughout the period of rehabilitation and to accommodate a range of foal sizes.

The upper part of the cradle should be rigidly attached to the actuated parts of the load-bearing device. The upper part should be constructed from an aluminum cage and would provide suspension support for the cradle sling described above. Again, adequate padding would serve to eliminate tissue damage from possible contact between the metal cage and the animal skin.

As the device is lifted off the ground, the foal carries the full weight of the device and cradle, suggesting that the total weight of the device should be used as a design-optimization criterion. The choice of aluminum provides a compromise between cost and strength-to-weight ratio.

Limb Frame Design

As the animal moves the supported limb, the device acts as a follower, mimicking the motion of the limb. It is only necessary for the load-bearing device to track the position of the hoof relative to the trunk of the foal in order to successfully offload the limb. This observation suggests the following device design illustrated in Figure 1-4. In particular, the load-bearing device is rigidly attached through a bracket to the aluminum cage that straddles the foal, from which the *lumbar* and thorax cradle sling is suspended. A rotary actuator between the bracket and the device corresponding to rotation about the transverse axis of the trunk would allow tracking of the cranial/caudal motion of the hoof. Distally from this actuator, a second rotary actuator about the longitudinal axis of the trunk would account for any abduction or adduction necessary to track the trunk and limb during turning and shifting of body weight. A telescoping actuator should be implemented distally from the abduction/adduction actuator. This actuator is responsible for tracking the position of the hoof relative to the trunk.

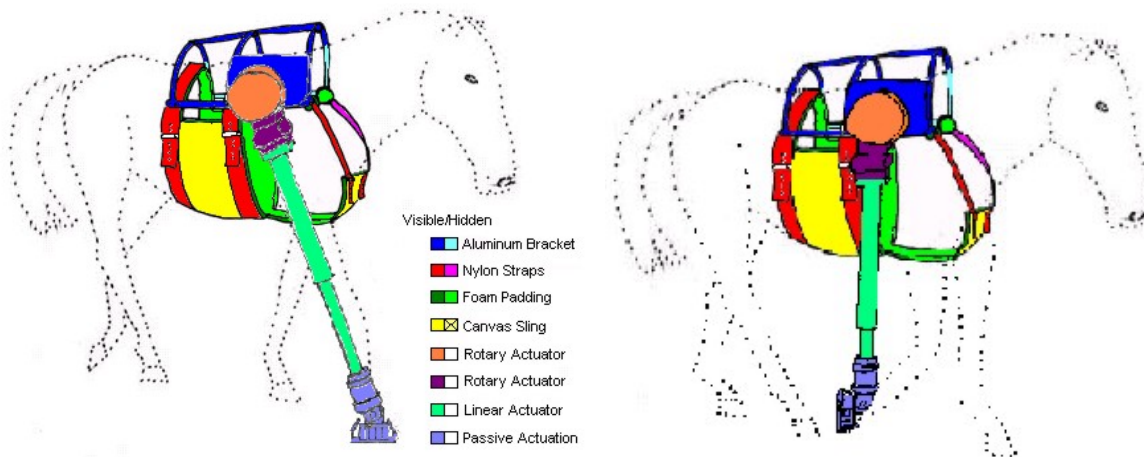


Figure 1-4: Schematics of the *bioassistive* device in two positions.

A shoe socket should be attached to the distal end of the telescoping actuator (Figure 1-5). This shoe would allow for passive actuation about multiple axes. It should be designed to offer sufficient friction at the contact with the ground in order to prevent slip and thus support the pivoting action that propels the body forward during gait. Bearings should

provide for unobstructed rotation of the shoe about the longitudinal axis (A) of the telescoping actuator. This would accommodate the rotation of the hoof relative to the trunk that accompanies turning during gait. The shoe should further be free to rotate about a transverse axis (B) at the junction of the telescoping actuator and the shoe to account for rotation of the *palmar* plane relative to the *dorsal* plane. Finally, a torsion spring should be introduced about the longitudinal axis (C) of the hoof forcing the shoe to lie flat against the base of the hoof. Here, the relaxed position of the torsion spring would be determined by the degree of abduction/adduction of the device. This would accommodate translational motion of the joints in the lateral direction that must accompany a lateral shifting of the foal's limb.

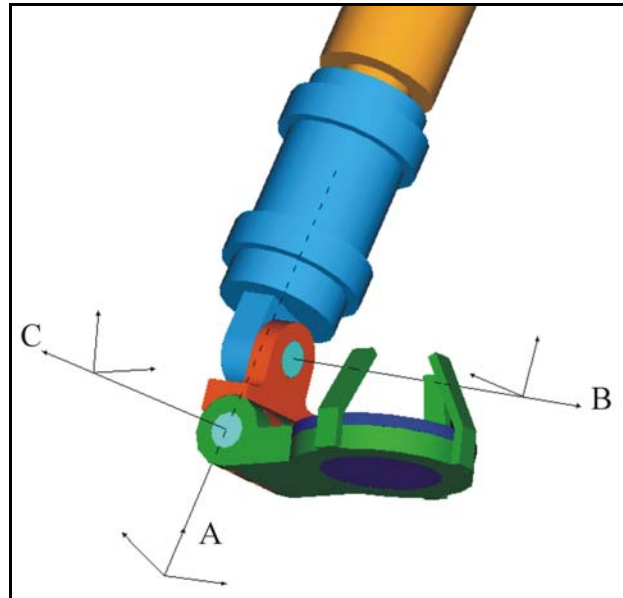


Figure 1-5: A schematic of the shoe socket indicating its three rotational degrees of freedom.

Should the limb be completely lifted off the ground, the weight of the assistive device would be fully carried by the animal. As suggested above, it is thus imperative that the device be as light as possible. The first generation prototype design should be based on a lightweight aluminum frame. In a later iteration of the design (and allowing for an increased manufacturing cost) the aluminum may be replaced by a composite structure. In addition to their weight characteristics, composite materials typically allow desirable structural reinforcement in the form of embedded fibers that can carry large loads. Composites components are also relatively straightforward to mold in a variety of forms allowing unobtrusive contoured shaping of the components and reduced risk of buckling.

The proposed design would all but eliminate all physical contact between the device limb and the skin. Primary contact would be reduced to the padded shoe socket in which the hoof rests. Sensors should be integrated within the shoe to detect the motion and load carried through the limb and the device. Pressure plates located on the top and bottom surfaces of the shoe would detect the total load transmitted to the ground and the load carried through the limb. Similarly, pressure sensors around the circumference of the shoe should be used to detect the change of position of the hoof relative to the device. These sensors would aid in the control of the device in conjunction with sensors imbedded in the sling. With these sensors, the load-bearing device would be capable of offloading a desired percentage of the

nominal load carried through the limb as well as allow unrestricted ambulation. While the device would not be intended to support *trot* or *canter*, it should handle the rapid motion and large force that would result from the foal attempting to kick the supportive structure from its limb. Additionally, since the device is intended to be used only in a controlled environment, the load-bearing device would not allow the foal the lower itself completely to the ground. Therefore, the device would be removed when the foal required rest and reapplied for routine exercise.

It is emphasized that the limb and hoof are not rigidly attached to the supporting structure. The structure is only rigidly strapped to the trunk, whereas all contact with the limb occurs via the padded structure and its embedded sensors.

Actuation Design

A variety of technologies exist for affecting force input on the mechanical device. These vary in the amount of load each actuator can carry, in their response times to control input, in the need for auxiliary equipment, weight and size, and in their up-front cost. An established and highly reliable technology is the use of hydraulic linear actuators. These afford an excellent compromise between the requirements for the load-bearing device, in particular reducing the projected cost of the final device significantly as compared with more recently developed technologies that may yield larger loads or faster responses.

Hydraulic actuators are essentially small cylinders with a valve and a controllable pressure difference between the two chambers resulting in a directed force on the piston. The pressure difference is maintained using a lubricant that is externally pressurized by a pump. For the proposed device, the pump should be contained in a small box attached to the ceiling in the stall with power cords and lubricant line fed to the horse below.

In contrast with traditional robotic applications, the successful design of the *bioassistive* device necessitates a careful analysis of the animal/device interface and the possibility of medical complications due to unnatural mechanical loading at this interface. For example, while the *musculoskeletal* system of the foal is particularly designed to carry the load of the trunk and transfer it to the ground, the proposed rehabilitative device requires large loads to be transferred via the skin of the animal. Sustained, large pressure on the skin, however, typically leads to tissue *ischemia* and ultimately *necrosis*. Similarly, any relative motion at the contact region between the horse's skin and the rehabilitative device can result in abrasion sores and skin damage.

The bioassistive device should rely on an alternating scheme to reduce or eliminate the risk for skin ischemia and necrosis. In particular, restrict attention to the case when the bioassistive device is applied parallel to the injured limb and consider the horse in stance. By controlling the amount of load carried through the device, the animal can be induced to rest its upper-body weight almost entirely on the device or almost entirely on the healthy limb. Indeed, by alternating between these two extremes, the control strategy mimics the natural shifting of the weight that occurs during stance as shown in Figure 1-6. The frequency of switching and duration of stance on the healthy limb and the device, respectively, should be design parameters that could be passively controlled by the human operator based on visual inspection of tissue condition during use, or actively controlled through feedback based on microcirculation sensors integrated with the device. During gait, a natural shifting would occur because of ambulation.



Figure 1-6: The natural shifting of the body weight between the two forelimbs.

Skin abrasion results largely from relative motion between the cradle sling or sling straps and the animal's skin. A secondary source for abrasion sores originates in large tangential forces at the skin/device interface, for example between the straps of a saddle and the skin. Sufficient normal pressure would eliminate the risk for relative motion because of large frictional forces. These frictional forces, however, may introduce small tears in the skin that further reduce its ability to sustain shear pressure.

In the proposed device, the two sources of abrasion damage would be dealt with independently, although they naturally overlap. In particular, the occurrence of relative motion would be addressed by an advantageous geometric sling design and the use of a layer of closed-cell foam between the skin and the sling as discussed earlier in the section on cradle design. Any relative motion between the horse and the cradle sling would then be carried within the foam layer. Moreover, the actuation of the abduction and adduction degree of freedom of the device's *shoulder joint* discussed earlier (see section on limb frame design) should be controlled in such a way as to align the sling to the desired orientation of the horse trunk. Again, pressure and shear sensors in the foam layer would provide information on the tangential forces that would feed back into the actuator control.

Related to the issue of tissue damage due to ischemia and abrasion is the conditioning of the skin because of perspiration and foreign particles. As suggested above, the device design should allow for quick and efficient donning and removal of the device. This would provide easy access to cleaning the skin from perspiration and particles that may have entered in between the foam and the skin and that otherwise increase the risk for tissue damage.

Also recognized is the need to allow for the natural growth of the foal during the treatment period, as well as to ensure that the device can be adapted to a range of foal sizes in the first place. There is a natural degree of variability in the shape of the horse and the orientation of the bones in the limbs. For example, the degree of obliquity of the scapula as well as its length may vary between full-grown individuals (Smythe, p. 29, 1972). Of course, limb lengths also vary greatly between foals at different stages of maturing. In the present context, the growth affects the extension of the trunk and the length of the limbs. These two aspects would be accommodated by the adjustable straps that provide a close fit of the sling to the body and by the telescopic component of the load-bearing device (shown above in figure 1-4).

Finally, it would be possible to adjust the relative load carried by the device throughout the period of rehabilitation. This would be advantageous in introducing small loads across a fracture site and thereby accelerating the healing process. Such adjustment could be effected by the operator in response to visual or other inspection of the health of the injured limb. The device could also make autonomous adjustments based on sensory input and the apparent magnitude of load that the foal is prepared to place on the injured limb during the load-shifting pulsations described above. At the beginning of the rehabilitation process, one would expect the foal to place an overwhelming portion of the load on the healthy limb when the device actuation was lowered. As the injured limb's condition improved, however, the amount carried by the injured limb would increase, thus reducing the need for the device to carry a large fraction of the load on the injured limb during stance and/or ambulation.

The development of the device will be facilitated through the initial construction of a robotic replica of a foal's limb with all significant functional degrees of freedom at the various joints as described in the main body of this thesis. The assistive device should be designed around this replica allowing full control over the motion of replica and device alike. Only after successful performance has been assured on the robotic replica, would the design be optimized for weight, fitting, obtrusiveness, cost, and subsequently readied for actual clinical trials.

In order to properly test the load-bearing device, the robotic replica must be capable of mimicking the anatomical motion of the forelimb of a typical foal. Therefore, it is our intent to design a robotic replica of a foal's forelimb that will simulate the anatomical motions that are anticipated during convalescence, such as shifting weight from one leg to the other, walking, and kicking.

1.3 Anatomic Forelimb Description

Since the robotic replica will be required to closely mimic the actual motion of the foal's forelimb, the replica will be designed as close to an anatomical model as possible. In the equine forelimb, there are seven primary joints of articulation, six of which are shown in Figure 1-7. Working from the ground up we will discuss each joint to be addressed in the foal's forelimb.

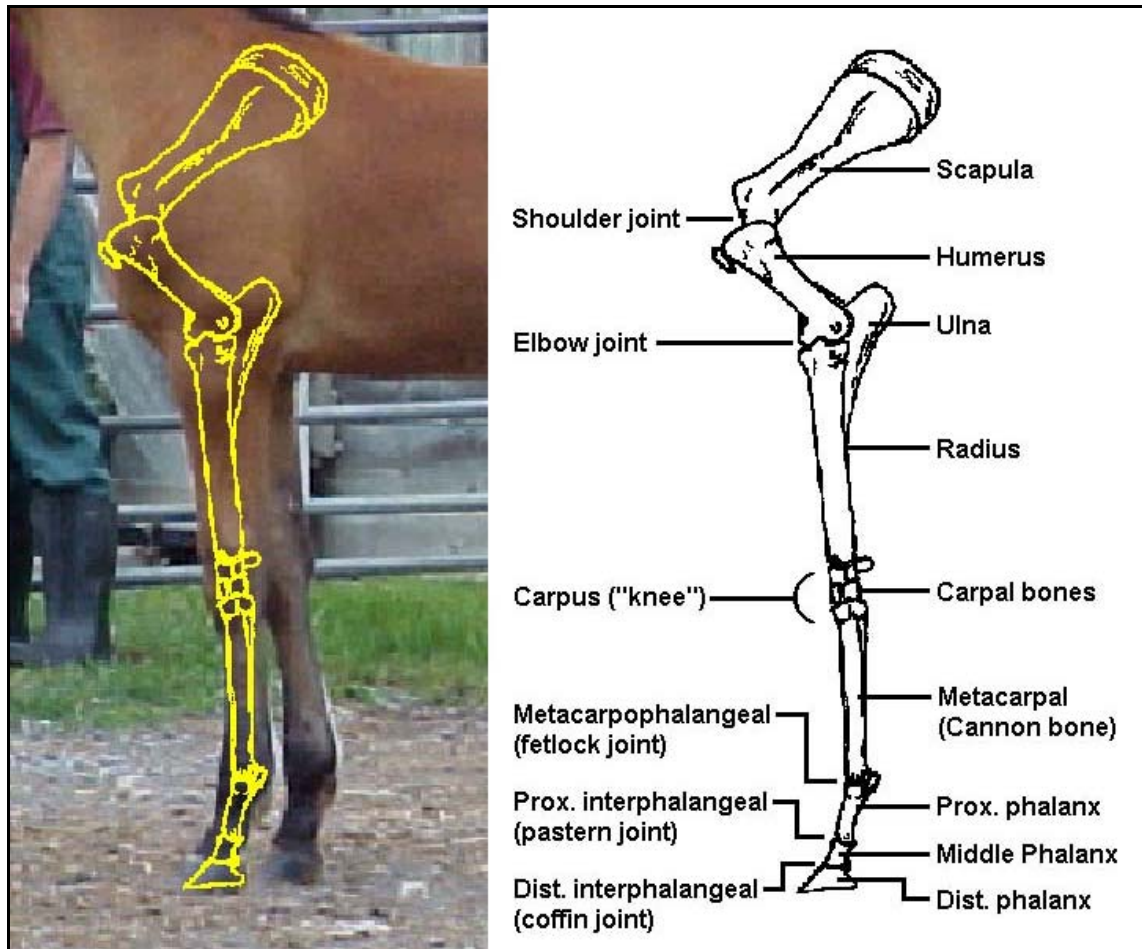


Figure 1-7: Skeletal structure of an equine forelimb.

The two most distal joints are the *coffin* and *pastern* joints (*distal and proximal interphalangeal joints* respectively). The *fetlock* joint (*metacarpophalangeal joint*) is located proximally to the interphalangeal joints. These three joints are considered the fetlock region. In a healthy horse without an ALD, each interface is a *saddle joint* (Pasquini et al, 1995) situated in a common *sagittal plane*. However, in a horse with a fetlock ALD, the plane of each joint is skewed from each other. The design considers a healthy limb and, therefore, will not further discuss fetlock ALD's. The majority of the articulation of the three joints occurs at the fetlock joint while the interphalangeal joints maintain a parallel plane between the hoof and the ground during stance. The interphalangeal joints, primarily the coffin joint, act as shock absorbers during gait dissipating energy from ground contact. However, the fetlock joint acts as a spring, storing and releasing energy during gait (Back and Clayton, 2001).

Moving proximally, the next joint encountered is the *carpal joint*. The carpal joint, a collection of eight bones that make up the joint of the equine forelimb similar to the human wrist, also acts in a sagittal plane as a series of hinge joints, see Figure 1-8. A joint that rotates through a sagittal plane is approximated to rotate about an axis (z) that is perpendicular to the plane (xy). The carpus is held together by several ligaments that spring the joint between the fully extended position and the flexed position. However, the carpal joint “doesn’t appear to play an important role in energy absorption or propulsion.” (Back and Clayton, 2001). Nevertheless, the carpal joint does act as a “propulsive strut” in

supporting the limb in stance. This support comes from the carpal bones locking together when the joint is hyper-extended.

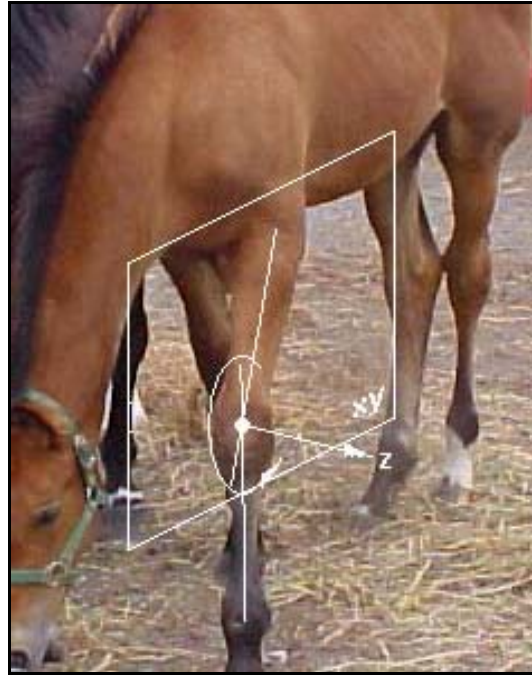


Figure 1-8: Rotation of carpal joint through a sagittal plane (xy).

Proximal to the carpus is the *elbow joint* (Humerus/*Radius* interface) that is a simple hinge joint in a sagittal plane. The elbow joint demonstrates early energy absorption during stance, followed by energy release at mid-stance (Back and Clayton, 2001).

The most proximal skeletal joint in the equine forelimb is the shoulder joint (Scapula/Humerus interface). The shoulder is a ball joint formed by the *glenoid cavity* and the head of the humerus. This ball joint is limited in its rotational motion about the longitudinal axis of limb due to the ligaments holding the joint together. However, this ball joint primarily allows for *protraction* and *retraction* as well as for abduction and adduction of the limb. The shoulder joint synchronically stores and releases energy with the elbow joint. However, the energy storage and release is followed by a “propulsive function” at the end of stance (Back and Clayton, 2001).

Finally, it can be noted that humans have a *clavicle* to aid in the location of the scapula relative to the axial bones. In contrast, the clavicle is completely absent in horses. Therefore, there is no skeletal connection between the scapula and the thorax of the horse. The connection of the scapula to the axial bones of the horse is accomplished through four muscle groups: *Trapezius*, *Rhomboids*, *Serratus Ventralis*, and *Omotransversarius* as shown in Figure 1-9 (Pasquini et al, 1995). The serratus ventralis transfers most of the load from the thorax to the limb. The other three muscle groups primarily locate the position of the scapula relative to the thorax to help position the forelimb. The primary challenge in designing the replica came from attempting to model this ‘floating’ joint. The scapula, held in this ‘cradle’ of muscle, has six degrees of freedom and is capable of limited motion in every direction. The primary motion of the scapula is protraction and retraction (Back and Clayton, 2001).

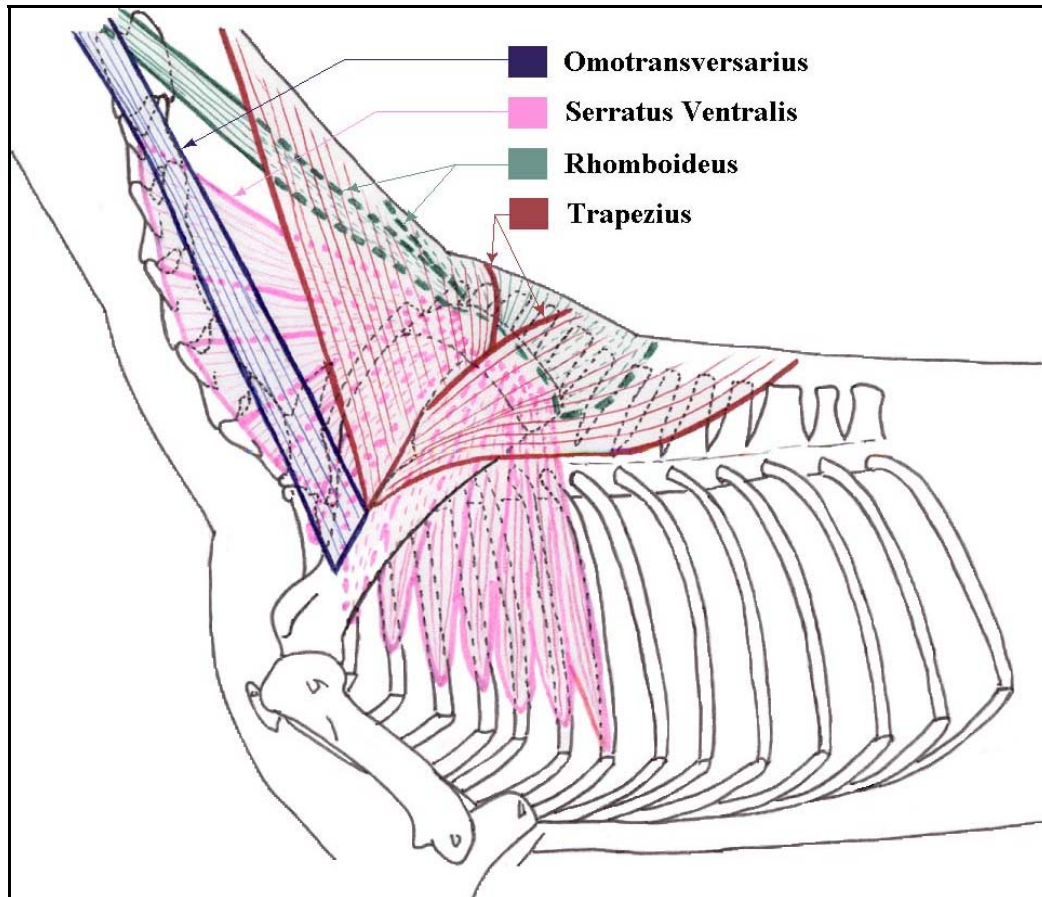


Figure 1-9: Muscular cradle supporting the scapula.

The horse has an interesting feature in its limbs that allows it to stand for extended durations with little muscular activity and, therefore, little fatigue. This is accomplished through a series of tendons and ligaments that do not tire. This series of tendons and ligaments is referred to as the ‘Stay Apparatus’. When the body weight pulls down on the scapula through the serratus ventralis, the shoulder is flexed. The flexing causes a chain reaction of tendons and ligaments stretching taut from the scapula down to the *distal sesamoid bone*. As the tendons and ligaments become taut, the load is transferred from the muscles to the Stay Apparatus. Two specific aspects of the ‘stay apparatus’ prevent hyperextension in the carpus and the fetlock. The carpus is made up of block shaped bones. These carpal bones along with the palmar carpal ligament lock the carpus and prevent it from going deep into hyperextension. Also, the suspensory apparatus and the digital flexor tendons and their accessory ligaments prevent hyperextension of the fetlock and digital joints during stance (Pasquini et al, 1995).

1.4 Approach to Robotic Replica

As discussed in Chapter 2, through dissection and measurements on *anesthetized* and conscious foals, we obtained the anatomical construction and range of motion of the foal’s forelimb. From this information, simplifications were suggested in the modeling of the limb

joints. Since many of the joints rotate primarily through a sagittal plane, it was reasonable to reduce their implementation to mechanical hinge joints. Furthermore, several of the joints were simplified from their anatomical models to a more restricted mechanical model. For instance, the pastern joint which has very little dorsopalmar movement was absorbed into the fetlock joint as shown in Figure 1-10 because of its proximity and direction of rotation. Both the fetlock and the pastern joint have a negative rotation, relative to Figure 1-1 shown earlier, during the first half of stance while the coffin joint has a positive rotation. Therefore, the fetlock joint is replicated with two hinge joints that allow rotation in a sagittal plane. Due to the compliant nature of the coffin joint to the ground, it had been determined that the coffin joint of the robotic replica can be passively controlled with a torsion spring. This spring allows the hoof to lie flat on the ground during stance. However, the proximal, fetlock joint is actively controlled. The insertion point of the actuator is on the fetlock while the origin is located on the metacarpus. This reduces the compilation of forces up to the next actuator. Similar to the natural 'stay apparatus' the fetlock reaches a maximum extension where the actuators will discontinue their increase of force. Instead, the load is taken structurally through stops.

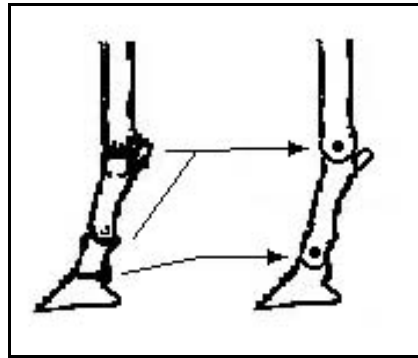


Figure 1-10: Reduction of number of joints in the fetlock region.

Through physical inspection and measurements of several foals, it was possible to reduce the carpus to two hinge joints spaced appropriately to simulate the position of the radius and metacarpus in both the flexed and extended position. Both carpal hinge joints are actively controlled in a sagittal plane by two actuators. However, when the joints go into hyperextension in the stance phase of gait, the joints lock out on hard stops. These hard stops simulate the locking of the carpal bones in hyperextension. Utilizing stops during stance reduces the maximum force required by the actuators. However, while the insertion points of the actuators lie on different rigid bodies (carpus and metacarpal), both origins lie on one rigid body (radius). This must be done due to the space available on the carpus and the minimum length of the actuator. A sketch of this design can be seen in Figure 1-11.

A single hinge joint is capable of robotically simulating the elbow joint. This joint is actively controlled in a sagittal plane similar to the previous joints. The origin of the actuator controlling the elbow joint is on the humerus while the insertion point is located on the radius.

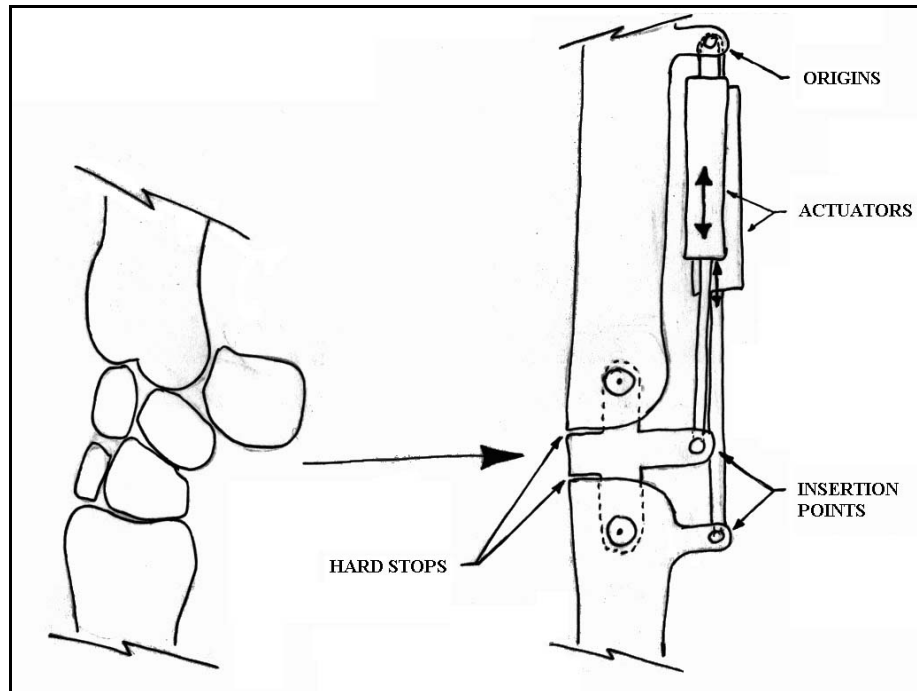


Figure 1-11: Sketch of the carpal design for the robotic replica.

The shoulder joint is mimicked through an actively controlled ball joint allowing protraction and retraction as well abduction and adduction. The humerus is positioned relative to the scapula by three actuators as shown in Figure 1-12. This method of actuation allows for the limited rotation about the longitudinal axis (2) of the robotic limb. This rotational motion is necessary to replicate turning of the foal during gait. All of the points of origin of the actuators are located on the scapula and all of the insertions are on the humerus.

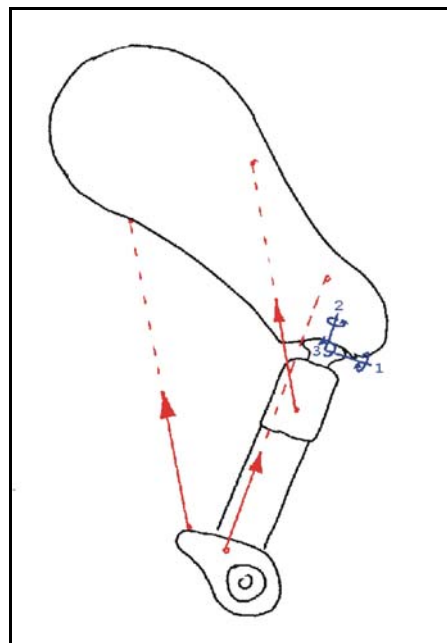


Figure 1-12: Three actuators controlling the three degrees of freedom of the humerus.

The scapula is actuated on an angled plane to closely represent the external surface of the ribs and *intercostal* muscles. This plane has active actuation in the vertical direction to simulate the effect of the serratus ventralis. However, the horizontal motion is passive to allow for the relative motion of a contralateral scapula. This passive motion is accomplished through springs and dampers. In addition to the two degrees of freedom allowed through the plane, the scapula is also situated on a ball joint relative to the plane allowing for three additional degrees of freedom. These three degrees of freedom are actuated by three actuators as shown in Figure 1-13.

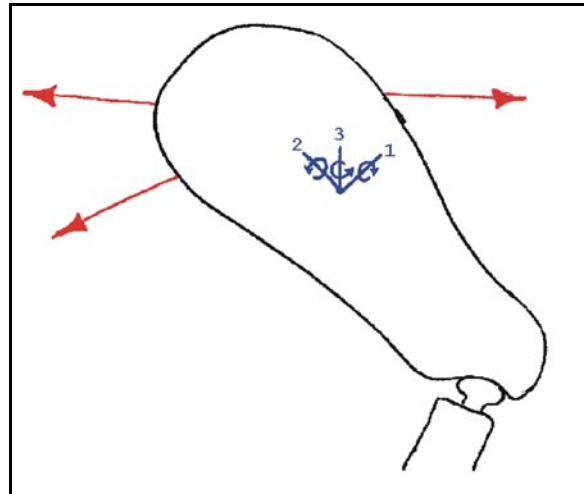


Figure 1-13: Three actuators controlling the three degrees of freedom of the scapula.

The final robotic replica can have one of two different configurations. The first configuration would have two opposing forelimbs with a mass located on top of them and a stabilization unit. This robot would be capable a freestanding motion. However, the second configuration would apply a vertical pneumatic cylinder to one robotic forelimb to simulate the weight of the foal as well as the impact forces generated through the anticipated motion. Both robotic replicas are capable of simulating a range of motions including normal gait through a straight line, turning during gait, kicking in various directions, and shifting weight to and from the leg during rest.

In order to get the robotic replica to follow the motion of an equine forelimb, positions, velocities, and acceleration as a function of stride must be known. Extensive research on equine gait analysis has already been performed by numerous experimenters. Therefore, gait analysis was not replicated. This is discussed in detail in Chapter 2.

The positions, velocities, and accelerations of the forelimb are controlled via several servo-valves and hydraulic actuators. The hydraulic actuators are located directly on the robotic replica as stated earlier. However, the servo-valves and the rest of the hydraulic system (accumulator, pump, etc.) are remotely located to reduce the mass and mass moment of inertia of each segment of the robotic replica. The actuators are specified based on the dynamics of the robotic replica.

1.5 Scope

The scope of this project is limited to the design, analysis, and procedure of construction of a robotic replica and the creation of detailed and assembly drawings. With this work completed, funding needs to be sought to invest in the hardware necessary for construction. Testing and subsequent optimization of the replica design would then follow.

The design of the robotic replica encompasses three primary aspects, namely, the replica structural design, joint kinematics, and joint actuation. Specifically, the definition of the range of motion is derived from investigation of equine gait through literature and experimentation. Because the load-bearing device will be used in a controlled environment, the foal's motion will be limited, thus limiting the requirements on the robotic replica as discussed in Chapter 2.

The structural design of the limb replica includes specifications of structural members as well as actuators. Detailed drawings and assembly drawings are necessary to fabricate the structural members of the limb. These drawings have been created directly from the computer-aided design (CAD) of the limb. In an attempt to minimize the total cost of the robotic replica, off-the-shelf parts have been utilized when possible. These parts have been specified from the hoof up to the thorax. To retain the choice between a single standalone forelimb and a pair of front limbs, as discussed earlier, the vertical actuator has been left unspecified. This gives the producer of the robot the choice to create a single standalone forelimb or a pair of front legs as discussed later. High-pressure actuators (≥ 3000) are not offered as a standard item with bore diameters less than 1½in. Therefore, the hydraulic actuators will be custom built due to their size and operating pressure. Due to the uncertainty of the manufacturer, the actuators are only given overall dimensions and force requirements. With the freedom of choosing the actuators comes the choice of sensors. Hence, this thesis does not cover the final “nervous” system of the replica. Only a theoretical control system is designed. The control system is based on linear sensors on each actuator.

From the structural design and the kinematics of a foal's forelimb, a complete dynamic analysis has been performed. First, an inverse dynamic analysis on equine gait-analysis data yielded the forces required to reproduce the gait motion in the replica. Next, a finite element analysis (FEA) was implemented to ensure that the robotic replica would not fail during use. Finally, a forward dynamic analysis (FDA) was performed using open-loop as well as closed-loop control and compared to the original gait data. Details on the analysis methodology and the comparison between simulation predictions and actual gait are found in Chapters 3 and 4.

2 Equine Locomotion

Most of the biological functions associated with athletic performance are more superior in the horse than in the human (Wilson, 1991). Their superiority and the fact that horses are domestic animals make them an excellent choice for competition. Because horses are used extensively for competition, their gaits have been extensively analyzed to classify good and bad gaits. There are four basic forms of equine gait—walk, trot, canter, and gallop—all of which are used for different competitions. Each gait is typically associated with a particular range of speed for an individual horse. Generally, an increase in speed within each gait is accomplished primarily through an increase in stride length. However, once a horse has reached moderate gallop, the speed is increased by increasing the pace (Dušek *et al.*, 1970).

The walk is the slowest of the four gaits performed by the horse. Starting with the contact of the right hind hoof, the right fore hoof is the next to impact the ground. The right fore hoof is followed by the left hind and then the left fore foot. This cycle is repeated to form the walking gait shown in Figure 2-1 where FL, FR, HL, and HR stand for front left, front right, hind left, and hind right respectively. Walk is classified as a rhythmic four-beat gait. (Back and Clayton, 2001)



Figure 2-1: Foot placement as a function of stride for walk.

Trot, on the other hand, is a two-beat gait. This two-beat motion is characterized by diagonal pairs of fore and hind limbs moving in synch and often is accompanied by a suspension phase. The foot placement of this gait is displayed in Figure 2-2 below. The trot of a quadruped is often referred to as jogging. (Back and Clayton, 2001)



Figure 2-2: Foot placement as a function of stride for trot.

Canter is a gait that is frequently seen in competitions. The canter is characterized as an asymmetric gait. ‘There is so great a variety in the mode adopted by different horses for performing the canter, that no single description will suffice, nor indeed is it easy . . . to define any one of them.’—J. H. Walsh (Porter, 1998). It can be said, however, to be a quicker pace than the trot. Yet, the canter is slower than the gallop. One form of canter can be seen in Figure 2-3. This version is referred to as a right leading canter due to the left hindlimb and left forelimb following the right hindlimb and the right forelimb respectively.

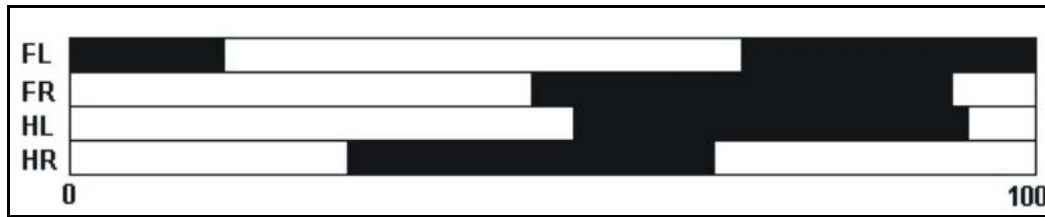


Figure 2-3: Foot placement as a function of stride for a right lead canter.

The natural fast-paced gait of a horse is called the gallop. Gallop is described as bounding by alternately lifting the fore hoofs and the hind hoofs. Gallop can't be specified as a two, three, or four-beat gait due to the variation among horses. However, it can be noted that gallop has a phase where the horse is suspended. (Back and Clayton, 2001) For comparison with the other gaits, Figure 2-4 shows the foot placement for one stride of a right lead transverse gallop.

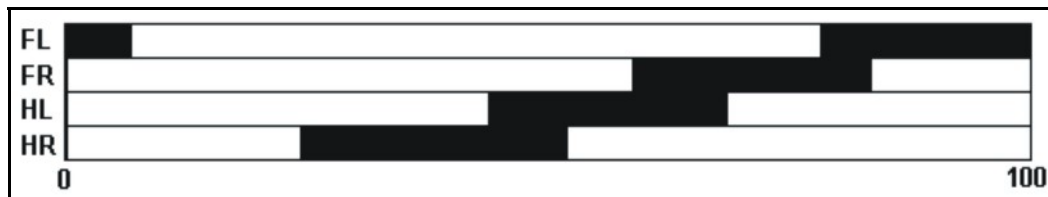


Figure 2-4: Foot placement as a function of stride for a right lead transverse gallop.

In addition to their kinematic characteristics, the gaits described above may be differentiated by the peak ground reaction forces on the four limbs. For example, during walk, a foal weighing 200kg would create a peak ground reaction force in the forelimbs of approximately 1360N. A 68% increase in the reaction force would be seen as the gait was changed to trot. However, changing from a trot to a canter only increases the ground force by 9%. (Back and Clayton, 2001)

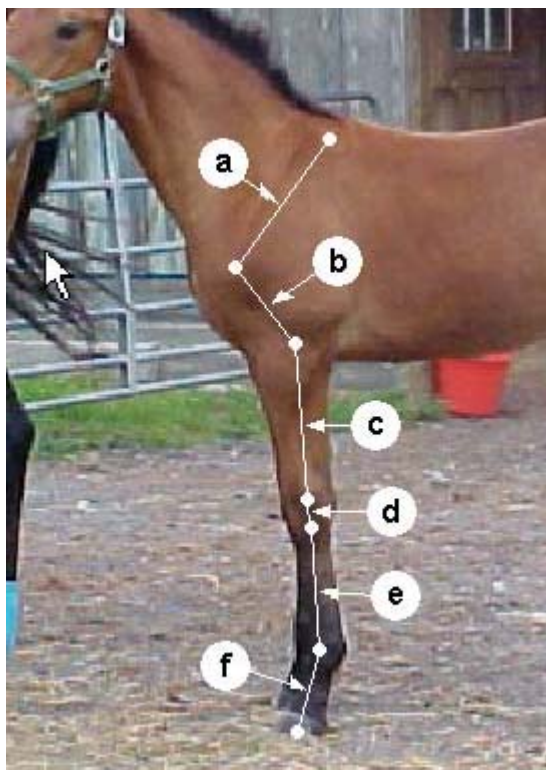
Two immediate constraints on the design of the bioassistive, rehabilitative device are the speed of locomotion of the animal and impact and contact forces during use. Since the device is to be used in a controlled environment, say a stall, its design needs only accommodate a restricted speed of locomotion, typically below that of canter and gallop. However, in the event that the foal attempts to kick the device free, the device should be designed to withstand the resultant larger impact forces. As trot results in a significantly larger ground reaction force relative to walking, it thus appears reasonable to use trot as a nominal kinematic and kinetic reference. Hence, the robotic replica was designed to replicate trot.

2.1 Structural Size Data

There is great variation in the size of a foal through its development to a mature horse. Rapid growth in the foal's forelimb occurs primarily in the first month and continues at a lower pace for the next two months. Overall limb development takes place over a nine-month period. With this in mind, the size of the robotic replica was selected to correspond to an average four-month-old foal, thus ensuring that the foal had completed its initial rapid growth, although not yet reached its full size.

2 Equine Locomotion

Due to availability of foals on the Virginia Tech campus, the foals used for the structure size were all Quarter-horse/Thoroughbred mixes and Warm-bloods. Following the above observation on growth, the foals used for collecting size data were all four-month-old males. The average mass at four months of the foals used was about 206kg. The variation of the mass was $\pm 8.7\%$. All of the foals used for collecting size data were males. This selection allowed length data to be gathered while the foals were routinely anesthetized for *castration*. While each foal was unconscious, each leg segment was measured from rotation center to rotation center. The center of rotation was approximated by flexing and extending the sections as shown in Figure 2-5. The average lengths of the forelimb segments from the measured sample of four-month-old foals are shown in Table 2-1. The length of the scapula was not measured on any of the specimens, as the connective tissue between the scapula and the axial bones made an accurate determination of the location of the center of rotation of the scapula relative to the thorax impossible. Instead, the overall length of the scapula was used, as determined from skeletal remains and scaling to the measured data. The largest variation in the forelimb was $\pm 4.2\%$ for the radius. Comparing the variation in length to that of the mass demonstrates that there is good forelimb length uniformity between foals of similar breeds and ages.



a: Distance from scapular cartilage to shoulder joint.

b: Distance between shoulder and elbow joint.

c: Elbow to carpus length.

d: Approximation of distance between radial-carpus and metacarpal-carpus rotation.

e: Distance from carpus to fetlock joint.

f: Distance from fetlock joint to the ground.

Figure 2-5: Length of segments of the equine forelimb.

Table 2-1: Forelimb length data

Notation	Section	Length (cm)
a	Scapula	32
b	Humerus	20
c	Radius	36
d	Carpus	5
e	Metacarpal	30
f	Fetlock	19

In addition to the structural data described above, the kinematic characteristics of gait as a function of time were obtained from the literature as discussed below.

2.2 Walk Data

Gait data has been compiled by numerous investigators (Back and Clayton, 2001). The general method used for determining the relative angles between limb segments is to use markers and high-speed cameras. Markers are placed at key locations on the limb and body (centers of rotation and bony protrusions) to measure the relative orientation of the bones with respect to each other. Next, the horse is filmed during the desired gait with the high-speed camera. Once the footage is collected, the position of each bone is determined as a function of stride. This is often done through automated software programs that digitize the coordinates and produce specific sets of gait data. Depending on the position of the markers, the motion of the skin relative to the skeleton must be subtracted. Finally, the relative angles between limb segments are derived and plotted as a function of stride (see Chapter 3 in Back and Clayton (2001) for a more in-depth discussion on the data-gathering methodology).

Using previously collected data (Back and Clayton, 2001), the time histories of the various joint angles were determined. The first gait that was investigated was walk. Walk is the gait that will be seen most during convalescence due to the nature of the expected injuries. Therefore, it is necessary for the robotic forelimb to replicate not only trot for worst-case scenarios, but also walk so the rehabilitative device can be designed and optimized at that gait. From the figures for angle as a function of stride, a data point was estimated every 5% of stride for each joint; shoulder, elbow, carpus, and fetlock. However, to determine the angle of the scapula relative to the ground, data from another source was used (Schamhardt et al, 1994). Due to the lack of walk data for the scapula, the position of the scapula relative to the ground during trot was used for both trot and walk. This data produced a normal motion of the equine forelimb during walk. Each graph was enlarged and a grid overlaid. This enlargement and grid allowed for an estimation of the angle at specific instances throughout the motion.

With the relative angles for each section, the absolute angles relative to the ground were calculated for each joint as a function of stride. Each angle was defined relative to the ground with the horse moving from left to right as shown in Figure 2-6. The angular position of the scapula was already relative to ground. Therefore, the scapula data was used unmodified as seen in Figure 2-7a. However, the subsequent joint angles were determined from the previous joint's angle. These angles are displayed in Figure 2-7b, Figure 2-8, and Figure 2-9.

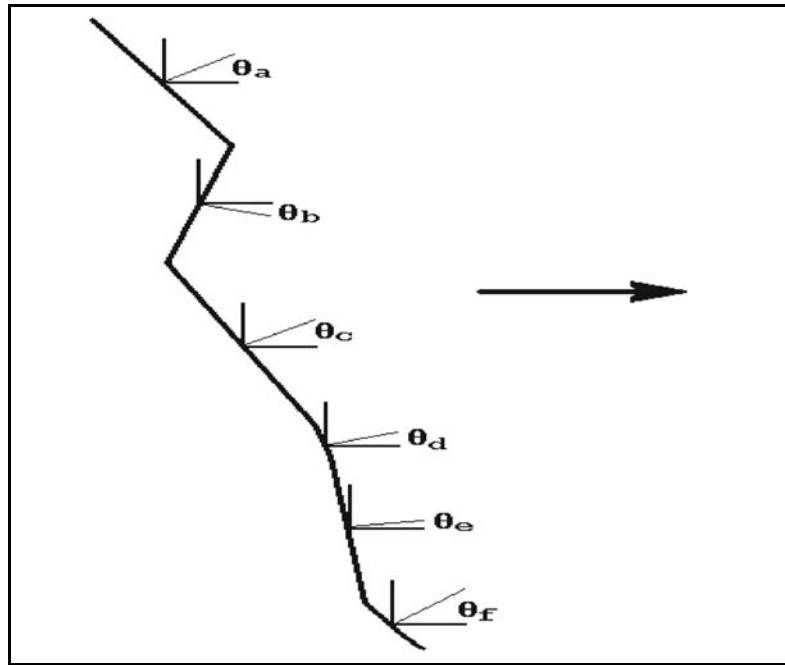


Figure 2-6: Definition of absolute angles for each limb section.

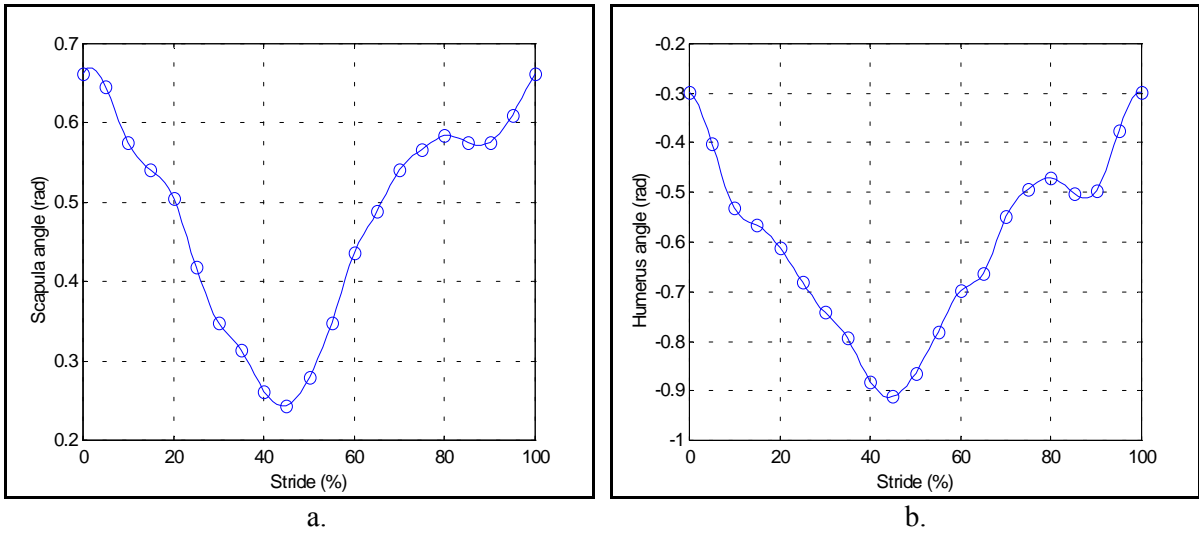


Figure 2-7: Joint angles relative to the ground as a function of stride for walking.
a. Scapula, b. Humerus.

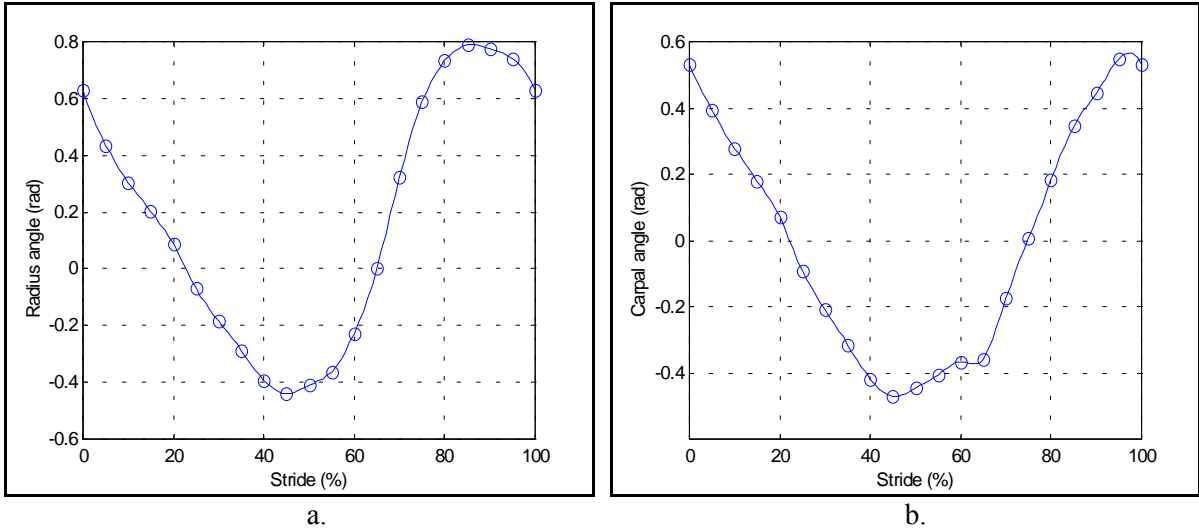


Figure 2-8: Joint angles relative to the ground as a function of stride for walking.
a. Radius, b. Carpus.

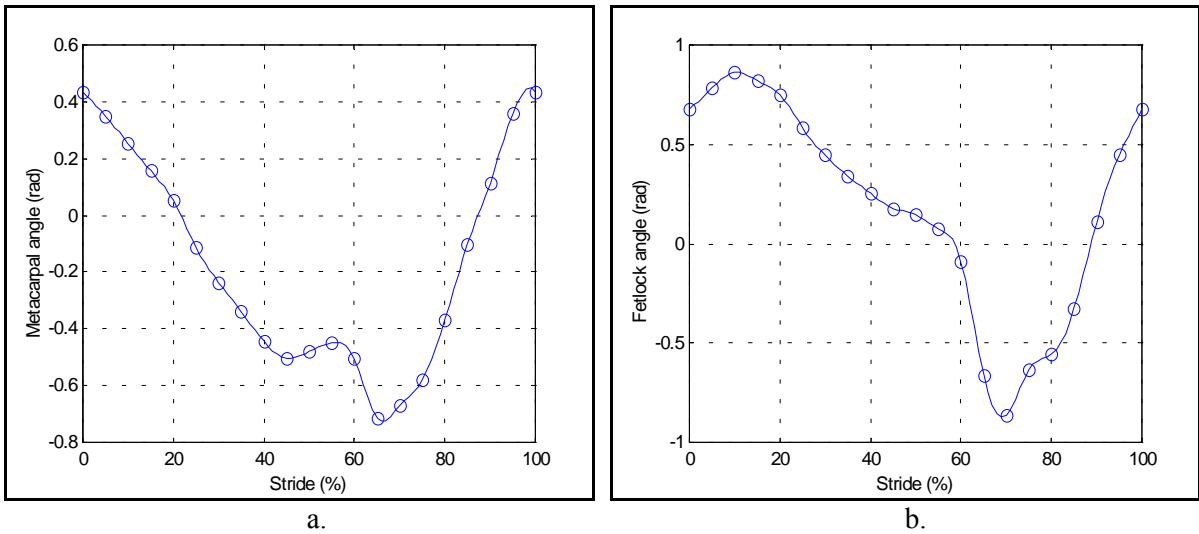


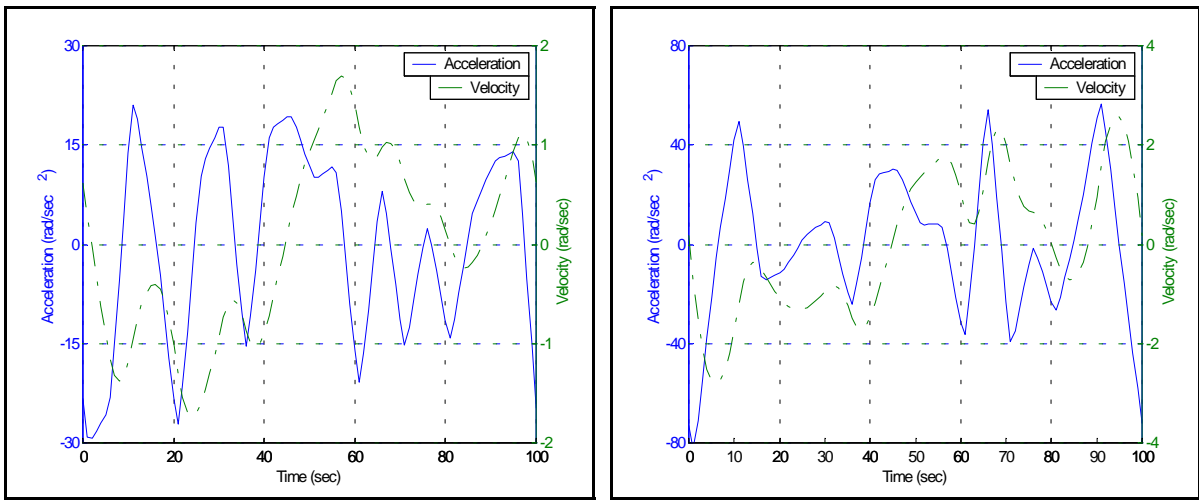
Figure 2-9: Joint angles relative to the ground as a function of stride for walking.
a. Metacarpal, b. Fetlock.

Next, from the angular position data, the average angular velocity relative to the fixed reference frame was calculated. First, a cubic spline was fit to the periodic gait data using points at one percent increments of the stride. These curves can be seen in the previous figure relative to the original 20 data points collected. Then, the velocity calculation was accomplished by taking the difference of the current position estimated by the cubic spline and the previous position of the spline and dividing by the elapsed time for every one percent of stride,

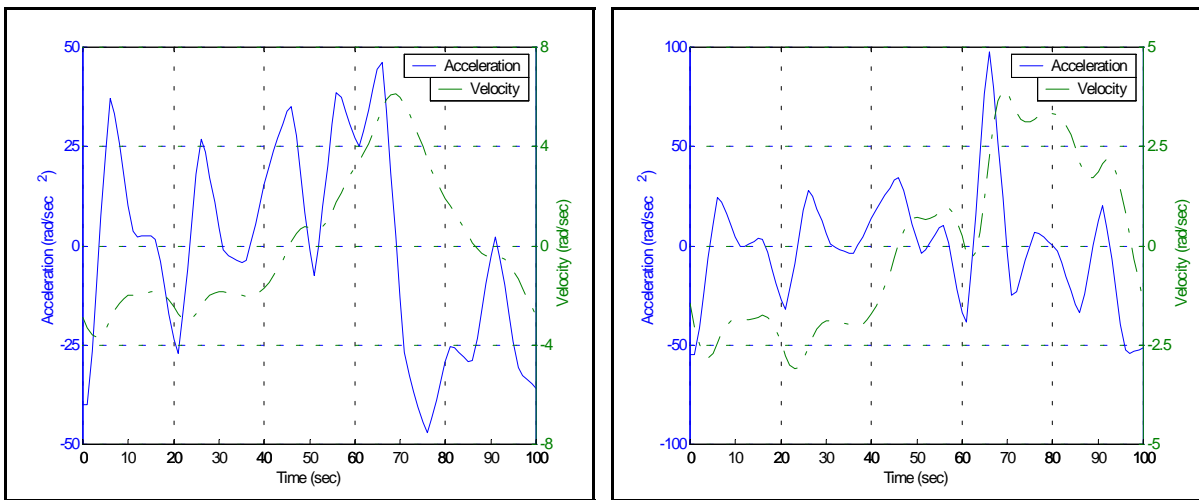
$$\omega = \frac{\Delta\theta}{\Delta t}, \alpha = \frac{\Delta\omega}{\Delta t}, \quad (2.1)$$

where ω is the velocity, $\Delta\theta$ is the change in position, Δt is the change in time, α is the acceleration, and $\Delta\omega$ is the change in velocity. This method computed the average velocity

using many finely spaced points. The resulting curve was a piecewise quadratic curve that closely approximated the actual derivatives of the positions. The gait was repeated as a periodic motion to obtain a continuous velocity through each stride. This means that the velocity at the beginning of the stride will be the same as at the end of stride. The time of each stride used for walk was 1.09 seconds. The percent of time spent in stance for each stride of the forelimbs was 63.2% (0.69sec) (Back and Clayton, 2001). Similar to the velocity calculation, the angular acceleration relative to the fixed reference frame was found for each joint using Eq. (2.1). This computation resulted in piecewise linear approximations of the actual acceleration. The angular velocity and acceleration for each limb section are shown in Figures 2-10 through 2-12.



a. b.
Figure 2-10: Angular velocities and accelerations per stride during walk, relative to the ground.
a. Scapula, b. Humerus.



a. b.
Figure 2-11: Angular velocities and accelerations per stride during walk, relative to the ground.
a. Radius, b. Carpus.

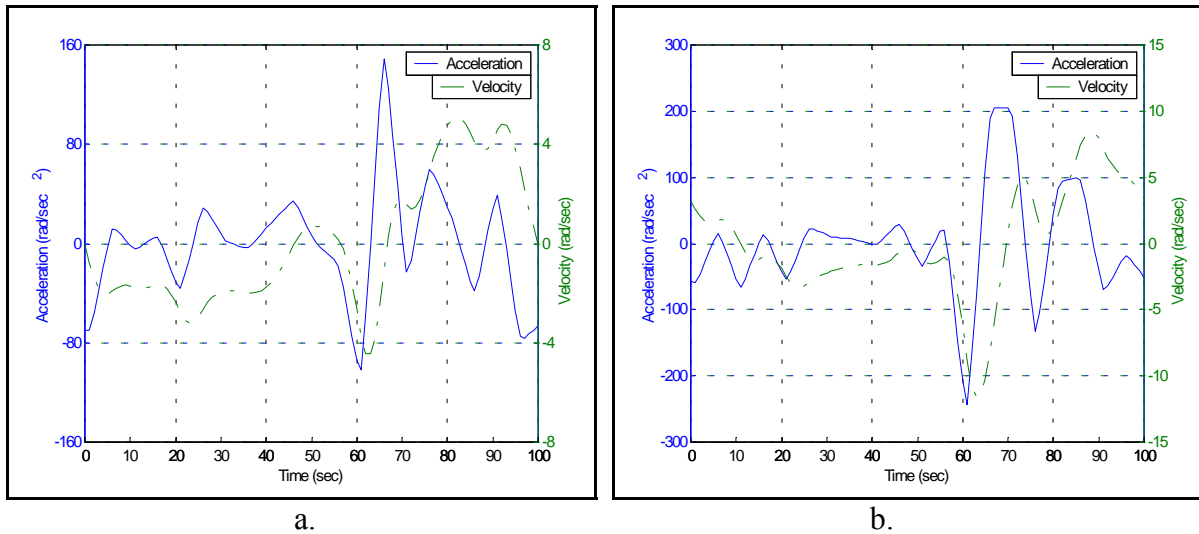


Figure 2-12: Angular velocities and accelerations per stride during walk, relative to the ground. a. Metacarpal, b. Fetlock.

2.3 Trot Data

The forequarters actually produce almost zero percent of the forward propulsion during gait. The hindquarters of the horse are the primary source of propulsion pivoting about the pelvis. The forelimbs are used for support and balance as the hind limbs propel the horse forward (Back and Clayton, 2001). Therefore, as the horse transitions from walk to trot, the load carried through the forelimbs increases substantially as the horse's center of mass translates through a larger height.

Adequate data for generating plots of the relative angles between limb segments as a function of percent of stride were found in the reviewed literature (Schamhardt et al, 1994). From the data in the literature, angles relative to the ground were calculated for each joint in the same manner as for walk. The absolute angle relative to the ground of each section of the forelimb during trot can be seen in Figure 2-13.

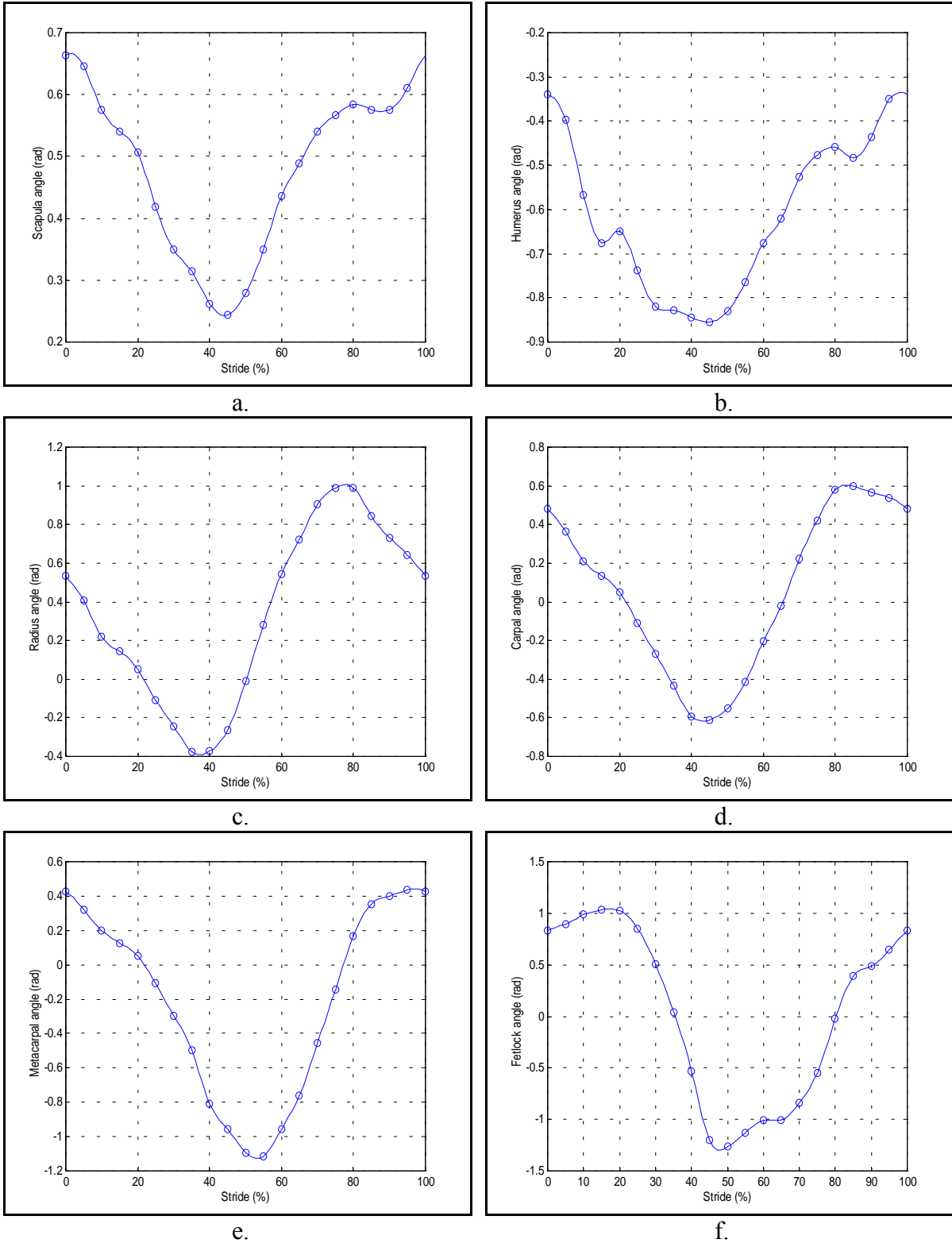


Figure 2-13: Joint angle relative to the ground as a function of stride for trotting.
 a. Scapula, b. Humerus, c. Radius, d. Carpus, e. Metacarpal, f. Fetlock.

In addition to the relative angles during trot, the angular velocities and accelerations were calculated for trot as they were for walk. The results of these computations are displayed in Figures 2-14 through 2-16. The time of each stride used for trot was 0.67 seconds. The percent of time spent in stance for each stride of the forelimbs was 40.3% (0.27sec). (Back and Clayton, 2001)

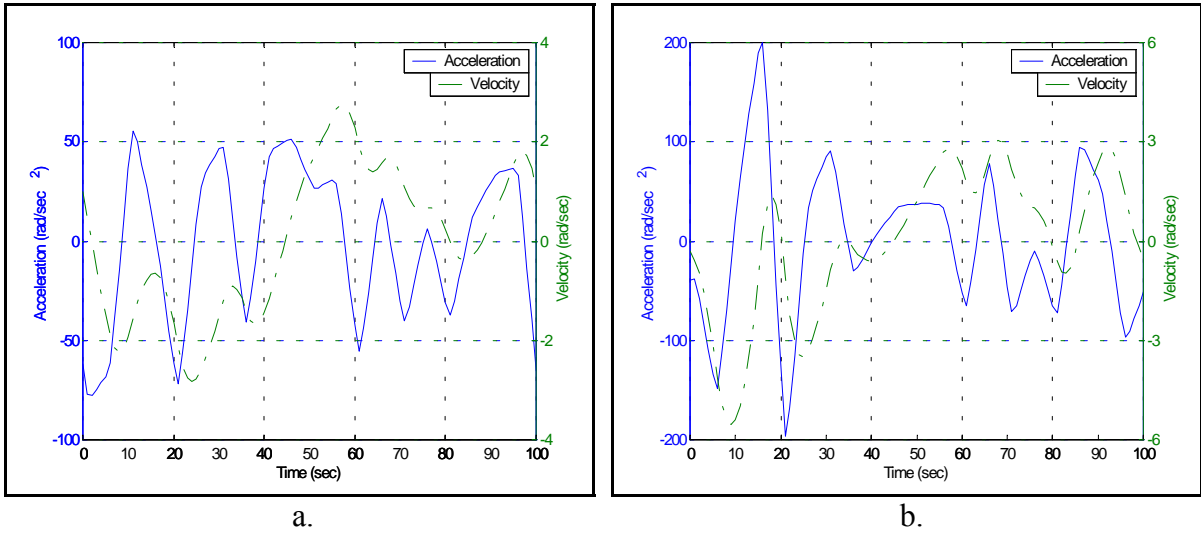


Figure 2-14: Angular velocities and accelerations per stride during trot, relative to the ground. a. Scapula, b. Humerus.

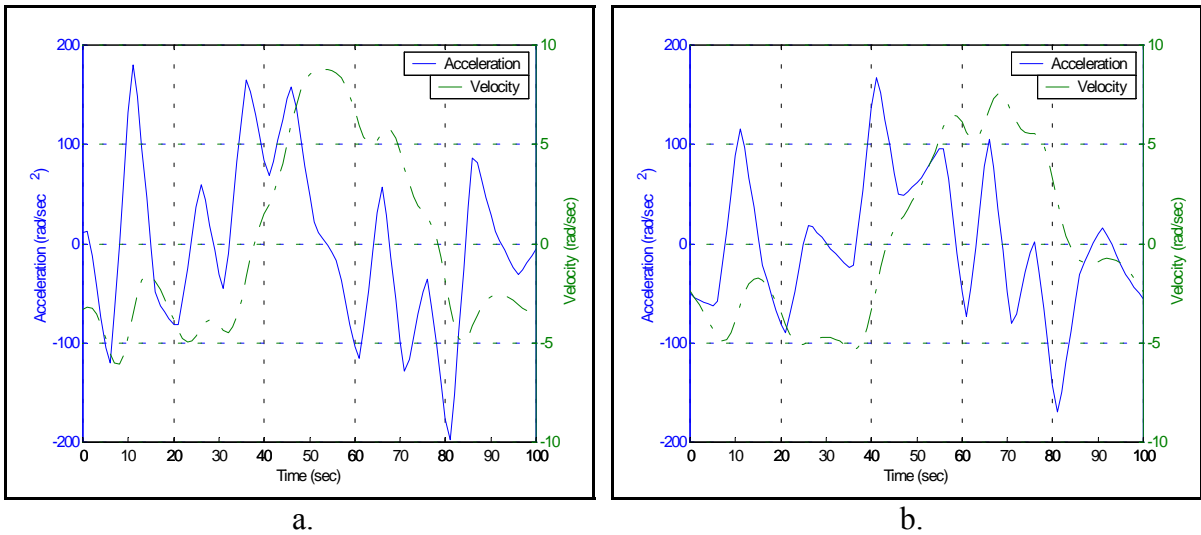


Figure 2-15: Angular velocities and accelerations per stride during trot, relative to the ground. a. Radius, b. Carpus.

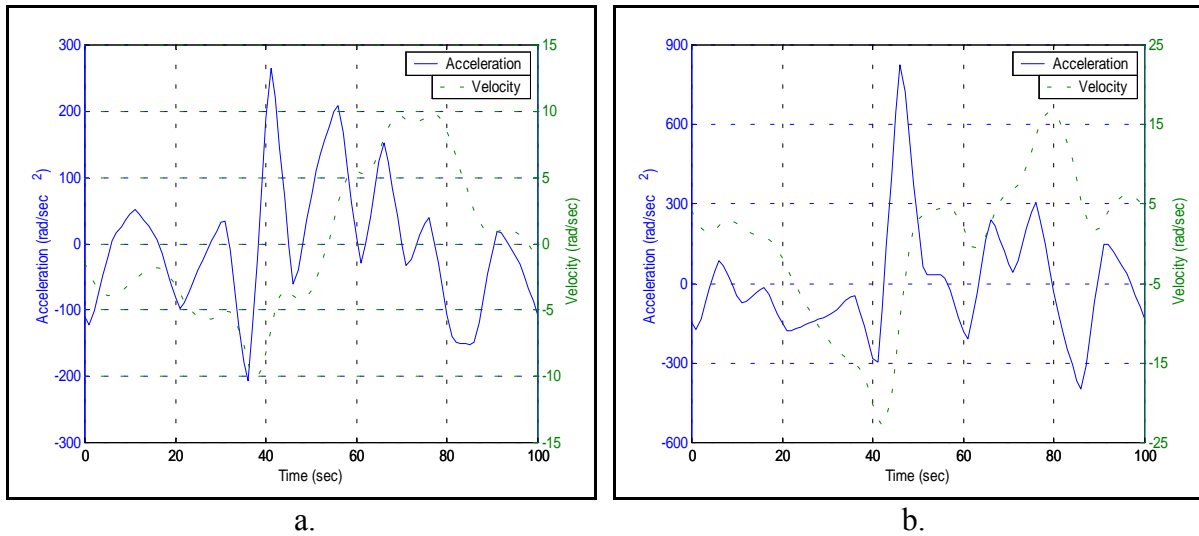


Figure 2-16: Angular velocities and accelerations per stride during trot, relative to the ground. a. Metacarpal, b. Fetlock.

In addition to the angles of each joint as a function of stride, the total articulation of each joint was investigated. The total articulation was determined on anesthetized foals with the use of a large transparent protractor and recorded. The averages of the angles measured are shown in Table 2-2. These angles were then compared to the difference between the largest positive and largest negative joint angles during trot.

Table 2-2: Forelimb joint articulation range.

Joint	Manually measured		Trot data	
	(rad)	(deg)	(rad)	(deg)
Scapula	?	?	0.42	24
Shoulder	?	?	0.30	17
Elbow	1.31	75	1.24	71
Knee	2.44	140	1.57	90
Fetlock	0.96	55	1.83	105

As the foals were lying on the ground during the manual measurements, it was very difficult to manually move the scapula relative to the thorax, thus preventing a quantitative determination of the scapula range of motion. Similar difficulties in manually manipulating the humerus about the shoulder joint as well as the surrounding muscle mass prevented a quantitative determination of the shoulder range of motion.

Observations of healthy and active foals led to the conclusion that the range of motion in the knee joint that is required for the animal to lower and raise itself from the ground greatly exceeds that utilized during gait. This was suggested as the likely explanation of the discrepancy in Table 2-2 between the knee range of motion during gait and during manual manipulation.

Similarly, two possible explanations were proposed to explain the discrepancies in Table 2-2 between the fetlock range of motion during gait and during manual manipulation. On the one hand, it was noted that the forces used to articulate the fetlock as the foal was

anesthetized were significantly smaller than those imposed on the joint during gait. On the other hand, it was noted that some of the difference could be attributed to differences in the methods of measurement. In particular, during both gait and manual manipulation, the flexion of the fetlock region appeared to be the same. In the manual measurements, the angle was taken between the *cannon bone* and the proximal phalanx. The gait measurements, however, used markers placed on the fetlock joint and on the hoof. The difference of the flexion angle can be noted in Figure 2-17. Since the difference in both extension and flexion are accumulative, the large deviation between manual articulation and gait-induced articulation can be understood.

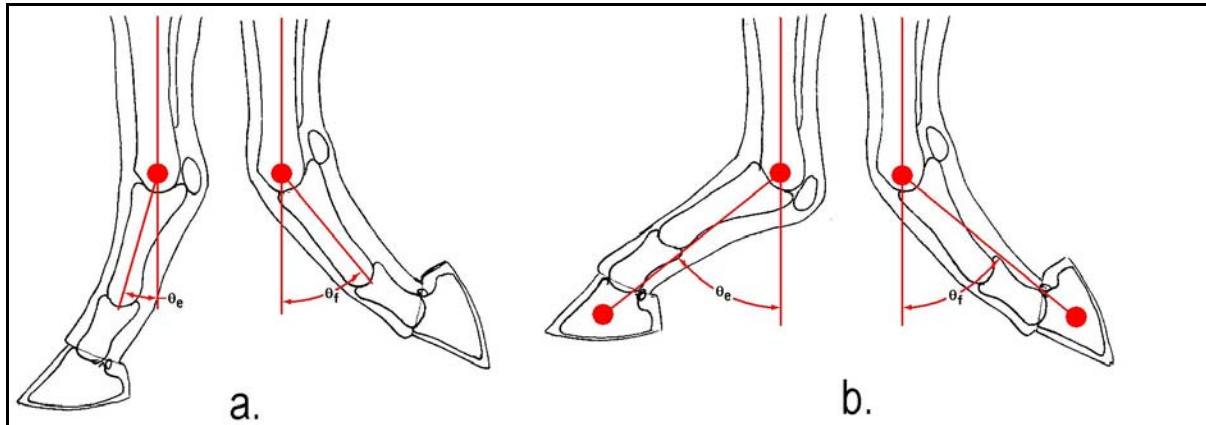


Figure 2-17: Extension and flexion angles for fetlock.
a. Motion achieved by human manipulation. b. Articulation during trot.

The scapula-to-ground and shoulder joint angles were modeled from the trot data because there was no information obtained during manual inspection of the range of motion. In addition, the range of motion for the elbow joint was similar in both applications. Therefore, no selection between the two methods of measurement was necessary.

As noted above, the range of motion of the knee joint, however, differed significantly between human manipulation and trot (50deg). The actuator used to control the length of the rehabilitative load-bearing device will not possess the necessary motion to allow the foal to lower itself completely to the ground due to mechanical restrictions. Since the rehabilitative device will be used in a controlled environment and not allow the foal to lie down, the range of motion at the knee joint will not be permitted to reach that necessary value to lie down. Therefore, the robotic replica doesn't need to simulate the entire range of motion that a healthy foal is capable of producing. However, the replica can simulate an attempt of the foal to lower to the ground with a range of motion of 122 degrees in the carpus. This attempt will allow a testing of the rehabilitative in the event the foal does attempt to lie down. A large range of motion was unachievable due to the mechanical limitation of the hydraulic actuators selected for the given geometry of the robotic replica.

During testing of the rehabilitative, collateral, load-bearing device the robotic replica will simulate trot in an attempt to test the robustness of the rehabilitative device. Hence, the robotic replica was designed to simulate the range of motion experienced in the fetlock throughout trot.

With the kinematics of the forelimb defined for walk and trot and the desired geometry described, a preliminary design of the robotic replica was drafted. The overall geometry for the robotic replica, shown in figure 2-18, was selected based on the skeletal structure of the foal and the range of motion that must be achieved.

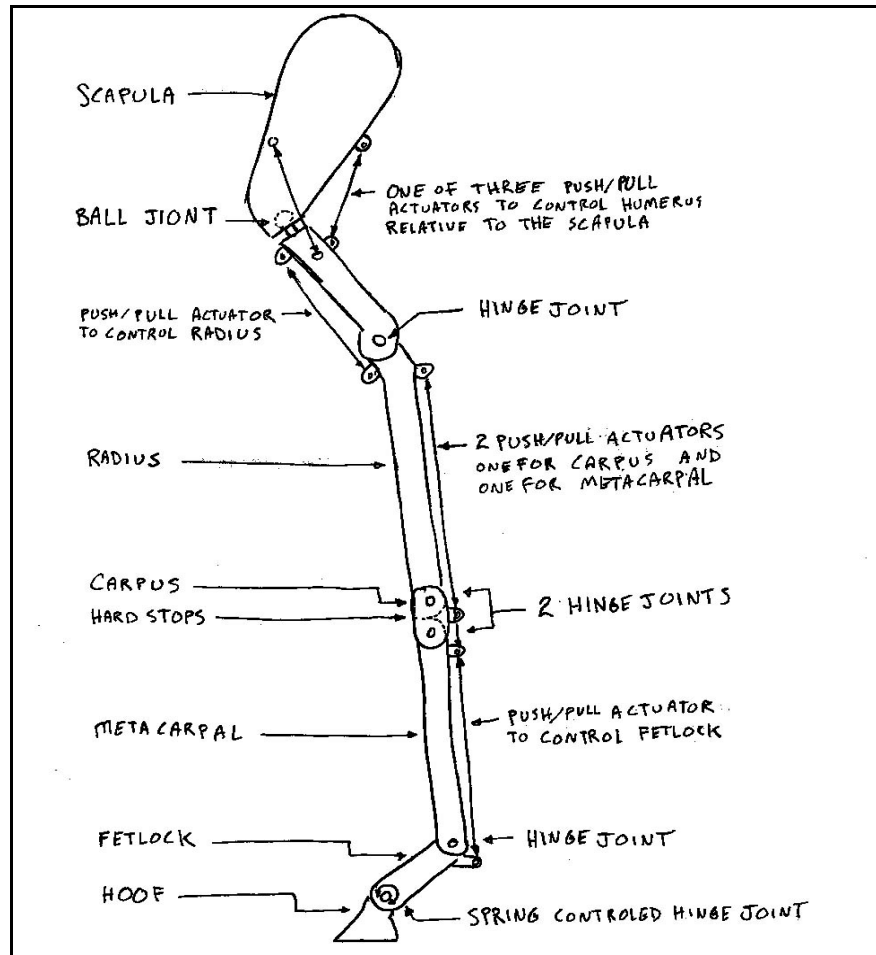


Figure 2-18: Preliminary design of the robotic replica.

First, the foal's skeletal structure determined the location of each joint relative to each other. The lengths from Table 2-1 and an approximation of the diameter of the legs bones (45mm) were used to get a rough model.

Secondly, the range of motion helped design each specific joint. The joints were positioned to optimize the positions of the limb sections used during the desired gaits. In addition, the shapes of the joints were design to closely mimic the actual anatomical design taking advantage of the evolutionary optimization. For example, the carpus was designed with hard stops in hyperextension to simulate the locking of the carpal bones as described in Chapter 1.

With the preliminary design of the replica complete, the next step taken in the design process of the robotic replica was a dynamic analysis. This dynamic analysis aided in the optimization of the geometry of the robot in addition to the locations of the origins and insertion of the actuators. The dynamic analysis is covered in detail in Chapter 3.

3 Design of Robotic Replica

To design the robotic replica, the Computer Aided Design (CAD) program SDRC 8m2 produced by I-DEAS was used. A three-dimensional CAD model of the robotic replica was produced from the preliminary design discussed in Chapter 2. From this model the mass properties of the replica were obtained for a dynamical analysis. The mass properties included the mass of each rigid body (representing the different limb segments), the center of mass relative to the joint, and the mass moment of inertia about each axis. Next, an inverse dynamic analysis was performed to determine the required force to generate the desired motion. These forces were inspected to determine if hydraulic actuators could generate them within the restricted space of the replica. The origin and insertion points of the actuators were arranged to optimize the required force within the mechanical limits of the actuators. After obtaining the forces, a free-body diagram was drawn for each limb segment and a finite-element analysis (FEA) was performed. The FEA process aided in determining the appropriate robustness of the components in the robotic limb. Through an iterative process, the final design of the robotic replica was achieved. Finally, a forward dynamic analysis was performed to determine if the designed robotic replica would produce the required motion. Both open-loop and closed-loop control algorithms were tested in reproducing the desired motions.

3.1 Mass Properties

The I-DEAS program SDRC has a function that allows the user to input a density for a homogeneous material. From this density, SDRC will calculate the mass through the volume of the part as shown in Figure 3-1. This process of determining the mass was repeated for each limb component that is moved with hydraulic actuators.

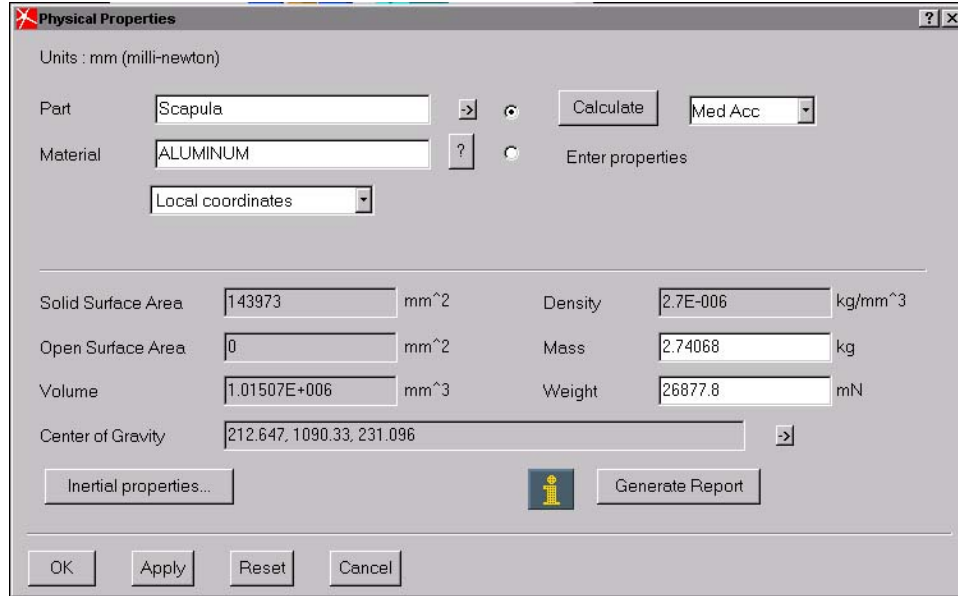


Figure 3-1: I-DEAS window displaying mass and associated properties.

Also calculated by the program was the center of gravity (see Figure 3-1 on the previous page). This value was recorded and used later to determine the position of the joint centers relative to the center of mass.

Next, the mass moment of inertia for each component was determined through the program as displayed in Figure 3-2. The axes of each component were oriented such that the y-axis of the part would coincide with its longitudinal axis as shown in Figure 3-3. In addition, the z-axis was arranged to lie perpendicular to the plane of protraction and retraction. This consideration for orienting the xyz-triad to the part was done to facilitate the use of the inertial properties directly to the Maple code discussed later in this chapter. The process of determining the inertial properties of each limb component was repeated for each iteration until the final values were obtained. These values can be seen in the code in appendix A where the mass is in kilograms and the mass moment of inertia is in kilograms times meters squared.

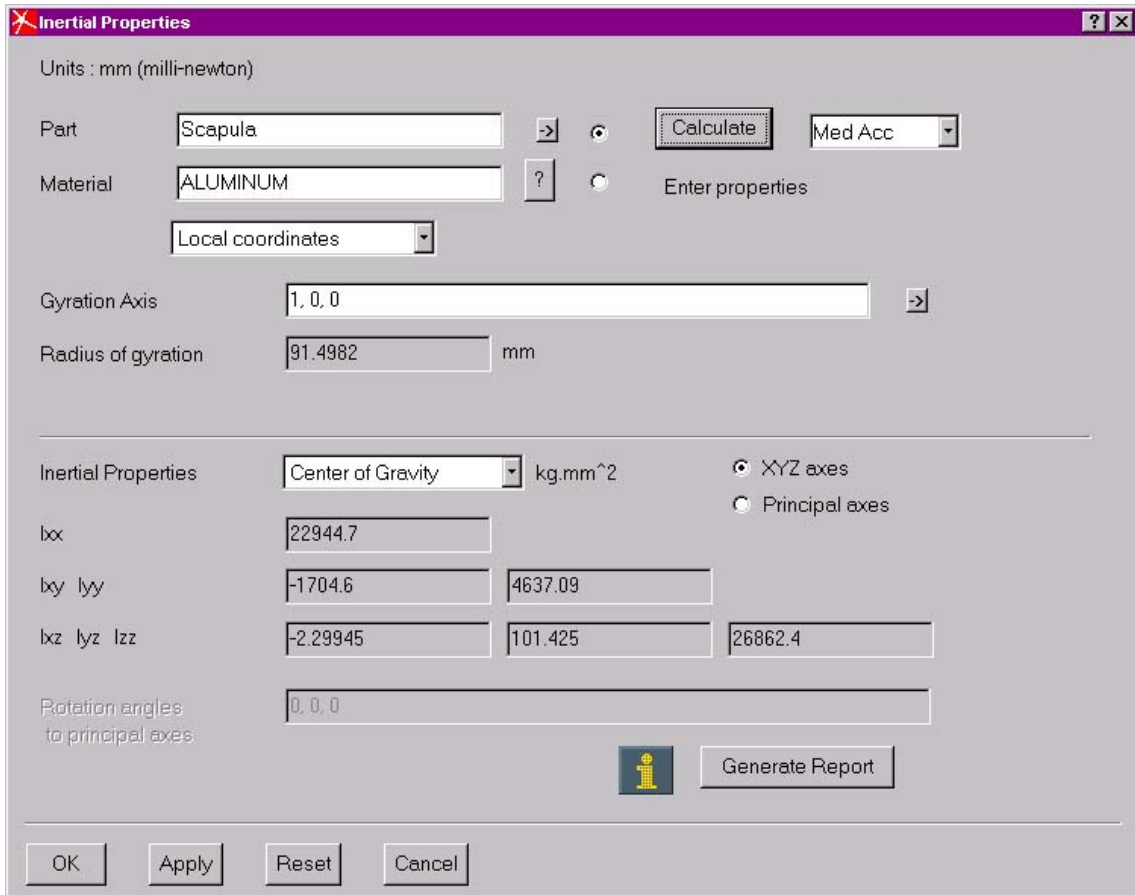


Figure 3-2: Inertia properties as displayed by I-DEAS.

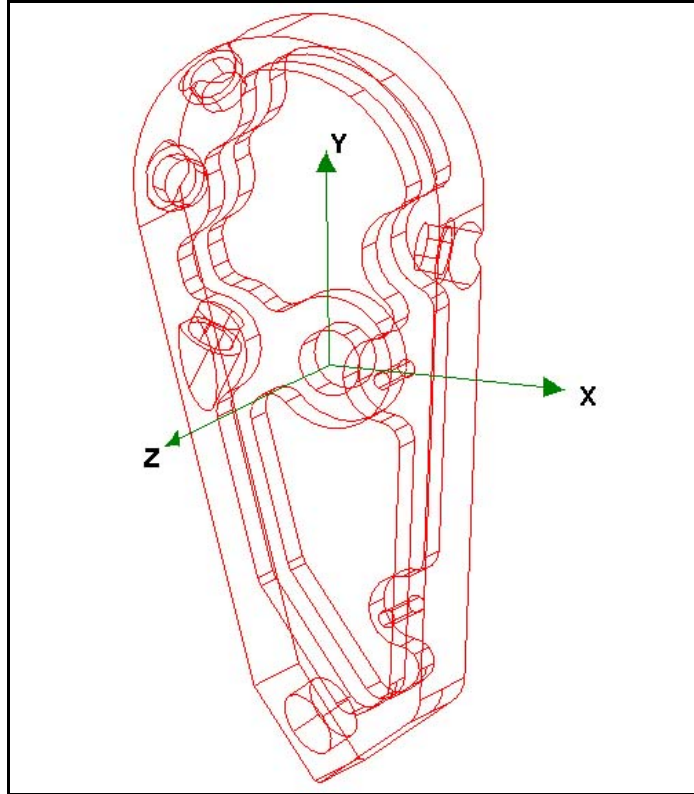


Figure 3-3: Orientation of xyz-triad to the scapula.

The actual masses of the different limb sections for a four-month old foal were not determined. It was decided that the actual mass of the limb was irrelevant for testing the rehabilitative device. The function of the load-bearing device is to follow the hoof of the foal and transfer load from the trunk of the horse to the ground by bypassing the limb. In addition, the device doesn't produce resistance against normal ambulation. Therefore, the position, velocity, and acceleration are of primary importance. Hence, the mass of the limb is irrelevant for testing the device. The resistance of the limb to the device is accomplished by the forces generated by the actuators. For this reason, a comparison of the mass properties of the robotic replica to the actual forelimb was not performed.

The mass of each component of the robotic forelimb, however, was kept to a minimum to reduce the required energy to replicate equine gait. Hollow cylinders were used to connect several of the joints together. Tubes offer the mechanical advantage of increasing the area moment of inertia while reducing the mass. Also, material was removed from machined parts where the material didn't provide a structural function. The reduction of mass was aided by the use of stress analysis through FEA to maintain the structural integrity while reducing the mass of each component. The process of reducing the mass while sustaining a structural integrity sufficient for supporting the required loads is an iterative process. The final finite element analysis is discussed later in this chapter.

3.2 Dynamics of Robot

The dynamics of the robot is the relationship of the motion of the limb with the forces acting on the limb. These forces can be internal and/or external forces. However, the analysis of the limb was broken down into several rigid bodies representing the individual limb sections. Therefore, the only forces applied to each limb segment were external forces generated by the hydraulic actuators and the joint connections. These external forces then resulted in internal stresses in the components in addition to the motion of the limb. These stresses were investigated to ensure that the robotic replica wouldn't fail during operation. Since the motion of the robot was specified, the forces were obtained through an inverse dynamic analysis. These forces formed the basis for the formulation of two control algorithms for reproducing the observed gait characteristics. The open-loop architecture relied on inputting the computed forces back into the equations of motion. In contrast, the closed-loop architecture superimposed corrective actuation on top of the computer forces based on a comparison between desired and observed motion of the replica.

Force calculations

To actuate the robotic replica, pressures are applied to the hydraulic actuators generating forces on the connection points of the hydraulic actuators thus generating torques about each joint. These forces determine the subsequent changes in angular motion of each of the limb segments. Since the angular positions, velocities, and accelerations of each limb section are known, the forces required to move the designed robotic replica have already been established. These forces must be calculated from the kinematics and the mass properties.

The process of finding the forces from the motion and mass properties of a system is commonly referred to as an inverse dynamic analysis. This inverse analysis was performed through the implementation of d'Alembert's principle of virtual work. For an explanation of d'Alembert's principle and how it's used to determine the forces applied to a system, *Mechanics Problems and their Solutions* by Dankowicz (1998) should be reviewed.

To execute d'Alembert's principle, a program was written in Maple 6 with an appending software package, Sophia Light, for multibody modeling developed by Harry Dankowicz. This code for the dynamic analysis can be seen in Appendix A. The code started by defining a list of rotation axes. In particular, the command

```
>DeclareRotationList([n,torso,1,evalf(Pi/12)], [n,o1,1,q3], [o1,o2,2,q4], [o2,a,3,q5], [n,b1,1,q6], [b1,b2,2,q8], [b2,b,3,q7], [n,c,3,q9], [n,d,3,q10], [n,e,3,q11], [n,f,3,q12]):
```

defines a list of body-fixed, right-handed, orthonormal coordinate systems associated with each of the limb segments and their relative rotations including all relevant degrees of freedom. Here, the first rotation, `[n,torso,1,evalf(Pi/12)]`, defines the constant orientation of the thorax relative to the ground through a rotation about the common x-axis. The orientation of the scapula relative to the ground is here decomposed into three subsequent rotations: an angle `q3` about the x-axis of the ground coordinate system, an angle `q4` about the y-axis of the intermediate `o1` coordinate system, and an angle `q5` about the z-axis of the intermediate `o2` coordinate system. (cf. Figure 3-3 above). For this work, the 'x' rotation was held constant to match the orientation of the thoracic plane. Therefore, with no rotation about the 'y' axis, the 'z' rotation was used as the angles of walk and trot. The subsequent rotations defined the orientations of the remaining limb segments relative to the ground.

The next stage of the code defines all of the constant parameters of the model, such as the coordinates of the position vectors from the joint centers to the centers of mass of each limb segment and to the actuator insertion and origin points, the segment masses, and the segment mass moments of inertia. First a matrix of all of the values was defined,

```
> ptable:=matrix(7,25,[[ -0.0296,-0.0422,0.0275, 0.0267,-0.1201,-0.0085, 0.0685,-  
0.1449,0.0065, -0.0425,-0.0726,-0.0024, -0.0522,-0.1765, 0.0329,-0.1899, -0.0016,-0.0252,  
0.0016,-0.0248, -0.0300,-0.1677, 0.0300,-0.1353, -0.0015],
```

Then these values were assigned to their appropriate names for later use in the code,

```
> eqs:={p1=ptable[1,1], p2=ptable[1,2], p3=ptable[1,3], p4=ptable[1,4], p5=ptable[1,5],  
p6=ptable[1,6], p7=ptable[1,7], p8=ptable[1,8], p9=ptable[1,9], p10=ptable[1,10],
```

With all of the constants of the limb defined, vectors describing the geometry of the robotic replica could be established. First, the position vector from the origin of the ground coordinate system to the proximal joint center of the thorax was defined.

```
> rN01:=CreateVector(q1,q2,0,n):
```

Here, it is implicitly assumed that the thorax is fixed in the x-y plane of the ground coordinate system. Subsequently, position vectors describing the location of the center of mass of each limb segment relative to its joint centers were defined.

```
> rA1A0:=subs(eqs,CreateVector(p1,p2,p3,a)):
```

Here, the second and fourth letters represent the label of the corresponding limb segment. These are specified in Figure 2-5 with the exception of the thorax which is labeled by 0. The numbers in the name refer to the point of reference; **0** is the center of mass, **1** is the proximal joint center, and **2** is the distal joint center. Each adjacent limb section share joint centers. Therefore, **B2** and **C1** are the same point. With each character defined, the name **rA1A0** refers to the vector from the proximal joint center of the scapula to the center of mass of the scapula as shown in Figure 3-4.

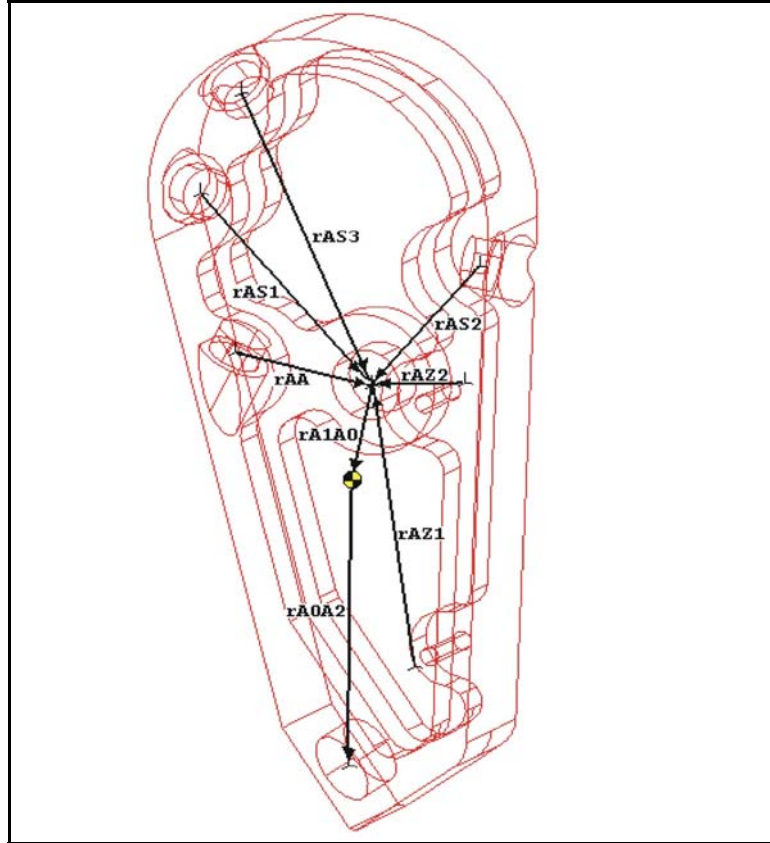


Figure 3-4: Vectors relative to the scapula.

The next phase of the vector definition command defined the insertion and origin points of all of the hydraulic actuators. The notation for these vector definitions first noted the limb section that the vector was to be related to. Next, the actuator insertion/origin point was specified for the particular actuator. All vectors for the insertion and origin points of the actuators go to the proximal joint center of the limb section. Therefore, the name `rAS1` refers to the vector from the insertion point of the caudal-dorsal scapula actuator to the proximal joint of the scapula shown in Figure 3-4 above.

```
> rAS1:=subs(eqs,CreateVector(p38,p39,p40,a)):
```

With the previous vectors defined, vectors relating the centers of mass of each limb section to the Newtonian reference frame were then established. These vectors were accomplished by adding and subtracting the previously established vectors to each other until the desired vector was constructed. For example, the center of mass of the thorax can be established by going from the Newtonian frame to the proximal joint of the thorax, `rNO1`, and then going from the proximal joint to the center of mass of the thorax, `rO100`.

```
> rNO0:=rNO1 &++ rO100:
```

Additionally, vectors defining the actuators were created in a similar manner.

```
> ro1:=rAS1 &-- rO002 &-- rO100 &-- rOS1:
```

The vector r_{o1} defines the path between the insertion point and the origin of the caudal-dorsal scapula actuator. Using the previously defined vectors, whose magnitude remains constant but orientation changes throughout gait, the vector of the actuator can be define as shown in Figure 3-5 dependent only on the previously established variables, $q_1, q_2, q_3, q_4, q_5, q_6, q_7, q_8, q_9, q_{10}, q_{11}, q_{12}$.

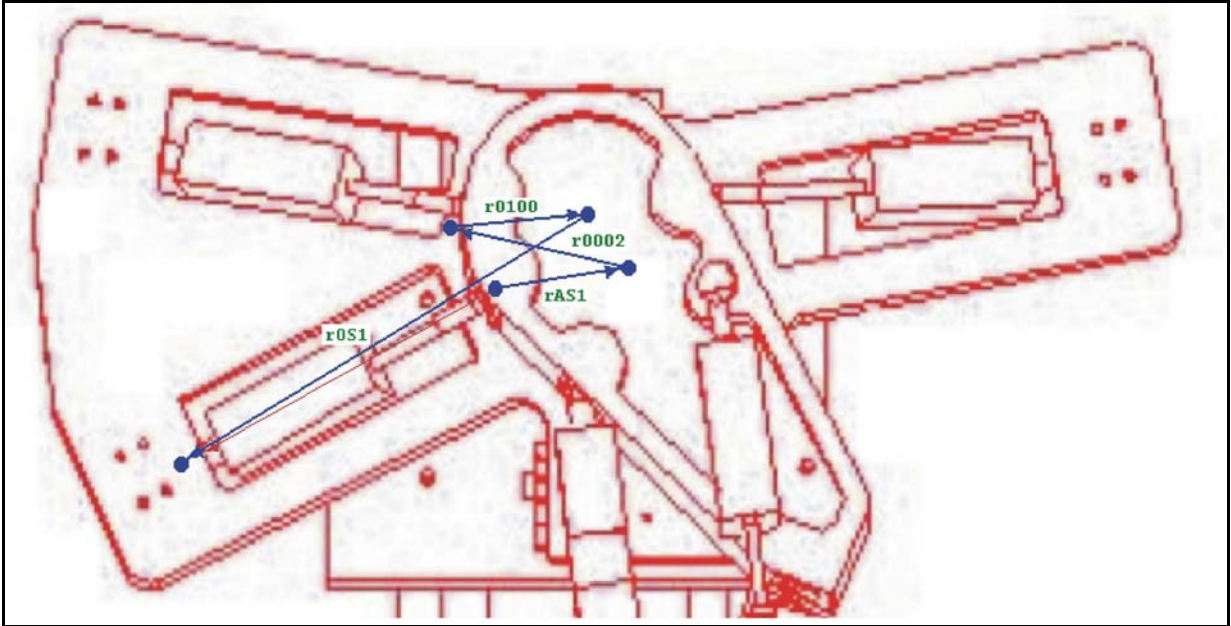


Figure 3-5: Vector defining the caudal-dorsal scapula actuator.

With all of the descriptive vectors of the robotic replica defined, motion of the replica was established. First, all time-dependent configuration coordinates and independent velocity coordinates were declared.

```
> DependsTime (seq (cat (q, i), i=1..12), seq (cat (u, i), i=1..12)) :
```

Next, the velocities of the centers of mass were computed by taking the time derivative of the position vectors of each center of mass relative to the Newtonian reference frame.

```
> v00:=DiffTime (rNO0, n) :
```

Using the time dependent variables, the kinematic differential equations of the system were identified.

```
>kde:={q1t=u1, q2t=u2, q3t=u3, q4t=u4, q5t=u5, q6t=u6, q7t=u7, q8t=u8, q9t=u9, q10t=u10, q11t=u11, q12t=u12} :
```

The use of d'Alembert's principle requires the time derivative of the momentum. Therefore, the masses and mass moment of inertias are required in addition to the velocities. The mass moment of inertias of each limb section were calculated relative to the coordinate system defined in the *Mass Properties* section of this chapter.

```
>mass:=subs (eqs, LiftDescription (mA &**  
UnitDyad (n), CreateDyad (IA11, IA12, IA13, IA21, IA22, IA23, IA31, IA32, IA33), a)
```

With both a mass matrix and the velocities the momentum and the time derivative of momentum can be derived respectively.

```
> p:=Transpose(vel) &o mass:
> pt:=subs(kde,DiffTime(p,n)):
```

Next, a collection of allowable kinematic directions of motion was extracted from the velocity description of the mechanism (see Dankowicz, 1998).

```
> beta:=BetaExtract(vel, [u1,u2,u3,u4,u5,u6,u7,u8,u9,u10,u11,u12]):
```

To calculate the applied forces to be used in the equation of virtual work, the actuator vectors were normalized,

```
> Norms := (Ero1 = EuclideanNorm(ro1),
```

such that dividing the actuator vectors by the normalized vectors would produce unit directional vectors that could be multiplied by the actuation forces acting on each body.

```
(F01/Ero1) &** (ro1)
```

When applying the forces to each limb section, the force resulting from gravity was first applied. Next, all actuator forces were defined as positive when the actuator attempts to contract—pull on the rigid body. Finally, the ground reaction force was applied to the fetlock. These forces make up all of the applied forces. The ensuing free-body-diagrams contain only applied forces since the virtual work equation is independent of the constraint—joint reaction—forces and follow as Figures 3-6 through 3-8.

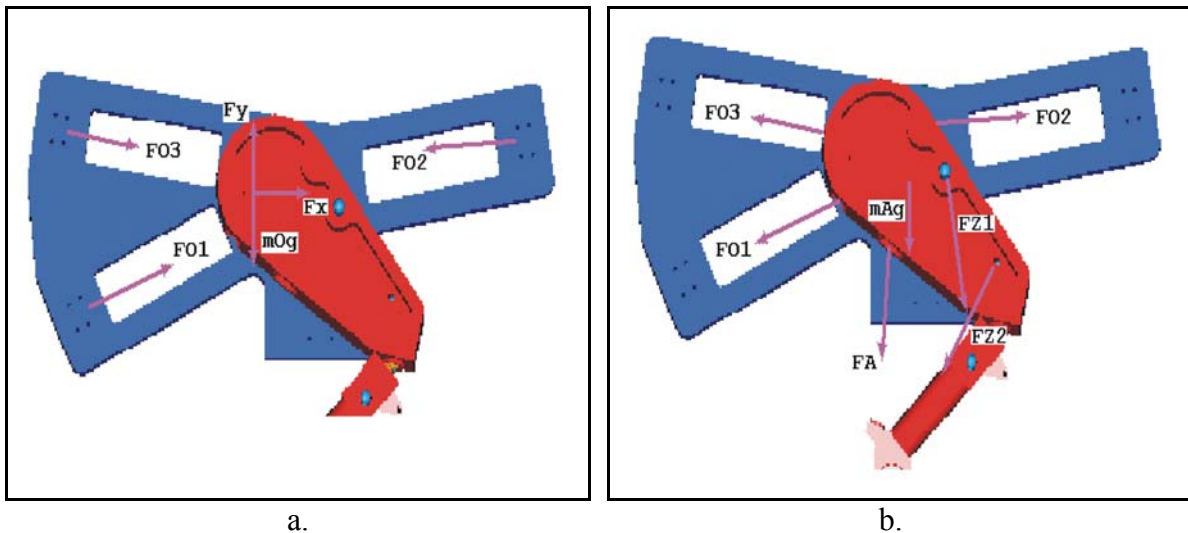


Figure 3-6: Free-body-diagram.
a. Thorax, b. Scapula.

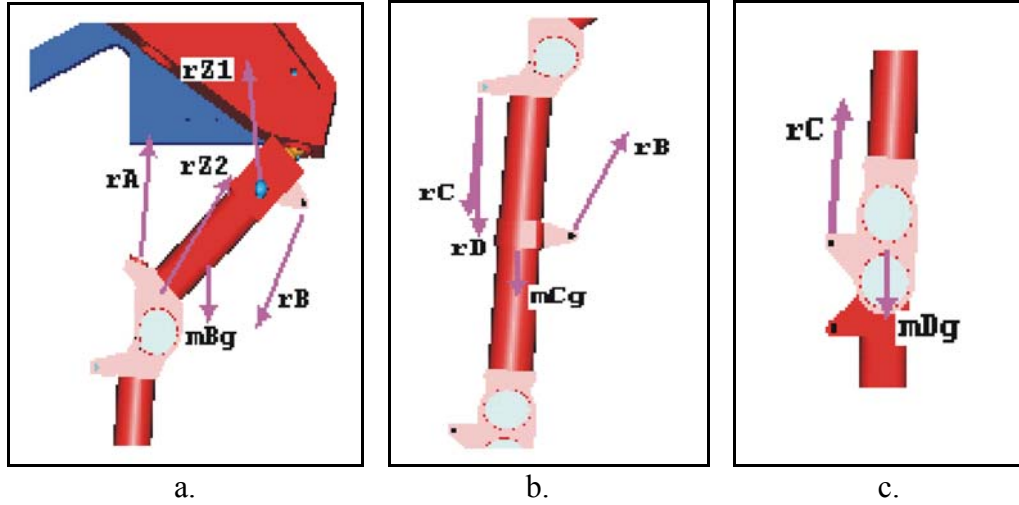


Figure 3-7: Free-body-diagram.
a. Humerus, b. Radius, c. Carpus.

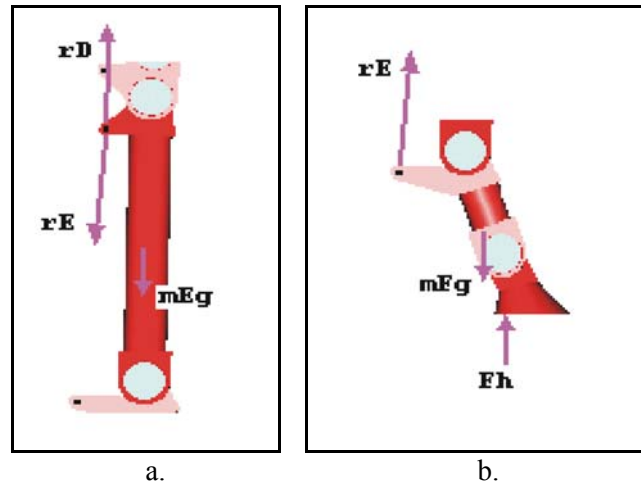


Figure 3-8: Free-body-diagram.
a. Metacarpal, b. Fetlock.

The description of the forces and moments of each limb section was then executed. Forces acting on each rigid body were then translated to the center of mass and torques applied to compensate for the relocation of these forces, as demonstrated in Figure 4-9. Therefore, as an example, the total forcing on scapula would be the vector,

```
> force:=subs(Norms union eqs,CotangentDescription(
CreateVector(0,-mA*g,0,n) &+ ((FO1/Ero1) &** (ro1)) &+ ((FO2/Ero2) &** (ro2)) &+
((FO3/Ero3) &** (ro3)) &- ((FA/Era) &** (ra)) &- ((FZ1/Erz1) &** (rz1)) &- ((FZ2/Erz2) &**
(rz2)), (((FO1/Ero1) &** (ro1)) &xx (rAS1 &+ rA1A0)) &+ (((FO2/Ero2) &** (ro2)) &xx (rAS2
&+ rA1A0)) &+ (((FO3/Ero3) &** (ro3)) &xx (rAS3 &+ rA1A0)) &- ((FA/Era) &** (ra)) &xx
(rAA &+ rA1A0)) &- ((FZ1/Erz1) &** (rz1)) &xx (rAZ1 &+ rA1A0)) &- ((FZ2/Erz2) &**
(rz2)) &xx (rAZ2 &+ rA1A0)),
```

The vector for the total ‘force’ includes both forces and moments about the center of mass resulting from those forces. Careful consideration was taken to ensure that all of the actuator

forces were positive when pulling on each rigid body and that the moments were defined as positive counter-clockwise.

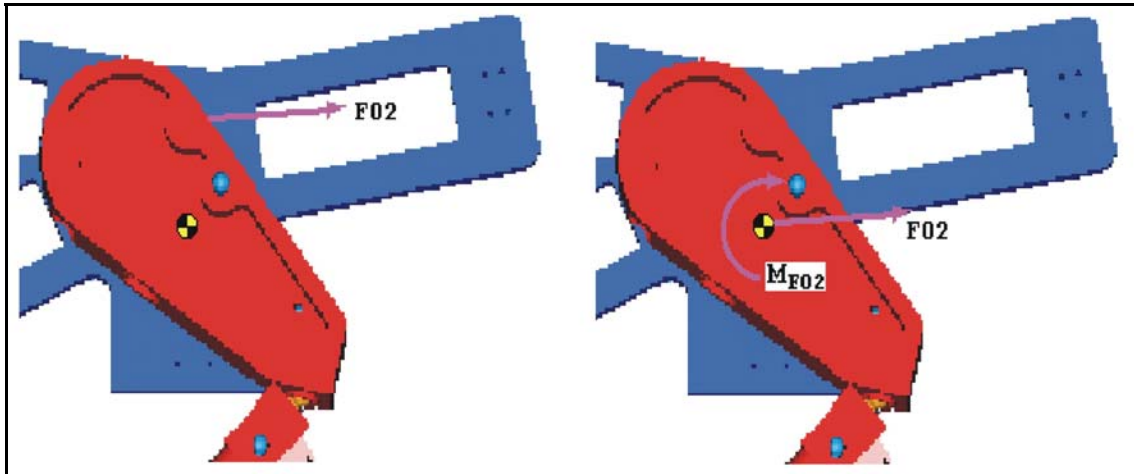


Figure 3-9: Relocation of an actuator force to the center of mass.

With all of the parameters necessary to execute d'Alembert's principle of virtual work, the equation was written for use in performing the inverse dynamics.

```
> eq:=(force &-- pt) &o beta:
> eq:=convert(eq,set):
```

Finally, a matrix of the values of the variables throughout stride was created. Each row defines the positions (q), velocities (u), and accelerations (udots) of each degree of freedom, and the vertical ground reaction force. The rows represent different time steps. For this calculation, the stride was broken down into one hundred steps—a data point at every one percent of stride.

```
> valtable:=matrix(101,37,[0.0,0.0000,-0.2618,0.0,0.6629,0.0,-
0.2966,0.0,0.6280,0.5321,0.4361,0.6803,0.0,0.078,0.0,0.0,0.611,0.0,0.166,0.0,-2.878,-1.443,-
0.008,3.214,0.0,26.49,0.0,0.0,-23.29,0.0,-73.02,0.0,-39.94,-55.02,-70.01,-56.94,0.0],
```

The last step of the code performs the inverse dynamics on the equations by evaluating the replica at each described orientation and calculating the unknown forces—twelve degrees of freedom and twelve unknown forces.

```
> inversedynamics:=proc(eq)
for i from 1 to 101 do
equs:=evalf(subs(q1=valtable[i,1], q2=valtable[i,2], q3=valtable[i,3], q4=valtable[i,4],
q5=valtable[i,5], q6=valtable[i,6], q7=valtable[i,7], q8=valtable[i,8], q9=valtable[i,9],
q10=valtable[i,10], q11=valtable[i,11], q12=valtable[i,12], u1=valtable[i,13],
u2=valtable[i,14], u3=valtable[i,15], u4=valtable[i,16], u5=valtable[i,17],
u6=valtable[i,18], u7=valtable[i,19], u8=valtable[i,20], u9=valtable[i,21],
u10=valtable[i,22], u11=valtable[i,23], u12=valtable[i,24], u1t=valtable[i,25],
u2t=valtable[i,26], u3t=valtable[i,27], u4t=valtable[i,28], u5t=valtable[i,29],
u6t=valtable[i,30], u7t=valtable[i,31], u8t=valtable[i,32], u9t=valtable[i,33],
u10t=valtable[i,34], u11t=valtable[i,35], u12t=valtable[i,36], Fh=valtable[i,37], FG=0,
FH=0,eq)):
forcevals:=subs(fsolve(equs,{Fx,Fy,FO1,FO2,FO3,FA,FZ1,FZ2,FB,FC,FD,FE})
```

Once the forces were derived for the desired motion they were transferred to a spreadsheet for examination. These forces are reported and discussed later in Chapter 4. From the force examination it was determined if the positioning of the origin and insertion points of the actuators was appropriate. These actuation points were adjusted to minimize the required forces while maintaining the desired range of motion and the anatomical likeness of a foal. However, with these modifications the geometry and mass properties had to be recalculated. Also, it was necessary to repeat the inverse-dynamic analysis to obtain the new actuation forces. This iterative design process is shown through a block diagram in Figure 3-10.

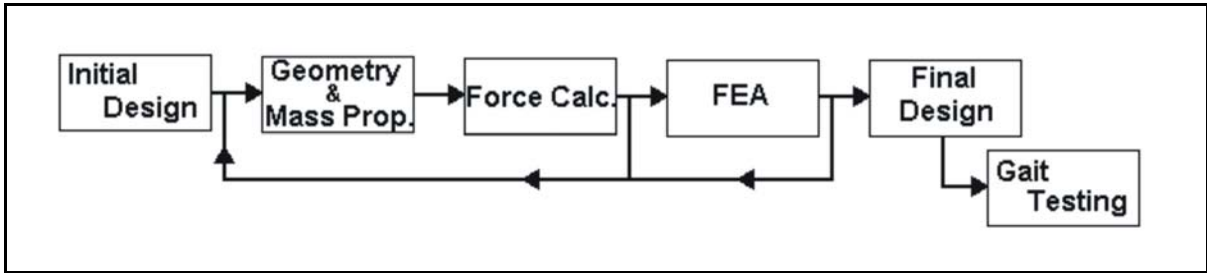


Figure 3-10: Block diagram of design process.

Finite Element Analysis

With the required actuator forces established, a finite element analysis had to be performed to ensure that the design of the robot was sufficient to carry the required load. In addition, it was desirable to minimize the weight of the robotic replica. Therefore, the analysis also ensured that the design wasn't unnecessarily robust.

To perform the FEA, the CAD models were first simplified to reduce the number of elements. This simplification involved removing radii between surfaces. A small radius between two surfaces requires a large number of elements to model in the FEA program. The absence of the radius will increase the actual stress in the localized area of that radius. Therefore, the removal of these radii is justified. Also, the bearings, bearing-shafts, and joint-shafts were incorporated into the limb component. Incorporating the bearings and shafts eliminates the necessity of contact elements in the model and doesn't reduce the accuracy of the analysis for this situation. Finally, mounting holes were removed where bolts were to be affixed in order to maintain a relatively low number of elements.

The models were imported into an FEA program called ANSYS. The program ANSYS was chosen due to its availability. However, difficulty was encountered transferring models between IDEAS and ANSYS. The method of transferring a model between the two programs was through the use of an IGES file. An IGES file is used to transfer digital information of a 2D or 3D model between different programs in a neutral data format. Generally, each CAD company includes a translator to export a model into an IGES file that can then be imported into another program through their translator. However, the 'flavor' of the IGES file exported by IDEAS is of a more sophisticated level than ANSYS is capable of interpreting. Therefore, after the file had been imported into ANSYS, extensive surface operations were necessary to prepare the model for *meshing*. During this preparation, further simplification of the model was required to closely remodel the components of the robotic limb in the FEA program. Due to the low stress levels at these locations, seen in the results (Chapter 4), the model was deemed acceptable for the purpose of stress analysis.

The next stage in the process is to define the material properties of the model. Due to the strength and mass characteristics and availability, the aluminum parts were specified to be constructed from aluminum 6061-T6. This material has a yield strength of approximately 275 MPa. The steel components were designed out of a stainless steel to prevent corrosion. In addition, the series 304 was used. The material has been specified to be annealed at 1950°F, water quenched, and 2% cold drawn. This material has been tested to a yield strength of about 510 MPa.

With the preprocessing phase of the FEA completed, the forces and constraints were applied to the models. Since the ground reaction force was known and the actuator forces were solved for, the joint reaction forces needed to be calculated. The joint reaction forces were determined for the position of the leg which experienced the highest forces. These forces were applied to the distal end of each limb section. The actuator forces were then applied to the appropriate connection points. Finally, the proximal end of each section was constrained in space to allow for a static analysis of the components. Additional forces were applied to the proximal end of the metacarpal, carpus, and distal end of the radius. These forces represent the implantation of the stay apparatus. First, the peak forces of the radius-metacarpal and radius-carpus actuators were established for the duration that the carpus is in full extension. The moments about the joints were then calculated for static equilibrium with the forces revealed through the inverse dynamics. However, with the reduced actuation forces, the moments about the joints were maintained through the addition of forces in the stops of the carpus as shown in Figure 3-11. These forces were calculated based on the previously determined forces and moments and the appropriate moment arms.

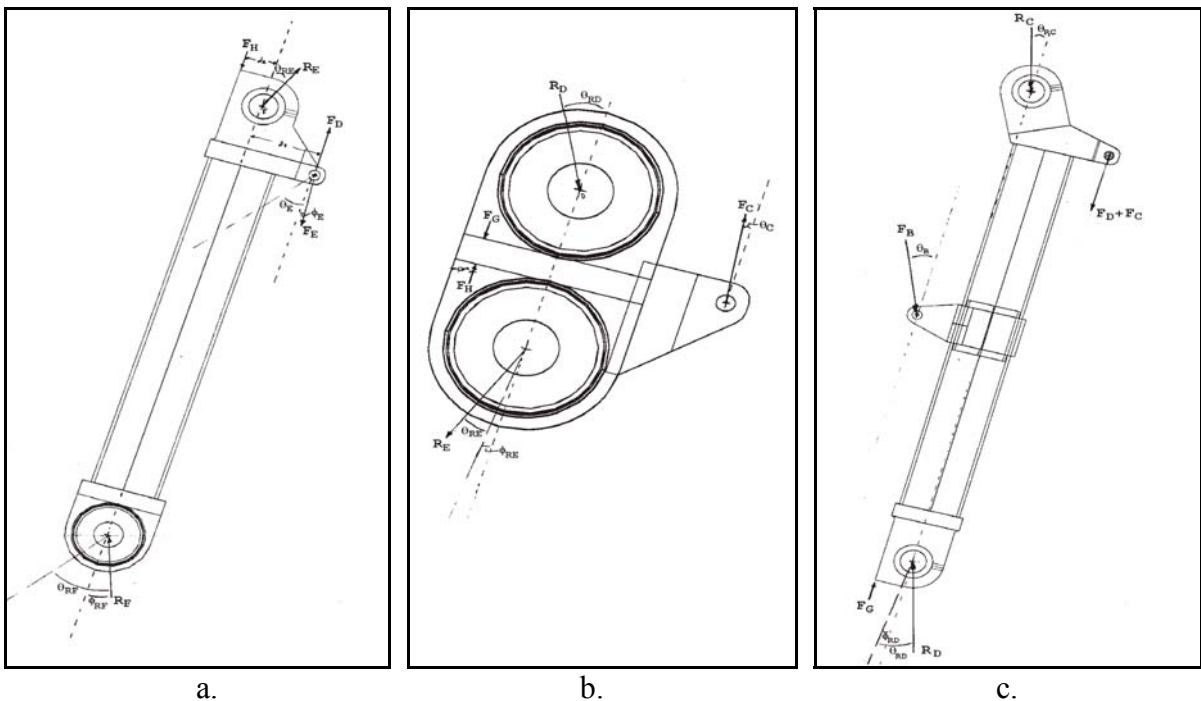


Figure 3-11: Free-body diagrams for FEA.
a. Metecarpal, b. Carpus, c. Radius.

The forces developed through the stay apparatus were only utilized in the stress analysis. Since the moments about the joints remained unchanged, the carpal stops were not

included in the forward dynamic analysis discussed in a later section. Instead, this analysis used the forces calculated in the inverse-dynamical analysis.

With the forces applied to each model, the solver was then initiated and the stresses calculated. Finally, these stresses were investigated through the postprocessor. If the stresses were above the yield point of the selected material, the model was redesigned to reduce the stress in the localized areas. However, if the stress was negligible, material was removed from particular parts of the robot if possible.

Iterating through the different steps as shown in Figure 3-10, the final structural design of the robotic replica was arrived at. This design and accompanying assembly instructions are shown in detailed in Chapter 5.

3.3 Control System of Robot

With the limb completed, the replica next needed to be theoretically tested. Ideally, the forces calculated through the inverse-dynamical analysis should produce precisely the same motion when fed back into the equations of motions as the motion used to derive the forces. However, due to the method of interpolating between the points as discussed in Chapter 2, error will be introduced into the model. In addition to this error, the sensitivity of the replica will influence how controllable it is. Therefore, it may not be possible to control the robotic replica with an open-loop control algorithm. Thus, the response of the system to both an open-loop and a closed-loop control algorithm were investigated.

Open Loop Control

The first control method investigated was open-loop control. Open-loop control is the simplest method of control. This method involves applying an input to the system and obtaining an output. The input in this situation is independent of the output as shown in Figure 3-11. Since the information simply feeds through a straight line it is referred to as an ‘open-loop’ system. Since there is no communication between the input and output, there can be no compensation for errors between the desired output and the actual output. These errors can grow unchecked until the model collapses. For an in depth discussion on control systems, review Dorf and Bishop (2001).

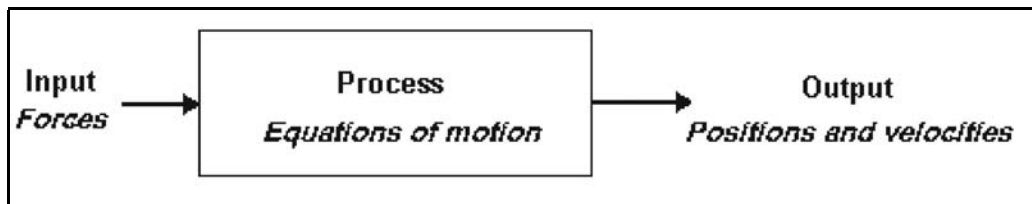


Figure 3-12: Block diagram of an open-loop control system.

To develop our control system, the equations of motion were exported from the Maple file discussed earlier to a C file using ExMex—a program developed at the Royal Institute of Technology in Stockholm, Sweden. Additionally, C code was written to determine the actuation forces at all times, Appendix A. This required interpolating between the one hundred data point for each force produced by the cubic spline fit of the position data as discussed in Chapter 2.

```
f2_open=(para[i+358]*(t-para[i-1+156])+para[i-1+358]*(para[i+156]-t))/(para[i+156]-para[i-1+156]);
```

Here, the parameters (in the vector para) are defined in the exported code of the equations of motion—para[i+358] refers to the actuation forces while para[i+156] is the time.

Finally, a matlab code was written to simulate the open-loop controlled motion. First, a list of the values of all of the parameters was established

```
% VALUES FOR PARAMETER LIST
P = [-0.0296,-0.0422, 0.0275, 0.0267,-0.1201,-0.0085, 0.0685,-0.1449, 0.0065,-0.0425,...
A = [5.507, 0.04093, 0.00660, 0.00122, 0.00660, 0.02248,-0.00271, 0.00122,-0.00271, 0.05916];
B = [3.026, 0.01654,-0.00619,-0.00024,-0.00619, 0.00922, 0.00033,-0.00024, 0.00033, 0.02478];
C = [3.686, 0.03956, 0.00065,-0.00016, 0.00065, 0.00275, 0.00007,-0.00016, 0.00007, 0.03983];
D = [0.617, 0.00057, 0.00000, 0.00002, 0.00000, 0.00030, 0.00000, 0.00002, 0.00000, 0.00055];
E = [2.666, 0.02266,-0.00009, 0.00001,-0.00009, 0.00153, 0.00003, 0.00001, 0.00003, 0.02352];
F = [0.882, 0.00207,-0.00033, 0.00000,-0.00033, 0.00054, 0.00000, 0.00000, 0.00000, 0.00206];
O = [3.000, 0.03000, 0.03000, 0.03000];
G = 9.81;
```

where ‘P’ is the section of the maple code ptable that describes the vectors of each limb section. A, B, C, D, E, and F refer to the mass properties of the limb section as described in Figure 2-5. The vector O is the mass properties of the thorax. The value of gravity was then defined using the standard notation of G. It should be noted that all of the values are in the metric system using meters, kilograms, and seconds.

The time variable was introduced as the vector

```
for tj=1:101
    T(1,tj) = 0+(tj-1)*(0.67/100);
end
```

to be used in the parameter list for each specified orientation of gait.

Next, the forces at an interval of one percent of stride calculated from the inverse dynamics were loaded into the program

```
load Ft_t.txt Ft = Ft_t'; load Fh_t.txt Fh = Fh_t'; Ft=[Ft;Fh];
```

With all of the values of the parameters defined, the values were arranged in to a vector corresponding to the vector generated for the equations of motion.

```
% positions
parameters(1:91,1) = P(1,:);
% mass and inertia properties
parameters(92:101,1)=A(1,:); parameters(102:111,1)=B(1,:); parameters(112:121,1)=C(1,:);
parameters(122:131,1)=D(1,:); parameters(132:141,1)=E(1,:); parameters(142:151,1)=F(1,:);
parameters(152:155,1)=O(1,:);
% gravity
parameters(156,1) = G;
% time
parameters(157:257,1) = T(1,:);
% forces
for k=1:13
    parameters(258+(k-1)*101:358+(k-1)*101,1) = Ft(k,:);
end
```

Next, the initial conditions of the limb were defined for position and velocity of each limb section respectively for the desired starting point in the stride.

```
% INITIAL CONDITIONS AT 0% OF STRIDE
theta_i = [0,0.0750,-0.2618,0,0.6629,0,-0.3402,0,0.5321,0.4797,0.4274,0.8286];
omega_i = [0,-0.483,0,0,0.994,0,-0.314,0,-3.285,-2.361,-1.439,4.115];
IC = [theta_i,omega_i];
```

Finally, the time of investigation was defined and the differential equations of motion solved for.

```
% TIME
Ti = 0; Tf = .67;
% GAIT
[Time,QU] = ode45('equine_eq_forelimb_v5',[Ti:.01:Tf],IC,options,parameters);
```

With the code written for running the open-loop control system, a simulation of the motion could be attempted at various times during gait. This motion could then be compared to the desired gait to determine the adequacy of the open-loop system. With the open-loop system tested, the process next moved to the closed-loop control system.

Closed Loop Control

Conversely to the open-loop system, the closed loop system does not feed the input straight through to the output. A closed-loop system is characterized by a feedback signal returning to the input side of the system as shown in Figure 3-12. This returning signal is a measurement of the outputs. The measurement is first sent through an amplifier, after which the signal is combined with the input. This allows the system to correct for any outside disturbances or unforeseen errors. Hence, a closed-loop increases the controllability of a system.

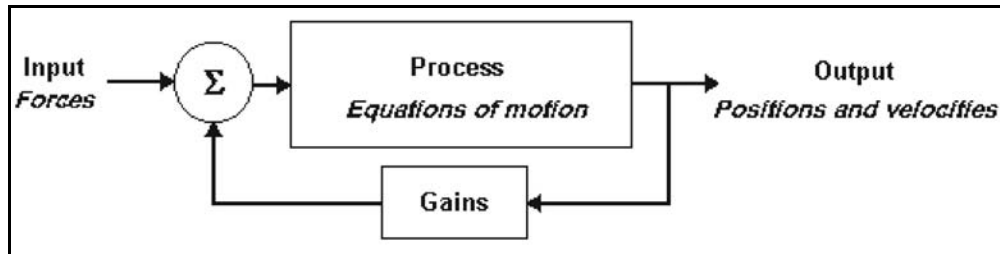


Figure 3-13: Block diagram of a closed-loop control system.

Since, the closed-loop control considers the outputs as inputs to the system, the outputs that are to be fed back to the inputs must be defined. The inputs to the equations of motion are forces. Therefore, the total forces supplied to the system are the sum of the open-loop forces and the closed-loop forces. The closed-loop forces were determined using proportional and derivate control.

The proportional control was achieved by monitoring the squares of the lengths of the actuator cylinders and comparing them to the desired squares of the lengths. The equations defining the squares of the lengths of the actuators were determined in maple, `EuclideanNorm(ra)^2`. The position of the limb was then input into the equation to determine the current magnitude of the squares of the lengths. Next, the desired values of the squares of the lengths were calculated.

```
>for i from 1 to 101 do
lengths:=evalf(subs(q1=valtable[i,1], q2=valtable[i,2], q3=valtable[i,3], q4=valtable[i,4],
q5=valtable[i,5], q6=valtable[i,6], q7=valtable[i,7], q8=valtable[i,8], q9=valtable[i,9],
q10=valtable[i,10], q11=valtable[i,11], q12=valtable[i,12], [q1, q2, EuclideanNorm(ro1)^2,
EuclideanNorm(ro2)^2, EuclideanNorm(ro3)^2, EuclideanNorm(ra)^2,...]));
od:
```

With the desired and actual value of the squares of the lengths determined for a particular instance in time, the difference could be calculated. The differences of the lengths were then multiplied by gains to yield the proportional part of the closed-loop forces.

```
f12_close=para[2793]*(pow((para[i+2681]*(t-para[i-1+156])+para[i-1+2681]*(para[i+156]-t))^(para[i+156]-para[i-1+156]),2)-E);
```

Next, the derivative control was achieved through the use of the change of the square of the length as a function of time. Since the equations of motions output the velocities in addition to the positions, it was possible to relate the outputs to the desired outputs for both the lengths and the velocities. Again, using maple the equations of the squares was obtained,

```
subs(GlobalImplicit,kde,diff(subs(GlobalExplicit,EuclideanNorm(ra)^2),t));
```

Subsequently, the desired values of the change in the squares of the length as a function of time were calculated to compare with the actual values.

```
>for i from 1 to 101 do
dlengths:=evalf(subs(seq(cat(q,j)=valtable[i,j],j=1..12),seq(cat(u,j)=valtable[i,12+j],j=1..12),[subs(GlobalImplicit,kde,diff(subs(GlobalExplicit,q1),t)),subs(GlobalImplicit,kde,diff(subs(GlobalExplicit,q2),t)),subs(GlobalImplicit,kde,diff(subs(GlobalExplicit,EuclideanNorm(ro1)^2),t)),subs(GlobalImplicit,kde,diff(subs(GlobalExplicit,EuclideanNorm(ro2)^2),t)),subs(GlobalImplicit,kde,diff(subs(GlobalExplicit,EuclideanNorm(ro3)^2),t)),subs(GlobalImplicit,kde,diff(subs(GlobalExplicit,EuclideanNorm(ra)^2),t)),subs(GlobalImplicit,kde,diff(subs(GlobalExplicit,EuclideanNorm(rz1)^2),t)),subs(GlobalImplicit,kde,diff(subs(GlobalExplicit,EuclideanNorm(rz2)^2),t)),subs(GlobalImplicit,kde,diff(subs(GlobalExplicit,EuclideanNorm(rb)^2),t)),subs(GlobalImplicit,kde,diff(subs(GlobalExplicit,EuclideanNorm(rc)^2),t)),subs(GlobalImplicit,kde,diff(subs(GlobalExplicit,EuclideanNorm(rd)^2),t)),subs(GlobalImplicit,kde,diff(subs(GlobalExplicit,EuclideanNorm(re)^2),t)))]));
od:
```

Similar to the proportional control, the differences of the actual velocities and the desired velocities were multiplied by gains to obtain the derivative portion of the closed-loop forces.

```
f12_close_d=para[2805]*((para[i+3816]*(t-para[i-1+156])+para[i-1+3816]*(para[i+156]-t))^(para[i+156]-para[i-1+156]))-dE);
```

Both the proportional closed-loop forces and the derivative closed-loop forces were combined to achieve the total closed-loop forces. The sum of the closed-loop forces was combined with the open-loop force, `return (f2_open + f2_close + f2_close_d);`, to yield the actuator force required to generate the desired gait.

The Matlab code introduces the desired squares of the lengths and velocities in addition to the gains for the proportional and derivative control,

```
load length_t.txt lengths = length_t'; load dlength_t.txt dlength = dlength_t';
K=[k1,k2,k3,k4,k5,k6,k7,k8,k9,k10,k11,k12,dk1,dk2,dk3,dk4,dk5,dk6,dk7,dk8,dk9,dk10,dk11,dk12];

% lengths of cylinders
for k=1:12
parameters(1571+(k-1)*101:1671+(k-1)*101,1) = lengths(k,:);
end
```

```
% gains
parameters(2783:2806,1) = K(1,:);
% derivatives of lengths
for k=1:11
    parameters(2807+(k-1)*101:2907+(k-1)*101,1) = dlength(k,:);
end
```

Using the code developed for the open-loop control and the closed-loop additions the closed-loop system was ready for simulation (cf. Appendix A). The feedback gains were manually adjusted to determine their optimal values for accurately reproducing the limb kinematics while using forces that are close to the open-loop control forces computed in the inverse-dynamical analysis. The code could then be executed numerous times while adjusting the gains to determine the optimal gains. The final gains should yield similar positions of the limb segments as the collected data while using forces that oscillate closely around the open-loop control forces. From this analysis, the feasibility of the robotic replica could be validated.

4 Results and Discussion

The completed design of the robotic replica of a foal's forelimb was modeled in I-DEAS' SDRC 8m2 computer aided design (CAD) program. This three-dimensional model of the robotic replica is structurally strong enough to produce the forces required for trot. The structure integrity of the replica was proven through the use of Finite Element Analysis (FEA) discussed later in this Chapter. First, the forces required by the actuators for the desired gait were determined using an inverse dynamics approach. These forces were determined to be within the limits of hydraulic actuators that can fit in the restricted space of the replica. Then, the FEA program, ANSYS, was utilized to determine the resulting stresses due to the actuator forces. With the predicted stresses below the yield limit of the materials used, the analysis of the replica progressed to the forward dynamics.

The forward dynamic analysis of the robotic replica demonstrated that it was not possible to replicate the desired gait with an open-loop control algorithm. However, utilizing a proportional derivative (PD) controller, the robotic replica is capable of replicating the desired motions with reasonable actuator forces. Therefore, the designed robotic replica is sufficient for the purpose of testing the proposed rehabilitative, load-bearing device.

4.1 Structural Design

Several simplifications of the foal's forelimb were made throughout the design process in order to properly model the limb within a realistic space. First, the fetlock region was simplified to use only two joints of rotation in a sagittal plane. The pastern joint was absorbed into the fetlock joint while the coffin joint remained to allow for compliance with the ground plane. This absorption was possible due to the direction of rotation of the two proximal joints during gait. Both the fetlock and the pastern joint rotate in the same direction during stance.

The second simplification came with the design of the carpus. As discussed in Chapter 1, the carpal joint was reduced to two hinge joints. Due to position of the radius relative to the metacarpal when the forelimb was extended and flexed it was possible to reduce the region of the eight carpal bones to two joints.

Finally, the scapula was simplified from the floating joint to a series of rigid joints. Instead of floating over the curved surface of the ribs, the replica's scapula slides on a flat plane that closely represents the surface of the ribs. In addition to these two degrees of freedom, a ball joint was used to add three more degrees of freedom. However, the seventh degree of freedom, displacement perpendicular to the thorax, was completely removed from the model due to the lack of relative motion in that direction.

The remaining joints experienced very little simplification. The elbow joint was modeled using a single hinge joint that allowed for the required motion. Also the shoulder joint is capable of all of the natural degrees of freedom. The motion of the shoulder in the replica is generated through a ball joint. This joint not only allows for protraction, retraction, abduction, and adduction, but also allows for the natural rotation about the longitudinal axis of the humerus.

Mass and Geometry of Robotic Replica

The final design of the robotic closely resembles the anatomical model of the foal's forelimb. This can be noted in Figure 4-1. The dimensions of the replica were selected directly from actual foals. Hence, the height of the limb and locations of the joints are similar. In addition, the structural members were kept to a minimum size, therefore, allowing the overall size of the limb to remain close to the anatomical version. In addition to the size and geometry of the replica, the final design of the robotic replica makes it possible to actuate the robotic limb through the range of motion discussed in Chapter 2. With this closeness of the robotic replica to a foal's forelimb, testing and optimization of the rehabilitative load-bearing device will be possible and realistic.

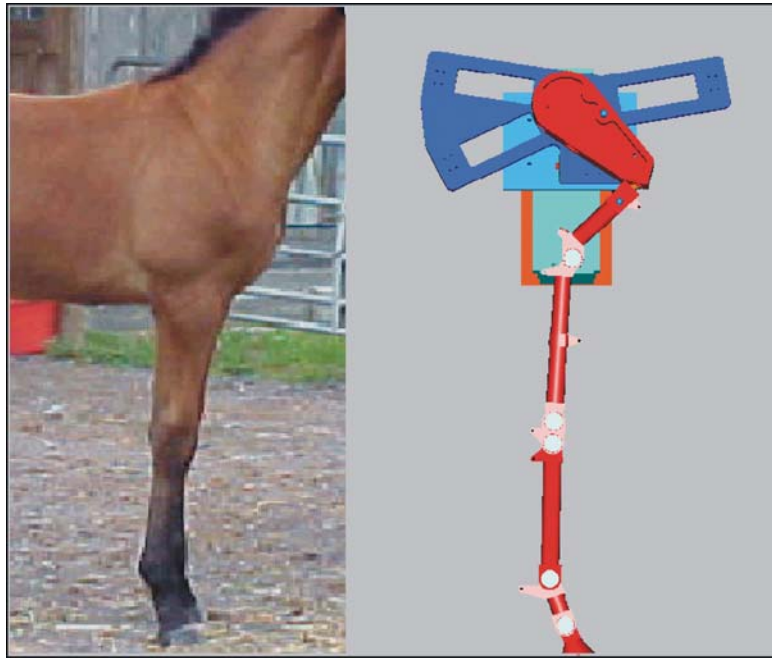


Figure 4-1: Side view of replica and side view of foal's forelimb.

The material used in the replica is primarily aluminum and steel. Given the similarities in the structural size of the replica to the foal's limb, it is logical to assume that the mass of the replica will be greater. Nevertheless, this assumption is irrelevant. As stated in Chapter 3, the position, velocity, and acceleration are of primary importance. Hence, the mass of the limb is irrelevant for testing the load-bearing device. However, the mass of each component was recorded for use in the actuator force calculation. The masses used were determined through the CAD software and estimations of the hydraulic actuators. The CAD software gave accurate masses of the designed section. However, due to the variability in manufacture of the hydraulic cylinders, the total mass of each section is uncertain. Nonetheless, the masses used for the replica are as follows: The mass of the scapula and associated actuators was estimated at 5.5 kilograms. The humerus and associated actuator mass was 3 kilograms. A mass of 3.7 kilograms was estimated for the radius and the two associated actuators originated on it. The carpus weights only 0.6 kilograms due to its size and the fact that no actuators originate there. The metacarpal and the actuator originating there yielded a mass of approximately 2.7 kilograms. Finally, the fetlock has a mass of 0.9 kilograms. The masses of the preceding components included the hydraulic actuators

originating on each limb section. These actuators were considered to be rigidly attached to each component for the analysis due to their relatively small angular deviation from the limb section compared to the angular deviation of that limb section to the previous limb section. This was chosen to significantly simplify the model. The total estimated mass of the robotic replica, including the mass of the thoracic-scapula joint and thoracic plate is estimated at 41 kilograms. The majority of the mass is proximally located in the thorax region of the robotic replica keeping the inertia of the distal components relatively low. A large percentage of this mass originates from the purchased parts used in the thoracic design.

Actuator Forces

With the dimensions and masses of the robotic replica determined, forces required by the actuators to generate the desired motion needed to be calculated. There are a total of 13 degrees of freedom to account for. However, since the coffin joint is only used to maintain the hoof parallel to the ground during stance, it can be controlled passively. The final concept of the coffin joint was designed with a torsion spring that applied pressure to maintain the hoof in an extended position. However, when the hoof comes in contact with the ground it will be forced to lay flat due to the ground reaction force.

Also, the scapula will not be actively controlled in the horizontal direction. The motion in the cranial-caudal direction is passive to allow for the relative motion of a contralateral scapula. This passive motion is accomplished through springs and dampers.

All of the other degrees of freedom, totaling eleven, will be actively controlled. The vertical actuation of the scapula relative to the rib cage is controlled with a ball-screw actuator, specified in the parts list (appendix B). This motion simulates the vertical motion of the scapula relative to the thorax as a result of the serratus ventralis. The peak ground force that will be generated by the replica is 2201 Newtons. This force was determined from data collected by other researchers (pg.67, Back and Clayton, 2001). Therefore, the maximum dynamic force of the THK ball-screw actuator of 7700 Newtons is adequate for this application.

There are a total of ten hydraulic actuators used to control the motion of the remaining ten degrees of freedom. The actuator for the fetlock originates on the proximal end of the metacarpal and inserts on the proximal end of the fetlock. It was found that the maximum force required from the fetlock actuator to produce the ground reaction forces during trot was slightly higher than 10000 Newtons as shown in Figure 4-2. It was discovered, however, that this peak force comes when the fetlock is in its maximum extension. Therefore, the natural stay apparatus of the horse was utilized. When the fetlock reaches its full extent, the hydraulic cylinder also reaches its full extent; allowing a portion of the load to be carried through a stop at the end of the cylinder reducing the maximum force needed by the actuator. Therefore, the maximum actuation force can be reduced to approximately 6000 Newtons through the use of the 'stay apparatus'.

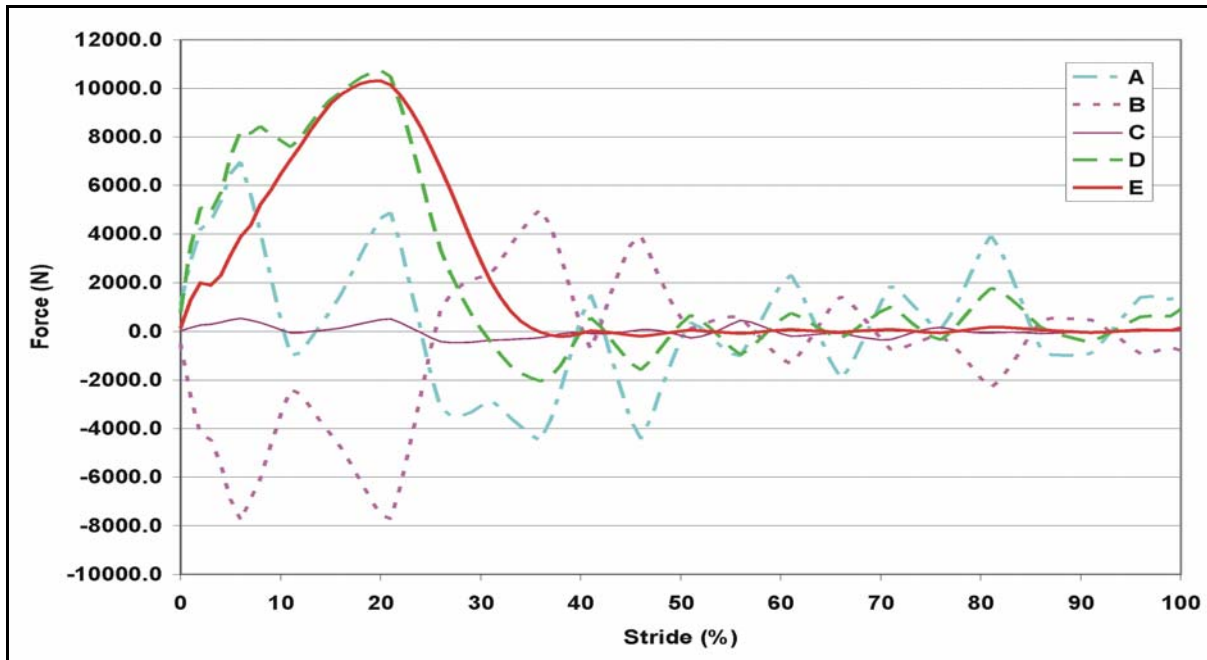


Figure 4-2: Actuator control forces at trot. A: Scapula-Humerus, B: Humerus-Radius, C: Radius-Carpus, D: Radius-Metacarpal, E: Metacarpal-Fetlock.

The two hinge joints of the carpal joint are controlled via two hydraulic actuators. Both actuators share a similar point of origin on the proximal end of the radius. However, the insertion points are located on the carpus and the metacarpal. The maximum actuator forces calculated for the two actuators were about 10,700 Newtons to the metacarpal and 530 Newtons to the carpus as shown above in Figure 4-2. Again, the maximum actuation forces occur at maximum extension of the joint. Therefore, the stay apparatus was also used to reduce the actuation force required in the carpus. Hard-stops engage when the joints go into hyperextension during the stance phase of gait. This locking of the ‘carpal bones’ reduces the required peak force of the radius-metacarpal actuator to approximately 6000 Newtons from the 10,700 Newtons. However, the carpal joint doesn’t go into hyperextension until approximately 10 percent of stride for trot. It can be noted from Figure 4-2 that the actuator force of the Radius-Metacarpal (D) goes above the 6000 Newtons before both hard-stops can be engaged. Nevertheless, the 6000 Newton actuator force can be achieved by utilizing the distal stop and increasing the Radius-Carpus actuator force. To achieve the required torques on each limb section, the Radius-Carpus peak actuator force must be increased from 530 Newtons to about 2360 Newtons. The resulting force is insignificant when compared to the other actuation forces.

Moving proximally, the next actuator encountered is that which controls the angle of the radius relative to the humerus. A force of approximately 7800 Newtons is required to actuate this joint through trot as seen in Figure 4-2 above. The origin of this actuator is located on the proximal end of the humerus. However, the insertion point of the actuator was positioned midway on the radius. This position was selected due to the optimization of the required force for actuation and the change in length of the actuator. As the actuator moved distally from this location, the actuation force began to decrease at a lower rate while the change in length began to increase at a high rate. It was found that for the given length, it would still be possible to construct an actuator that could undergo the change in length.

However, moving the insertion point to the distal end of the radius increased the required actuation length to a point that it would not be possible to create the needed hydraulic actuator.

Next, the ball joint of shoulder was considered. The position of the humerus relative to the scapula had to be located by three actuators due to the three degrees of freedom. The primary actuator (A) was located on the caudal side of the limb. The other two actuators, Z1 and Z2, were situated on the lateral and medial side of the limb respectively. These three positions allowed for all of the required motions to be achieved. The calculated forces of these actuators during trot are displayed in Figure 4-3 below. It can be noted that the maximum force of these actuators is approximately 7000 Newtons.

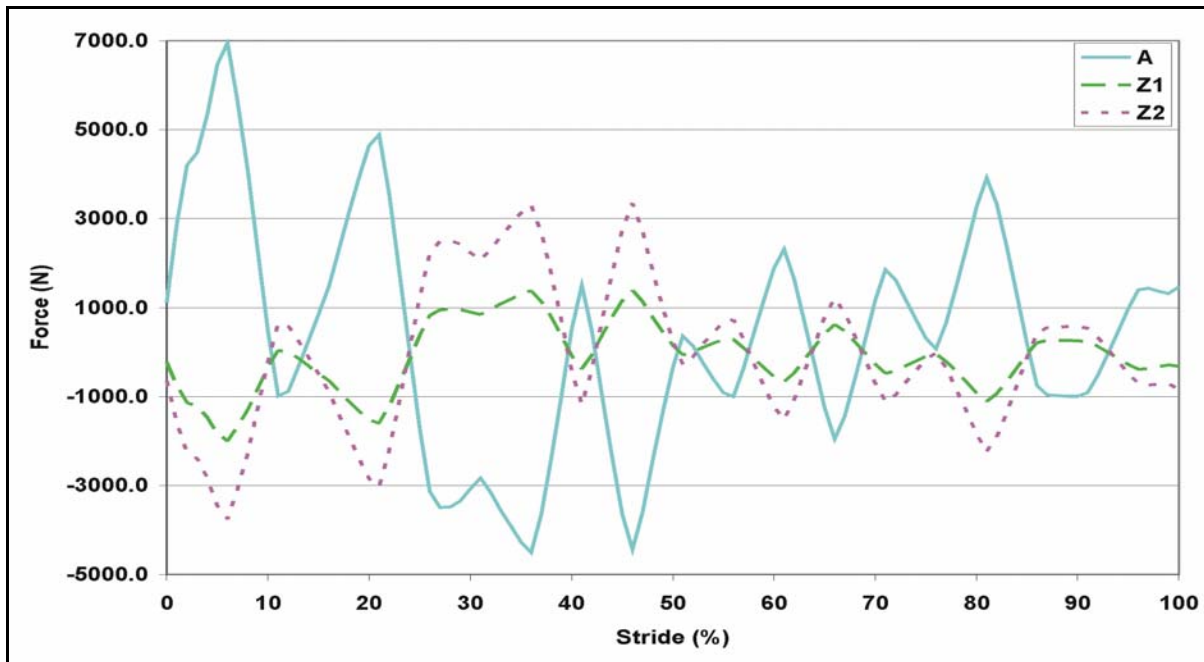


Figure 4-3: Shoulder actuator forces for trot. A: Caudal, Z1: Lateral, Z2: Medial.

In addition to the two degrees of freedom allowed through the plane, the scapula is also situated on a ball joint relative to the plane allowing for three additional degrees of freedom. These three degrees of freedom are actuated by three hydraulic actuators as shown in Figure 4-1 earlier. The origins of these actuators have been situated medially from the scapula to maintain the anatomical structure of the foal. The first actuator (O1) inserts on the caudal ridge of the scapula. The second (O2) was given an insertion point on the cranial ridge. Finally, ventrally to the first actuator, the last actuator (O3) was positioned on the caudal ridge. The forces required by these actuators vary significantly from one to the other. This variation can be seen in Figure 4-4. The greatest force generated by the caudal-dorsal actuator during trot is 5300 Newtons. However, the greatest force of the caudal-ventral actuator required to replicate trot is 36600 Newtons. The cranial actuator needs a peak force between the other two, just under 10000 Newtons. With these three actuators it is possible to move the scapula through the anatomical range of motion desired.

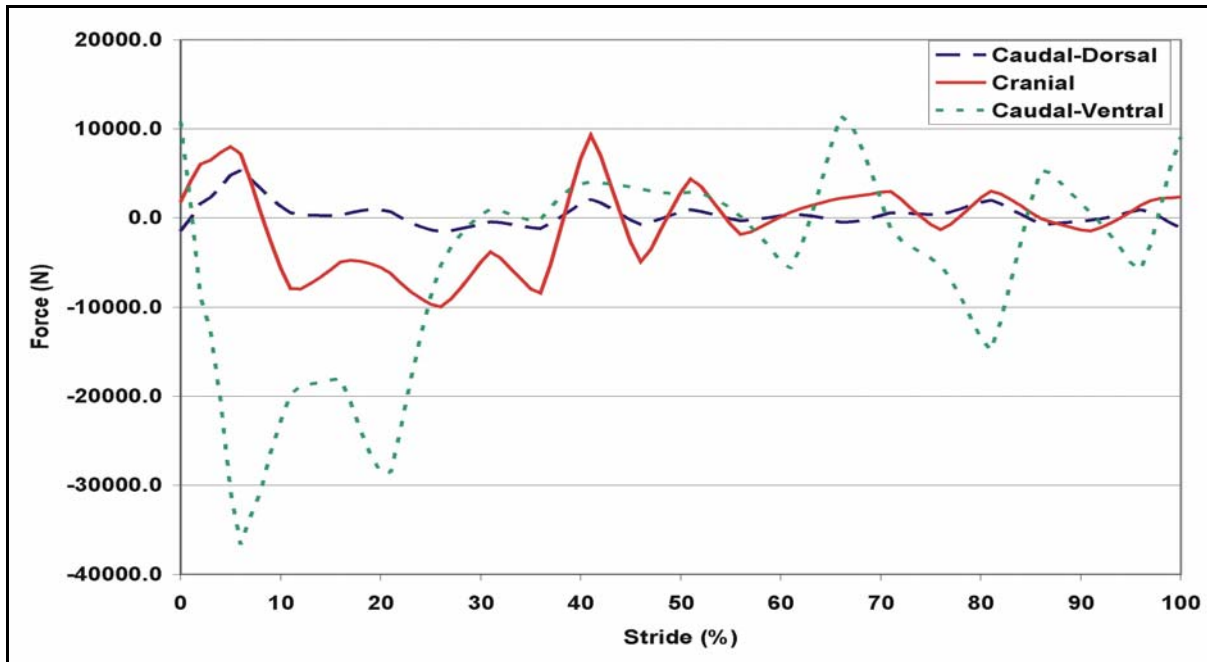


Figure 4-4: Scapula hydraulic actuator forces at trot.
O1: Caudal-Dorsal, O2: Cranial, O3: Caudal-Ventral.

All of the required forces for the actuators have been defined from the fetlock to the thorax. However, one detail remains to be discussed. The design of the robotic replica has been left to have one of two different configurations. The first configuration would have two opposing forelimbs with a mass located on top of them and a stabilization unit. This model would be a close representation of the actual foal with the capability of freestanding motion. However, a second configuration could be fit with a vertical pneumatic/hydraulic cylinder to one robotic forelimb. This single limb would need to be tested on a treadmill due to its inability to ambulate freely. The vertical actuator would be responsible for simulating the forces on the limb from the weight of the foal. Both robotic replicas are capable of simulating a range of motions including normal gait through a straight line, turning during gait, kicking in various directions, and shifting weight to and from the leg during rest.

FEA

Once the forces required for actuation of the robotic replica were calculated, an FEA was performed to guarantee that the robotic replica wouldn't fail while testing the rehabilitative load-bearing device. The FEA process, discussed in detail in Chapter 3, determined the maximum stresses that will be encountered while the replica is in use. Since the replica's peak forces are experienced during trot, the forces from trot were used for the analysis. It was determined from the analysis that the designed components did not exceed the yield strength of the specified materials. The aluminum specified to be used in the construction of the replica was Aluminum 6061-T6. Reynolds' aluminum of this type has been tested to have a yield strength of 275 MPa. The steel used in the design was series 304, annealed at 1950°F, water quenched, and 2% cold drawn. This steel has a yield strength of approximately 510 MPa.

Using the peak ground reaction force experienced during trot, the fetlock was first examined. The ground reaction force was transposed from the ground contact to the rotation

center of the coffin joint. This was done to simplify the FEA model and justified by the compliant natural of the coffin joint. The resulting stress from the ground reaction force and the hydraulic actuator can be seen in Figure 4-5. A peak stress of approximately 200 MPa was noted on the corner of the support for the actuator. However, radii in this location were removed from this model to simplify the analysis. Therefore, it can be speculated that the peak force would be less than 200 MPa. Nonetheless, the maximum stress of 200 MPa is below the yield strength of the material and therefore is adequate for the task of producing trot.

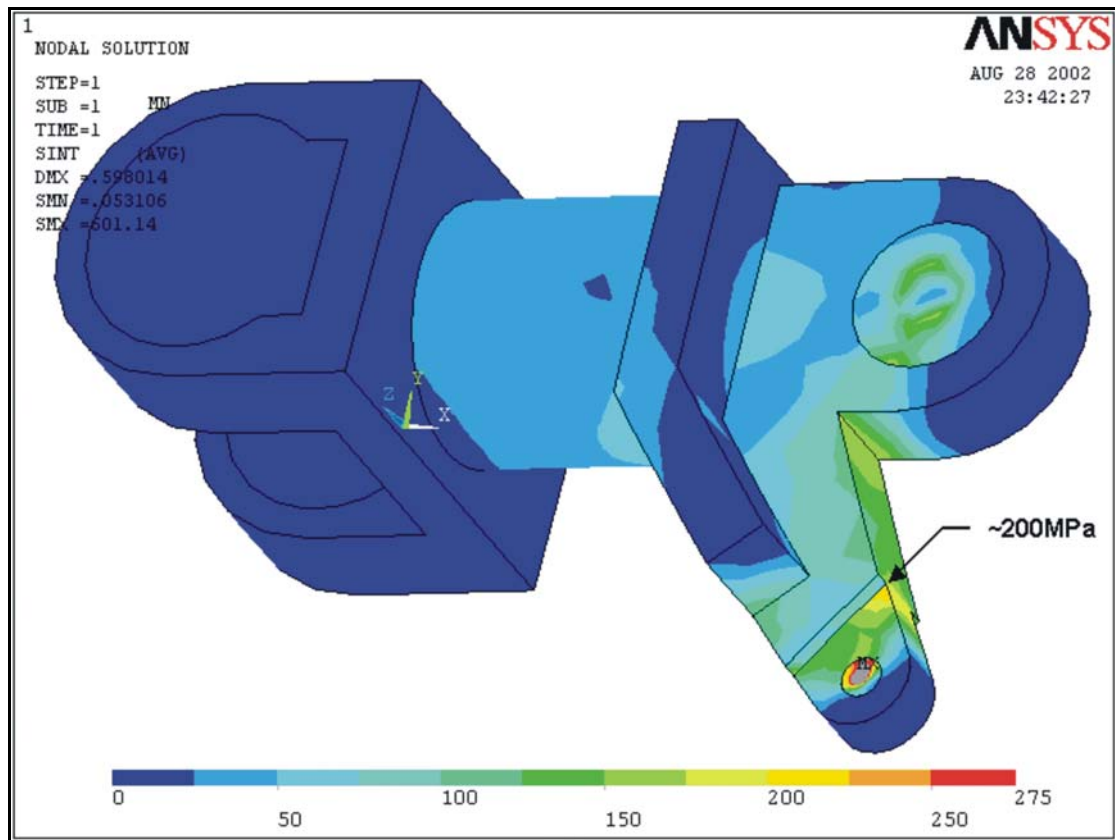


Figure 4-5: Stress analysis of the fetlock during trot.

Knowing the ground reaction force and the actuator force, the fetlock joint reaction force was calculated. Next the force was transposed to the distal end of the metacarpal. From there the hydraulic actuator force was applied and the stresses solved for. After obtaining the forces, they were transposed to the joint rotation centers from which an FEA was done. The resulting stress can be seen in Figure 4-6. Localized peaks in the stress were observed at the actuator mounting locations. The highest stress experienced in the aluminum was 250 MPa. Due to the location of this stress, the simplifications of this model would have little effect on the stress at the given location. Therefore, the actual stress would be that noted in the FEA analysis. Still below the yield strength of the material, the peak stress is close enough to the maximum permissible stress that this replica shouldn't be cycled continuously at trot. It is possible that a stress fracture could propagate from the location of the peak stress due to fatigue. Yet, the robotic replica will be capable of replicating trot for the purpose of testing the robustness of the rehabilitative load-bearing device.

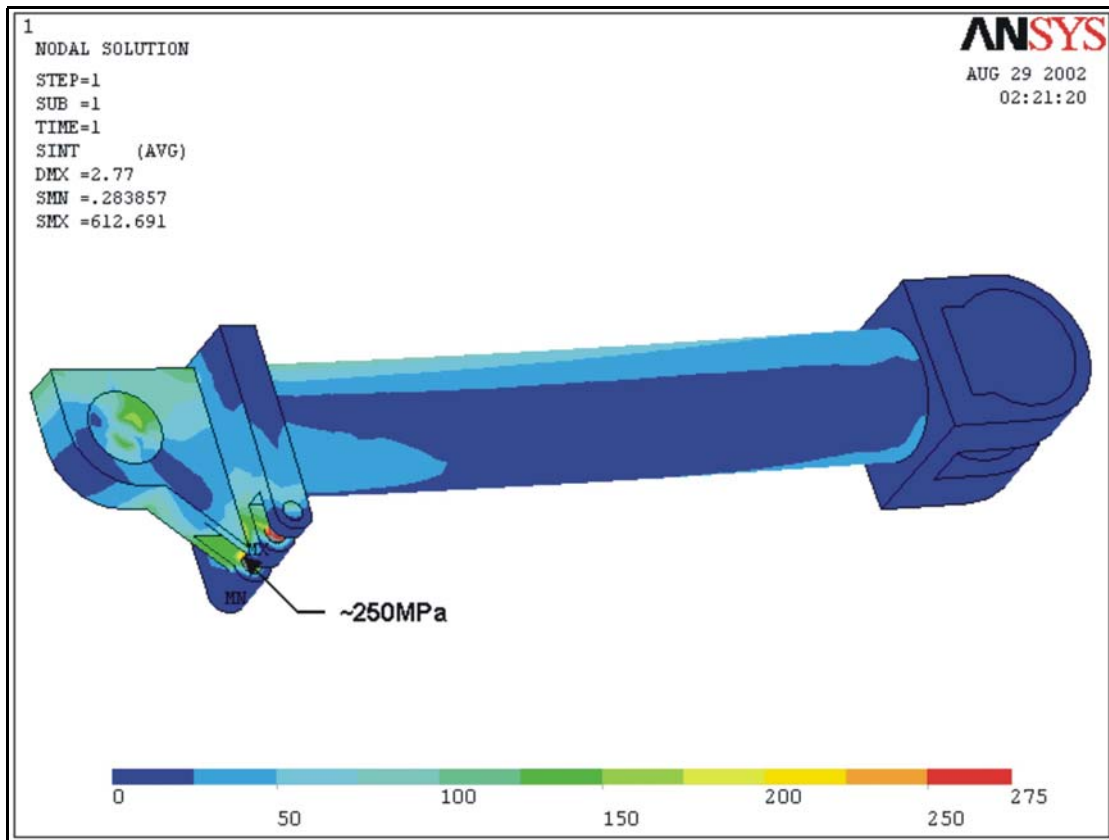


Figure 4-6: Stress analysis of metacarpal at trot.

Next, the stresses in the carpal joint were examined through ANSYS as discussed in Chapter 3. The bulk of the mass of the carpal joint, however, is bearings. Therefore, little could be done about optimizing the mass of the carpus. It was found that the maximum stress experienced from trot was only about 80 MPa as seen in Figure 4-7. This stress occurs at the insertion point of the actuator similar to the metacarpal.

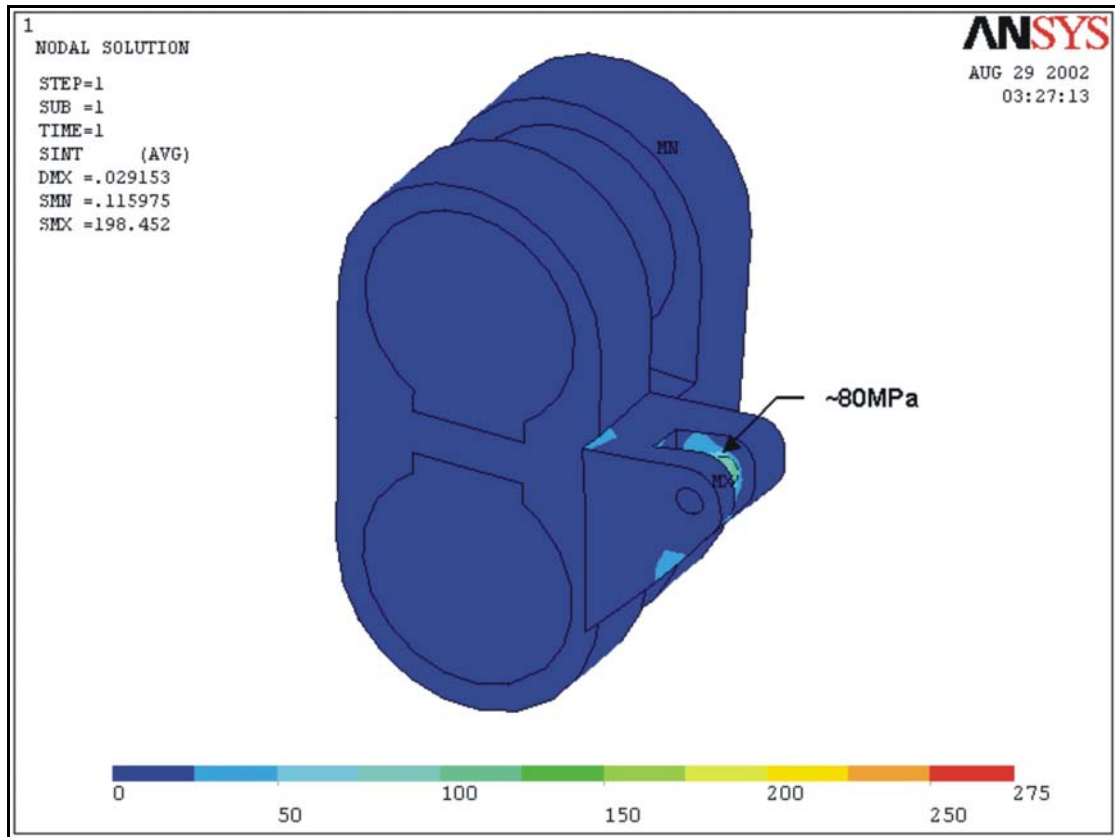


Figure 4-7: Stress analysis of carpal joint at trot.

In contrast, when the radius is analyzed, the maximum stress isn't located at the origin points of the actuators. The maximum stress in the radius occurs at the junction point of the tubular members and the ends that house the bearings as seen in Figure 4-8. Inspection through postprocessor revealed that the maximum stress was 275 MPa. This peak stress crops up in two locations. Both locations have been simplified to remove the radius of the weld. This extra material aids in distributing the stress. Therefore, the actual peak stress would be lower than that computed by the FEA program. However, this high stress still warrants caution when cycling the replica through trot. As suggested due to the stress seen in the metacarpal, the replica shouldn't be cycled continuously at trot, but is adequate for the required function of testing the rehabilitative device.

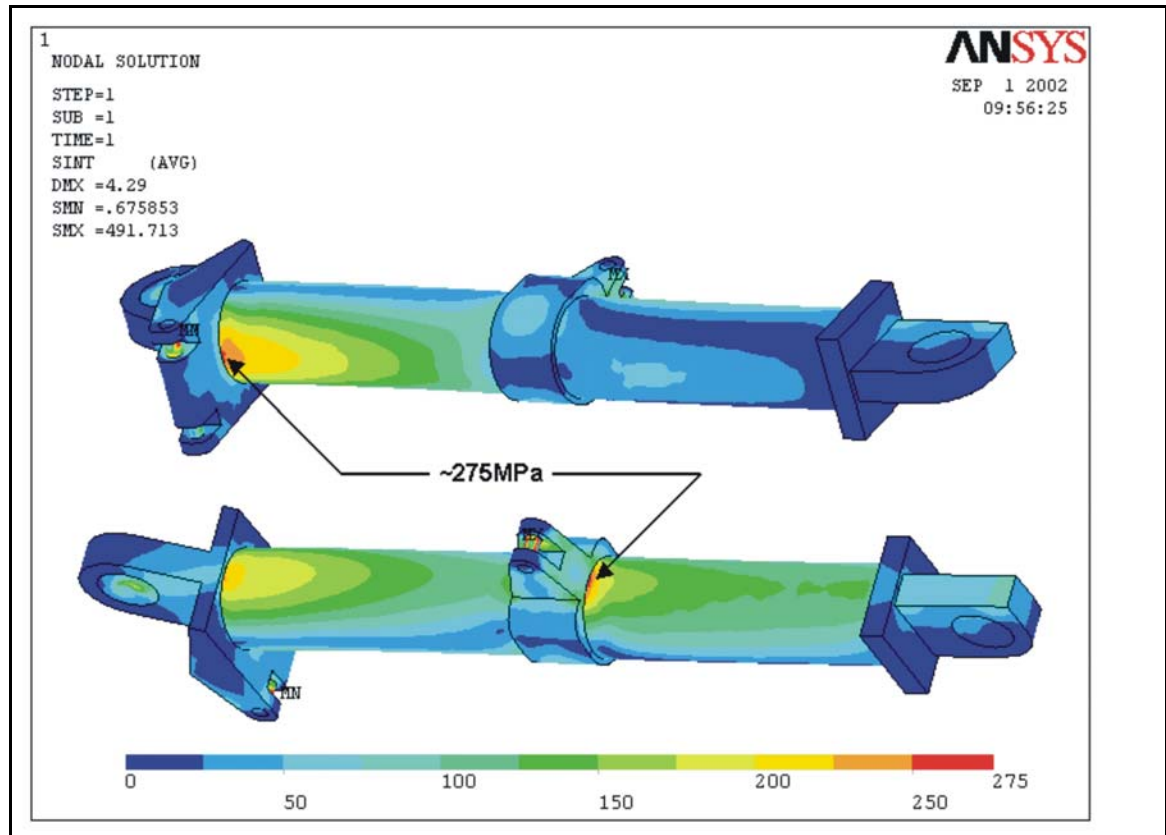


Figure 4-8: Stress analysis of radius at trot.

Moving proximally, the humerus was next investigated. After applying the appropriate forces and constraints, ANSYS determined the maximum stress to be approximately 230 MPa as shown in Figure 4-9. This stress occurs at the location of the origin point of the humerus-radius actuator. This level of stress is near 85 percent of the yield stress. Therefore, similar precautions should be taken as on the previous limb segments. However, the stress in the remaining portion of the humerus link was insignificantly low. Nevertheless, material shouldn't be removed due to the insertion points of the scapula-humerus actuators and the added cost of machining.

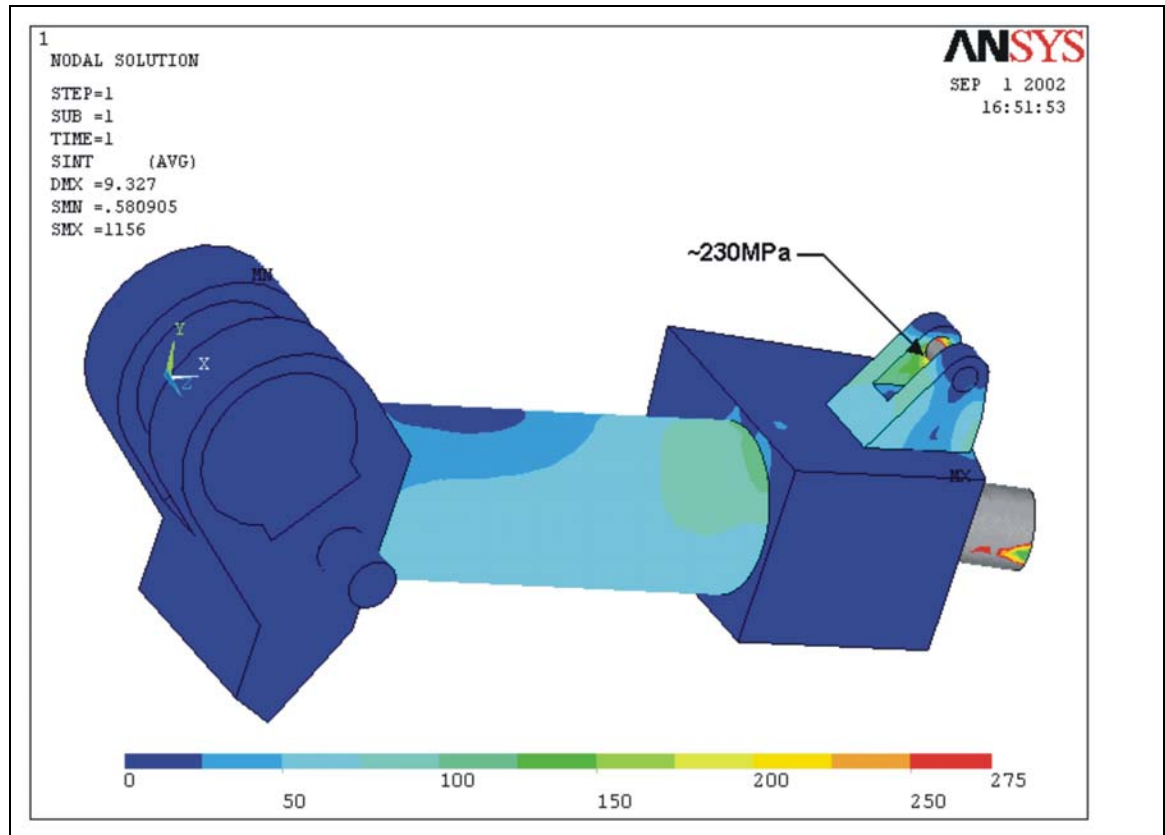


Figure 4-9: Stress analysis of humerus at trot.

Finally, the scapula was investigated for stresses induced by trot. The final design of the scapula yielded peak stresses well below the yield limit of the material. The peak stress in the final design is approximately 160 MPa at the location of the ball-joint connecting the forelimb to the planar positioning table as shown in Figure 4-10. It was also noted that the material removed from the body of the scapula did not increase the stress to a level of concern. Therefore, the decrease in mass is only a cost of machining and not that of stress.

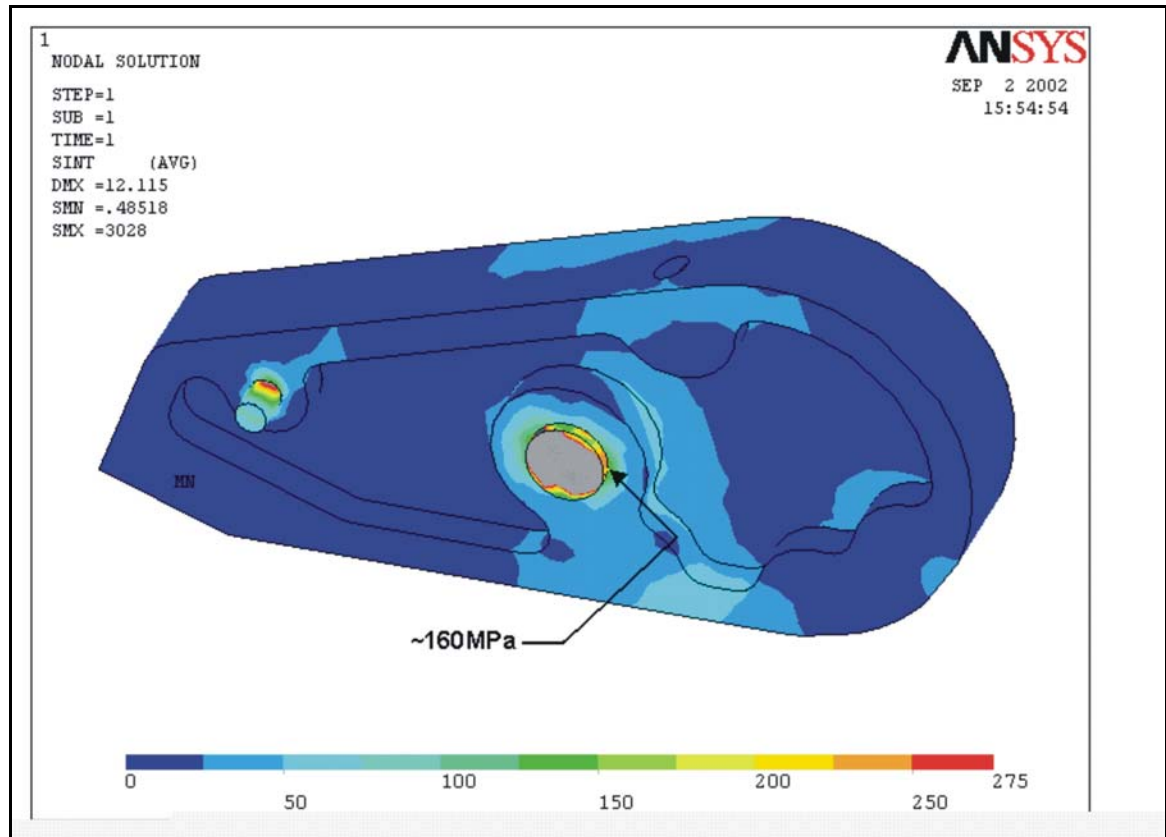


Figure 4-10: Stress analysis of scapula at trot.

The final design of the robotic replica shown in Chapter 5 is structurally sufficient for producing trot for the purpose of testing the bioassistive load-bearing device. In addition, it was proven that the design of the replica was not unnecessarily robust. This is demonstrated by the stress analysis above. However, the next question to address is whether the replica will be able to reproduce the motion when the forces are applied to the limb. This concern is addressed next in a comparison of the gait of the replica produced by the forces to that of an actual horse.

4.2 Comparison with Equine Gait

To compare the gait produced by the replica to that of the horse, control algorithms were developed as discussed in Chapter 3. The first gait to be examined was trot due to the large forces and significantly higher accelerations and velocities. First an open-loop control was attempted. After the open-loop was tested, the closed-loop control was applied to the model for trot. Finally, the design was tested at walk with the final control design.

Trot

The design was initially tested using open-loop control. Since the equations of motions are the same for the inverse dynamics as those used in the control loops, the forces determined for the inverse dynamics should yield the same motion when applied to the control loop. Therefore, theoretically the open-loop should be sufficient to replicate the desired motion.

However, the angles of each joint quickly diverge to impracticable values as seen in the radius angle shown in Figure 4-11a. Starting the replica with the hoof in contact with the ground resulted in a system that went unstable in less than 0.03 seconds. It was then speculated that the large forces associated with ground contact resulted in the unstable system. Therefore, the replica was then tested starting with the hoof in the air. The robotic replica was able to maintain the desired gait for a much greater length of time. As shown in Figure 4-11b, it took approximately fifteen times longer for the radius angle to become unstable when starting with the hoof in the air opposed to in contact with the ground. Nevertheless, the replica still became unstable and rotated through ridiculously large angles.

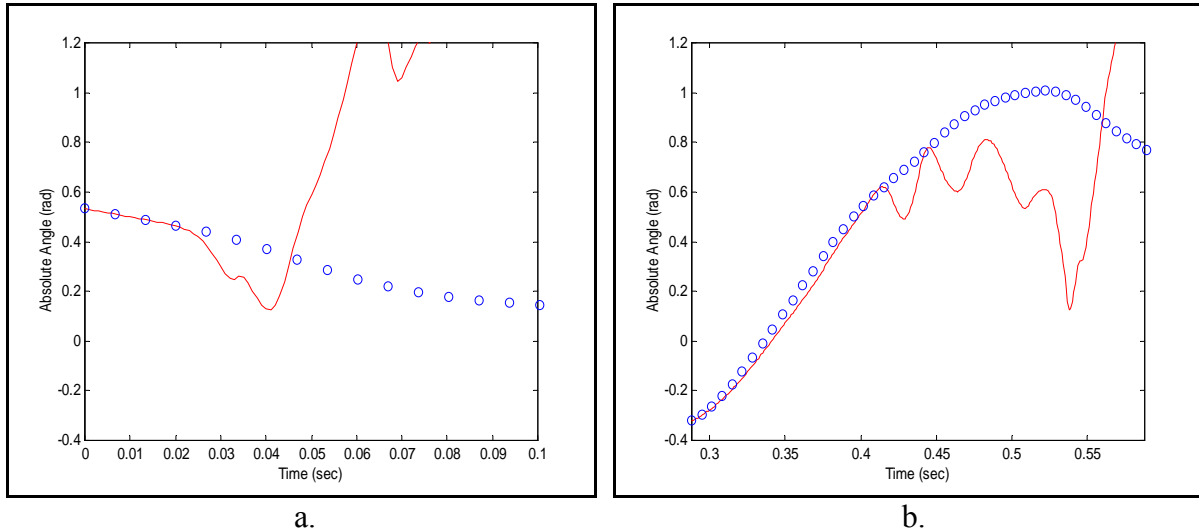


Figure 4-11: Open-loop response of radius angle for robotic replica.
a. starting at time=0sec, b. starting at time=0.2881sec

To address this issue, a closed-loop control algorithm was written to introduce feedback into the model of the robotic replica. The first closed-loop system utilized position control—proportional control as described in Chapter 3. This system was able to mimic the desired gait. It was possible to force all of the angles to follow the exact path of the collected data. However, this motion came at a great cost. The resulting forces of the closed-loop system were astronomical. Since the robotic replica was modeled without any inherent damping and the control model only used position control, the system acted as a spring. In order to create a controllable ‘spring’, the stiffness of the spring was increased to a level that resulted in the ridiculously large actuator forces.

To reduce these forces, damping was added to the system through the control loop. This damping came in the form of velocity control. The velocity, derivative, control was used in conjunction with position control resulting in a proportional-derivative (PD) controller. This controller is discussed in more detail in Chapter 3. After numerous iterations, gains for both the proportional and derivative feedbacks of each actuator were attained. These gains yielded a gait that closely mimicked the desired gait. The proximal limb sections follow the collected data with little inaccuracy. Also, the distal joint angles still follow the desired path close enough to be used for replicating trot. The angles of the scapula and fetlock as a function of time can be seen in Figure 4-12. From the two plots, it can be noted that it is possible to replicate trot with the designed robotic replica.

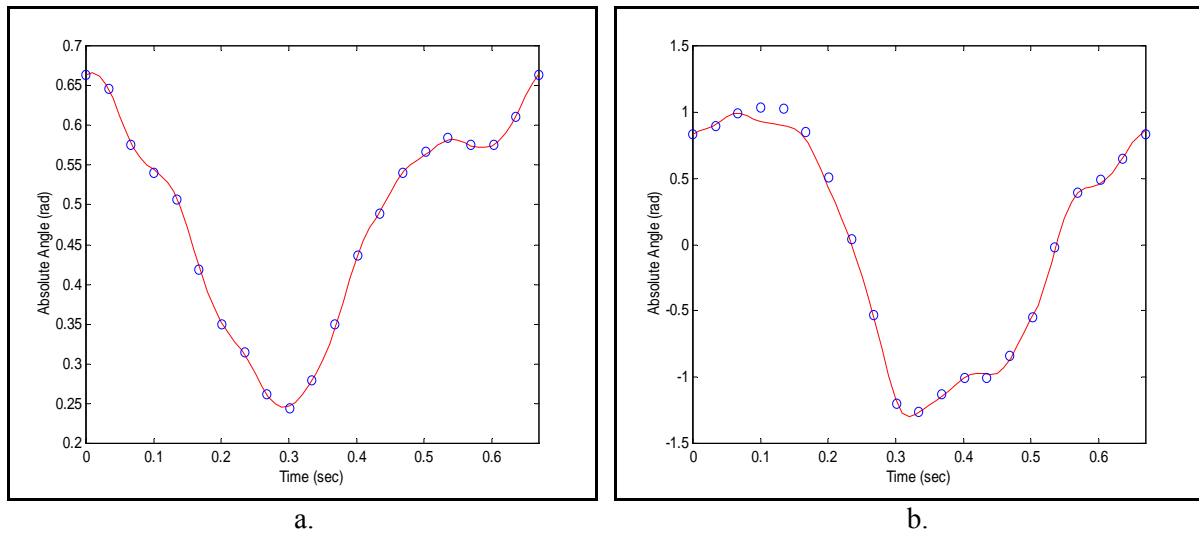


Figure 4-12: Path of robotic replica (line) compared to collected data (points) for trot.
a. Scapula-Ground angle, b. Fetlock-Ground angle

The gains of the PD controller were not only selected based on the replication of trot, but also for the closed-loop force required to produce that motion. It was discovered that several of the peak actuator forces needed to be increased slightly to attain the desired motion. However, some of the actuator forces decreased with the introduction of feedback. The scapula actuators all experienced increases in their peak forces. The caudal-dorsal and caudal-ventral actuators increased from 5300 to 6930 Newtons and 36600 to 37100 Newtons respectively. However, the cranial actuator increased to 17200 from 10000 Newtons. The scapula to humerus actuator's peak forces remained relatively unchanged while the forces oscillated about the open-loop forces predicted through the inverse dynamics. Both the humerus-radius and radius-metacarpal peak actuation forces decreased from the predicted open-loop forces. The humerus-radius force decreased from 7800 to 6370 Newtons and the radius-metacarpal force decreased from 10700 to 9360 Newtons. However, the radius-carpal actuator peak force increased from 530 to 820 Newtons. Finally, a reduction in the peak force of the metacarpal-fetlock actuator was noted, 10000 to 8830 Newtons.

As the Close-loop control forces varied from the open-loop forces, it was noted that they did so in an oscillatory manner. Some actuators oscillated about the open-loop force more than other. As noted in Figure 4-13, the force of the cranial-ventral actuator tended to vary more than that of the metacarpal-fetlock actuator. However, over-shooting of the control force was noted in all of the actuators. Therefore, a more sophisticated control algorithm may be warranted. For example, a proportional, integral, derivative (PID) controller may control the robotic replica to a similar or improved gait while requiring lower actuation forces with less oscillation.

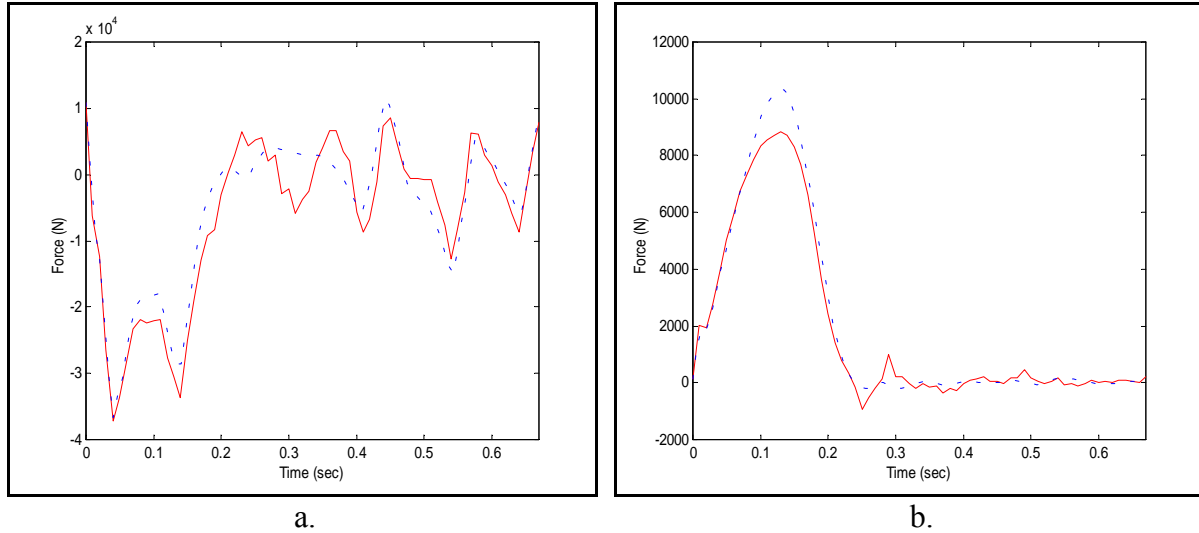


Figure 4-13: Comparison of closed-loop force (solid) to the open-loop force (dotted) for trot. a. Cranial-Ventral actuator, b. Metacarpal-Fetlock actuator

The current control design is sufficient to replicate trot. The closed-loop forces required to actuate the replica through trot are at acceptable levels that can be generated by high pressure hydraulic actuators in the given space. Also, the path of each limb segment is close enough to the collected data to adequately produce trot for testing of the rehabilitative load-bearing device.

Walk

During convalescence, the foal will spend the majority of its ambulatory time pacing back and forth in the stall. Therefore, the rehabilitative load-bearing device that the foal will don should be optimized for walk. Therefore, the robotic replica must be able to replicate walk to properly test the rehabilitative device. The ability of the replica to replicate trot is solely for the purpose of testing the robustness and responsiveness of the load-bearing device to the bucking and kicking of the foal in an attempt to free itself from the device. Therefore, walk will be the gait at which the replica will be actuated for the greater part of its use.

The algorithm used for trot was implemented to test the replica's ability to reproduce walk. The length of time it takes to complete one stride for walk is over 60% greater than that of trot. This longer stride time leads to lower accelerations of the various limb segments as shown in Chapter 2. Therefore, with the lower accelerations, the replica was capable of replicating walk to a satisfactory level with the algorithm designed for trot. The proximal limb segments moved through the desired paths with little difficulty and reasonable actuation forces shown in Figure 4-14a and Figure 4-15a. Additionally, moving distally, the limb segments continued to follow the desired paths as seen in Figure 4-14b. All of the closed-loop actuation forces experienced during walk were lower than that of the forces used in trot. This emphasizes that the design for trot will be adequate for reproducing walk to test the load-bearing device.

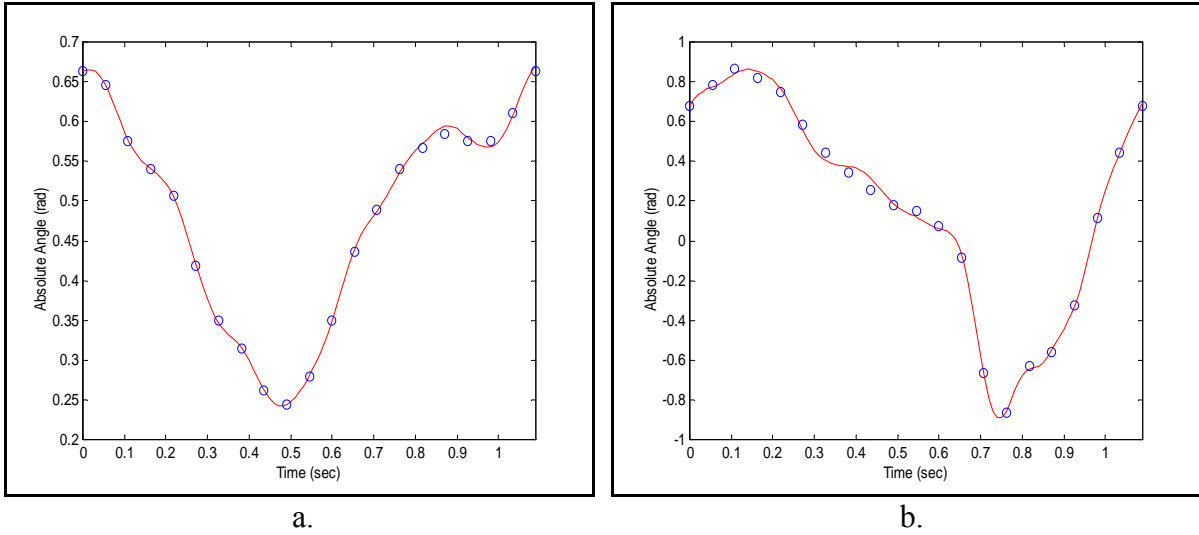


Figure 4-14: Path of robotic replica (line) compared to collected data (points) for walk. a. Scapula-Ground angle, b. Fetlock-Ground angle.

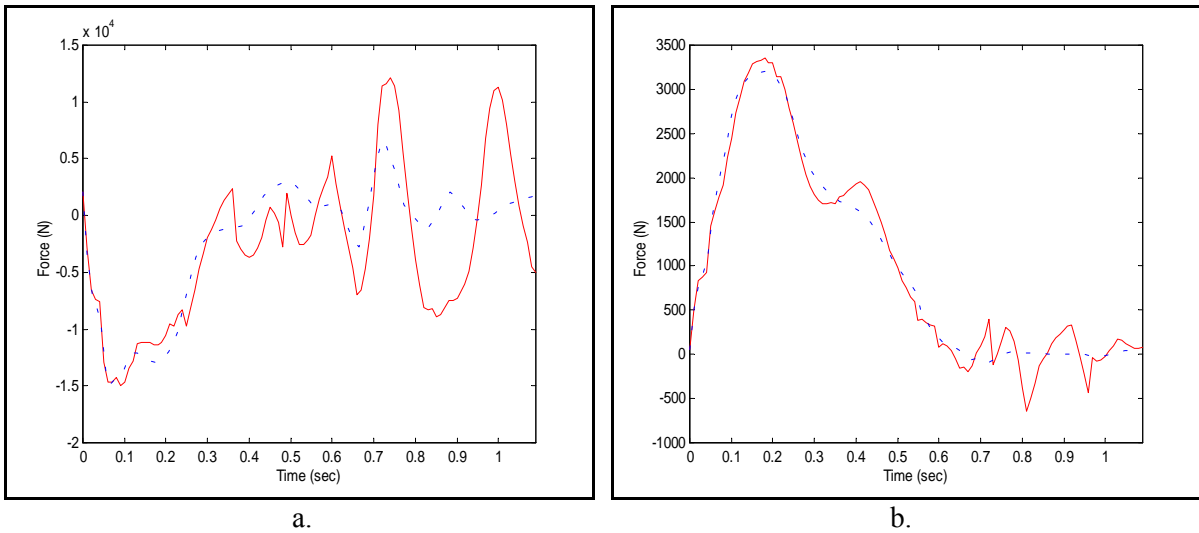


Figure 4-15: Comparison of closed-loop force (solid) to the open-loop force (dotted) for walk. a. Cranial-Ventral actuator, b. Metacarpal-Fetlock actuator.

The design of the limb is sufficient to produce a structural robotic replica of a foal's limb as mentioned earlier. Also, the robotic replica is capable of mimicking the anatomical motion of the forelimb of a typical foal as discussed above. Therefore, we have designed a robotic replica of a foal's forelimb that is capable of simulating the anatomical motions, such as shifting weight from one leg to the other, walking, and kicking, that are anticipated during convalescence to properly test the load-bearing device.

5 Construction of Robotic Replica

This section covers the assembly of the robotic replica in its entirety, which is shown in Figure 5-1. With every section of the robot being designed, including the load-bearing members and the hydraulic system, all of the parts can be fabricated and purchased accordingly. A complete list of the required components can be found in Appendix B. After obtaining all of the components, the construction of the replica begins with the assembly of the structural members. Next, assembly of the hydraulic system should be completed. Finally, the installation of the central nervous system of the robot (sensors and PC) takes place. After construction, the replica needs to be tested. This section will be organized in the order that the replica is constructed.

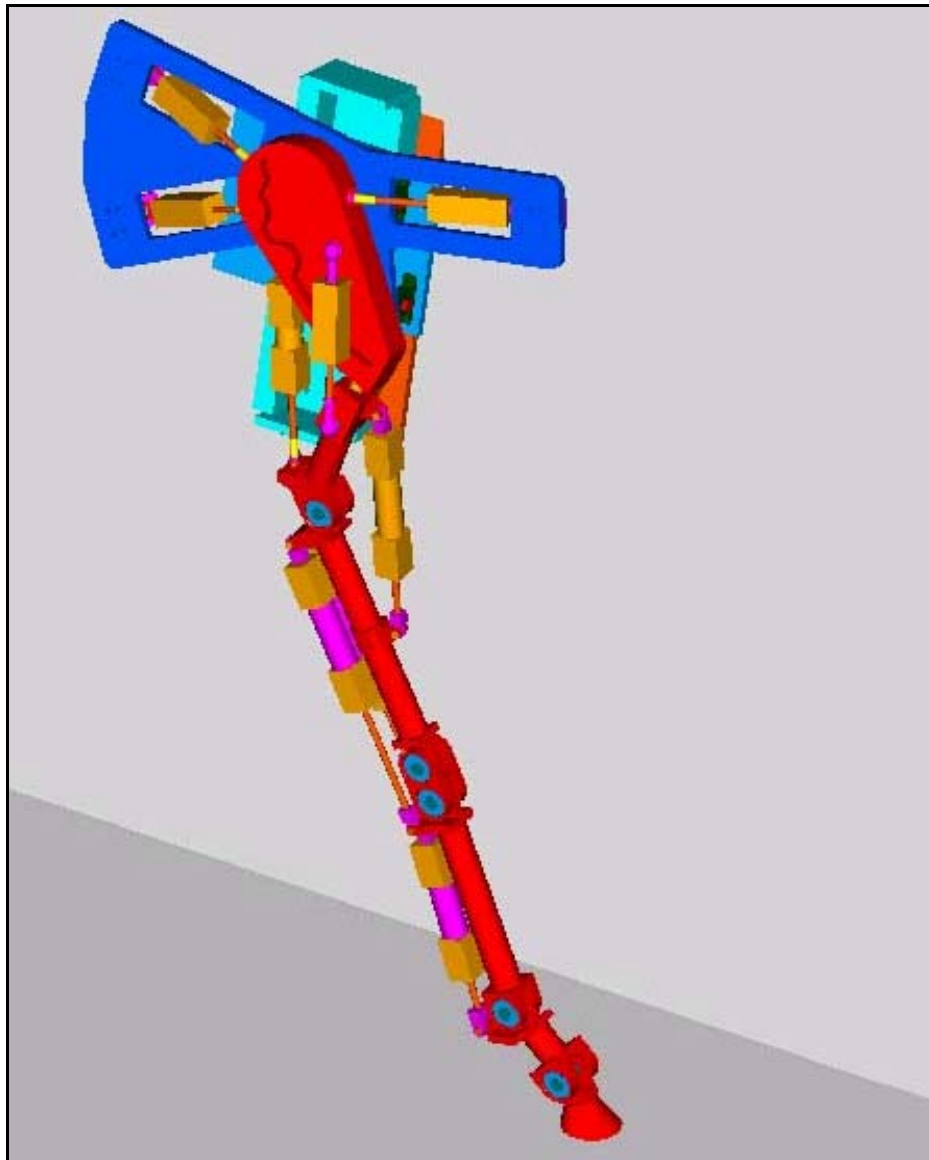


Figure 5-1: Assembled robotic replica.

5.1 Assembly of Structural Members

After the design of the robotic replica is completed, detailed drawings are generated as introduced in Chapter 3. These drawings are located in Appendix C. The required parts for the robotic replica can be fabricated from these drawings. With all of the fabricated parts and the required purchased parts accounted for, the assembly of the robotic replica begins. The order in which the structural members of replica are assembled is from the ground up, starting with the hoof.

Because of to the fusion of the hoof (distal phalanx) with the middle phalanx, the middle (215DSR) and distal (216DSR) phalanx sections are bolted together with three M4 bolts (603DSR) as shown in Figure 5-2. Next, one bearing (601DSR) is pressed into one side of the proximal phalanx (214DSR) and retained with the snap ring (602DSR). The proximal phalanx is held in a vice to immobilize it while pressing the bearing. Once the bearing is installed correctly, the part is flipped to expose the space for the other bearing. Carefully placing the return spring (105DSR) into the receiving hole of the middle phalanx, the middle phalanx is raised into its final position with the other end of the returning spring coming to rest in the appropriate hole of the proximal phalanx.

The middle phalanx is then clamped into position relative to the proximal phalanx. The shaft (104DSR) is then pressed through the middle phalanx and into the bearing of the proximal phalanx. Pressing the second bearing into the opposite side of the first bearing constrains the free end of the shaft. Finally, the fetlock assembly is completed by installing the second snap ring. The fetlock is then tested to ensure that the spring has been installed properly. The hoof is held firmly in the dorsal position by the spring. Pushing the hoof in the *palmar* direction should result in an increasing returning force. After the hoof is released, it should return to its dorsal position. This component is now considered operational and the construction continues.

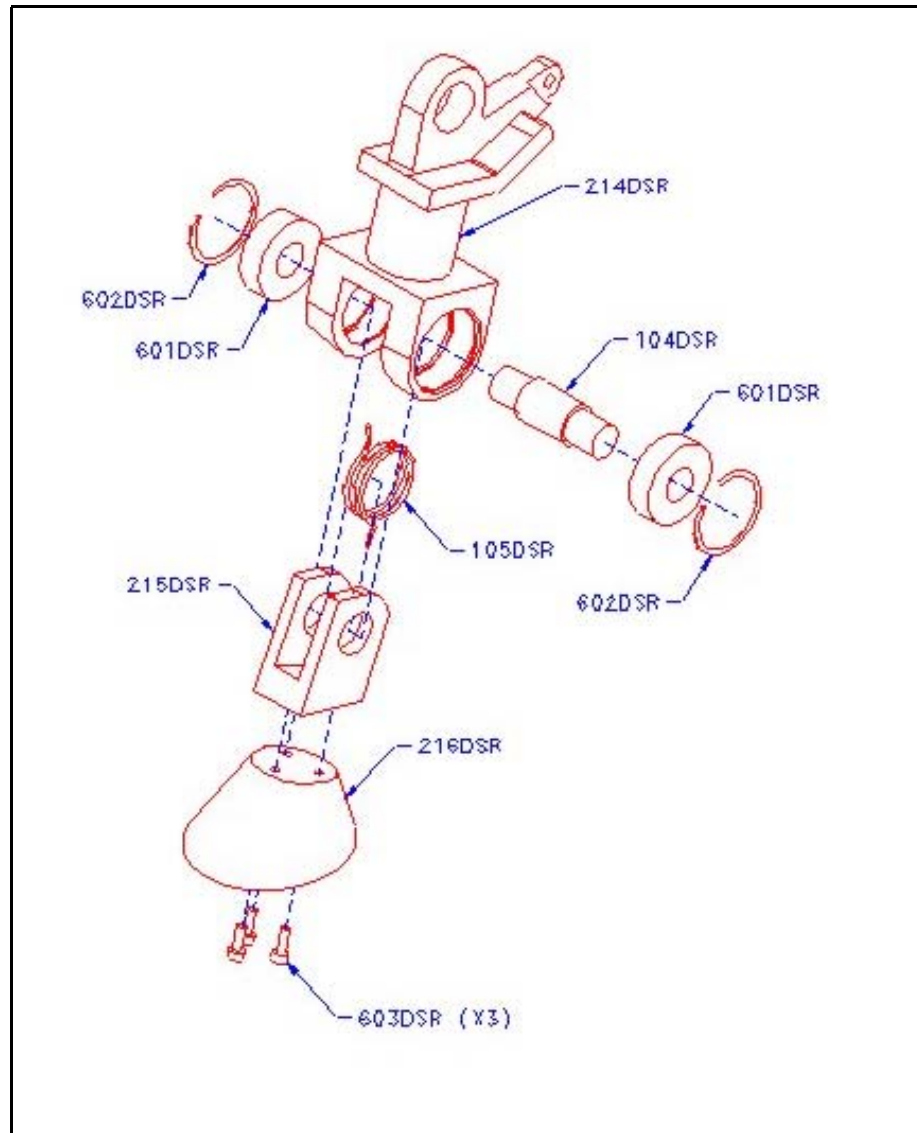


Figure 5-2: Assembly drawing of the phalangeal section.

Moving proximally, the joint encountered next is that between the fetlock assembly and the metacarpal (the fetlock joint). This joint is assembled in much the same fashion as the joint between the middle and the proximal phalanx. However, there is no spring to install in the metacarpal-fetlock interface, as seen in Figure 5-3. Therefore, the positioning of the fetlock (214DSR) relative to the metacarpal (206DSR) is simplified. It must be noted, however, that the direction of the metacarpal must be considered before completing the assembly. The attachment points for the hydraulic actuators are located caudally on the metacarpal as was shown back in Figure 5-1. The bearings and shaft are all pressed into the assembly in the same order and manner as in the fetlock assembly. Once the bearings have been contained on each side with their respective snap rings, a setscrew is installed to prevent the shaft from rotating relative to the fetlock. A setscrew was not used on the previous assembly because of the lack of space. With this joint assembled, the construction is continued on what is commonly referred to as the knee joint of the horse, the carpus.

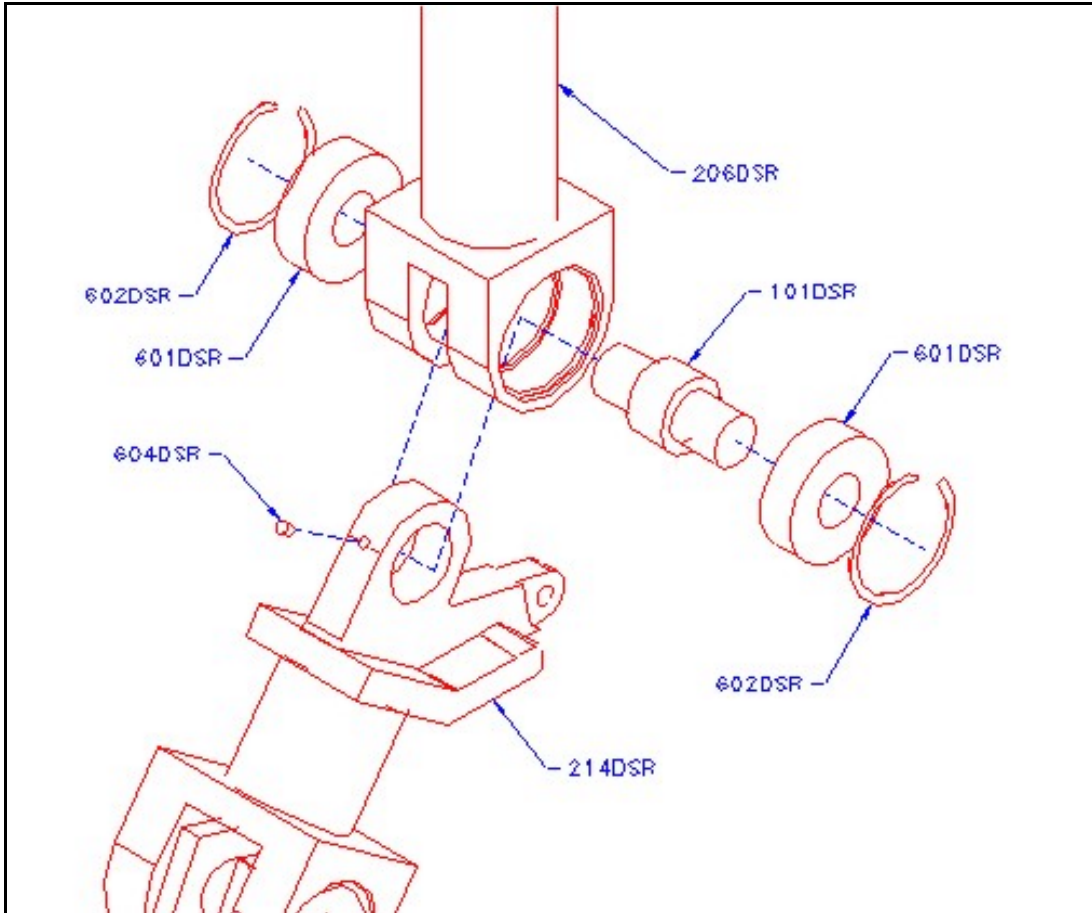


Figure 5-3: Fetlock joint.

The carpus (301DSR) in the horse is made up of eight bones. Since this joint rotates in a sagittal plane, hinge joints are used to perform the articulation as discussed in Chapter 1. The number of joints determined to achieve the appropriate positioning of the radius relative to the metacarpal was two. These joints are assembled in the same way as the metacarpal-fetlock interface (see Figure 5-4). Because of the incorporation of the stay apparatus, also discussed in Chapter 1, the carpal section is required to act as a 'hard stop' during articulation. This stop is implemented at the extreme extension of the knee joint. Using a large protractor, the angles of the assembled carpal joint can be tested and verified to be accurate for this application. The angle between the radius and metacarpal should be approximately two degrees into hyperextension.

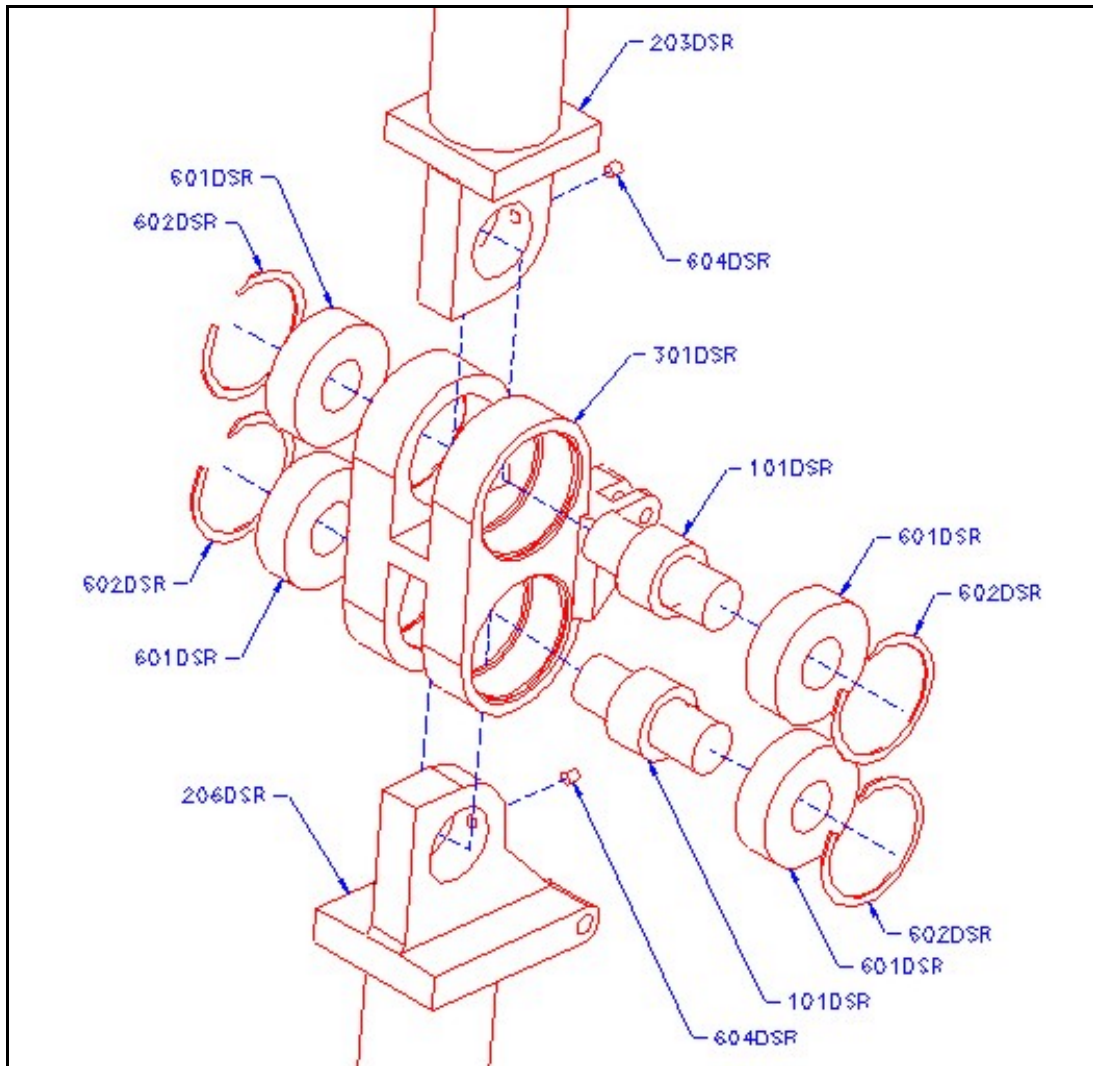


Figure 5-4: Knee joint (Carpus).

With the double hinge joint for the carpus completed, the final hinge joint of the robot shall be erected. The most proximal hinge joint of an equine forelimb is the humerus-radius joint, or the elbow joint. Again, the procedure for assembling this joint is identical to the fetlock joint, as can be seen in Figure 5-5. Again, careful consideration should be taken to orient the components in the proper cranial-caudal positions prior to assembly. With the final hinge joint assembled, each joint should be articulated to ensure that it is free to swing through the required range of motion discussed in Chapter 2. With the joints articulating as designed the assembly of the robot progresses further proximally to the shoulder joint.

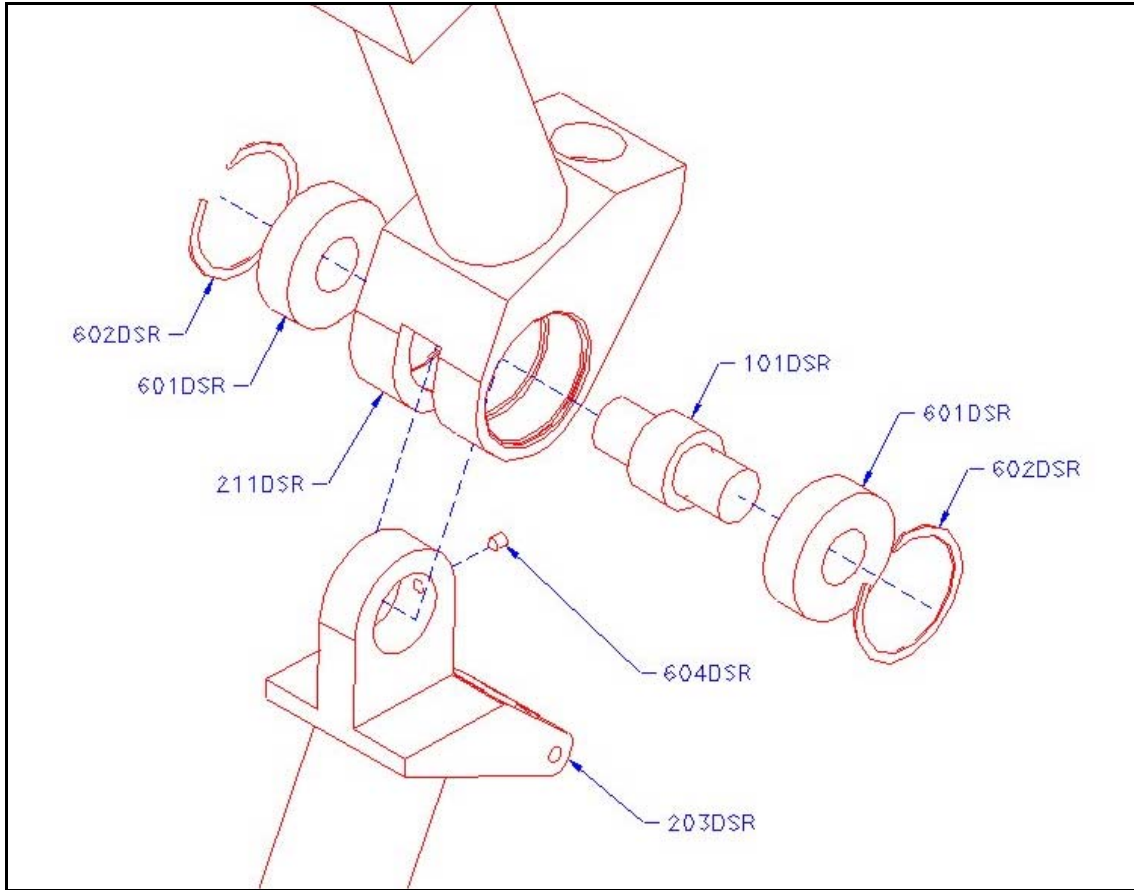


Figure 5-5: Elbow joint.

The shoulder joint—scapula-humerus interface—is a balljoint. For this reason, a commercial ball is used in the construction. The balljoint (605DSR) is simply threaded into the respective components and secured, as shown in Figure 5-6.

With the all of the skeletal joints of the equine forelimb completed, the construction moved to the muscular connection of the scapula to the axial bones. The design of the muscular cradle incorporates planar motion across an approximation of the rib cage and rotation about three axes. The rotation is achieved with another balljoint. However, the planar motion is divided into two components: an actively controlled, vertical component and a passively controlled, horizontal component. The construction of this cradle begins with the vertical cylinder that generates the force and position of the thorax relative to the limb. This cylinder is connected to the aluminum plate (217DSR) that holds the linear THK actuator (618DSR).

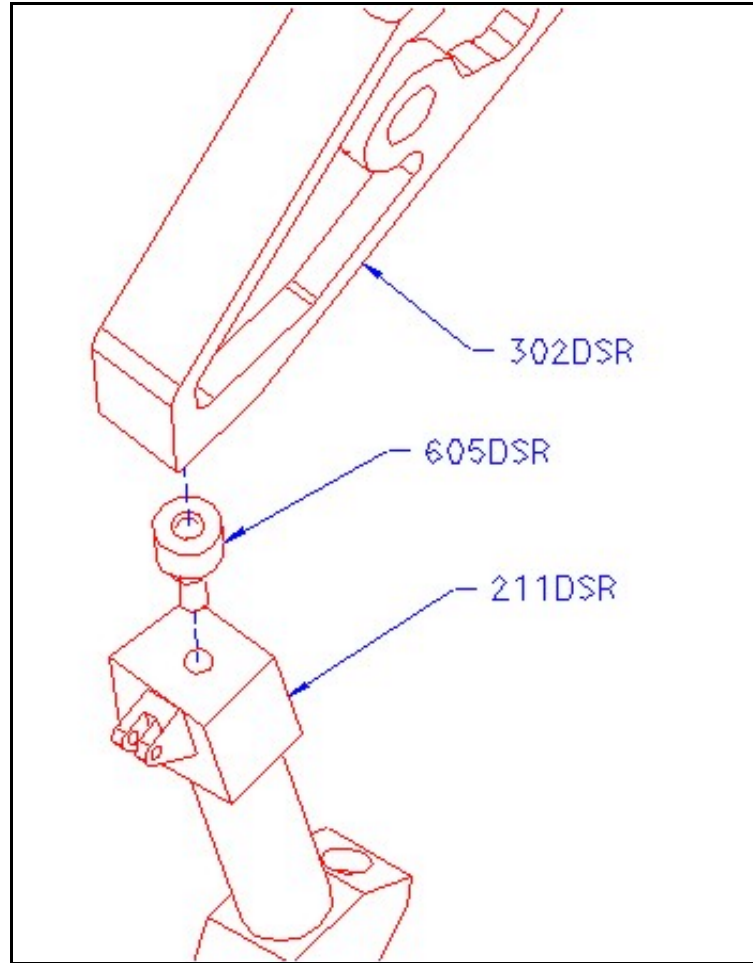


Figure 5-6: Shoulder joint.

As the horse moves through gait, the scapula moves up and down relative to the thorax through the muscular cradle. The vertical motion of the scapula relative to the thorax is achieved via a THK linear guide and ball screw (618DSR). The THK actuator is connected to the aluminum plate, 217DSR, with six M5x25 bolts as shown in Figure 5-7. The sliding tray of the actuator is then connected to an intermediate plate (218DSR) between the vertical and horizontal positioning mechanisms. The attachment of the intermediate plate to the sliding tray is accomplished with four M8x30 bolts. All of the bolts are threaded into their appropriate holes before being tightened. This procedure finishes the construction of the vertical actuator.

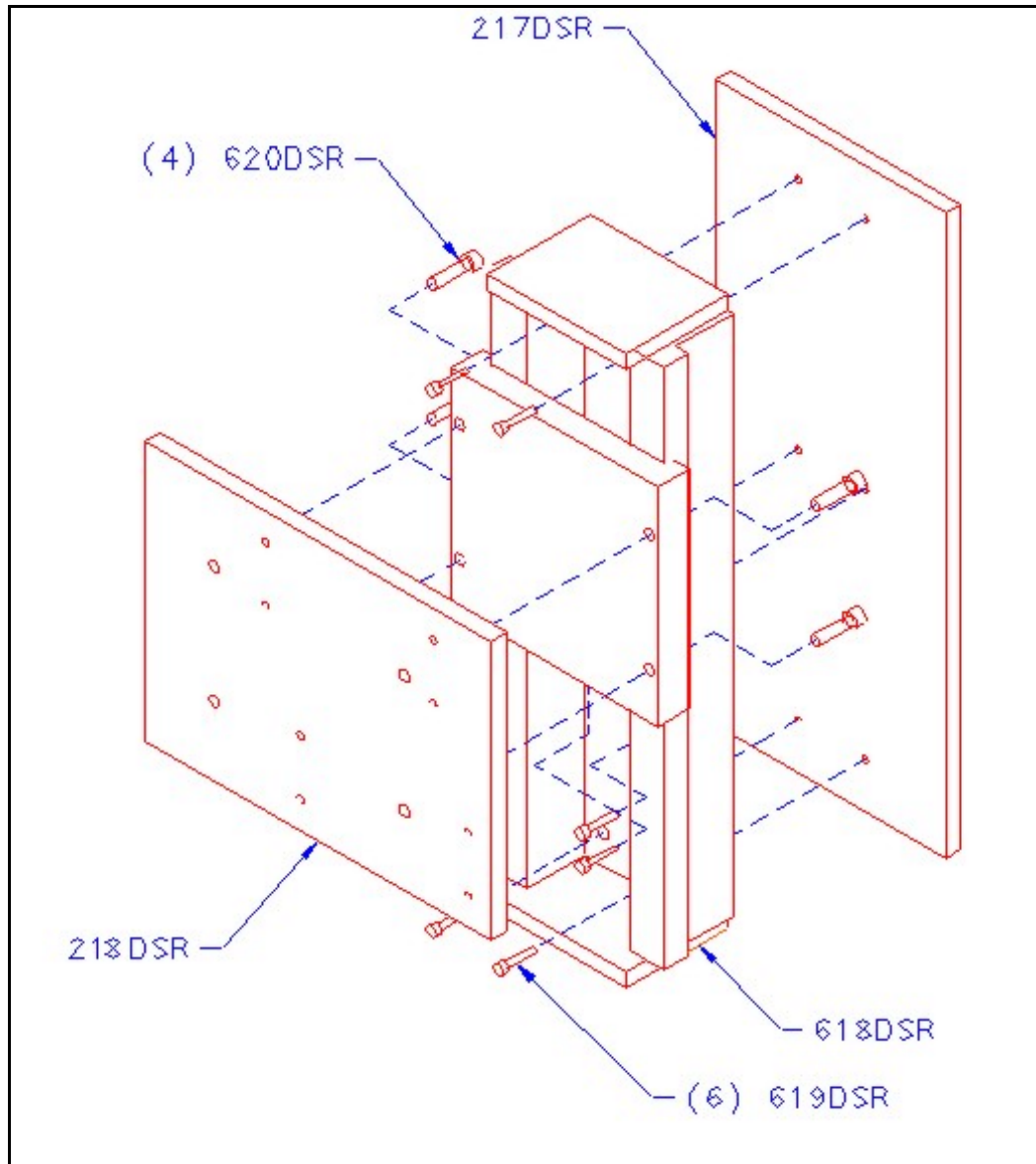


Figure 5-7: Vertical actuation of cradle.

Next, the construction of the horizontal positioning mechanism is executed. First, the shaft supports are connected to the intermediate plate with #10 bolts. However, the bolts are not tightened to ensure proper alignment of the bearings. Then, #8 bolts are installed as to lightly secure the bearings (608DSR) to the horizontal positioning aluminum plate (219DSR). Sliding the shafts (609DSR) into position temporarily allows for the supports and bearings to be tightened in their proper positions while moving the plates back and forth. The shafts are then removed to torque the bolts. Finally, the shafts are reinstalled through the supports and bearing blocks with the compression springs (622DSR) in place, as shown in Figure 5-8. The shafts are secured with #10 bolts as shown in Figure 5-9.

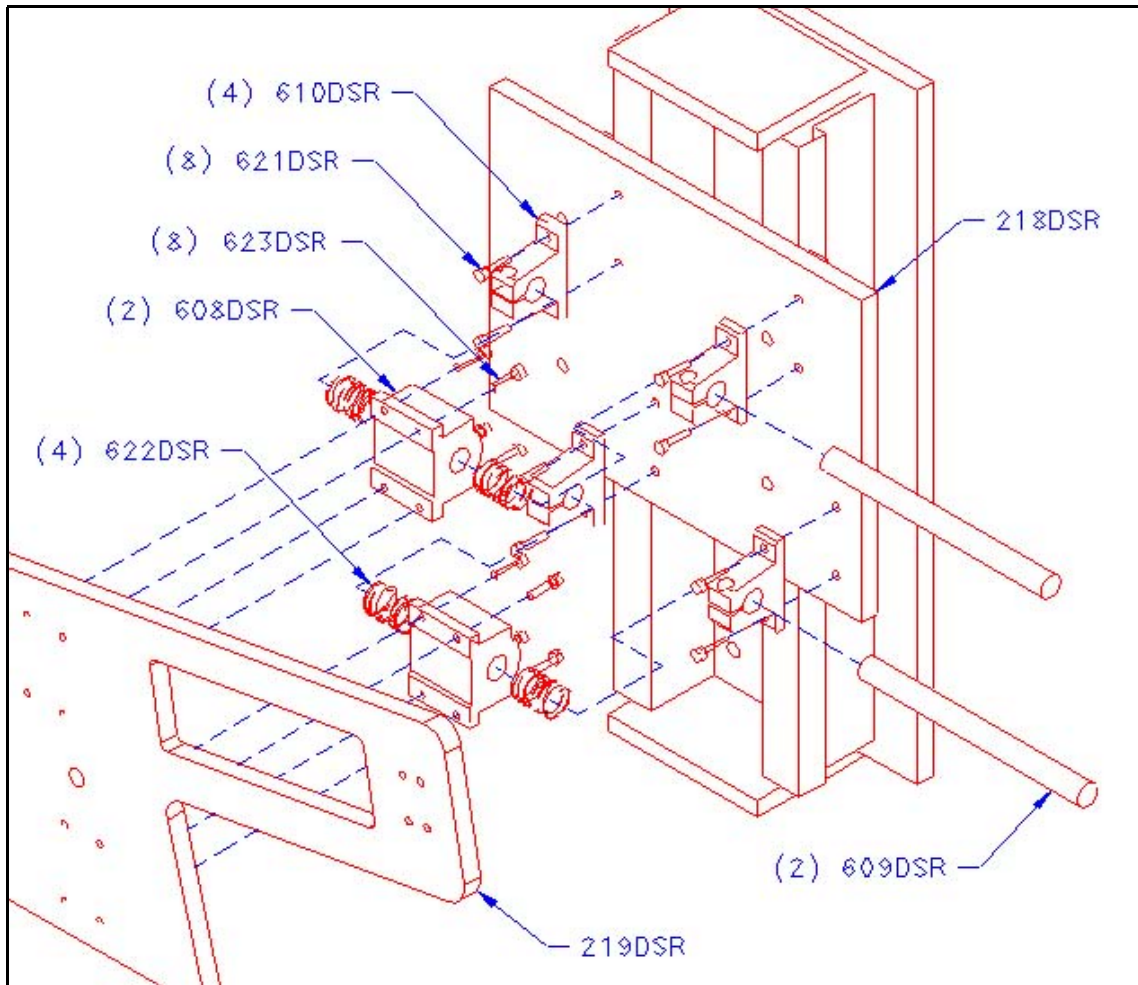


Figure 5-8: Horizontal control of cradle.

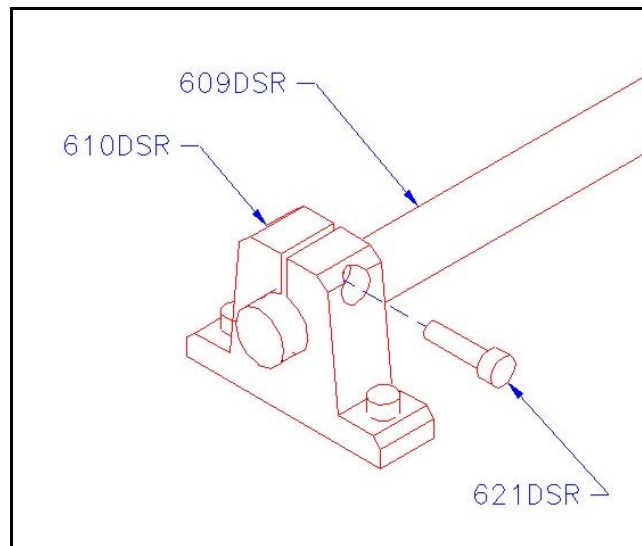


Figure 5-9: Secure shaft when in position.

The horizontal positioning of the scapula is passive. A damper is required to over-damp the horizontal positioning of the scapula. This over-damping prevents the scapula from experiencing unnecessary oscillatory motion. The damper (625DSR) is connected to the two plates that move horizontally relative to each other. This connection completes the construction of the muscular cradle for the planar positioning of the scapula relative to the thorax.

The structural construction is finalized by connecting the robotic forelimb to the thorax through the cradle. The connection between the forelimb and the planar positioning table is achieved with a balljoint (605DSR), as shown in Figure 5-10. With the installation of this balljoint, the construction of the robotic replica proceeds to the assembly of the hydraulic system.

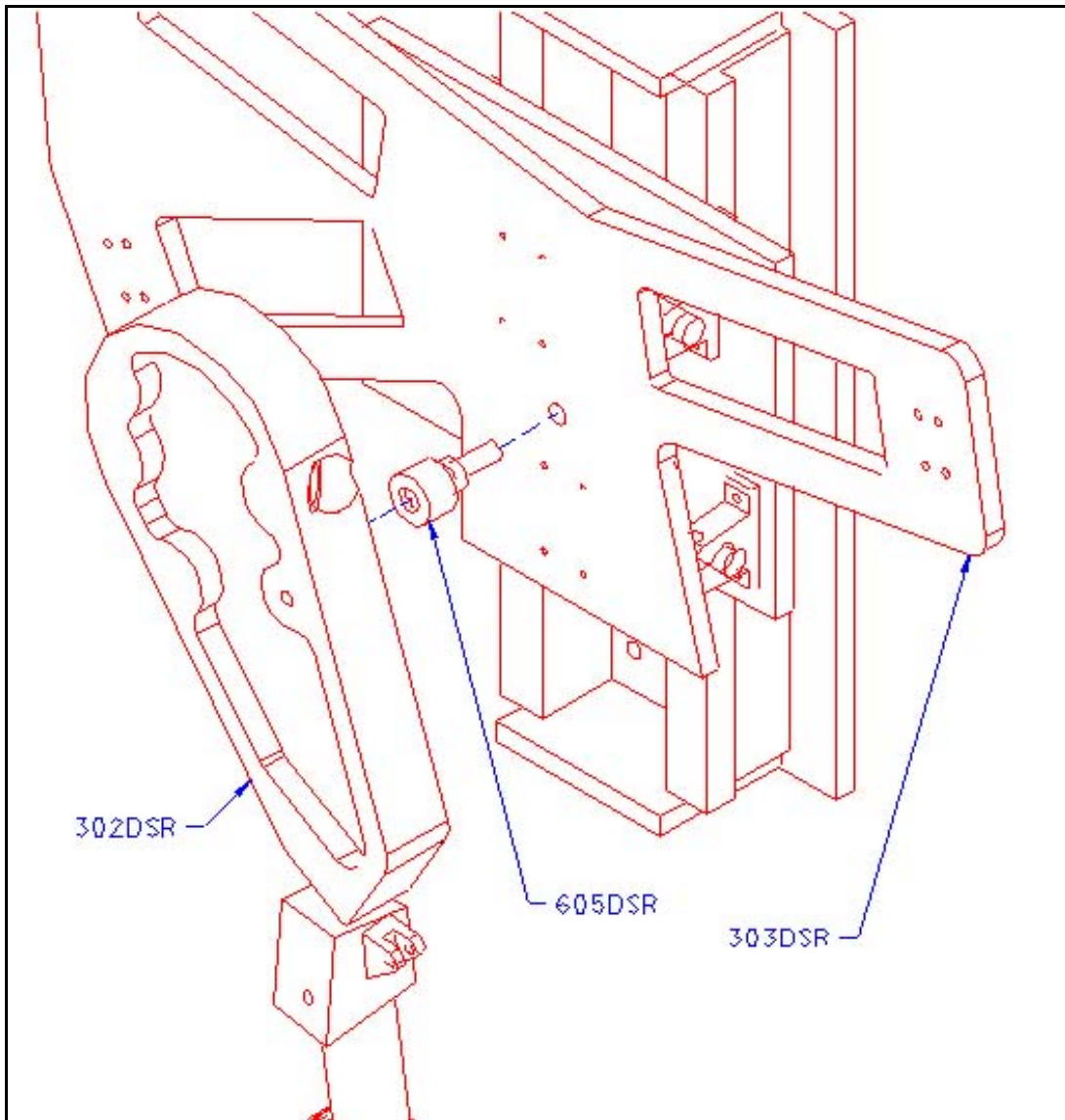


Figure 5-10: Scapula to thorax connection.

5.2 Assembly of Hydraulic System

Now that the procedure for the assembly of the structural members of the robotic replica is completed, we move to the installation of the hydraulic actuators. The current state of the robotic replica should be that of Figure 5-11. The installation of the actuators is covered from proximal to distal. This order of installation makes it easier to manipulate the limb sections into the required position for securing the endpoints of the actuators.

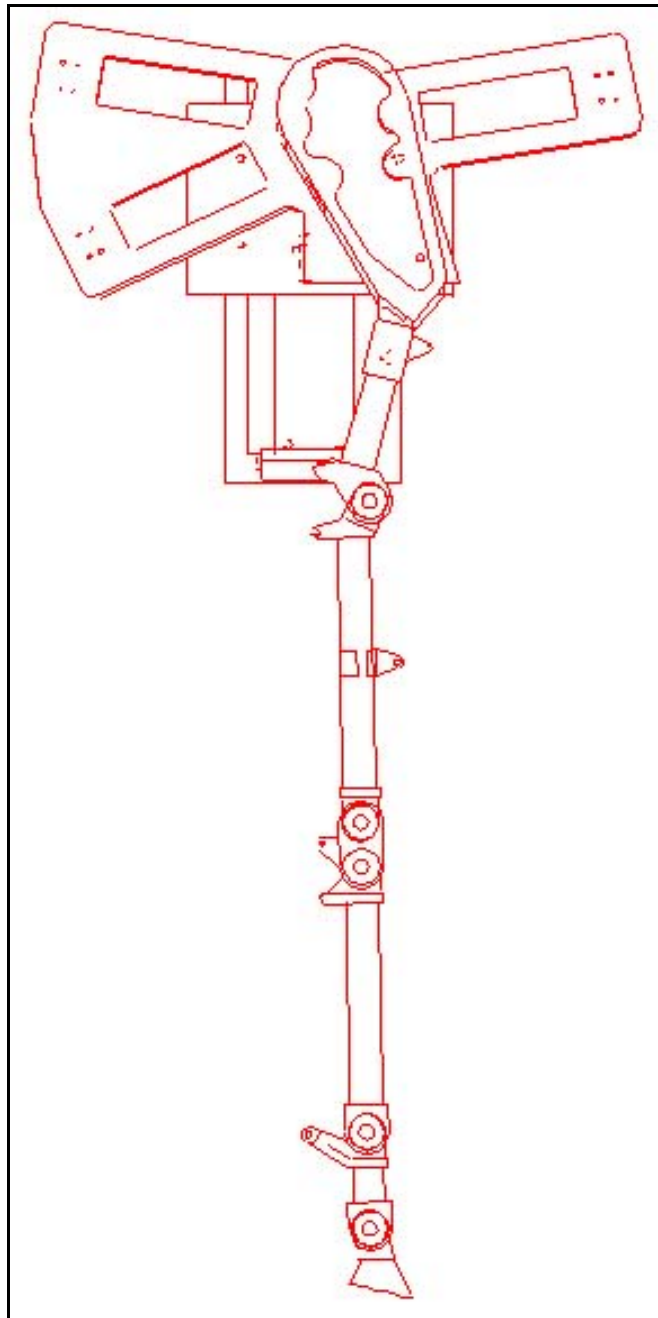


Figure 5-11: Assembled robotic replica before installation of the actuators.

To initiate the installation of the actuators, mounting blocks have to be fixed to the horizontal positioning plate of the muscular cradle. Since the scapula is articulated about a balljoint, three actuators are required to fully constrain the scapula relative to the plate (303DSR). Therefore, three mounting blocks (102DSR) are fixed to the plate. Twelve M5 bolts are required to connect the components together. First, the bolts are placed through the holes in the plate (303DSR) and loosely threaded into the mounting blocks. The orientation of the blocks is shown in Figure 5-12. Once all of the bolts are in place, they are torqued to properly restrain the mounts.

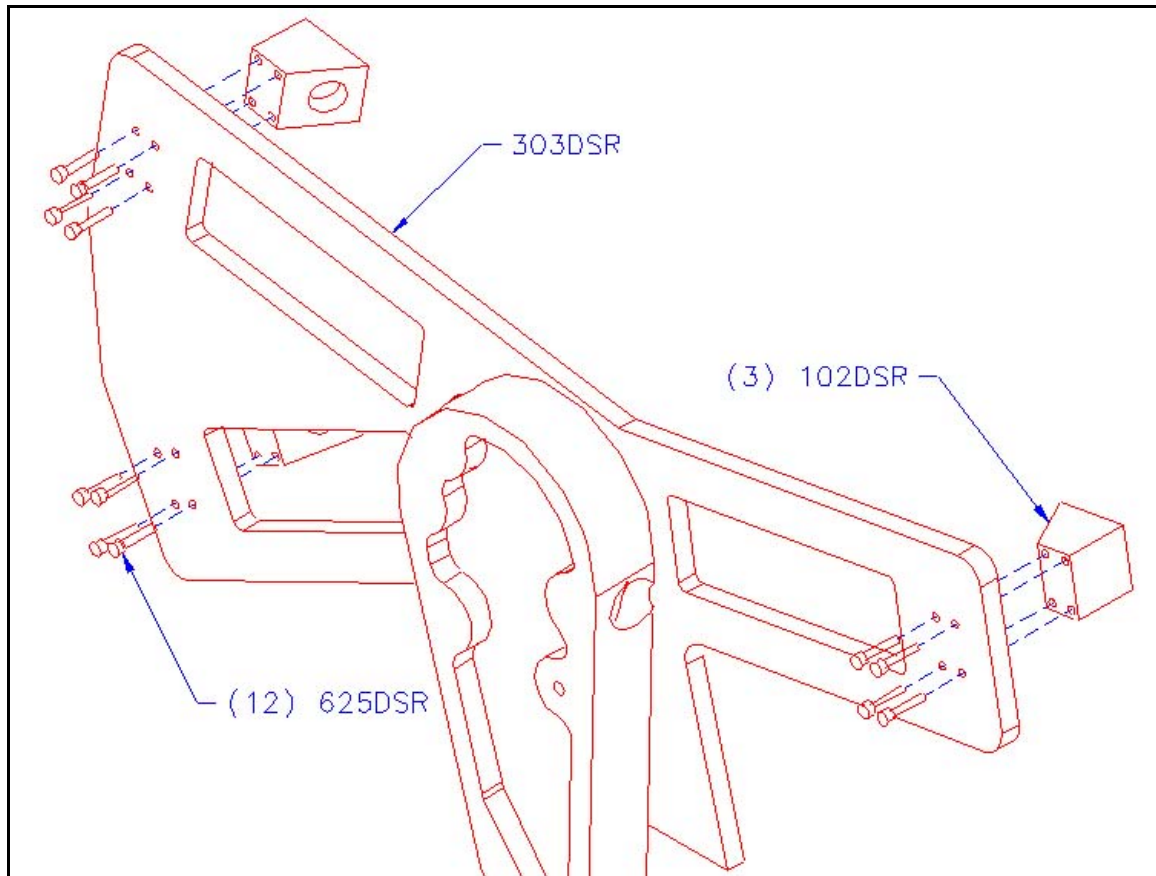


Figure 5-12: Installation of mounts for origins of scapula actuator.

Next, the three actuators for controlling the scapula are installed. All three actuators are identical to one another and the mounting hardware and procedure is also the same. Each actuator requires two THK balljoints (606DSR) and one locknut sleeve (624DSR) for complete installation. First, the nut sleeve is threaded onto one of the balljoints. Next, the open end of the nut sleeve is secured to the rod end of the actuator as shown in Figure 5-13. Then, the second balljoint is installed in the cylinder end of the actuator. Finally, the actuator is ready to connect the scapula to the mounting blocks. The balljoints are securely threaded into both the mounting block and the scapula. This procedure is repeated for the remaining two actuators as seen in Figure 5-13. It is noted at this point that the rod ends of the actuators are all pointing towards the scapula. This orientation of the cylinder remains constant for the rest of the installation of the hydraulic actuators. The bored end of the actuator is always oriented proximal to the thorax of the robot relative to its rod end.

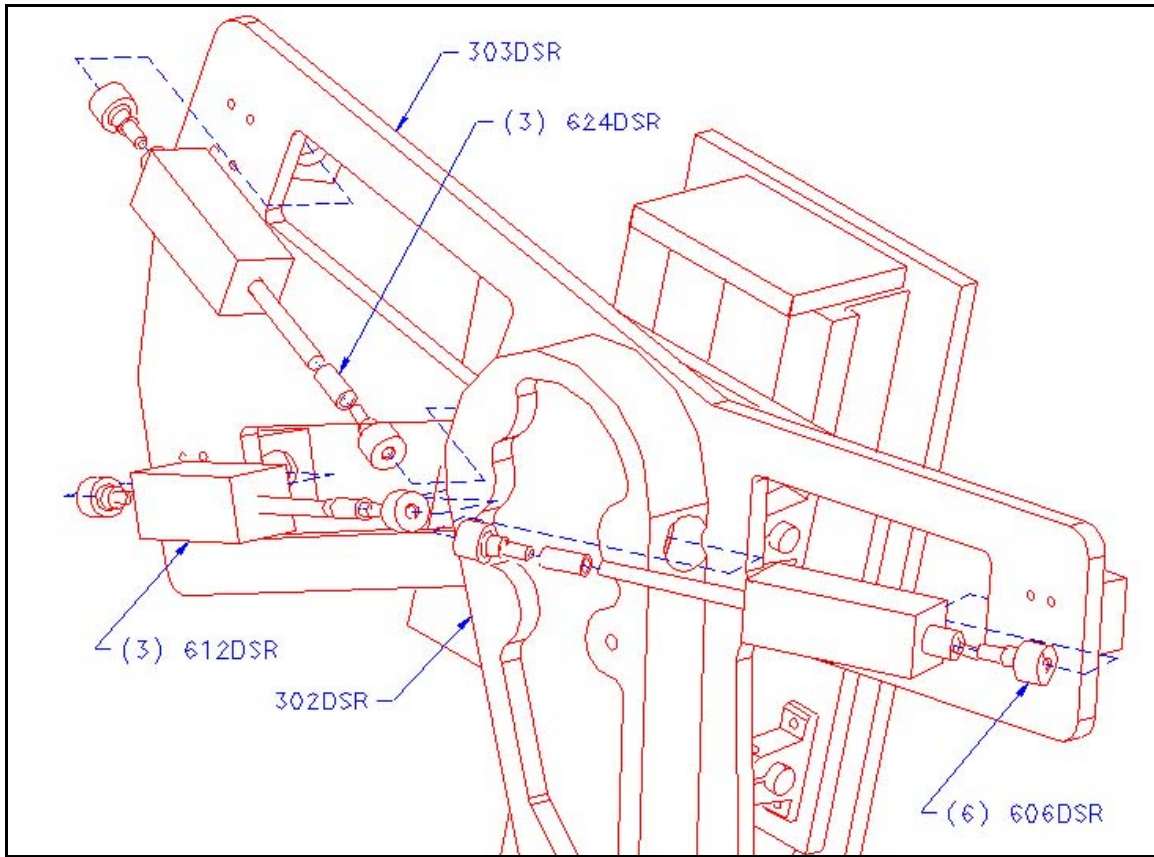


Figure 5-13: Installation of scapula actuators.

Similar to the previous joint, the scapula-humerus joint is controlled by three actuators. However, only two of the three actuators used to control the humerus relative to the scapula are the same. As before, balljoints are used to make the connection between the two structural members. The two identical actuators (611DSR) are both fitted with THK RBL8D balljoints on each end. However, the other actuator (613DSR) is fitted with the same balljoints used in the previous joint. The actuators are then connected to the humerus and scapula as demonstrated in Figure 5-14 using the balljoints. With these three actuators in place, the humerus can be controlled relative to the scapula as described in Chapter 3.

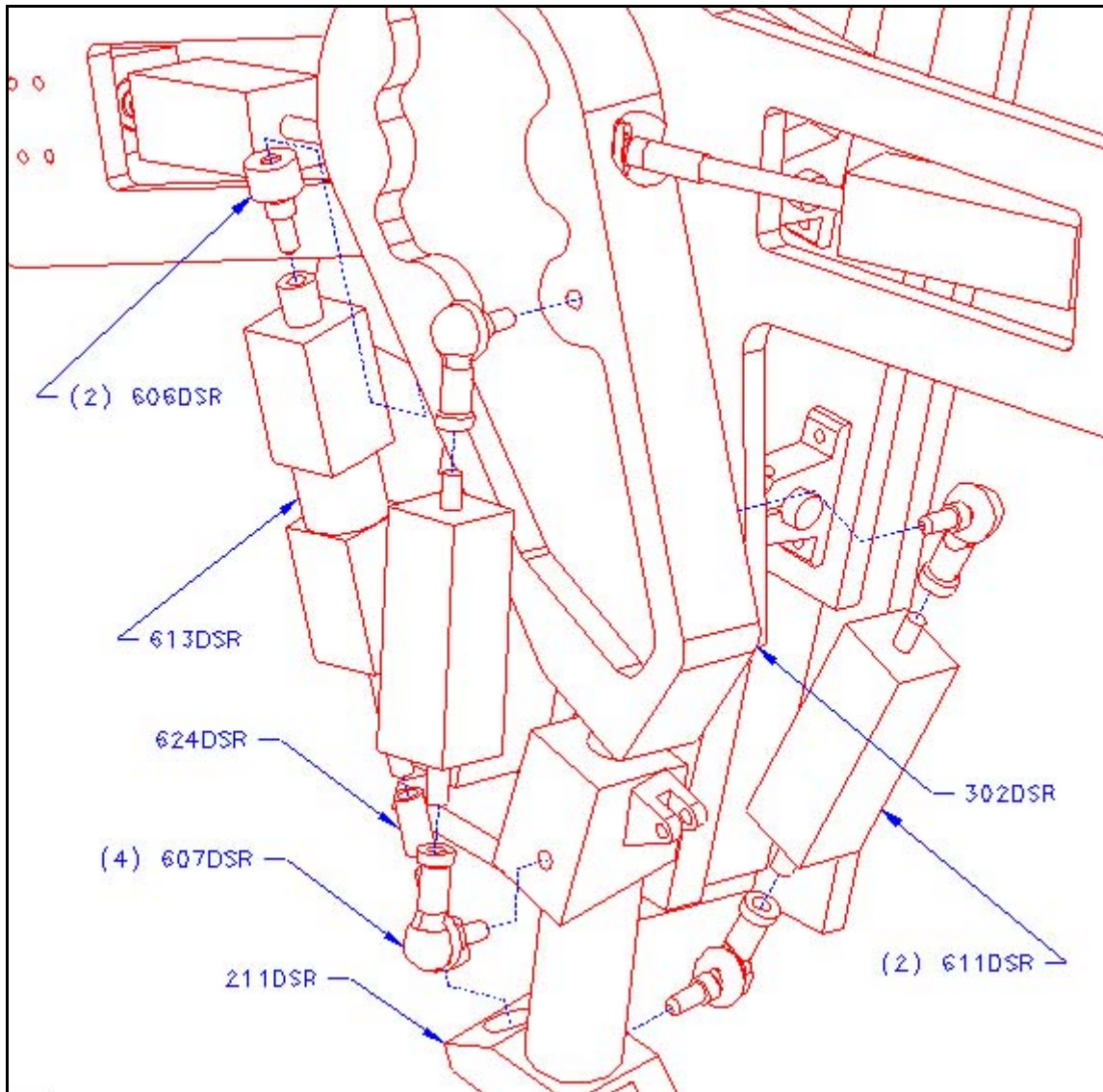


Figure 5-14: Installation of actuators for controlling the humerus.

The remaining joints of articulation are hinge joints. Therefore, the joints only need to be controlled about one degree of freedom as discussed earlier in Chapter 3. Balljoint attachments are not necessary to connect the remaining actuators since there is only one degree of freedom for each joint. Therefore, the actuators should be ordered with clevis attachments as their endpoints.

The actuator controlling the humerus-radius interface is fitted with a male clevis on each end of the hydraulic actuator. First, the origin of the actuator is located and held in place with a pin (113DSR). This pin is then secured using a cotter pin. Similarly, the insertion point of the actuator is positioned in its receiving slot of the radius and is retained in the same fashion as the origin of the actuator as shown in Figure 5-15.

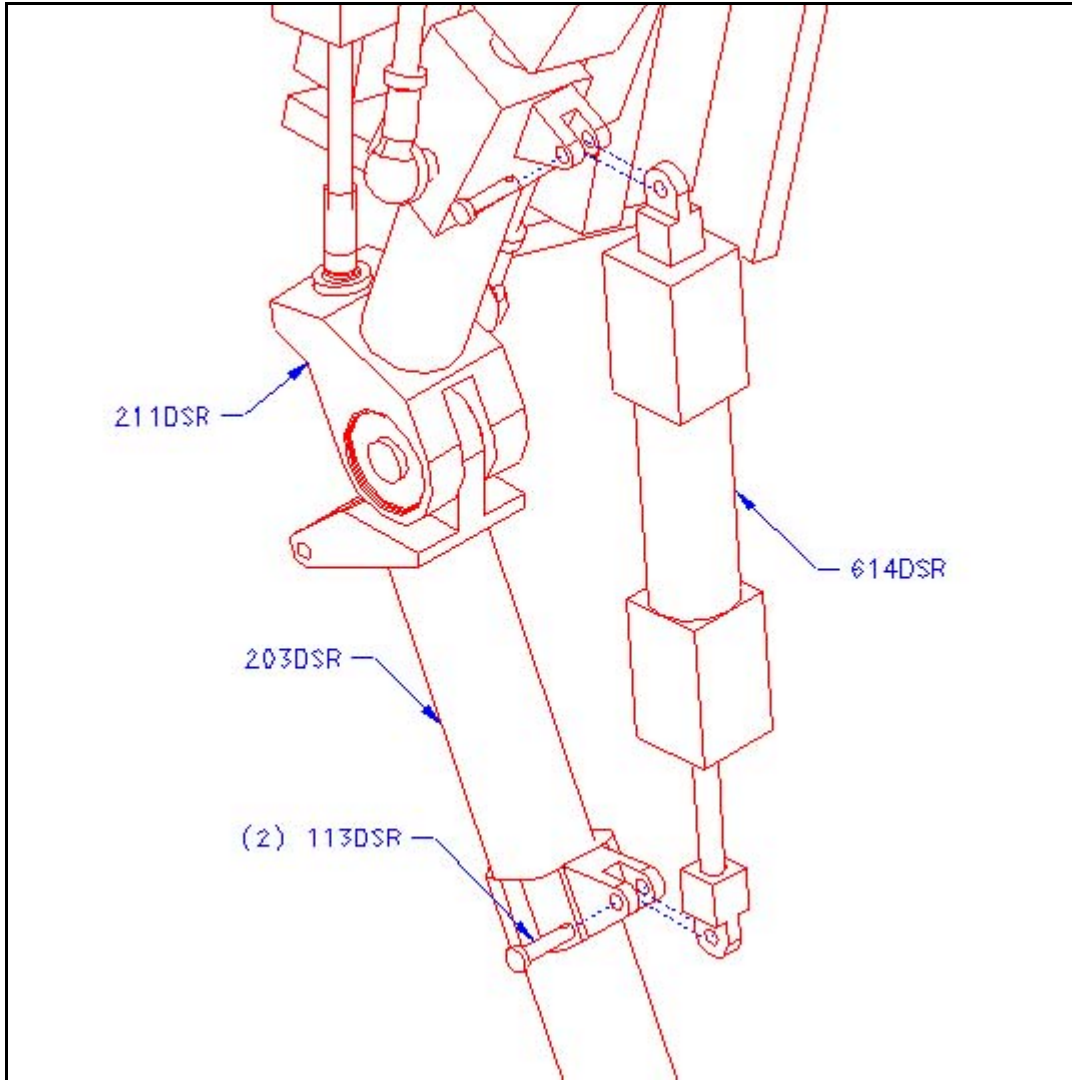


Figure 5-15: Installation of radius actuator.

The position of the carpus and the metacarpal are both controlled from the same origin as described in Chapter 1. Since they have a mutual point of origin, both the carpal and metacarpal actuators are installed at the same time. Their installation is the same as that of the previous actuator for the humerus-radius motion. This can be seen in Figure 5-16. However, consideration must be taken when inserting the pin (112DSR). This is because the pin has different diameters at each end to accommodate the different clevis attachments. Once the parts are inspected, it will be evident how the pin must be inserted.

The insertion point of the carpal actuator (615DSR) is then connected to the carpus using the appropriate pin (111DSR). Again, the process for connecting this actuator is identical to the previous installations as seen in Figure 5-17.

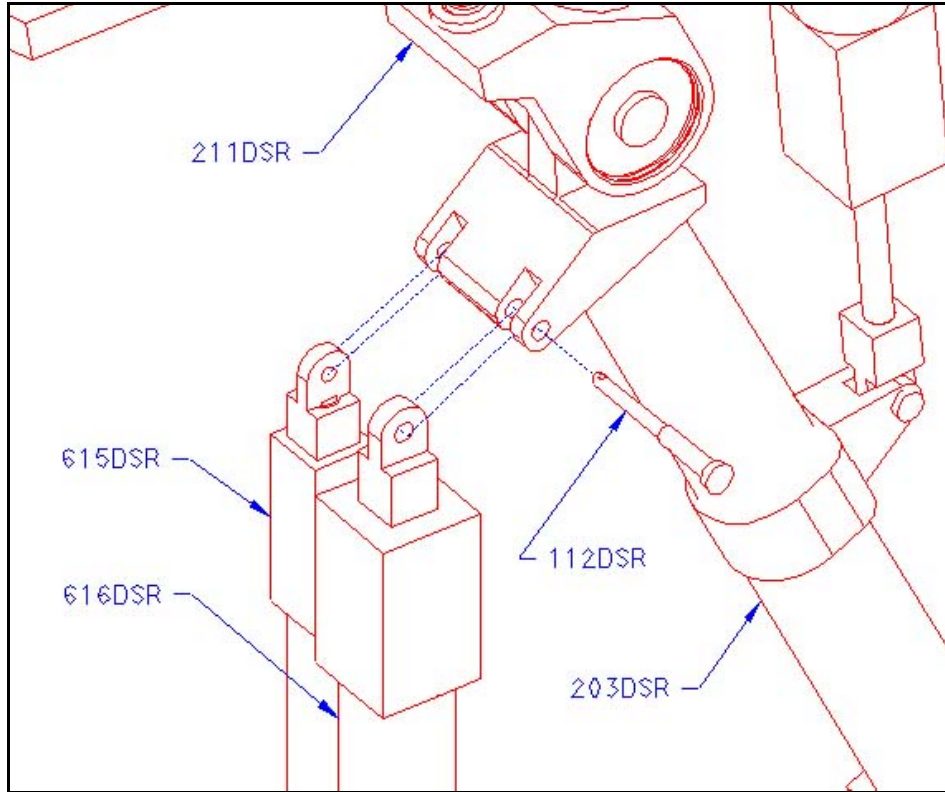


Figure 5-16: Assembly of origins of carpal and metacarpal actuators on the radius.

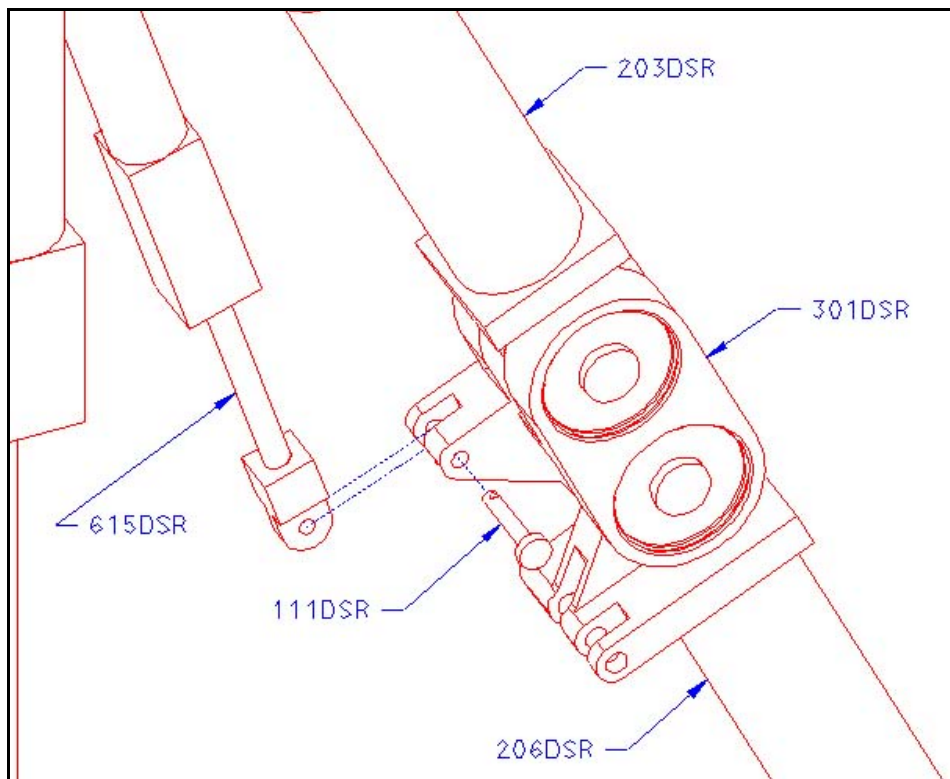


Figure 5-17: Installation of insertion point of carpal actuator.

Finally, the last actuator is installed. It is noted that the insertion end of the fetlock actuator (617DSR) has a female clevis instead of the typical male clevis. The first step to installing this actuator is to position both the insertion point of the metacarpal actuator (616DSR) and the origin of the fetlock actuator in their proper receiving slots. Next, they are secured as where the previous actuators. Finally, the insertion end of the last actuator is retained as shown in Figure 5-18. This completes the installation of the actuators.

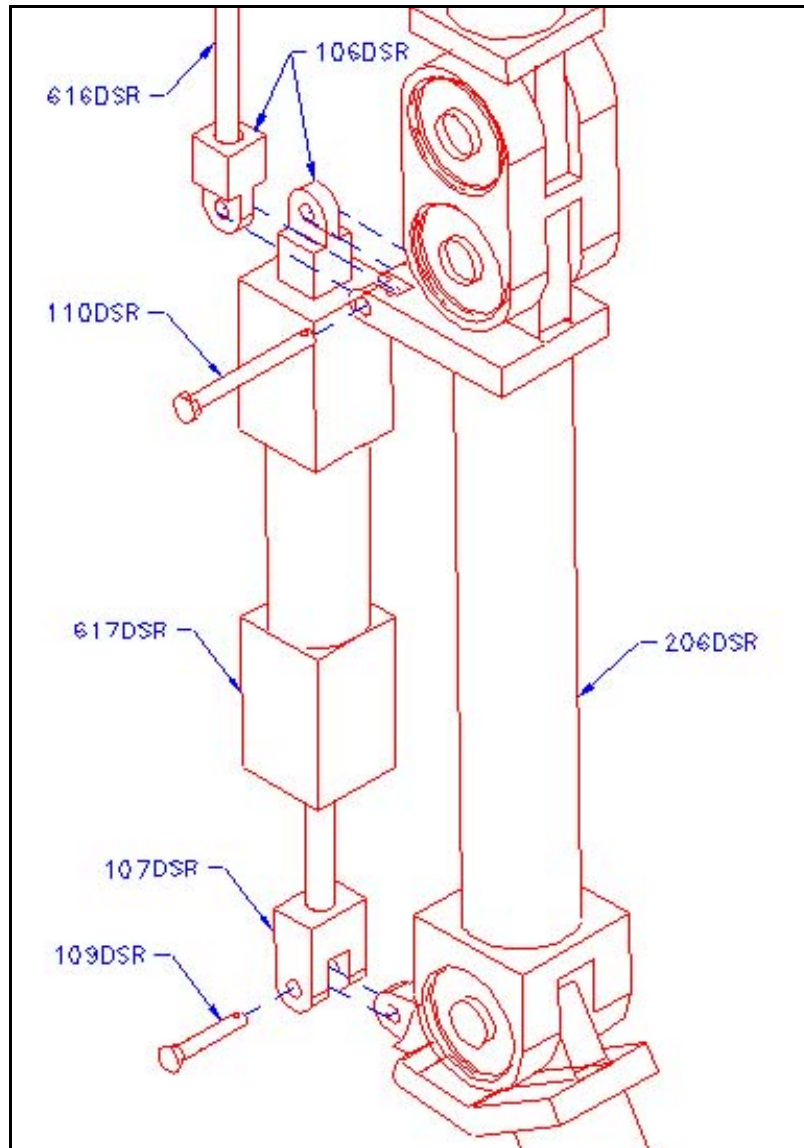


Figure 5-18: Installation of fetlock actuator and insertion point of metacarpal actuator.

With the actuators installed as shown in Figure 5-19, the remaining portion of the hydraulic system is assembled. This portion of the system includes the accumulator, pump, servo-actuated valves, hydraulic lines and fittings, and oil. Due to the variety in manufactures of hydraulic cylinders, this thesis does not include the specification of the hydraulic system. Therefore, the specifics of the remaining fraction of the system have been left for future work. It will, however, be noted here that the hydraulic pump, accumulator, and valves are

5 Construction of Robotic Replica

remotely located as to minimize the weight of the robotic forelimb. The pressurized oil will be carried through the hydraulic lines from the remote station to each actuator for controlling the robot.

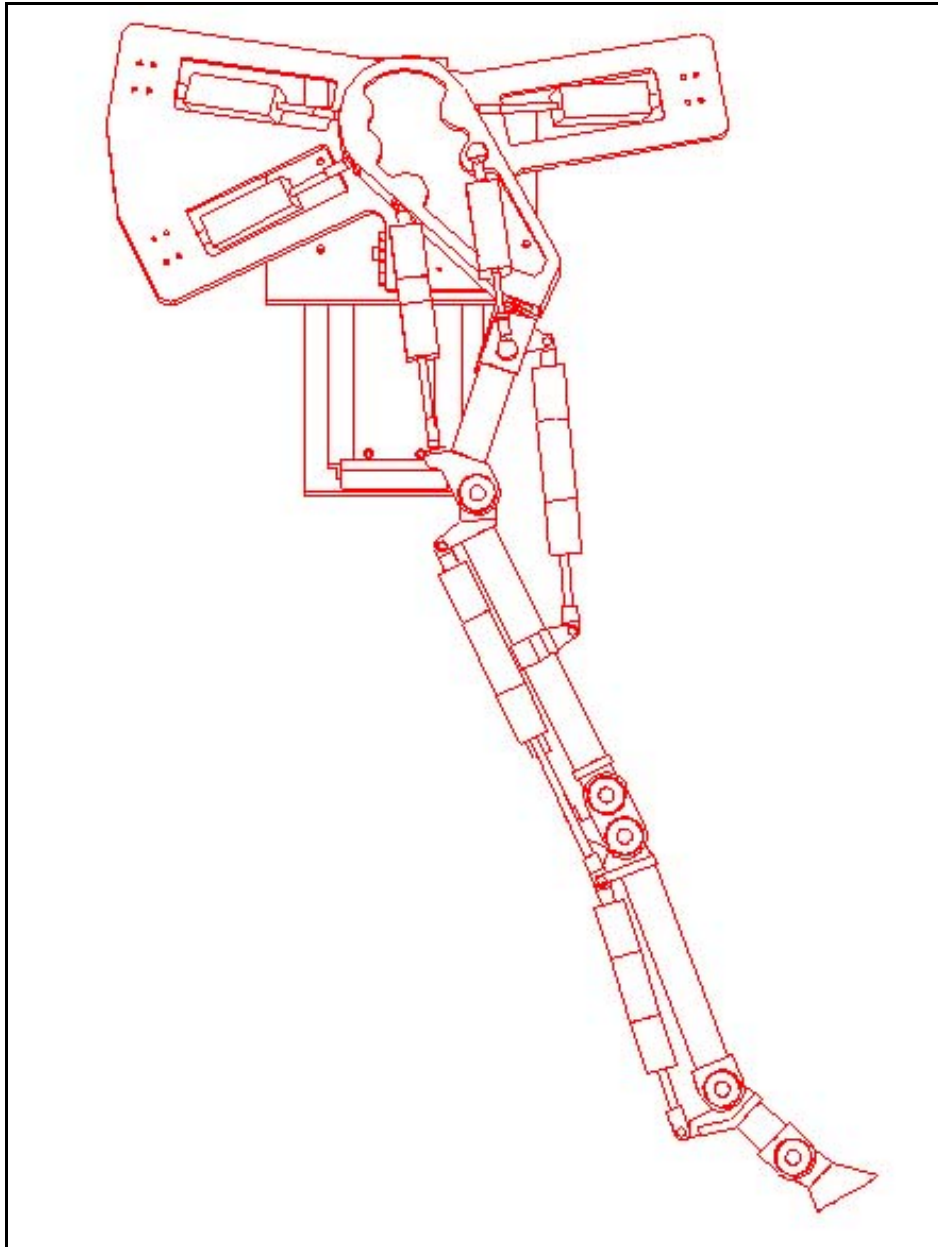


Figure 5-19: Assembled robotic replica with hydraulic actuators.

6 Conclusion and Recommendations

A load-bearing, bioassistive device has been proposed to reduce the incidence of angular limb deformities and gait abnormalities in foals with limb fractures. The proposed collateral load-bearing device discussed in Chapter 1 allows for a sufficient range of articulation of all of the joints in the forelimb to support physical exercise and therapy. The structure of this device is relatively unobtrusive and designed from common materials and parts thus reducing the overall cost. Additionally, a cradle for transferring the load of the foal off of the injured limb and through the device has been considered and a preliminary design drafted. This cradle addresses the issues of skin abrasion and ischemia through material and structural design and control methods. The load-bearing device will be simple to operate and the total weight kept to a minimum. The low weight is achieved through material selection and locating all of the auxiliary equipment, such as valves, pumps, accumulators, and other external components, in a closed box remotely to the animal, such as the stall ceiling. This rehabilitative device will also be highly adaptive allowing for the rapid growth of the foal during convalescence and a variety of foal geometries.

The assistive device will be developed around a robotic replica of a foal's limb. Developing the device around a robot forestalls the possibility of injuring a foal in the preliminary stages of the devices maturation. Also, a robotic replica allows the investigator total control of both the limb and the bioassistive device throughout testing and optimization.

Through my preliminary investigations, I found that a robotic replica of a foal's forelimb was not available for testing load-bearing devices. In addition, I couldn't find a commercial method of replicating the motion of the scapula, which is completely suspended by muscle and void of any skeletal connection to the thorax. Therefore, to facilitate the complete testing of the load-bearing device, a robotic replica has been designed with all of the significant functional degrees of freedom required of the limb and capable of mimicking the forelimb kinematics anticipated during convalescence. This design includes a scapula-thorax joint with five degrees of freedom to closely mimic the natural motion of the scapula in its muscular cradle.

The analysis in this thesis strongly supports the claim that the designed replica can reproduce trot and walk as required for testing the bioassistive device. The finite element analysis demonstrated the structural integrity of the robotic replica by ensuring that the anticipated stress during trot is below the yield strength of the selected materials. The FEA model used a static situation to calculate the joint reaction forces for use in the stress analysis. A more accurate model would have used a d'Alembert analysis to calculate the dynamic joint reaction forces. These forces will differ from the static forces used in this analysis and therefore leave the analysis here in question. Before an investment is made in constructing a robotic replica, it would be prudent to perform a full finite element analysis using the closed loop control forces and the dynamic joint reaction force in a dynamic FEA model with the limb segment in motion. Nevertheless, the crude analysis performed herein indicates that the design is adequate for the intended purpose.

In addition to the FEA, dynamic control simulations were performed for both walk and trot. The resulting motion of the closed-loop control system was in reasonable agreement with the collected data.

Once the robotic replica is constructed, an assistive device can be designed around this replica allowing full control over the motion of replica and device alike. After successful performance has been assured on the robotic replica, the design can then be optimized for weight, fitting, obtrusiveness, cost, and subsequently readied for actual clinical trials.

6.1 Alternative Application of Current Work

As a result of this thesis, it has been proven that is feasible to construct a robotic replica to replicate trot and walk of a foal. This work was done to allow for the future construction of a robotic replica. This replica will then be used for the development of a collateral load-bearing device. However, the work from this paper can also be used to aid in diagnosing forelimb injuries in addition to building a physical representation of a foal's forelimb.

With a soft tissue injury, the horse will sense pain if it attempts to overload the tissue. Therefore, the peak force allowable in that tissue will be reduced. This soft tissue could be muscles, tendons, or ligaments. With the reduced capacity to carry the load in the tissue, the horse will not be able to reproduce the correct motion of gait. The motion of the injured limb will be adjusted to reduce the resulting force in the injured tissue to a level of tolerable pain. Therefore, if one collected angular position data of the ensuing gait, one could determine the required forces to generate such motion. With the kinematics of the injured limb revealed, an inverse dynamic analysis can be performed as developed in this thesis. Using the code from Appendix A, the forces required for the motion could be determined. With the required forces discovered, they could be investigated and compared with the forces associated with normal gait. From this comparison, the injury could be isolated to a particular muscle group. The location of the injured tissue would now be known.

With the knowledge of the location of the injured muscle group further investigation of the injured limb would be necessary to isolate the exact injured tissue. With this collective knowledge, the injury could be properly treated by the veterinarian. However, a properly trained equine specialist can determine the injured region through a simple inspection. This is achieved from anatomical knowledge of the limbs and experience with previous injuries. Therefore, collecting gait data as describe above to determine the required forces to replicate the gait of an injured horse could be used to mimic the injury in the designed robotic replica for training purposes. This idea is discussed in a little more detail in the following section which discusses the possibility of continuation of this research.

6.2 Future Work

The closed-loop forces required to replicate gait in the robotic replica are not the same as those determined through the inverse dynamics. However, the determined forces are acceptable for producing trot and walk for the purpose of testing a load-bearing rehabilitative device.

The ground is modeled as a varying force on the hoof. One can image that as the position of the hoof deviates from the ground plane that the force on the hoof should also deviate from that of the desired gait. However, this model does not account for the position of the ground, but the force that the ground is supposed to be producing. An alternative

6 Conclusion and Recommendations

model to the one generated here would not apply a ground reaction force, but incorporate a surface with a stiffness to simulate an actual ground. With the absence of an applied ground reaction force, force on the scapula from the rest of the horse would have to be applied instead of varied. This model would more closely represent the physical model. Nevertheless, the current model seems to predict the forces within a reasonable range. Noting the difference between the open-loop and closed-loop force in stance and during swing (cf. Figure 4-13 and 4-15) it is noted that the lack of a 'true' ground does not cause problems with the closed-loop model.

An immense improvement in the control forces of the replica was seen from the change from the position controller to the position velocity controller. Hence, one could assume that an improvement in the difference between the predicted forces and the required forces would be seen by including the acceleration into the control feedback. Therefore, to accurately replicate equine motion using forces closer to the predicted forces, a controller should be developed that includes position, velocity, and acceleration feedback. Even though the closed-loop forces are not the exactly the same as the predicted forces, they are close enough to replicate gait using the designed robot.

Due to lack of funding the robotic replica has not been constructed. The total estimated cost to build the robotic replica is approximately \$16000. The structure assembly of the replica accounts for roughly 60 percent of the cost. The machined parts were quoted at about \$9000 by the Engineering Science and Mechanics machine shop. In addition, the hydraulic system will cost approximately \$4000 because most of the actuators have to be custom built due to size requirements and availability. However, once funding is accrued the construction of the robotic assembly can begin as described in Chapter 5.

With a completed robotic replica the development of the collateral load-bearing device can begin as discussed in Chapter 1. However, there is potential to use the robotic replica to facilitate the development of other rehabilitative devices and investigate equine gait.

Laminitis (founder) is another problem that can occur in the limbs of horses. The situation, laminitis, results in the separation of the *laminae dermis* and *epidermis*. This separation allows the tendons to rotate the cranial point of the distal phalanx down into the sole of the hoof. Once this rotation ensues, the foot drops or founders as a ship's captain would say as the vessel sinks. To alleviate the damage while the horse heals, a brace could be used to partially or completely offload the fetlock. This brace would transfer the load from the metacarpal through the padded brace and then to the ground. In order to test the effectiveness of this device prior to implementation, the robotic replica could be modified slightly to accommodate the testing of the brace. This accommodation would come about through the addition of foam inserts and a synthetic skin to replicate more closely the shape and texture of the metacarpal of a horse. Implanting sensors in the synthetic skin would allow a researcher to determine the shear forces on the skin and also the effectiveness of offloading the fetlock.

Other possible uses of the robotic replica could be the replication of soft tissue injuries in the forelimb. For example, if a horse injures a particular muscle or muscle group, the maximum forces in the actuators could be restricted. This restriction would be based on the magnitude of the injury; severed tendon, torn muscle, or other soft tissue injuries. With the injury specified, the peak force of the actuators could be determined and gait attempted. The control algorithm would move the limb through the particular motion. However, as the

6 Conclusion and Recommendations

peak forces of the actuators are encountered, the motion of the limb would be adjusted accordingly to complete the stride. This adjustment might involve increases in actuator forces on other limb sections. Based on the magnitude of these increased forces, one might be able to determine if the resulting motion would be possible. Once the motion is determined feasible, the resulting gait could be investigated and compared with known forelimb injuries. With the motion of the simulated injury confirmed, this simulation of injuries could be used for education of equine specialist to speed diagnosing of limb injuries.

Glossary of Terms

- abduction: to draw away from the midline of the body or from an adjacent part or limb.
- adduction: to draw inward toward the median axis of the body or toward an adjacent part or limb.
- anesthetized: rendered insensible/unconscious by means of general anesthesia.
- articulation: a fixed or movable joint between bones.
- bioassistive: providing assistance for a biological organism.
- cannon bone: the section of the lower leg between the hock or knee and the fetlock, the third metacarpal bone.
- canter: a smooth gait that is slower than a gallop but faster than a trot.
- carpal joint: the articulation of the carpus; there are three (two movable) joints in the carpus.
- carpus: the group of eight bones forming the joint between the radius and the metacarpals.
- cartilage: a tough, elastic, fibrous connective tissue found in various parts of the body, such as the joints.
- castration: the removal of the testicles of a male.
- caudal: of, at, or near the tail or hind parts; posterior.
- clavicle: one of the bones of the pectoral girdle in many vertebrates.
- coffin: distal interphalangeal joint.
- cranial: of or relating to the skull or cranium.
- descending pectorals: the superficial part of the flat muscle extending from the sternum to the cranial surface of the humerus.
- distal: anatomically located far from a point of reference; in quadrupeds, away from the trunk.
- distal interphalangeal joint: the connection of the middle and distal phalanges; coffin joint.
- distal sesamoid bone: the furthest most, small modular bone which developed in a tendon of the forelimb; navicular bone.
- dorsal: of, toward, on, in, or near the back or upper surface of an organ, part, or organism. In horses, the “front” of the limb surface between the ground and the carpus.
- elbow joint: a hinge joint between the forearm (radius and *ulna*) and upper arm (humerus) marked by the protrusion of the *olecranon*.
- fetlock: metacarpophalangeal joint or region thereabouts.
- digit: a projection on the lower part of the leg, composed of the phalanges.
- glenoid cavity: the concavity in the head of the scapula that receives the head of the humerus to form the shoulder joint.

humerus: the long bone extending from the shoulder to the elbow.

intercostals: a space, muscle, or part situated between the ribs.

ischemia: a decrease in the blood supply to a bodily organ, tissue, or part caused by pressure, constriction or obstruction of the blood vessels.

laminae: the thin layers of sensitive vascular tissue in the hoof.

laminar dermis: inner lay of laminae containing sensitive vascular tissue.

laminar epidermis: outer, protective, nonvascular layer of lamina.

laminitis: inflammation and breakdown of the sensitive *laminae* of the hoof.

lumbar: of, near, or situated in the part of the back and sides between the lowest ribs and the pelvis.

meshing: The formation of a network of elements in a model to be analyzed by finite element analysis.

Metacarpus: a bone that lies between the knee (carpus) and the fetlock in the forelimb.

musculoskeletal: relating to or involving the muscles and the skeleton.

necrosis: death of cells or tissues through injury or disease.

olecranon: the large process on the upper end of the ulna that projects behind the elbow joint and forms the point of the elbow.

Omotransversarius: the muscle that extends from the shoulder region to the cervical vertebrae.

ossification: the hardening or calcification of soft tissue into a bonelike material.

palmar: of, relating to, or corresponding to the bottom of the hoof (or solar). Also the “back” surface of the limb distal to the carpus.

pastern: the part of a horse's foot between the fetlock and hoof.

pastern joint: proximal interphalangeal joint.

proximal: nearer to a point of reference such as an origin, a point of attachment, or the midline of the body.

proximal interphalangeal joint: the connection of the proximal and middle phalanges.

protraction: the act of extending or protruding.

Proximal Phalanx: the bone in the fetlock that is adjacent to the metacarpal.

Radius: The preaxial bone of the forelimb spanning between the elbow and the carpus’.

retraction: the act of drawing back or in.

raphe: a seam like line or ridge between to similar parts of a body.

Rhomboids: the extrinsic muscle extending from the median *raphe* of the neck, thoracic vertebral spines, and the skull to the dorsal border of the scapula and scapular cartilage.

saddle joint: a part which is hollowed out to fit upon a convex surface and serve as a means of attachment or support.

sagittal plane: a longitudinal plane that divides the body or part thereof of a bilaterally symmetrical animal into right and left sections.

scapula: either of two large, flat, triangular bones forming the proximal aspect of the shoulder.

Serratus Ventralis: the serrated, fan shaped muscle extending from the last five cervical vertebrae and the first seven thoracic and first seven or eight ribs to the medial surface of the scapula.

shoulder joint: a ball-and-socket joint between the head of the humerus and a cavity of the scapula also scapulohumeral joint.

sternum: a long flat bone that is situated along the ventral midline of the thorax and articulates with the ribs.

tendon: a band of tough, inelastic fibrous tissue that connects a muscle with its bony attachment.

thoracic: of, relating to, or situated in or near the thorax.

thorax: the part of vertebrates between the neck and the diaphragm, partially encased by the ribs and containing the heart and lungs; the chest.

Trapezius: the triangular muscle extending from the dorsal-medial neck and thorax to the spine of the scapula.

trot: the gait between a walk and a canter in speed, in which diagonal pairs of legs move forward together

ulna: the bone extending from the elbow to the 'knee' with the Radius.

Valgus: a deformity in which the hoof is turned abnormally outward; displace outward from the centerline of the body.

Varus: a deformity of the leg causing them to bend inward.

ventrally: relating to or situated on or close to the abdomen. Opposite of dorsal or toward the topline in a quadruped

References

- [1] Allen, D., "Equine Fracture Management and Repair", *Musculoskeletal Diseases of Large Animals LMS 536*, Department of Large Animal Medicine, University of Georgia, Athens, GA, March 1996
- [2] Auer, J., *Angular Limb Deformities in Equine Surgery*, Philadelphia, W.B. Saunders, 1999.
- [3] Back, W., Clayton, H., *Equine Locomotion*, W.B. Saunders, 2001.
- [4] Cohen, N.D., Peloso, J.G., Mundy, G.D., et al, "Racing Related Factors and Results of Pre-race Physical Inspection and their Association with Musculoskeletal Injuries Incurred in Thoroughbreds during Racing", *Journal of American Veterinary Medical Association*, pp. 454-463, 1997.
- [5] Dankowicz, H., *Mechanics Problems and their Solutions*, Stockholm, Sweden: Department of Mechanics of the Royal Institute of Technology, 1998.
- [6] Dorf, R.C., Bishop, R.H., *Modern Control Systems*, 9th Edition, Prentice Hall, 2001
- [7] Dušek, J., Ehrlein, H.-J., Engelhardt, W.V. and Hornicke, H., "Beziehungen zwischen Trittlänge, Trittfrequenz und Geschwindigkeit bei Pferden", *A Tierzucht ZuchtBiol*, 1970.
- [8] Hynes, P.F., Robinson, R.A., "Racetrack Breakdown Pilot Study Summary", *34th Annual American Association of Equine Practitioners*, pp. 673-676, 1988.
- [9] King, C., Mansmann, R., *Equine Lameness*, Equine Research Inc., Texas, 1997.
- [10] Kobluk, C.N., "Epidemiologic Studies of Racehorse Injuries", *Current Techniques in Equine Surgery and Lameness*, Philadelphia, W.B. Saunders, pp.564-569, 1998.
- [11] Martin, R.B., Burr, D.B., Sharkey, N.A., *Skeletal Tissue Mechanics*, Springer, 1998.
- [12] McKee, S.L., "An Update on Racing Fatalities in the UK", *Equine Veterinarian Education*, 7, pp. 202-204, 1995.
- [13] Mohammed, H.O., Hill, T., Lowe, J., "Risk Factors Associated with Injuries in Thoroughbred Horses", *Equine Veterinary Journal*, supplement #23, pp. 445-448, 1991.
- [14] Mueller, E., "Equine Distal Limb Fractures", *Musculoskeletal Diseases of Large Animals LMS 536*, Department of Large Animal Medicine, University of Georgia, Athens, GA, March 1996.
- [15] Pasquini, C., Spurgeon, T., and Pasquini, S., *Anatomy of Domestic Animals*, 8th edition, Sudz Publishing, Texas, 1995.
- [16] Peloso, J.G., Mundy, G.D., Cohen, N.D., "Prevalence of and Factors Associated with Musculoskeletal racing injuries of Thoroughbreds during Racing", *Journal of American Veterinary Medical Association*, pp. 620-626, 1994
- [17] Porter, N., *Webster's Revised Unabridged Dictionary*, MICRA, Inc, New Jersey, 1998

- [18] Schamhardt, H.C., Clayton, H.M., and Wade, J.F., "Proceedings of the Second International Workshop on Animal Locomotion," *Equine Veterinary Journal*, Supplement #17, pp. 51-55, June 1994.
- [19] Smythe, R.H., "The Horse: Structure and Movement", *J. Allen & Co, Ltd.*, 2nd ed., 1972.
- [20] White, N. A., "Fracture of the Equine Forelimb", *Equine Medicine & Surgery 1 VM 8695*, Marion duPont Scott Equine Medical Center, Leesburg, Virginia, 2002.
- [21] Wilson, A. M., "The effect of exercise intensity on the biochemistry, morphology and mechanical properties of tendon", *PhD. Thesis*, University of Bristol, UK, 1991.

Appendix A: Computer Codes

Code for performing an inverse dynamic analysis of the robot.

```
> with(SophiaLight):
> Restart():
> DeclareRotationList([n,torso,1,evalf(Pi/12)], [n,o1,1,q3], [o1,o2,2,q4], [o2,a,3,q5], [n,b1,1,q6
], [b1,b2,2,q8], [b2,b,3,q7], [n,c,3,q9], [n,d,3,q10], [n,e,3,q11], [n,f,3,q12]):
> ptable:=matrix(7,25,[-0.0296,-0.0422,0.0275, 0.0267,-0.1201,-0.0085, 0.0685,-
0.1449,0.0065, -0.0425,-0.0726,-0.0024, -0.0522,-0.1765, 0.0329,-0.1899, -0.0016,-0.0252,
0.0016,-0.0248, -0.0300,-0.1677, 0.0300,-0.1353, -0.0015],
[-0.0959, 0.0075,-0.0849, 0.2941,0.0514,0.0579, -0.2514,-0.1093,0.0579, 0.3138,-
0.1323,0.0579, 0.0725,-0.0765,-0.0183, -0.0566,-0.0601,-0.0191, 0.0575,-0.122,-0.0134,
0.0539,-0.0094,-0.0190, -0.0397],
[-0.0033,-0.0575, -0.0368,0.1092,0.0195, -0.0023,0.0545,-0.0573, -0.0003,0.1924,0.0358,
0.0348,0.1919,-0.0052, -0.0413,0.0319,-0.0052, -0.0269,0.1844, 0.0609,0.0349, -0.0007,0.3864,
0.0453,0.0225],
[0.0200,0.0210, 0.0200,0.0290, 0.0415,0.0360, -0.0200,-0.0200, 0.0659,0.0060,
0,0,0,0,0,0,0,0,0,0,0,0,0,0,0,0,0,0,0],
[5.507,0.04093,0.00660,0.00122,0.00660,0.02248,-0.00271,0.00122,-0.00271,0.05916,
3.026,0.01654,-0.00619,-0.00024,-0.00619,0.00922,0.00033,-0.00024,0.00033,0.02478,
3.686,0.03956,0.00065,-0.00016,0.00065],
[0.00275,0.00007,-0.00016,0.00007,0.03983,
0.617,0.00057,0.00000,0.00002,0.00000,0.00030,0.00000,0.00002,0.00000,0.00055,
2.666,0.02266,-0.00009,0.00001,-0.00009,0.00153,0.00003,0.00001,0.00003,0.02352],
[0.882,0.00207,-0.00033,0.00000,-0.00033,0.00054,0.00000,0.00000,0.00000,0.00206, 9.81,
3.000,0.03000,0.03000,0.03000,0,0,0,0,0,0,0,0,0,0,0,0,0]):
> eqs:=[p1=ptable[1,1], p2=ptable[1,2], p3=ptable[1,3], p4=ptable[1,4], p5=ptable[1,5],
p6=ptable[1,6], p7=ptable[1,7], p8=ptable[1,8], p9=ptable[1,9], p10=ptable[1,10],
p11=ptable[1,11], p12=ptable[1,12], p13=ptable[1,13], p14=ptable[1,14], p15=ptable[1,15],
p16=ptable[1,16], p17=ptable[1,17], p18=ptable[1,18], p19=ptable[1,19], p20=ptable[1,20],
p21=ptable[1,21], p22=ptable[1,22], p23=ptable[1,23], p24=ptable[1,24], p25=ptable[1,25],
p26=ptable[2,1], p27=ptable[2,2], p28=ptable[2,3], p29=ptable[2,4], p30=ptable[2,5],
p31=ptable[2,6], p32=ptable[2,7], p33=ptable[2,8], p34=ptable[2,9], p35=ptable[2,10],
p36=ptable[2,11], p37=ptable[2,12], p38=ptable[2,13], p39=ptable[2,14], p40=ptable[2,15],
p41=ptable[2,16], p42=ptable[2,17], p43=ptable[2,18], p44=ptable[2,19], p45=ptable[2,20],
p46=ptable[2,21], p47=ptable[2,22], p48=ptable[2,23], p49=ptable[2,24], p50=ptable[2,25],
p51=ptable[3,1], p52=ptable[3,2], p53=ptable[3,3], p54=ptable[3,4], p55=ptable[3,5],
p56=ptable[3,6], p57=ptable[3,7], p58=ptable[3,8], p59=ptable[3,9], p60=ptable[3,10],
p61=ptable[3,11], p62=ptable[3,12], p63=ptable[3,13], p64=ptable[3,14], p65=ptable[3,15],
p66=ptable[3,16], p67=ptable[3,17], p68=ptable[3,18], p69=ptable[3,19], p70=ptable[3,20],
p71=ptable[3,21], p72=ptable[3,22], p73=ptable[3,23], p74=ptable[3,24], p75=ptable[3,25],
p76=ptable[4,1], p77=ptable[4,2], p78=ptable[4,3], p79=ptable[4,4], p80=ptable[4,5],
p81=ptable[4,6], p82=ptable[4,7], p83=ptable[4,8], p84=ptable[4,9], p85=ptable[4,10],
p86=ptable[4,11], p87=ptable[4,12], p88=ptable[4,13], p89=ptable[4,14], p90=ptable[4,15],
p91=ptable[4,16], p92=ptable[4,17], p93=ptable[4,18], p94=ptable[4,19], p95=ptable[4,20],
p96=ptable[4,21], p97=ptable[3,22], p98=ptable[4,23], p99=ptable[4,24],
p100=ptable[4,25], mA=ptable[5,1], IA11=ptable[5,2], IA12=ptable[5,3], IA13=ptable[5,4],
IA21=ptable[5,5], IA22=ptable[5,6], IA23=ptable[5,7], IA31=ptable[5,8], IA32=ptable[5,9],
IA33=ptable[5,10], mB=ptable[5,11], IB11=ptable[5,12], IB12=ptable[5,13], IB13=ptable[5,14],
IB21=ptable[5,15], IB22=ptable[5,16], IB23=ptable[5,17], IB31=ptable[5,18], IB32=ptable[5,19],
IB33=ptable[5,20], mC=ptable[5,21], IC11=ptable[5,22], IC12=ptable[5,23], IC13=ptable[5,24],
IC21=ptable[5,25], IC22=ptable[6,1], IC23=ptable[6,2], IC31=ptable[6,3], IC32=ptable[6,4],
IC33=ptable[6,5], mD=ptable[6,6], ID11=ptable[6,7], ID12=ptable[6,8], ID13=ptable[6,9],
ID21=ptable[6,10], ID22=ptable[6,11], ID23=ptable[6,12], ID31=ptable[6,13],
ID32=ptable[6,14], ID33=ptable[6,15], mE=ptable[6,16], ID11=ptable[6,17], ID12=ptable[6,18],
ID13=ptable[6,19], ID21=ptable[6,20], IE22=ptable[6,21], ID23=ptable[6,22],
ID31=ptable[6,23], ID32=ptable[6,24], IE33=ptable[6,25], mF=ptable[7,1], ID11=ptable[7,2],
ID12=ptable[7,3], ID13=ptable[7,4], ID21=ptable[7,5], IF22=ptable[7,6], IF23=ptable[7,7],
IF31=ptable[7,8], IF32=ptable[7,9], IF33=ptable[7,10], g=ptable[7,11], mO=ptable[7,12],
IO11=ptable[7,13], IO22=ptable[7,14], IO33=ptable[7,15]]:
> rN01:=CreateVector(q1,q2,0,n):
rO100:=subs(eqs,CreateVector(p86,p87,p88,torso)):
rO002:=subs(eqs,CreateVector(p89,p90,p91,torso)):
rA1A0:=subs(eqs,CreateVector(p1,p2,p3,a)):
```

```

rA0A2:=subs (eqs,CreateVector (p4,p5,p6,a)) :
rB1B0:=subs (eqs,CreateVector (p7,p8,p9,b)) :
rB0B2:=subs (eqs,CreateVector (p10,p11,p12,b)) :
rC1C0:=subs (eqs,CreateVector (p13,p14,0,c)) :
rC0C2:=subs (eqs,CreateVector (p15,p16,0,c)) :
rD1D0:=subs (eqs,CreateVector (p17,p18,0,d)) :
rD0D2:=subs (eqs,CreateVector (p19,p20,0,d)) :
rE1E0:=subs (eqs,CreateVector (p21,p22,0,e)) :
rE0E2:=subs (eqs,CreateVector (p23,p24,0,e)) :
rF1F0:=subs (eqs,CreateVector (p25,p26,0,f)) :
rF0F2:=subs (eqs,CreateVector (p27,p28,0,f)) :
rOS1:=subs (eqs,CreateVector (p29,p30,p31,torso)) :
rOS2:=subs (eqs,CreateVector (p32,p33,p34,torso)) :
rOS3:=subs (eqs,CreateVector (p35,p36,p37,torso)) :
rAS1:=subs (eqs,CreateVector (p38,p39,p40,a)) :
rAS2:=subs (eqs,CreateVector (p41,p42,p43,a)) :
rAS3:=subs (eqs,CreateVector (p44,p45,p46,a)) :
rAA:=subs (eqs,CreateVector (p47,p48,p49,a)) :
rAZ1:=subs (eqs,CreateVector (p50,p51,p52,a)) :
rAZ2:=subs (eqs,CreateVector (p53,p54,p55,a)) :
rBZ1:=subs (eqs,CreateVector (p56,p57,p58,b)) :
rBZ2:=subs (eqs,CreateVector (p59,p60,p61,b)) :
rBA:=subs (eqs,CreateVector (p62,p63,p64,b)) :
rBB:=subs (eqs,CreateVector (p65,p66,p67,b)) :
rCB:=subs (eqs,CreateVector (p68,p69,0,c)) :
rCC:=subs (eqs,CreateVector (p70,p71,0,c)) :
rCD:=rCC:
rDC:=subs (eqs,CreateVector (p74,p75,0,d)) :
rED:=subs (eqs,CreateVector (p80,p81,0,e)) :
rEE:=rED:
rFE:=subs (eqs,CreateVector (p84,p85,0,f)) :
> rNO0:=rNO1 &++ rO100:
rNA0:=rNO1 &++ rO002 &++ rA1A0:
rNB0:=rNA0 &++ rA0A2 &++ rB1B0:
rNC0:=rNB0 &++ rB0B2 &++ rC1C0:
rND0:=rNC0 &++ rC0C2 &++ rD1D0:
rNE0:=rND0 &++ rD0D2 &++ rE1E0:
rNF0:=rNE0 &++ rE0E2 &++ rF1F0:
ro1:=rAS1 &-- rO002 &-- rO100 &-- rOS1:
ro2:=rAS2 &-- rO002 &-- rO100 &-- rOS2:
ro3:=rAS3 &-- rO002 &-- rO100 &-- rOS3:
ra:=rBA &-- rA0A2 &-- rA1A0 &-- rAA:
rz1:=rBZ1 &-- rA0A2 &-- rA1A0 &-- rAZ1:
rz2:=rBZ2 &-- rA0A2 &-- rA1A0 &-- rAZ2:
rb:=rCB &-- rB0B2 &-- rB1B0 &-- rBB:
rc:=rDC &-- rC0C2 &-- rC1C0 &-- rCC:
rd:=rED &-- rD0D2 &-- rD1D0 &-- rC0C2 &-- rC1C0 &-- rCD:
re:=rFE &-- rE0E2 &-- rE1E0 &-- rEE:
> DependsTime (seq (cat (q,i),i=1..12),seq (cat (u,i),i=1..12)) :
> vO0:=DiffTime (rNO0,n) :
vA0:=DiffTime (rNA0,n) :
vB0:=DiffTime (rNB0,n) :
vC0:=DiffTime (rNC0,n) :
vD0:=DiffTime (rND0,n) :
vE0:=DiffTime (rNE0,n) :
vF0:=DiffTime (rNF0,n) :
>
kde:={q1t=u1,q2t=u2,q3t=u3,q4t=u4,q5t=u5,q6t=u6,q7t=u7,q8t=u8,q9t=u9,q10t=u10,q11t=u11,q12t=u
12} :
>
vel:=subs (kde,TangentDescription (vO0,AngularVelocity (n,torso),vA0,AngularVelocity (n,a),vB0,An
gularVelocity (n,b),vC0,AngularVelocity (n,c),vD0,AngularVelocity (n,d),vE0,AngularVelocity (n,e)
,vF0,AngularVelocity (n,f))) :
> mass:=subs (eqs,LiftDescription (mO &**)
UnitDyad (n),CreateDyad (IO11,0,0,0,IO22,0,0,0,IO33,torso),mA &**)
UnitDyad (n),CreateDyad (IA11,IA12,IA13,IA21,IA22,IA23,IA31,IA32,IA33,a),mB &**)
UnitDyad (n),CreateDyad (IB11,IB12,IB13,IB21,IB22,IB23,IB31,IB32,IB33,b),mC &**)
UnitDyad (n),CreateDyad (IC11,IC12,IC13,IC21,IC22,IC23,IC31,IC32,IC33,c),mD &**)
UnitDyad (n),CreateDyad (ID11,ID12,ID13,ID21,ID22,ID23,ID31,ID32,ID33,d),mE &**)
UnitDyad (n),CreateDyad (IE11,IE12,IE13,IE21,IE22,IE23,IE31,IE32,IE33,e),mF &**)
UnitDyad (n),CreateDyad (IF11,IF12,IF13,IF21,IF22,IF23,IF31,IF32,IF33,f)) :

```

```

> p:=Transpose(vel) &o mass:
> pt:=subs(kde,DiffTime(p,n)):
> beta:=BetaExtract(vel,[u1,u2,u3,u4,u5,u6,u7,u8,u9,u10,u11,u12]):
> Norms := {Ero1 = EuclideanNorm(ro1),
            Ero2 = EuclideanNorm(ro2),
            Ero3 = EuclideanNorm(ro3),
            Era = EuclideanNorm(ra),
            Erb = EuclideanNorm(rb),
            Erc = EuclideanNorm(rc),
            Erd = EuclideanNorm(rd),
            Ere = EuclideanNorm(re),
            Erz1 = EuclideanNorm(rz1),
            Erz2 = EuclideanNorm(rz2)}:
> force:=subs(Norms union eqs,CotangentDescription(
CreateVector(0,-mO*g,0,n) &+ CreateVector(Fx,Fy,0,n) &-- ((FO1/Ero1) &** (ro1)) &--
((FO2/Ero2) &** (ro2)) &-- ((FO3/Ero3) &** (ro3)),NullVector(),

CreateVector(0,-mA*g,0,n) &+ ((FO1/Ero1) &** (ro1)) &+ ((FO2/Ero2) &** (ro2)) &+
((FO3/Ero3) &** (ro3)) &-- ((FA/Era) &** (ra)) &-- ((FZ1/Erz1) &** (rz1)) &-- ((FZ2/Erz2) &**
(rz2)), (((FO1/Ero1) &** (ro1)) &xx (rAS1 &+ rA1A0)) &+ (((FO2/Ero2) &** (ro2)) &xx (rAS2
&+ rA1A0)) &+ (((FO3/Ero3) &** (ro3)) &xx (rAS3 &+ rA1A0)) &-- ((FA/Era) &** (ra)) &xx
(rAA &+ rA1A0)) &-- ((FZ1/Erz1) &** (rz1)) &xx (rAZ1 &+ rA1A0)) &-- ((FZ2/Erz2) &**
(rz2)) &xx (rAZ2 &+ rA1A0)),

CreateVector(0,-mB*g,0,n) &+ ((FA/Era) &** (ra)) &+ ((FZ1/Erz1) &** (rz1)) &+ ((FZ2/Erz2)
&** (rz2)) &-- ((FB/Erb) &** (rb)), (((FA/Era) &** (ra)) &xx (rBA &+ rB1B0)) &+
(((FZ1/Erz1) &** (rz1)) &xx (rBZ1 &+ rB1B0)) &+ ((FZ2/Erz2) &** (rz2)) &xx (rBZ2 &+
rB1B0)) &-- ((FB/Erb) &** (rb)) &xx (rBB &+ rB1B0)),

CreateVector(0,-mC*g,0,n) &+ ((FB/Erb) &** (rb)) &-- ((FC/Erc) &** (rc)) &-- ((FD/Erd) &**
(rd)), (((FB/Erb) &** (rb)) &xx (rCB &+ rC1C0)) &-- ((FC/Erc) &** (rc)) &xx (rCC &+
rC1C0)) &-- ((FD/Erd) &** (rd)) &xx (rCD &+ rC1C0)),

CreateVector(0,-mD*g,0,n) &+ ((FC/Erc) &** (rc)), (((FC/Erc) &** (rc)) &xx (rDC &+ rD1D0)),

CreateVector(0,-mE*g,0,n) &+ ((FD/Erd) &** (rd)) &-- ((FE/Ere) &** (re)), (((FD/Erd) &**
(rd)) &xx (rED &+ rE1E0)) &-- ((FE/Ere) &** (re)) &xx (rEE &+ rE1E0)),

CreateVector(0,-mF*g,0,n) &+ ((FE/Ere) &** (re)) &+ CreateVector(0,Fh,0,n),
(((FE/Ere) &** (re)) &xx (rFE &+ rF1F0)) &+ (CreateVector(0,Fh,0,n) &xx ((-1) &**
rFOF2))))):
> eq:=(force &-- pt) &o beta:
> eq:=convert(eq,set):
> valtable:=matrix(101,37,[0.0,0.0000,-0.2618,0.0,0.6629,0.0,-
0.2966,0.0,0.6280,0.5321,0.4361,0.6803,0.0,0.078,0.0,0.0,0.611,0.0,0.166,0.0,-2.878,-1.443,-
0.008,3.214,0.0,26.49,0.0,0.0,-23.29,0.0,-73.02,0.0,-39.94,-55.02,-70.01,-56.94,0.0],
[0.0,0.0043,-0.2618,0.0,0.6661,0.0,-
0.3046,0.0,0.5919,0.5098,0.4277,0.7083,0.0,0.390,0.0,0.0,0.293,0.0,-0.732,0.0,-3.313,-2.043,-
0.771,2.568,0.0,28.68,0.0,0.0,-29.16,0.0,-82.41,0.0,-39.94,-55.03,-70.01,-59.29,224.4],
[0.0,0.0110,-0.2618,0.0,0.6658,0.0,-
0.3210,0.0,0.5526,0.4827,0.4127,0.7308,0.0,0.623,0.0,0.0,-0.027,0.0,-1.506,0.0,-3.601,-
2.491,-1.380,2.062,0.0,21.35,0.0,0.0,-29.37,0.0,-71.04,0.0,-26.43,-41.15,-55.79,-
46.39,367.2],
[0.0,0.0192,-0.2618,0.0,0.6622,0.0,-
0.3439,0.0,0.5122,0.4527,0.3931,0.7497,0.0,0.750,0.0,0.0,-0.334,0.0,-2.100,0.0,-3.705,-
2.751,-1.794,1.739,0.0,11.64,0.0,0.0,-28.16,0.0,-54.47,0.0,-9.54,-23.79,-38.01,-29.67,408.0],
[0.0,0.0276,-0.2618,0.0,0.6553,0.0,-
0.3713,0.0,0.4727,0.4219,0.3711,0.7671,0.0,0.771,0.0,0.0,-0.628,0.0,-2.513,0.0,-3.625,-
2.821,-2.014,1.598,0.0,1.92,0.0,0.0,-26.96,0.0,-37.90,0.0,7.35,-6.44,-20.23,-12.96,469.2],
[0.0,0.0351,-0.2618,0.0,0.6454,0.0,-
0.4012,0.0,0.4361,0.3925,0.3489,0.7850,0.0,0.686,0.0,0.0,-0.909,0.0,-2.746,0.0,-3.361,-
2.702,-2.041,1.639,0.0,-7.79,0.0,0.0,-25.75,0.0,-21.33,0.0,24.23,10.92,-2.45,3.75,673.2],
[0.0,0.0408,-0.2618,0.0,0.6327,0.0,-
0.4318,0.0,0.4039,0.3659,0.3280,0.8046,0.0,0.521,0.0,0.0,-1.161,0.0,-2.806,0.0,-2.958,-
2.436,-1.914,1.798,0.0,-15.10,0.0,0.0,-23.15,0.0,-5.58,0.0,37.01,24.38,11.68,14.61,754.8],
[0.0,0.0449,-0.2618,0.0,0.6183,0.0,-
0.4616,0.0,0.3756,0.3420,0.3085,0.8244,0.0,0.382,0.0,0.0,-1.324,0.0,-2.731,0.0,-2.594,-
2.193,-1.792,1.820,0.0,-12.80,0.0,0.0,-14.97,0.0,6.90,0.0,33.35,22.29,11.16,2.03,816.0],
[0.0,0.0481,-0.2618,0.0,0.6032,0.0,-
0.4891,0.0,0.3504,0.3201,0.2898,0.8423,0.0,0.294,0.0,0.0,-1.383,0.0,-2.529,0.0,-2.315,-
2.015,-1.716,1.641,0.0,-8.09,0.0,0.0,-5.40,0.0,18.56,0.0,25.57,16.30,6.98,-16.40,877.2],

```

[0.0,0.0509,-0.2618,0.0,0.5886,0.0,-
0.5131,0.0,0.3272,0.2993,0.2714,0.8561,0.0,0.257,0.0,0.0,-1.338,0.0,-2.200,0.0,-2.121,-
1.903,-1.685,1.262,0.0,-3.38,0.0,0.0,4.17,0.0,30.22,0.0,17.80,10.31,2.80,-34.83,958.8],
[0.0,0.0539,-0.2618,0.0,0.5757,0.0,-
0.5321,0.0,0.3053,0.2791,0.2529,0.8635,0.0,0.271,0.0,0.0,-1.188,0.0,-1.743,0.0,-2.012,-
1.856,-1.700,0.681,0.0,1.33,0.0,0.0,13.74,0.0,41.88,0.0,10.03,4.32,-1.37,-53.26,1003.7],
[0.0,0.0574,-0.2618,0.0,0.5652,0.0,-
0.5452,0.0,0.2838,0.2588,0.2338,0.8631,0.0,0.325,0.0,0.0,-0.959,0.0,-1.206,0.0,-1.973,-
1.861,-1.749,-0.034,0.0,4.89,0.0,0.0,20.99,0.0,49.30,0.0,3.56,-0.46,-4.43,-65.57,1040.4],
[0.0,0.0614,-0.2618,0.0,0.5570,0.0,-
0.5537,0.0,0.2626,0.2385,0.2144,0.8564,0.0,0.366,0.0,0.0,-0.752,0.0,-0.772,0.0,-1.948,-
1.865,-1.782,-0.616,0.0,3.82,0.0,0.0,18.97,0.0,39.78,0.0,2.32,-0.36,-3.03,-53.42,1060.8],
[0.0,0.0656,-0.2618,0.0,0.5506,0.0,-
0.5590,0.0,0.2416,0.2183,0.1949,0.8455,0.0,0.384,0.0,0.0,-0.593,0.0,-0.489,0.0,-1.922,-
1.855,-1.787,-0.999,0.0,1.61,0.0,0.0,14.62,0.0,26.01,0.0,2.39,0.95,-0.50,-35.16,1081.2],
[0.0,0.0697,-0.2618,0.0,0.5453,0.0,-
0.5629,0.0,0.2210,0.1983,0.1757,0.8326,0.0,0.377,0.0,0.0,-0.481,0.0,-0.355,0.0,-1.895,-
1.830,-1.765,-1.183,0.0,-0.61,0.0,0.0,10.28,0.0,12.25,0.0,2.45,2.26,2.02,-16.89,1101.6],
[0.0,0.0735,-0.2618,0.0,0.5408,0.0,-
0.5669,0.0,0.2006,0.1788,0.1570,0.8199,0.0,0.346,0.0,0.0,-0.416,0.0,-0.371,0.0,-1.868,-
1.791,-1.716,-1.168,0.0,-2.82,0.0,0.0,5.93,0.0,-1.51,0.0,2.52,3.57,4.54,1.37,1107.7],
[0.0,0.0767,-0.2618,0.0,0.5364,0.0,-
0.5725,0.0,0.1804,0.1597,0.1389,0.8088,0.0,0.298,0.0,0.0,-0.403,0.0,-0.511,0.0,-1.851,-
1.755,-1.661,-1.016,0.0,-4.46,0.0,0.0,1.27,0.0,-12.82,0.0,1.48,3.32,5.06,13.94,1115.9],
[0.0,0.0795,-0.2618,0.0,0.5315,0.0,-
0.5797,0.0,0.1598,0.1402,0.1205,0.7982,0.0,0.256,0.0,0.0,-0.453,0.0,-0.667,0.0,-1.895,-
1.790,-1.687,-0.975,0.0,-3.79,0.0,0.0,-4.66,0.0,-14.30,0.0,-3.97,-3.18,-2.45,3.75,1122.0],
[0.0,0.0820,-0.2618,0.0,0.5252,0.0,-
0.5886,0.0,0.1379,0.1193,0.1007,0.7861,0.0,0.229,0.0,0.0,-0.572,0.0,-0.812,0.0,-2.009,-
1.912,-1.817,-1.108,0.0,-2.55,0.0,0.0,-10.91,0.0,-13.33,0.0,-10.52,-11.24,-11.95,-
12.13,1111.8],
[0.0,0.0844,-0.2618,0.0,0.5170,0.0,-
0.5989,0.0,0.1139,0.0962,0.0783,0.7707,0.0,0.214,0.0,0.0,-0.759,0.0,-0.947,0.0,-2.195,-
2.122,-2.051,-1.413,0.0,-1.30,0.0,0.0,-17.16,0.0,-12.36,0.0,-17.07,-19.30,-21.46,-
28.01,1107.7],
[0.0,0.0867,-0.2618,0.0,0.5059,0.0,-
0.6106,0.0,0.0872,0.0698,0.0523,0.7501,0.0,0.214,0.0,0.0,-1.014,0.0,-1.071,0.0,-2.453,-
2.421,-2.389,-1.891,0.0,-0.05,0.0,0.0,-23.41,0.0,-11.39,0.0,-23.62,-27.35,-30.97,-
43.90,1083.2],
[0.0,0.0891,-0.2618,0.0,0.4916,0.0,-
0.6235,0.0,0.0572,0.0396,0.0219,0.7230,0.0,0.221,0.0,0.0,-1.311,0.0,-1.181,0.0,-2.748,-
2.768,-2.787,-2.483,0.0,0.68,0.0,0.0,-27.25,0.0,-10.08,0.0,-27.07,-31.86,-36.49,-
54.28,1081.2],
[0.0,0.0914,-0.2618,0.0,0.4748,0.0,-0.6372,0.0,0.0251,0.0068,-
0.0115,0.6909,0.0,0.214,0.0,0.0,-1.545,0.0,-1.262,0.0,-2.946,-3.009,-3.071,-2.948,0.0,-
0.65,0.0,0.0,-21.45,0.0,-7.45,0.0,-18.13,-22.15,-26.06,-42.67,1060.8],
[0.0,0.0935,-0.2618,0.0,0.4563,0.0,-0.6515,0.0,-0.0077,-0.0270,-
0.0464,0.6557,0.0,0.187,0.0,0.0,-1.689,0.0,-1.311,0.0,-3.106,-3.198,-3.227,0.0,-
2.49,0.0,0.0,-13.24,0.0,-4.48,0.0,-6.09,-8.88,-11.63,-25.56,1040.4],
[0.0,0.0950,-0.2618,0.0,0.4373,0.0,-0.6660,0.0,-0.0398,-0.0604,-
0.0809,0.6195,0.0,0.140,0.0,0.0,-1.744,0.0,-1.328,0.0,-2.947,-3.058,-3.167,-3.319,0.0,-
4.33,0.0,0.0,-5.03,0.0,-1.51,0.0,5.95,4.39,2.79,-8.45,1026.1],
[0.0,0.0958,-0.2618,0.0,0.4187,0.0,-0.6803,0.0,-0.0698,-0.0916,-
0.1134,0.5844,0.0,0.073,0.0,0.0,-1.710,0.0,-1.312,0.0,-2.751,-2.866,-2.980,-3.225,0.0,-
6.17,0.0,0.0,3.18,0.0,1.45,0.0,17.99,17.66,17.21,8.66,1020.0],
[0.0,0.0957,-0.2618,0.0,0.4013,0.0,-0.6941,0.0,-0.0966,-0.1195,-0.1425,0.5519,0.0,-
0.010,0.0,0.0,-1.598,0.0,-1.267,0.0,-2.457,-2.564,-2.672,-2.981,0.0,-
7.58,0.0,0.0,10.28,0.0,4.12,0.0,26.96,27.68,28.24,22.37,1015.9],
[0.0,0.0947,-0.2618,0.0,0.3854,0.0,-0.7073,0.0,-0.1206,-0.1446,-0.1686,0.5221,0.0,-
0.089,0.0,0.0,-1.456,0.0,-1.206,0.0,-2.199,-2.294,-2.391,-2.736,0.0,-
7.27,0.0,0.0,12.96,0.0,5.56,0.0,23.65,24.74,25.71,22.50,1020.0],
[0.0,0.0930,-0.2618,0.0,0.3713,0.0,-0.7196,0.0,-0.1425,-0.1674,-0.1923,0.4946,0.0,-
0.160,0.0,0.0,-1.298,0.0,-1.133,0.0,-2.011,-2.092,-2.176,-2.526,0.0,-
6.52,0.0,0.0,14.53,0.0,6.69,0.0,17.26,18.55,19.79,19.23,1030.2],
[0.0,0.0905,-0.2618,0.0,0.3590,0.0,-0.7310,0.0,-0.1631,-0.1887,-0.2144,0.4689,0.0,-
0.223,0.0,0.0,-1.122,0.0,-1.048,0.0,-1.893,-1.957,-2.025,-2.352,0.0,-
5.77,0.0,0.0,16.10,0.0,7.83,0.0,10.88,12.36,13.86,15.97,1040.4],
[0.0,0.0875,-0.2618,0.0,0.3489,0.0,-0.7414,0.0,-0.1832,-0.2093,-0.2355,0.4448,0.0,-
0.278,0.0,0.0,-0.930,0.0,-0.950,0.0,-1.844,-1.890,-1.938,-2.213,0.0,-
5.03,0.0,0.0,17.67,0.0,8.97,0.0,4.50,6.18,7.94,12.70,1056.7],

[0.0,0.0840,-0.2618,0.0,0.3409,0.0,-0.7507,0.0,-0.2034,-0.2298,-0.2563,0.4219,0.0,-0.325,0.0,0.0,-0.736,0.0,-0.856,0.0,-1.854,-1.881,-1.908,-2.105,0.0,-4.31,0.0,0.0,17.75,0.0,8.68,0.0,-0.92,0.87,2.79,9.91,1081.2],
[0.0,0.0800,-0.2618,0.0,0.3343,0.0,-0.7597,0.0,-0.2239,-0.2504,-0.2770,0.4000,0.0,-0.366,0.0,0.0,-0.607,0.0,-0.827,0.0,-1.880,-1.891,-1.900,-2.007,0.0,-3.73,0.0,0.0,11.82,0.0,2.67,0.0,-2.45,-0.93,0.70,8.99,1101.6],
[0.0,0.0756,-0.2618,0.0,0.3282,0.0,-0.7693,0.0,-0.2448,-0.2712,-0.2978,0.3791,0.0,-0.400,0.0,0.0,-0.559,0.0,-0.879,0.0,-1.913,-1.911,-1.907,-1.914,0.0,-3.18,0.0,0.0,4.40,0.0,-4.76,0.0,-3.01,-1.86,-0.61,8.54,1122.0],
[0.0,0.0709,-0.2618,0.0,0.3217,0.0,-0.7803,0.0,-0.2660,-0.2924,-0.3188,0.3592,0.0,-0.429,0.0,0.0,-0.592,0.0,-1.012,0.0,-1.952,-1.941,-1.928,-1.826,0.0,-2.63,0.0,0.0,-3.03,0.0,-12.20,0.0,-3.58,-2.78,-1.93,8.09,1162.8],
[0.0,0.0660,-0.2618,0.0,0.3140,0.0,-0.7937,0.0,-0.2878,-0.3140,-0.3402,0.3402,0.0,-0.452,0.0,0.0,-0.706,0.0,-1.225,0.0,-1.997,-1.982,-1.963,-1.743,0.0,-2.08,0.0,0.0,-10.45,0.0,-19.63,0.0,-4.14,-3.70,-3.24,7.64,1197.5],
[0.0,0.0609,-0.2618,0.0,0.3045,0.0,-0.8099,0.0,-0.3100,-0.3360,-0.3620,0.3220,0.0,-0.467,0.0,0.0,-0.875,0.0,-1.487,0.0,-2.038,-2.022,-2.003,-1.668,0.0,-1.38,0.0,0.0,-15.47,0.0,-24.00,0.0,-3.77,-3.70,-3.64,6.91,1224.0],
[0.0,0.0558,-0.2618,0.0,0.2936,0.0,-0.8280,0.0,-0.3322,-0.3581,-0.3839,0.3045,0.0,-0.468,0.0,0.0,-0.994,0.0,-1.663,0.0,-2.035,-2.022,-2.007,-1.612,0.0,-0.07,0.0,0.0,-10.88,0.0,-16.12,0.0,0.34,0.00,-0.36,5.10,1264.8],
[0.0,0.0509,-0.2618,0.0,0.2823,0.0,-0.8468,0.0,-0.3537,-0.3796,-0.4053,0.2872,0.0,-0.453,0.0,0.0,-1.036,0.0,-1.719,0.0,-1.976,-1.972,-1.965,-1.579,0.0,1.38,0.0,0.0,-3.88,0.0,-5.18,0.0,5.38,4.63,3.83,3.02,1305.6],
[0.0,0.0463,-0.2618,0.0,0.2714,0.0,-0.8648,0.0,-0.3740,-0.4000,-0.4258,0.2701,0.0,-0.422,0.0,0.0,-1.002,0.0,-1.656,0.0,-1.863,-1.871,-1.878,-1.569,0.0,2.84,0.0,0.0,3.11,0.0,5.76,0.0,10.41,9.25,8.02,0.93,1336.2],
[0.0,0.0422,-0.2618,0.0,0.2617,0.0,-0.8809,0.0,-0.3925,-0.4187,-0.4448,0.2529,0.0,-0.375,0.0,0.0,-0.892,0.0,-1.474,0.0,-1.694,-1.719,-1.744,-1.581,0.0,4.30,0.0,0.0,10.10,0.0,16.70,0.0,15.45,13.88,12.21,-1.15,1368.8],
[0.0,0.0388,-0.2618,0.0,0.2539,0.0,-0.8939,0.0,-0.4086,-0.4353,-0.4619,0.2355,0.0,-0.312,0.0,0.0,-0.717,0.0,-1.192,0.0,-1.474,-1.520,-1.566,-1.600,0.0,5.72,0.0,0.0,16.02,0.0,25.92,0.0,20.21,18.33,16.34,-1.70,1377.0],
[0.0,0.0362,-0.2618,0.0,0.2482,0.0,-0.9035,0.0,-0.4218,-0.4492,-0.4765,0.2185,0.0,-0.236,0.0,0.0,-0.525,0.0,-0.884,0.0,-1.214,-1.279,-1.345,-1.558,0.0,6.97,0.0,0.0,17.63,0.0,28.28,0.0,23.85,22.09,20.26,3.90,1393.3],
[0.0,0.0346,-0.2618,0.0,0.2446,0.0,-0.9097,0.0,-0.4318,-0.4601,-0.4883,0.2028,0.0,-0.147,0.0,0.0,-0.327,0.0,-0.568,0.0,-0.917,-0.999,-1.083,-1.437,0.0,8.19,0.0,0.0,18.17,0.0,28.92,0.0,27.20,25.69,24.13,11.03,1393.3],
[0.0,0.0341,-0.2618,0.0,0.2433,0.0,-0.9124,0.0,-0.4382,-0.4675,-0.4968,0.1893,0.0,-0.045,0.0,0.0,-0.123,0.0,-0.246,0.0,-0.584,-0.680,-0.777,-1.239,0.0,9.40,0.0,0.0,18.71,0.0,29.55,0.0,30.56,29.28,27.99,18.16,1377.0],
[0.0,0.0349,-0.2618,0.0,0.2442,0.0,-0.9115,0.0,-0.4405,-0.4710,-0.5015,0.1788,0.0,0.071,0.0,0.0,0.087,0.0,0.083,0.0,-0.215,-0.321,-0.430,-0.964,0.0,10.62,0.0,0.0,19.24,0.0,30.19,0.0,33.92,32.87,31.86,25.29,1346.4],
[0.0,0.0370,-0.2618,0.0,0.2474,0.0,-0.9070,0.0,-0.4387,-0.4704,-0.5022,0.1717,0.0,0.194,0.0,0.0,0.298,0.0,0.409,0.0,0.168,0.054,-0.061,-0.649,0.0,11.31,0.0,0.0,19.35,0.0,29.95,0.0,35.11,34.45,33.87,28.87,1326.0],
[0.0,0.0403,-0.2618,0.0,0.2528,0.0,-0.8995,0.0,-0.4335,-0.4665,-0.4995,0.1668,0.0,0.302,0.0,0.0,0.491,0.0,0.695,0.0,0.470,0.359,0.249,-0.450,0.0,9.92,0.0,0.0,17.75,0.0,26.23,0.0,27.66,28.01,28.44,18.26,1244.4],
[0.0,0.0446,-0.2618,0.0,0.2600,0.0,-0.8893,0.0,-0.4263,-0.4602,-0.4942,0.1624,0.0,0.390,0.0,0.0,0.662,0.0,0.931,0.0,0.666,0.573,0.479,-0.405,0.0,8.00,0.0,0.0,15.72,0.0,21.63,0.0,18.04,19.57,21.15,4.10,1193.4],
[0.0,0.0495,-0.2618,0.0,0.2689,0.0,-0.8771,0.0,-0.4180,-0.4527,-0.4874,0.1568,0.0,0.456,0.0,0.0,0.812,0.0,1.116,0.0,0.758,0.694,0.630,-0.515,0.0,6.09,0.0,0.0,13.69,0.0,17.02,0.0,8.43,11.12,13.86,-10.06,1120.0],
[0.0,0.0550,-0.2618,0.0,0.2791,0.0,-0.8635,0.0,-0.4099,-0.4448,-0.4797,0.1483,0.0,0.502,0.0,0.0,0.939,0.0,1.252,0.0,0.745,0.723,0.702,-0.779,0.0,4.18,0.0,0.0,11.67,0.0,12.42,0.0,-1.19,2.68,6.57,-24.22,1038.4],
[0.0,0.0608,-0.2618,0.0,0.2905,0.0,-0.8488,0.0,-0.4027,-0.4374,-0.4720,0.1358,0.0,0.529,0.0,0.0,1.049,0.0,1.346,0.0,0.664,0.683,0.702,-1.146,0.0,2.55,0.0,0.0,10.06,0.0,8.61,0.0,-7.48,-3.74,0.01,-33.64,785.4],
[0.0,0.0668,-0.2618,0.0,0.3032,0.0,-0.8332,0.0,-0.3955,-0.4302,-0.4648,0.1205,0.0,0.552,0.0,0.0,1.159,0.0,1.432,0.0,0.659,0.660,0.663,-1.409,0.0,2.08,0.0,0.0,10.14,0.0,7.93,0.0,-0.47,-2.04,-3.63,-24.14,754.8],
[0.0,0.0730,-0.2618,0.0,0.3171,0.0,-0.8167,0.0,-0.3871,-0.4228,-0.4584,0.1039,0.0,0.573,0.0,0.0,1.275,0.0,1.520,0.0,0.766,0.679,0.591,-1.517,0.0,1.89,0.0,0.0,10.65,0.0,8.05,0.0,9.87,1.69,-6.54,-9.90,673.2],

[0.0,0.0795,-0.2618,0.0,0.3323,0.0,-0.7991,0.0,-0.3764,-0.4147,-
0.4531,0.0879,0.0,0.591,0.0,0.0,1.397,0.0,1.609,0.0,0.987,0.738,0.488,-
1.469,0.0,1.71,0.0,0.0,11.16,0.0,8.16,0.0,20.21,5.41,-9.44,4.34,612.0],
[0.0,0.0861,-0.2618,0.0,0.3489,0.0,-0.7806,0.0,-0.3620,-0.4056,-
0.4492,0.0741,0.0,0.608,0.0,0.0,1.524,0.0,1.699,0.0,1.320,0.837,0.354,-
1.267,0.0,1.52,0.0,0.0,11.66,0.0,8.27,0.0,30.55,9.14,-12.35,18.58,571.2],
[0.0,0.0928,-0.2618,0.0,0.3668,0.0,-0.7613,0.0,-0.3430,-0.3953,-
0.4475,0.0627,0.0,0.610,0.0,0.0,1.643,0.0,1.772,0.0,1.740,0.949,0.157,-
1.045,0.0,0.22,0.0,0.0,10.91,0.0,6.70,0.0,38.59,10.30,-18.08,20.39,489.6],
[0.0,0.0987,-0.2618,0.0,0.3853,0.0,-0.7422,0.0,-0.3196,-0.3848,-
0.4500,0.0481,0.0,0.549,0.0,0.0,1.698,0.0,1.754,0.0,2.148,0.962,-0.226,-1.345,0.0,-
5.58,0.0,0.0,5.10,0.0,-1.60,0.0,37.43,1.19,-35.08,-27.51,438.6],
[0.0,0.1032,-0.2618,0.0,0.4036,0.0,-0.7244,0.0,-0.2922,-0.3755,-
0.4589,0.0230,0.0,0.413,0.0,0.0,1.677,0.0,1.628,0.0,2.518,0.848,-0.824,-2.302,0.0,-
12.51,0.0,0.0,-1.97,0.0,-11.59,0.0,33.97,-10.48,-54.91,-87.84,373.3],
[0.0,0.1054,-0.2618,0.0,0.4208,0.0,-0.7092,0.0,-0.2611,-0.3689,-0.4768,-
0.0197,0.0,0.201,0.0,0.0,1.579,0.0,1.393,0.0,2.851,0.607,-1.639,-3.917,0.0,-19.43,0.0,0.0,-
9.04,0.0,-21.58,0.0,30.51,-22.15,-74.74,-148.17,322.3],
[0.0,0.1045,-0.2618,0.0,0.4361,0.0,-0.6978,0.0,-0.2268,-0.3663,-0.5059,-0.0872,0.0,-
0.086,0.0,0.0,1.403,0.0,1.049,0.0,3.146,0.238,-2.670,-6.190,0.0,-26.35,0.0,0.0,-16.10,0.0,-
31.56,0.0,27.05,-33.82,-94.57,-208.49,263.2],
[0.0,0.0999,-0.2618,0.0,0.4489,0.0,-0.6907,0.0,-0.1895,-0.3683,-0.5471,-0.1835,0.0,-
0.418,0.0,0.0,1.175,0.0,0.651,0.0,3.419,-0.181,-3.779,-8.838,0.0,-30.43,0.0,0.0,-20.89,0.0,-
36.46,0.0,25.04,-38.45,-101.79,-242.96,179.5],
[0.0,0.0926,-0.2618,0.0,0.4598,0.0,-0.6861,0.0,-0.1488,-0.3720,-0.5952,-0.3005,0.0,-
0.670,0.0,0.0,0.995,0.0,0.422,0.0,3.733,-0.344,-4.418,-10.734,0.0,-23.13,0.0,0.0,-16.53,0.0,-
21.03,0.0,28.83,-14.94,-58.60,-173.98,128.5],
[0.0,0.0838,-0.2618,0.0,0.4694,0.0,-0.6816,0.0,-0.1041,-0.3739,-0.6437,-0.4269,0.0,-
0.811,0.0,0.0,0.887,0.0,0.417,0.0,4.104,-0.173,-4.449,-11.597,0.0,-12.99,0.0,0.0,-9.90,0.0,-
0.51,0.0,34.06,15.62,-2.80,-79.14,40.8],
[0.0,0.0746,-0.2618,0.0,0.4787,0.0,-0.6746,0.0,-0.0547,-0.3703,-0.6859,-0.5515,0.0,-
0.843,0.0,0.0,0.852,0.0,0.635,0.0,4.533,0.330,-3.871,-11.426,0.0,-2.85,0.0,0.0,-
3.26,0.0,20.01,0.0,39.30,46.17,52.99,15.69,0.0],
[0.0,0.0663,-0.2618,0.0,0.4884,0.0,-0.6629,0.0,0.0000,-0.3576,-0.7152,-0.6629,0.0,-
0.763,0.0,0.0,0.889,0.0,1.077,0.0,5.018,1.166,-2.685,-
10.221,0.0,7.29,0.0,0.0,3.38,0.0,40.52,0.0,44.53,76.72,108.79,110.53,0.0],
[0.0,0.0598,-0.2618,0.0,0.4990,0.0,-0.6447,0.0,0.0602,-0.3333,-0.7268,-0.7518,0.0,-
0.594,0.0,0.0,0.976,0.0,1.666,0.0,5.522,2.230,-1.064,-
8.155,0.0,15.48,0.0,0.0,8.02,0.0,54.12,0.0,46.27,97.56,148.70,189.55,0.0],
[0.0,0.0552,-0.2618,0.0,0.5102,0.0,-0.6218,0.0,0.1244,-0.2995,-0.7235,-0.8163,0.0,-
0.421,0.0,0.0,1.027,0.0,2.103,0.0,5.893,3.097,0.299,-
5.917,0.0,15.87,0.0,0.0,4.67,0.0,40.02,0.0,34.03,79.60,125.05,205.31,0.0],
[0.0,0.0523,-0.2618,0.0,0.5213,0.0,-0.5966,0.0,0.1908,-0.2596,-0.7101,-0.8564,0.0,-
0.266,0.0,0.0,1.020,0.0,2.310,0.0,6.093,3.663,1.231,-3.680,0.0,14.30,0.0,0.0,-
0.67,0.0,19.00,0.0,18.29,51.92,85.52,205.24,0.0],
[0.0,0.0510,-0.2618,0.0,0.5317,0.0,-0.5717,0.0,0.2576,-0.2168,-0.6912,-0.8721,0.0,-
0.127,0.0,0.0,0.954,0.0,2.288,0.0,6.120,3.927,1.732,-1.444,0.0,12.74,0.0,0.0,-6.02,0.0,-
2.01,0.0,2.55,24.25,45.99,205.18,0.0],
[0.0,0.0509,-0.2618,0.0,0.5408,0.0,-0.5495,0.0,0.3227,-0.1744,-0.6716,-0.8635,0.0,-
0.005,0.0,0.0,0.830,0.0,2.037,0.0,5.977,3.890,1.803,0.792,0.0,11.17,0.0,0.0,-11.36,0.0,-
23.03,0.0,-13.19,-3.42,6.46,205.12,0.0],
[0.0,0.0519,-0.2618,0.0,0.5481,0.0,-0.5319,0.0,0.3846,-0.1350,-0.6547,-
0.8319,0.0,0.096,0.0,0.0,0.665,0.0,1.611,0.0,5.683,3.616,1.549,2.897,0.0,9.25,0.0,0.0,-
15.14,0.0,-39.06,0.0,-26.95,-25.17,-23.23,193.11,0.0],
[0.0,0.0537,-0.2618,0.0,0.5538,0.0,-0.5186,0.0,0.4427,-0.0983,-0.6394,-
0.7845,0.0,0.160,0.0,0.0,0.528,0.0,1.228,0.0,5.325,3.363,1.402,4.350,0.0,5.89,0.0,0.0,-
12.63,0.0,-35.12,0.0,-32.82,-23.23,-13.52,133.34,0.0],
[0.0,0.0557,-0.2618,0.0,0.5585,0.0,-0.5083,0.0,0.4964,-0.0635,-0.6234,-
0.7298,0.0,0.184,0.0,0.0,0.434,0.0,0.943,0.0,4.925,3.195,1.468,5.022,0.0,2.17,0.0,0.0,-
8.55,0.0,-26.18,0.0,-36.71,-15.37,6.02,61.62,0.0],
[0.0,0.0575,-0.2618,0.0,0.5627,0.0,-0.5000,0.0,0.5452,-0.0296,-0.6044,-
0.6762,0.0,0.167,0.0,0.0,0.386,0.0,0.755,0.0,4.482,3.113,1.746,4.912,0.0,-1.55,0.0,0.0,-
4.47,0.0,-17.24,0.0,-40.60,-7.52,25.57,-10.10,0.0],
[0.0,0.0587,-0.2618,0.0,0.5669,0.0,-0.4928,0.0,0.5888,0.0044,-0.5800,-
0.6324,0.0,0.109,0.0,0.0,0.381,0.0,0.664,0.0,3.997,3.117,2.238,4.020,0.0,-5.27,0.0,0.0,-
0.39,0.0,-8.31,0.0,-44.49,0.34,45.12,-81.81,0.0],
[0.0,0.0590,-0.2618,0.0,0.5713,0.0,-0.4858,0.0,0.6268,0.0392,-0.5485,-
0.6044,0.0,0.025,0.0,0.0,0.407,0.0,0.644,0.0,3.486,3.188,2.892,2.566,0.0,-
7.74,0.0,0.0,2.37,0.0,-1.85,0.0,-46.94,6.56,59.96,-133.39,0.0],

[0.0,0.0586,-0.2618,0.0,0.5758,0.0,-0.4794,0.0,0.6596,0.0746,-0.5103,-0.5889,0.0,-0.032,0.0,0.0,0.406,0.0,0.587,0.0,3.011,3.256,3.502,1.428,0.0,-5.19,0.0,0.0,-0.13,0.0,-5.29,0.0,-43.58,6.22,55.94,-104.40,0.0],
[0.0,0.0581,-0.2618,0.0,0.5797,0.0,-0.4743,0.0,0.6878,0.1106,-0.4665,-0.5799,0.0,-0.047,0.0,0.0,0.363,0.0,0.464,0.0,2.588,3.302,4.016,0.826,0.0,-1.40,0.0,0.0,-3.95,0.0,-11.21,0.0,-38.78,4.23,47.22,-55.27,0.0],
[0.0,0.0579,-0.2618,0.0,0.5827,0.0,-0.4713,0.0,0.7120,0.1469,-0.4182,-0.5716,0.0,-0.021,0.0,0.0,0.278,0.0,0.278,0.0,2.218,3.327,4.436,0.759,0.0,2.40,0.0,0.0,-7.77,0.0,-17.12,0.0,-33.98,2.25,38.49,-6.14,0.0],
[0.0,0.0584,-0.2618,0.0,0.5844,0.0,-0.4710,0.0,0.7327,0.1832,-0.3663,-0.5582,0.0,0.0,0.047,0.0,0.0,0.152,0.0,0.0,0.027,0.0,1.900,3.330,4.760,1.228,0.0,6.19,0.0,0.0,-11.59,0.0,-23.04,0.0,-29.18,0.27,29.77,42.99,0.0],
[0.0,0.0600,-0.2618,0.0,0.5844,0.0,-0.4739,0.0,0.7504,0.2192,-0.3120,-0.5348,0.0,0.0,0.143,0.0,0.0,-0.002,0.0,-0.264,0.0,1.623,3.302,4.982,2.146,0.0,8.86,0.0,0.0,-14.10,0.0,-26.69,0.0,-25.37,-2.55,20.35,84.26,0.0],
[0.0,0.0624,-0.2618,0.0,0.5830,0.0,-0.4793,0.0,0.7650,0.2541,-0.2567,-0.5002,0.0,0.0,0.220,0.0,0.0,-0.125,0.0,-0.496,0.0,1.345,3.207,5.071,3.172,0.0,7.05,0.0,0.0,-11.32,0.0,-21.26,0.0,-25.55,-8.71,8.20,94.09,0.0],
[0.0,0.0653,-0.2618,0.0,0.5808,0.0,-0.4863,0.0,0.7765,0.2872,-0.2020,-0.4543,0.0,0.0,0.265,0.0,0.0,-0.204,0.0,-0.644,0.0,1.053,3.036,5.021,4.219,0.0,4.11,0.0,0.0,-7.23,0.0,-13.55,0.0,-26.73,-15.71,-4.65,96.07,0.0],
[0.0,0.0683,-0.2618,0.0,0.5782,0.0,-0.4940,0.0,0.7847,0.3176,-0.1493,-0.3966,0.0,0.0,0.278,0.0,0.0,-0.238,0.0,-0.707,0.0,0.749,2.788,4.830,5.288,0.0,1.18,0.0,0.0,-3.14,0.0,-5.85,0.0,-27.91,-22.70,-17.50,98.04,0.0],
[0.0,0.0711,-0.2618,0.0,0.5757,0.0,-0.5015,0.0,0.7894,0.3445,-0.1003,-0.3271,0.0,0.0,0.259,0.0,0.0,-0.228,0.0,-0.687,0.0,0.432,2.465,4.499,6.378,0.0,-1.76,0.0,0.0,0.95,0.0,1.85,0.0,-29.09,-29.70,-30.34,100.01,0.0],
[0.0,0.0733,-0.2618,0.0,0.5738,0.0,-0.5078,0.0,0.7907,0.3674,-0.0558,-0.2462,0.0,0.0,0.206,0.0,0.0,-0.178,0.0,-0.578,0.0,0.117,2.100,4.084,7.421,0.0,-4.83,0.0,0.0,4.62,0.0,9.99,0.0,-28.91,-33.46,-38.07,95.69,0.0],
[0.0,0.0746,-0.2618,0.0,0.5726,0.0,-0.5117,0.0,0.7892,0.3874,-0.0143,-0.1575,0.0,0.0,0.114,0.0,0.0,-0.106,0.0,-0.362,0.0,-0.137,1.835,3.808,8.142,0.0,-8.42,0.0,0.0,6.60,0.0,19.85,0.0,-23.32,-24.30,-25.34,66.17,0.0],
[0.0,0.0744,-0.2618,0.0,0.5724,0.0,-0.5121,0.0,0.7857,0.4060,0.0263,-0.0651,0.0,-0.018,0.0,0.0,-0.017,0.0,-0.033,0.0,-0.316,1.705,3.727,8.473,0.0,-12.14,0.0,0.0,8.15,0.0,30.14,0.0,-16.38,-11.91,-7.49,30.36,0.0],
[0.0,0.0723,-0.2618,0.0,0.5734,0.0,-0.5077,0.0,0.7812,0.4246,0.0682,0.0266,0.0,-0.191,0.0,0.0,0.089,0.0,0.407,0.0,-0.419,1.711,3.839,8.414,0.0,-15.87,0.0,0.0,9.71,0.0,40.44,0.0,-9.44,0.48,10.36,-5.45,0.0],
[0.0,0.0679,-0.2618,0.0,0.5757,0.0,-0.4972,0.0,0.7763,0.4448,0.1134,0.1134,0.0,-0.405,0.0,0.0,0.212,0.0,0.960,0.0,-0.446,1.851,4.147,7.964,0.0,-19.59,0.0,0.0,11.26,0.0,50.73,0.0,-2.50,12.87,28.21,-41.26,0.0],
[0.0,0.0609,-0.2618,0.0,0.5795,0.0,-0.4800,0.0,0.7717,0.4674,0.1632,0.1920,0.0,-0.639,0.0,0.0,0.349,0.0,1.579,0.0,-0.424,2.074,4.571,7.212,0.0,-21.54,0.0,0.0,12.60,0.0,56.75,0.0,2.08,20.51,38.90,-69.00,0.0],
[0.0,0.0520,-0.2618,0.0,0.5849,0.0,-0.4574,0.0,0.7667,0.4911,0.2155,0.2630,0.0,-0.818,0.0,0.0,0.492,0.0,2.077,0.0,-0.454,2.174,4.799,6.509,0.0,-16.39,0.0,0.0,13.09,0.0,45.68,0.0,-2.75,9.12,20.96,-64.47,0.0],
[0.0,0.0420,-0.2618,0.0,0.5918,0.0,-0.4311,0.0,0.7606,0.5140,0.2674,0.3277,0.0,-0.921,0.0,0.0,0.637,0.0,2.408,0.0,-0.562,2.097,4.754,5.943,0.0,-9.47,0.0,0.0,13.36,0.0,30.34,0.0,-9.95,-7.03,-4.14,-51.88,0.0],
[0.0,0.0316,-0.2618,0.0,0.6004,0.0,-0.4031,0.0,0.7525,0.5341,0.3157,0.3879,0.0,-0.949,0.0,0.0,0.786,0.0,2.571,0.0,-0.749,1.844,4.436,5.515,0.0,-2.56,0.0,0.0,13.64,0.0,14.99,0.0,-17.14,-23.17,-29.23,-39.28,0.0],
[0.0,0.0218,-0.2618,0.0,0.6106,0.0,-0.3751,0.0,0.7414,0.5495,0.3576,0.4448,0.0,-0.902,0.0,0.0,0.938,0.0,2.567,0.0,-1.014,1.416,3.843,5.224,0.0,4.36,0.0,0.0,13.91,0.0,-0.35,0.0,-24.33,-39.32,-54.33,-26.68,0.0],
[0.0,0.0132,-0.2618,0.0,0.6223,0.0,-0.3490,0.0,0.7267,0.5587,0.3906,0.4996,0.0,-0.785,0.0,0.0,1.074,0.0,2.398,0.0,-1.347,0.843,3.029,5.031,0.0,10.66,0.0,0.0,12.52,0.0,-15.49,0.0,-30.51,-52.59,-74.70,-17.72,0.0],
[0.0,0.0064,-0.2618,0.0,0.6345,0.0,-0.3264,0.0,0.7082,0.5614,0.4146,0.5517,0.0,-0.628,0.0,0.0,1.123,0.0,2.073,0.0,-1.702,0.250,2.199,4.777,0.0,14.48,0.0,0.0,4.47,0.0,-29.82,0.0,-32.60,-54.38,-76.15,-23.33,0.0],
[0.0,0.0017,-0.2618,0.0,0.6462,0.0,-0.3090,0.0,0.6856,0.5578,0.4299,0.5999,0.0,-0.435,0.0,0.0,1.066,0.0,1.594,0.0,-2.069,-0.331,1.405,4.422,0.0,17.68,0.0,0.0,-5.25,0.0,-43.95,0.0,-33.68,-53.30,-72.89,-32.58,0.0],
[0.0,-0.0006,-0.2618,0.0,0.6560,0.0,-0.2985,0.0,0.6589,0.5480,0.4369,0.6431,0.0,-0.207,0.0,0.0,0.902,0.0,0.961,0.0,-2.448,-0.900,0.646,3.966,0.0,20.88,0.0,0.0,-14.97,0.0,-58.07,0.0,-34.75,-52.22,-69.62,-41.83,0.0],

```

[0.0,0.0000,-0.2618,0.0,0.6629,0.0,-
0.2966,0.0,0.6280,0.5321,0.4361,0.6803,0.0,0.055,0.0,0.0,0.633,0.0,0.174,0.0,-2.838,-1.458,-
0.077,3.409,0.0,24.09,0.0,0.0,-24.68,0.0,-72.20,0.0,-35.83,-51.13,-66.35,-51.08,0.0]]):
> inversedynamics:=proc(eq)
  global valtable:
  local i, forcevals, equs:

for i from 1 to 101 do

equs:=evalf(subs(q1=valtable[i,1], q2=valtable[i,2], q3=valtable[i,3], q4=valtable[i,4],
q5=valtable[i,5], q6=valtable[i,6], q7=valtable[i,7], q8=valtable[i,8], q9=valtable[i,9],
q10=valtable[i,10], q11=valtable[i,11], q12=valtable[i,12], u1=valtable[i,13],
u2=valtable[i,14], u3=valtable[i,15], u4=valtable[i,16], u5=valtable[i,17],
u6=valtable[i,18], u7=valtable[i,19], u8=valtable[i,20], u9=valtable[i,21],
u10=valtable[i,22], u11=valtable[i,23], u12=valtable[i,24], u13=valtable[i,25],
u14=valtable[i,26], u15=valtable[i,27], u16=valtable[i,28], u17=valtable[i,29],
u18=valtable[i,30], u19=valtable[i,31], u20=valtable[i,32], u21=valtable[i,33],
u22=valtable[i,34], u23=valtable[i,35], u24=valtable[i,36], Fh=valtable[i,37], FH=0,
FH=0,eq)):

forcevals:=subs(fsolve(equs, {Fx, Fy, FO1, FO2, FO3, FA, FZ1, FZ2, FB, FC, FD, FE}),
[Fx, Fy, FO1, FO2, FO3, FA, FZ1, FZ2, FB, FC, FD, FE]):

  print(forcevals):
od:
end:

```

Appending code for exporting the equations of motion.

```

> eq1:=[seq(simplify(eq[1,i]),i=1..12)]:
> with(linalg):
> init_exmex():          exmex version 4.04, 2 August 2002
> inc:='includes'=['input_forces.c']:
> path:='d:/home/David/Code/':
> kde_ordered:=[q1t-u1, q2t-u2, q3t-u3, q4t-u4, q5t-u5, q6t-u6, q7t-u7, q8t-u8,
> q9t-u9, q10t-u10, q11t-u11, q12t-u12]:
> kane_eq:=eq1:
> nops(kane_eq):
> Force_list:=[Fx=fx(t, tt1, tt2, tt3, tt4, tt5, tt6, tt7, tt8, tt9, tt10, tt11, tt12, tt13, tt14, tt15,
tt16, tt17, tt18, tt19, tt20, tt21, f1_1, f1_2, f1_3, f1_4, f1_5, f1_6, f1_7, f1_8, f1_9, f1_10, f1_11, f1_12,
f1_13, f1_14, f1_15, f1_16, f1_17, f1_18, f1_19, f1_20, f1_21), Fy=fy(t, tt1, tt2, tt3, tt4, tt5, tt6, tt7,
tt8, tt9, tt10, tt11, tt12, tt13, tt14, tt15, tt16, tt17, tt18, tt19, tt20, tt21, f2_1, f2_2, f2_3, f2_4, f2_5,
f2_6, f2_7, f2_8, f2_9, f2_10, f2_11, f2_12, f2_13, f2_14, f2_15, f2_16, f2_17, f2_18, f2_19, f2_20, f2_21),
FO1=fO1(t, tt1, tt2, tt3, tt4, tt5, tt6, tt7, tt8, tt9, tt10, tt11, tt12, tt13, tt14, tt15, tt16, tt17, tt18,
tt19, tt20, tt21, f3_1, f3_2, f3_3, f3_4, f3_5, f3_6, f3_7, f3_8, f3_9, f3_10, f3_11, f3_12, f3_13, f3_14,
f3_15, f3_16, f3_17, f3_18, f3_19, f3_20, f3_21), FO2=fO2(t, tt1, tt2, tt3, tt4, tt5, tt6, tt7, tt8, tt9,
tt10, tt11, tt12, tt13, tt14, tt15, tt16, tt17, tt18, tt19, tt20, tt21, f4_1, f4_2, f4_3, f4_4, f4_5, f4_6,
f4_7, f4_8, f4_9, f4_10, f4_11, f4_12, f4_13, f4_14, f4_15, f4_16, f4_17, f4_18, f4_19, f4_20, f4_21),
FO3=fO3(t, tt1, tt2, tt3, tt4, tt5, tt6, tt7, tt8, tt9, tt10, tt11, tt12, tt13, tt14, tt15, tt16, tt17, tt18,
tt19, tt20, tt21, f5_1, f5_2, f5_3, f5_4, f5_5, f5_6, f5_7, f5_8, f5_9, f5_10, f5_11, f5_12, f5_13, f5_14,
f5_15, f5_16, f5_17, f5_18, f5_19, f5_20, f5_21), FA=fA(t, tt1, tt2, tt3, tt4, tt5, tt6, tt7, tt8, tt9, tt10,
tt11, tt12, tt13, tt14, tt15, tt16, tt17, tt18, tt19, tt20, tt21, f6_1, f6_2, f6_3, f6_4, f6_5, f6_6, f6_7,
f6_8, f6_9, f6_10, f6_11, f6_12, f6_13, f6_14, f6_15, f6_16, f6_17, f6_18, f6_19, f6_20, f6_21), FZ1=fZ1(t,
tt1, tt2, tt3, tt4, tt5, tt6, tt7, tt8, tt9, tt10, tt11, tt12, tt13, tt14, tt15, tt16, tt17, tt18, tt19, tt20,
tt21, f7_1, f7_2, f7_3, f7_4, f7_5, f7_6, f7_7, f7_8, f7_9, f7_10, f7_11, f7_12, f7_13, f7_14, f7_15, f7_16,
f7_17, f7_18, f7_19, f7_20, f7_21), FZ2=fZ2(t, tt1, tt2, tt3, tt4, tt5, tt6, tt7, tt8, tt9, tt10, tt11, tt12,
tt13, tt14, tt15, tt16, tt17, tt18, tt19, tt20, tt21, f8_1, f8_2, f8_3, f8_4, f8_5, f8_6, f8_7, f8_8, f8_9,
f8_10, f8_11, f8_12, f8_13, f8_14, f8_15, f8_16, f8_17, f8_18, f8_19, f8_20, f8_21), FB=fB(t, tt1, tt2, tt3,
tt4, tt5, tt6, tt7, tt8, tt9, tt10, tt11, tt12, tt13, tt14, tt15, tt16, tt17, tt18, tt19, tt20, tt21, f9_1,
f9_2, f9_3, f9_4, f9_5, f9_6, f9_7, f9_8, f9_9, f9_10, f9_11, f9_12, f9_13, f9_14, f9_15, f9_16, f9_17,
f9_18, f9_19, f9_20, f9_21), FC=fC(t, tt1, tt2, tt3, tt4, tt5, tt6, tt7, tt8, tt9, tt10, tt11, tt12, tt13,
tt14, tt15, tt16, tt17, tt18, tt19, tt20, tt21, f10_1, f10_2, f10_3, f10_4, f10_5, f10_6, f10_7, f10_8,
f10_9, f10_10, f10_11, f10_12, f10_13, f10_14, f10_15, f10_16, f10_17, f10_18, f10_19, f10_20, f10_21),
FD=fD(t, tt1, tt2, tt3, tt4, tt5, tt6, tt7, tt8, tt9, tt10, tt11, tt12, tt13, tt14, tt15, tt16, tt17, tt18,
tt19, tt20, tt21, f11_1, f11_2, f11_3, f11_4, f11_5, f11_6, f11_7, f11_8, f11_9, f11_10, f11_11, f11_12,
f11_13, f11_14, f11_15, f11_16, f11_17, f11_18, f11_19, f11_20, f11_21), FE=fE(t, tt1, tt2, tt3, tt4, tt5,
tt6, tt7, tt8, tt9, tt10, tt11, tt12, tt13, tt14, tt15, tt16, tt17, tt18, tt19, tt20, tt21, f12_1, f12_2,
f12_3, f12_4, f12_5, f12_6, f12_7, f12_8, f12_9, f12_10, f12_11, f12_12, f12_13, f12_14, f12_15, f12_16,

```

```

f12_17,f12_18,f12_19,f12_20,f12_21),Fh=fh(t,tt1,tt2,tt3,tt4,tt5,tt6,tt7,tt8,tt9,tt10,tt11,
tt12,tt13,tt14,tt15,tt16,tt17,tt18,tt19,tt20,tt21,f13_1,f13_2,f13_3,f13_4,f13_5,f13_6,f13_7,
f13_8,f13_9,f13_10,f13_11,f13_12,f13_13,f13_14,f13_15,f13_16,f13_17,f13_18,f13_19,f13_20,
f13_21),FG=fG(t),FH=fH(t)]:
> Force_set:=(Fx=fx(t,t1,t2,t3,t4,t5,t6,t7,t8,t9,t10,t11,t12,t13,t14,t15,t16,t17,t18,t19,t20,
t21,f1_1,f1_2,f1_3,f1_4,f1_5,f1_6,f1_7,f1_8,f1_9,f1_10,f1_11,f1_12,f1_13,f1_14,f1_15,f1_16,
f1_17,f1_18,f1_19,f1_20,f1_21),Fy=fy(t,t1,t2,t3,t4,t5,t6,t7,t8,t9,t10,t11,t12,t13,t14,t15,
t16,t17,t18,t19,t20,t21,f2_1,f2_2,f2_3,f2_4,f2_5,f2_6,f2_7,f2_8,f2_9,f2_10,f2_11,f2_12,f2_13,
f2_14,f2_15,f2_16,f2_17,f2_18,f2_19,f2_20,f2_21),FO1=fO1(t,t1,t2,t3,t4,t5,t6,t7,t8,t9,t10,
t11,t12,t13,t14,t15,t16,t17,t18,t19,t20,t21,f3_1,f3_2,f3_3,f3_4,f3_5,f3_6,f3_7,f3_8,f3_9,
f3_10,f3_11,f3_12,f3_13,f3_14,f3_15,f3_16,f3_17,f3_18,f3_19,f3_20,f3_21),FO2=fO2(t,t1,t2,t3,
t4,t5,t6,t7,t8,t9,t10,t11,t12,t13,t14,t15,t16,t17,t18,t19,t20,t21,f4_1,f4_2,f4_3,f4_4,f4_5,
f4_6,f4_7,f4_8,f4_9,f4_10,f4_11,f4_12,f4_13,f4_14,f4_15,f4_16,f4_17,f4_18,f4_19,f4_20,f4_21),
FO3=fO3(t,t1,t2,t3,t4,t5,t6,t7,t8,t9,t10,t11,t12,t13,t14,t15,t16,t17,t18,t19,t20,t21,f5_1,
f5_2,f5_3,f5_4,f5_5,f5_6,f5_7,f5_8,f5_9,f5_10,f5_11,f5_12,f5_13,f5_14,f5_15,f5_16,f5_17,
f5_18,f5_19,f5_20,f5_21),FA=fA(t,t1,t2,t3,t4,t5,t6,t7,t8,t9,t10,t11,t12,t13,t14,t15,t16,t17,
t18,t19,t20,t21,f6_1,f6_2,f6_3,f6_4,f6_5,f6_6,f6_7,f6_8,f6_9,f6_10,f6_11,f6_12,f6_13,f6_14,
f6_15,f6_16,f6_17,f6_18,f6_19,f6_20,f6_21),FZ1=fZ1(t,t1,t2,t3,t4,t5,t6,t7,t8,t9,t10,t11,t12,
t13,t14,t15,t16,t17,t18,t19,t20,t21,f7_1,f7_2,f7_3,f7_4,f7_5,f7_6,f7_7,f7_8,f7_9,f7_10,f7_11,
f7_12,f7_13,f7_14,f7_15,f7_16,f7_17,f7_18,f7_19,f7_20,f7_21),FZ2=fZ2(t,t1,t2,t3,t4,t5,t6,t7,
t8,t9,t10,t11,t12,t13,t14,t15,t16,t17,t18,t19,t20,t21,f8_1,f8_2,f8_3,f8_4,f8_5,f8_6,f8_7,
f8_8,f8_9,f8_10,f8_11,f8_12,f8_13,f8_14,f8_15,f8_16,f8_17,f8_18,f8_19,f8_20,f8_21),FB=fB(t,
t1,t2,t3,t4,t5,t6,t7,t8,t9,t10,t11,t12,t13,t14,t15,t16,t17,t18,t19,t20,t21,f9_1,f9_2,f9_3,
f9_4,f9_5,f9_6,f9_7,f9_8,f9_9,f9_10,f9_11,f9_12,f9_13,f9_14,f9_15,f9_16,f9_17,f9_18,f9_19,
f9_20,f9_21),FC=fC(t,t1,t2,t3,t4,t5,t6,t7,t8,t9,t10,t11,t12,t13,t14,t15,t16,t17,t18,t19,t20,
t21,f10_1,f10_2,f10_3,f10_4,f10_5,f10_6,f10_7,f10_8,f10_9,f10_10,f10_11,f10_12,f10_13,f10_14,
f10_15,f10_16,f10_17,f10_18,f10_19,f10_20,f10_21),FD=fD(t,t1,t2,t3,t4,t5,t6,t7,t8,t9,t10,t11,
t12,t13,t14,t15,t16,t17,t18,t19,t20,t21,f11_1,f11_2,f11_3,f11_4,f11_5,f11_6,f11_7,f11_8,
f11_9,f11_10,f11_11,f11_12,f11_13,f11_14,f11_15,f11_16,f11_17,f11_18,f11_19,f11_20,f11_21),
FE=fE(t,t1,t2,t3,t4,t5,t6,t7,t8,t9,t10,t11,t12,t13,t14,t15,t16,t17,t18,t19,t20,t21,f12_1,
f12_2,f12_3,f12_4,f12_5,f12_6,f12_7,f12_8,f12_9,f12_10,f12_11,f12_12,f12_13,f12_14,f12_15,
f12_16,f12_17,f12_18,f12_19,f12_20,f12_21),Fh=fh(t,t1,t2,t3,t4,t5,t6,t7,t8,t9,t10,t11,t12,
t13,t14,t15,t16,t17,t18,t19,t20,t21,f13_1,f13_2,f13_3,f13_4,f13_5,f13_6,f13_7,f13_8,f13_9,
f13_10,f13_11,f13_12,f13_13,f13_14,f13_15,f13_16,f13_17,f13_18,f13_19,f13_20,f13_21),
FG=fG(t),FH=fH(t)]:
> cse:=[op(Force_list)]:
> qts:=[q1t,q2t,q3t,q4t,q5t,q6t,q7t,q8t,q9t,q10t,q11t,q12t]:
> uts:=[u1t,u2t,u3t,u4t,u5t,u6t,u7t,u8t,u9t,u10t,u11t,u12t]:
> vars:=[q1,q2,q3,q4,q5,q6,q7,q8,q9,q10,q11,q12,u1,u2,u3,u4,u5,u6,u7,u8,u9,u10,u11,u12]:
> para:=[p1,p2,p3,p4,p5,p6,p7,p8,p9,p10,p11,p12,p13,p14,p15,p16,p17,p18,p19,p20,p21,p22,p23,
p24,p25,p26,p27,p28,p29,p30,p31,p32,p33,p34,p35,p36,p37,p38,p39,p40,p41,p42,p43,p44,p45,p46,
p47,p48,p49,p50,p51,p52,p53,p54,p55,p56,p57,p58,p59,p60,p61,p62,p63,p64,p65,p66,p67,p68,p69,
p70,p71,p72,p73,p74,p75,p76,p77,p78,p79,p80,p81,p82,p83,p84,p85,p86,p87,p88,p89,p90,p91,
mA,IA11,IA12,IA13,IA21,IA22,IA23,IA31,IA32,IA33,mB,IB11,IB12,IB13,IB21,IB22,IB23,IB31,IB32,IB33,
mC,IC11,IC12,IC13,IC21,IC22,IC23,IC31,IC32,IC33,mD,ID11,ID12,ID13,ID21,ID22,ID23,ID31,ID32,
ID33,mE,IE11,IE12,IE13,IE21,IE22,IE23,IE31,IE32,IE33,mF,IF11,IF12,IF13,IF21,IF22,IF23,IF31,
IF32,IF33,mO,IO11,IO22,IO33,g,seq(cat(tt,ii),ii=1..21),
seq(seq(cat(cat(f,j),_),i),i=1..21),j=1..13)]:
> b:=[[], []]:
> diff_eqns:=[op(kde_ordered),op(kane_eq)]:
> qts_uts := [op(qts),op(uts)]:
> exmex('equine_eq_forelimb_v6',path,[[op(diff_eqns)],[op(qts_uts)],[op(cse)],[op(qts),
op(uts)],[op(vars)],parameters=para,inc,'matlab'=[]];
> seq(subs(Force_set,kane_eq[1,i]),i=1..12);
> nops(uts);

```

C code to iterate between data points for forces applied to the robotic replica.

```
#define c3 cos(q[2]) #define c4 cos(q[3]) #define c5 cos(q[4]) #define c6 cos(q[5])
#define c7 cos(q[6]) #define c8 cos(q[7]) #define c9 cos(q[8]) #define c10 cos(q[9])
#define c11 cos(q[10]) #define c12 cos(q[11]) #define si3 sin(q[2]) #define si4 sin(q[3])
#define si5 sin(q[4]) #define si6 sin(q[5]) #define si7 sin(q[6]) #define si8 sin(q[7])
#define si9 sin(q[8]) #define si10 sin(q[9]) #define si11 sin(q[10]) #define si12 sin(q[11])

double fx(double t, double *q, double *para)
{
    double f1_open, f1_close, f1_close_d, x, dx;
    int i;
    for (i=0; i<=100 && t>=para[i+156]; i++);
    f1_open=(para[i+257]*(t-para[i-1+156])+para[i-1+257]*(para[i+156]-
t))/(para[i+156]-para[i-1+156]);
    x = q[0];
    dx = q[12];
    f1_close=para[2782]*((para[i+1570]*(t-para[i-1+156])+para[i-
1+1570]*(para[i+156]-t))/(para[i+156]-para[i-1+156])-x);
    f1_close_d = -para[2794]*dx;
    return (f1_open + f1_close + f1_close_d);
}
double fy(double t, double *q, double *para)
{
    double f2_open, f2_close, f2_close_d, y, dy;
    int i;
    for (i=0; i<=100 && t>=para[i+156]; i++);
    f2_open=(para[i+358]*(t-para[i-1+156])+para[i-1+358]*(para[i+156]-
t))/(para[i+156]-para[i-1+156]);
    y = q[1];
    dy = q[13];
    f2_close=para[2783]*((para[i+1671]*(t-para[i-1+156])+para[i-
1+1671]*(para[i+156]-t))/(para[i+156]-para[i-1+156])-y);
    f2_close_d=para[2795]*((para[i+2806]*(t-para[i-1+156])+para[i-
1+2806]*(para[i+156]-t))/(para[i+156]-para[i-1+156])-dy);
    return (f2_open + f2_close + f2_close_d);
}
double f01(double t, double *q, double *para)
{
    double f3_open, f3_close, f3_close_d, O1, d01;
    int i;
    for (i=0; i<=100 && t>=para[i+156]; i++);
    f3_open=(para[i+459]*(t-para[i-1+156])+para[i-1+459]*(para[i+156]-
t))/(para[i+156]-para[i-1+156]);
    O1=.2533832796e-2*c3*c4-.5026129890e-2*c3*si5+.5303433608e-2*c3*c5+.1076406e-
1*si4-.5026129890e-2*si3*si4*c5-.5303433608e-2*si3*si4*si5+.1059225185e-1*c3*si4*si5-
.1003840862e-1*si3*si5+.1003840862e-1*c3*si4*c5-.4499730e-1*c4*si5+.10393257-.1268664510e-
2*si3*c4+.1059225185e-1*si3*c5-.4264450e-1*c4*c5;
    d01=-.1059225185e-1*si3*q[14]*si4*si5-.4499730e-1*c4*c5*q[16]-.5026129890e-
2*c3*c5*q[16]-.2533832796e-2*si3*q[14]*c4-.1268664510e-2*c3*q[14]*c4+.4499730e-
1*si4*q[15]*si5+.1268664510e-2*si3*si4*q[15]-.2533832796e-2*c3*si4*q[15]+.1059225185e-
1*c3*q[14]*c5-.5303433608e-2*si3*q[14]*c5-.1003840862e-1*si3*c5*q[16]-.5303433608e-
2*c3*si5*q[16]-.1003840862e-1*c3*q[14]*si5-.1059225185e-1*si3*si5*q[16]+.5026129890e-
2*si3*q[14]*si5+.4264450e-1*si4*q[15]*c5+.4264450e-1*c4*si5*q[16]+.1076406e-
1*c4*q[15]+.1003840862e-1*c3*c4*q[15]*c5-.1003840862e-1*c3*si4*si5*q[16]-.5026129890e-
2*si3*c4*q[15]*c5-.5026129890e-2*c3*q[14]*si4*c5+.1059225185e-1*c3*c4*q[15]*si5+.1059225185e-
1*c3*si4*c5*q[16]+.5026129890e-2*si3*si4*si5*q[16]-.5303433608e-2*c3*q[14]*si4*si5-
.5303433608e-2*si3*c4*q[15]*si5-.5303433608e-2*si3*si4*c5*q[16]-.1003840862e-
1*si3*q[14]*si4*c5;
    f3_close=para[2784]*(pow((para[i+1772]*(t-para[i-1+156])+para[i-
1+1772]*(para[i+156]-t))/(para[i+156]-para[i-1+156]),2)-O1);
    f3_close_d=para[2796]*((para[i+2907]*(t-para[i-1+156])+para[i-
1+2907]*(para[i+156]-t))/(para[i+156]-para[i-1+156])-d01);
    return (f3_open + f3_close+ f3_close_d);
}
double f02(double t, double *q, double *para)
{
    double f4_open, f4_close, f4_close_d, O2, d02;
    int i;
    for (i=0; i<=100 && t>=para[i+156]; i++);
```

```

        f4_open=(para[i+560]*(t-para[i-1+156])+para[i-1+560]*(para[i+156]-
t))/ (para[i+156]-para[i-1+156]);
        O2=-.1449147012e-1*c3*c5-.1364754092e-1*c3*si5+.3322109682e-
2*c3*si4*si5+.4605442253e-2*si3*c4-.1364754092e-1*si3*si4*c5+.1449147012e-1*si3*si4*si5-
.3128642396e-2*c3*si4*c5-.960348e-2*si4-.2845848e-1*c4*c5+.3128642396e-2*si3*si5+.3021828e-
1*c4*si5+.1055778618e-2*c3*c4+.8568124e-1+.3322109682e-2*si3*c5;
        dO2=-.3322109682e-2*si3*q[14]*si4*si5+.3021828e-1*c4*c5*q[16]-.1364754092e-
1*c3*c5*q[16]-.1055778618e-2*si3*q[14]*c4+.4605442253e-2*c3*q[14]*c4-.3021828e-
1*si4*q[15]*si5-.4605442253e-2*si3*si4*q[15]-.1055778618e-2*c3*si4*q[15]+.3322109682e-
2*c3*q[14]*c5+.1449147012e-1*si3*q[14]*c5+.3128642396e-2*si3*c5*q[16]+.1449147012e-
1*c3*si5*q[16]+.3128642396e-2*c3*q[14]*si5-.3322109682e-2*si3*si5*q[16]+.1364754092e-
1*si3*q[14]*si5+.2845848e-1*si4*q[15]*c5+.2845848e-1*c4*si5*q[16]-.960348e-2*c4*q[15]-
.3128642396e-2*c3*c4*q[15]*c5+.3128642396e-2*c3*si4*si5*q[16]-.1364754092e-1*si3*c4*q[15]*c5-
.1364754092e-1*c3*q[14]*si4*c5+.3322109682e-2*c3*c4*q[15]*si5+.3322109682e-
2*c3*si4*c5*q[16]+.1364754092e-1*si3*si4*si5*q[16]+.1449147012e-
1*c3*q[14]*si4*si5+.1449147012e-1*si3*c4*q[15]*si5+.1449147012e-
1*si3*si4*c5*q[16]+.3128642396e-2*si3*q[14]*si4*c5;
        f4_close=para[2785]*(pow((para[i+1873]*(t-para[i-1+156])+para[i-
1+1873]*(para[i+156]-t))/ (para[i+156]-para[i-1+156]),2)-O2);
        f4_close_d=para[2797]*(para[i+3008]*(t-para[i-1+156])+para[i-
1+3008]*(para[i+156]-t))/ (para[i+156]-para[i-1+156])-dO2);
        return (f4_open + f4_close+ f4_close_d);
}
double fO3(double t, double *q, double *para)
{
    double f5_open, f5_close, f5_close_d, O3, dO3;
    int i;
    for (i=0; i<=100 && t>=para[i+156]; i++);
        f5_open=(para[i+661]*(t-para[i-1+156])+para[i-1+661]*(para[i+156]-
t))/ (para[i+156]-para[i-1+156]);
        O3=-.3483773672e-1*c3*c5+.1641942509e-1*c3*si5+.5291224344e-
2*c3*si4*si5+.3826439934e-2*si3*c4+.1641942509e-1*si3*si4*c5+.3483773672e-
1*si3*si4*si5+.2493814753e-2*c3*si4*c5+.840984e-2*si4-.3608700e-1*c4*c5-.2493814753e-
2*si3*si5-.765672e-1*c4*si5+.13769595+.5811672640e-3*c3*c4+.5291224344e-2*si3*c5;
        dO3=-.5291224344e-2*si3*q[14]*si4*si5-.765672e-1*c4*c5*q[16]+.1641942509e-
1*c3*c5*q[16]-.5811672640e-3*si3*q[14]*c4+.3826439934e-2*c3*q[14]*c4+.765672e-
1*si4*q[15]*si5-.3826439934e-2*si3*si4*q[15]-.5811672640e-3*c3*si4*q[15]+.5291224344e-
2*c3*q[14]*c5+.3483773672e-1*si3*q[14]*c5-.2493814753e-2*si3*c5*q[16]+.3483773672e-
1*c3*si5*q[16]-.2493814753e-2*c3*q[14]*si5-.5291224344e-2*si3*si5*q[16]-.1641942509e-
1*si3*q[14]*si5+.3608700e-1*si4*q[15]*c5+.3608700e-1*c4*si5*q[16]+.840984e-
2*c4*q[15]+.2493814753e-2*c3*c4*q[15]*c5-.2493814753e-2*c3*si4*si5*q[16]+.1641942509e-
1*si3*c4*q[15]*c5+.1641942509e-1*c3*q[14]*si4*c5+.5291224344e-2*c3*c4*q[15]*si5+.5291224344e-
2*c3*si4*c5*q[16]-.1641942509e-1*si3*si4*si5*q[16]+.3483773672e-
1*c3*q[14]*si4*si5+.3483773672e-1*si3*c4*q[15]*si5+.3483773672e-1*si3*si4*c5*q[16]-
.2493814753e-2*si3*q[14]*si4*c5;
        f5_close=para[2786]*(pow((para[i+1974]*(t-para[i-1+156])+para[i-
1+1974]*(para[i+156]-t))/ (para[i+156]-para[i-1+156]),2)-O3);
        f5_close_d=para[2798]*(para[i+3109]*(t-para[i-1+156])+para[i-
1+3109]*(para[i+156]-t))/ (para[i+156]-para[i-1+156])-dO3);
        return (f5_open + f5_close + f5_close_d);
}
double fA(double t, double *q, double *para)
{
    double f6_open, f6_close, f6_close_d, A, dA;
    int i;
    for (i=0; i<=100 && t>=para[i+156]; i++);
        f6_open=(para[i+762]*(t-para[i-1+156])+para[i-1+762]*(para[i+156]-
t))/ (para[i+156]-para[i-1+156]);
        A=-.1957380e-1*(-c8*si7*c4-(-(-
si6*si8*si7+c6*c7)*si3+(c6*si8*si7+si6*c7)*c3)*si4)*c5-.1957380e-1*(-(-
si6*si8*si7+c6*c7)*c3+(c6*si8*si7+si6*c7)*si3)*si5-.1195032e-1*(c8*c7*c4-(-
(si6*si8*c7+c6*si7)*si3+(-c6*si8*c7+si6*si7)*c3)*si4)*si5-.354960e-
2*((si6*si8*c7+c6*si7)*c3+(-c6*si8*c7+si6*si7)*si3)*si5-.354960e-2*(c8*c7*c4-(-
(si6*si8*c7+c6*si7)*si3+(-c6*si8*c7+si6*si7)*c3)*si4)*c5+.1195032e-
1*((si6*si8*c7+c6*si7)*c3+(-c6*si8*c7+si6*si7)*si3)*c5-.178568e-2*(-
si6*c8*c3+c6*c8*si3)*c5+.178568e-2*(si8*c4-(si6*c8*si3+c6*c8*c3)*si4)*si5+.53040e-3*(si8*c4-
(si6*c8*si3+c6*c8*c3)*si4)*c5+.53040e-3*(-si6*c8*c3+c6*c8*si3)*si5-.6589846e-1*(-c8*si7*c4-(-
-si6*si8*si7+c6*c7)*si3+(c6*si8*si7+si6*c7)*c3)*si4)*si5+.6589846e-1*(-(-
si6*si8*si7+c6*c7)*c3+(c6*si8*si7+si6*c7)*si3)*c5+.7014558e-1;
        dA=.53040e-3*(c8*q[19]*c4-si8*si4*q[15)-(c6*q[17]*c8*si3-
si6*si8*q[19]*si3+si6*c8*c3*q[14]-si6*q[17]*c8*c3-c6*si8*q[19]*c3-c6*c8*si3*q[14])*si4-

```

```

(si6*c8*si3+c6*c8*c3)*c4*q[15])*c5-.53040e-3*(si8*c4-(si6*c8*si3+c6*c8*c3)*si4)*si5*q[16]-
.1957380e-1*(si8*q[19]*si7*c4-c8*c7*q[18])*c4+c8*si7*si4*q[15]-((-c6*q[17]*si8*si7-
si6*c8*q[19]*si7-si6*si8*c7*q[18]-si6*q[17]*c7-c6*si7*q[18])*si3-(-
si6*si8*si7+c6*c7)*c3*q[14]+(-si6*q[17]*si8*si7+c6*c8*q[19]*si7+c6*si8*c7*q[18]+c6*q[17]*c7-
si6*si7*q[18])*c3-(c6*si8*si7+si6*c7)*si3*q[14])*si4-((-
si6*si8*si7+c6*c7)*si3+(c6*si8*si7+si6*c7)*c3)*c4*q[15])*c5+.1957380e-1*(-c8*si7*c4-((-
si6*si8*si7+c6*c7)*si3+(c6*si8*si7+si6*c7)*c3)*si4)*si5*q[16]-.6589846e-1*(si8*q[19]*si7*c4-
c8*c7*q[18])*c4+c8*si7*si4*q[15]-((-c6*q[17]*si8*si7-si6*c8*q[19]*si7-si6*si8*c7*q[18]-
si6*q[17]*c7-c6*si7*q[18])*si3-(-si6*si8*si7+c6*c7)*c3*q[14]+(-
si6*q[17]*si8*si7+c6*c8*q[19]*si7+c6*si8*c7*q[18]+c6*q[17]*c7-si6*si7*q[18])*c3-
(c6*si8*si7+si6*c7)*si3*q[14])*si4-((-
si6*si8*si7+c6*c7)*si3+(c6*si8*si7+si6*c7)*c3)*c4*q[15])*si5-.6589846e-1*(-c8*si7*c4-((-
si6*si8*si7+c6*c7)*si3+(c6*si8*si7+si6*c7)*c3)*si4)*c5*q[16]+.53040e-3*(-
c6*q[17]*c8*c3+si6*si8*q[19]*c3+si6*c8*si3*q[14]-si6*q[17]*c8*si3-
c6*si8*q[19]*si3+c6*c8*c3*q[14])*si5+.53040e-3*(-si6*c8*c3+c6*c8*si3)*c5*q[16]-.178568e-2*(-
si6*q[17]*c8*c3+si6*si8*q[19]*c3+si6*c8*si3*q[14]-si6*q[17]*c8*si3-
c6*si8*q[19]*si3+c6*c8*c3*q[14])*c5+.178568e-2*(-si6*c8*c3+c6*c8*si3)*si5*q[16]+.178568e-
2*(c8*q[19]*c4-si8*si4*q[15]-c6*q[17]*c8*si3-si6*si8*q[19]*si3+si6*c8*c3*q[14]-
si6*q[17]*c8*c3-c6*si8*q[19]*c3-c6*c8*si3*q[14])*si4-
(si6*c8*si3+c6*c8*c3)*c4*q[15])*si5+.178568e-2*(si8*c4-
(si6*c8*si3+c6*c8*c3)*si4)*c5*q[16]+.6589846e-1*(-c6*q[17]*si8*si7-si6*c8*q[19]*si7-
si6*si8*c7*q[18]-si6*q[17]*c7-c6*si7*q[18])*c3-(-si6*si8*si7+c6*c7)*si3*q[14]+(-
si6*q[17]*si8*si7+c6*c8*q[19]*si7+c6*si8*c7*q[18]+c6*q[17]*c7-
si6*si7*q[18])*si3+(c6*si8*si7+si6*c7)*c3*q[14])*c5-.6589846e-1*((-
si6*si8*si7+c6*c7)*c3+(c6*si8*si7+si6*c7)*si3)*si5*q[16]-.354960e-
2*((c6*q[17]*si8*c7+si6*c8*q[19]*c7-si6*si8*si7*q[18]-si6*q[17]*si7+c6*c7*q[18])*c3-
(si6*si8*c7+c6*si7)*si3*q[14]+(si6*q[17]*si8*c7-
c6*c8*q[19]*c7+c6*si8*si7*q[18]+c6*q[17]*si7+si6*c7*q[18])*si3+(-
c6*si8*c7+si6*si7)*c3*q[14])*si5-.354960e-2*((si6*si8*c7+c6*si7)*c3+(-
c6*si8*c7+si6*si7)*si3)*c5*q[16]+.1195032e-1*((c6*q[17]*si8*c7+si6*c8*q[19]*c7-
si6*si8*si7*q[18]-si6*q[17]*si7+c6*c7*q[18])*c3-
(si6*si8*c7+c6*si7)*si3*q[14]+(si6*q[17]*si8*c7-
c6*c8*q[19]*c7+c6*si8*si7*q[18]+c6*q[17]*si7+si6*c7*q[18])*si3+(-
c6*si8*c7+si6*si7)*c3*q[14])*c5-.1195032e-1*((si6*si8*c7+c6*si7)*c3+(-
c6*si8*c7+si6*si7)*si3)*si5*q[16]-.1957380e-1*((-c6*q[17]*si8*si7-si6*c8*q[19]*si7-
si6*si8*c7*q[18]-si6*q[17]*c7-c6*si7*q[18])*c3-(-si6*si8*si7+c6*c7)*si3*q[14]+(-
si6*q[17]*si8*si7+c6*c8*q[19]*si7+c6*si8*c7*q[18]+c6*q[17]*c7-
si6*si7*q[18])*si3+(c6*si8*si7+si6*c7)*c3*q[14])*si5-.1957380e-1*((-
si6*si8*si7+c6*c7)*c3+(c6*si8*si7+si6*c7)*si3)*c5*q[16]-.354960e-2*(-si8*q[19]*c7*c4-
c8*si7*q[18])*c4-c8*c7*si4*q[15]-((-c6*q[17]*si8*c7+si6*c8*q[19]*c7-si6*si8*si7*q[18]-
si6*q[17]*si7+c6*c7*q[18])*si3-(-si6*si8*c7+c6*si7)*c3*q[14]+(si6*q[17]*si8*c7-
c6*c8*q[19]*c7+c6*si8*si7*q[18]+c6*q[17]*si7+si6*c7*q[18])*c3-(-
c6*si8*c7+si6*si7)*si3*q[14])*si4-((-si6*si8*c7+c6*si7)*si3+(-
c6*si8*c7+si6*si7)*c3)*c4*q[15])*c5+.354960e-2*(c8*c7*c4-((-si6*si8*c7+c6*si7)*si3+(-
c6*si8*c7+si6*si7)*c3)*si4)*si5*q[16]-.1195032e-1*(-si8*q[19]*c7*c4-c8*si7*q[18])*c4-
c8*c7*si4*q[15]-((-c6*q[17]*si8*c7+si6*c8*q[19]*c7-si6*si8*si7*q[18]-
si6*q[17]*si7+c6*c7*q[18])*si3-(-si6*si8*c7+c6*si7)*c3*q[14]+(si6*q[17]*si8*c7-
c6*c8*q[19]*c7+c6*si8*si7*q[18]+c6*q[17]*si7+si6*c7*q[18])*c3-(-
c6*si8*c7+si6*si7)*si3*q[14])*si4-((-si6*si8*c7+c6*si7)*si3+(-
c6*si8*c7+si6*si7)*c3)*c4*q[15])*si5-.1195032e-1*(c8*c7*c4-((-si6*si8*c7+c6*si7)*si3+(-
c6*si8*c7+si6*si7)*c3)*si4)*c5*q[16];
f6_close=para[2787]*(pow((para[i+2075]*(t-para[i-1+156])+para[i-
1+2075]*(para[i+156]-t))/(para[i+156]-para[i-1+156])),2)-A);
f6_close_d=para[2799]*(para[i+3210]*(t-para[i-1+156])+para[i-
1+3210]*(para[i+156]-t))/(para[i+156]-para[i-1+156])-dA);
return (f6_open + f6_close + f6_close_d);
}
double fZ1(double t, double *q, double *para)
{
double f7_open, f7_close, f7_close_d, Z1, dZ1;
int i;
for (i=0; i<=100 && t>=para[i+156]; i++);
f7_open=(para[i+863]*(t-para[i-1+156])+para[i-1+863]*(para[i+156]-
t))/(para[i+156]-para[i-1+156]);
Z1=-.17710e-3*(-(si6*si8*c7+c6*si7)*si3+(-c6*si8*c7+si6*si7)*c3)*c4+.419650e-
2*(-(-si6*si8*si7+c6*c7)*si3+(c6*si8*si7+si6*c7)*c3)*c4-.441210e-2*(si6*c8*si3+c6*c8*c3)*c4-
.441210e-2*si8*si4+.464340e-2*(-c8*si7*c4-((-
si6*si8*si7+c6*c7)*si3+(c6*si8*si7+si6*c7)*c3)*si4)*c5+.464340e-2*((-
si6*si8*si7+c6*c7)*c3+(c6*si8*si7+si6*c7)*si3)*si5+.76176e-3*(c8*c7*c4-(-
si6*si8*c7+c6*si7)*si3+(-c6*si8*c7+si6*si7)*c3)*si4)*si5-.19596e-
3*((si6*si8*c7+c6*si7)*c3+(-c6*si8*c7+si6*si7)*si3)*si5-.19596e-3*(c8*c7*c4-(-

```



```

c6*c8*q[19]*c7+c6*si8*si7*q[18]+c6*q[17]*si7+si6*c7*q[18])*c3-(-
c6*si8*c7+si6*si7)*si3*q[14])*si4-(-(si6*si8*c7+c6*si7)*si3+(-
c6*si8*c7+si6*si7)*c3)*c4*q[15])*si5;
    f7_close=para[2788]*(pow((para[i+2176]*(t-para[i-1+156])+para[i-
1+2176]*(para[i+156]-t))/(para[i+156]-para[i-1+156])),2)-Z1);
    f7_close_d=para[2800]*((para[i+3311]*(t-para[i-1+156])+para[i-
1+3311]*(para[i+156]-t))/(para[i+156]-para[i-1+156]))-dZ1);
    return (f7_open + f7_close + f7_close_d);
}
double fZ2(double t, double *q, double *para)
{
    double f8_open, f8_close, f8_close_d, Z2, dz2;
    int i;
    for (i=0; i<=100 && t>=para[i+156]; i++);
        f8_open=(para[i+964]*(t-para[i-1+156])+para[i-1+964]*(para[i+156]-
t))/(para[i+156]-para[i-1+156]);
        Z2=.2310e-4*(-(si6*si8*c7+c6*si7)*si3+(-c6*si8*c7+si6*si7)*c3)*c4-.1481480e-
1*(-(-si6*si8*si7+c6*c7)*si3+(c6*si8*si7+si6*c7)*c3)*c4-.275660e-2*(si6*c8*si3+c6*c8*c3)*c4-
.275660e-2*si8*si4+.1527656e-1*(-c8*si7*c4-(-(si6*si8*si7+c6*c7)*c3+(c6*si8*si7+si6*c7)*c3)*c5+.1527656e-1*((-
si6*si8*si7+c6*c7)*c3+(c6*si8*si7+si6*c7)*si3)*si5+.3186e-4*(c8*c7*c4-(-
si6*si8*c7+c6*si7)*si3+(-c6*si8*c7+si6*si7)*c3)*si4)*si5-.2382e-4*((si6*si8*c7+c6*si7)*c3+(-
c6*si8*c7+si6*si7)*si3)*si5-.2382e-4*(c8*c7*c4-(-(si6*si8*c7+c6*si7)*si3+(-
c6*si8*c7+si6*si7)*c3)*c5+.3186e-4*((si6*si8*c7+c6*si7)*c3+(-
c6*si8*c7+si6*si7)*si3)*c5+.380196e-2*(-si6*c8*c3+c6*c8*si3)*c5-.380196e-2*(si8*c4-
si6*c8*si3+c6*c8*c3)*si4)*si5+.284252e-2*(si8*c4-(si6*c8*si3+c6*c8*c3)*si4)*c5+.284252e-2*(-
si6*c8*c3+c6*c8*si3)*si5-.2043288e-1*(-c8*si7*c4-(-(si6*si8*si7+c6*c7)*c3+(c6*si8*si7+si6*c7)*c3)*si4)*si5+.2043288e-1*((-
si6*si8*si7+c6*c7)*c3+(c6*si8*si7+si6*c7)*si3)*c5+.2310e-4*c8*c7*si4+.1481480e-
1*c8*si7*si4+.4417744e-1;
        dz2=.275660e-2*(si6*c8*si3+c6*c8*c3)*si4*q[15]-.2043288e-1*((-
si6*si8*si7+c6*c7)*c3+(c6*si8*si7+si6*c7)*si3)*si5*q[16]-.2043288e-1*(-c8*si7*c4-(-(si6*si8*si7+c6*c7)*c3+
(c6*si8*si7+si6*c7)*c3)*si4)*c5*q[16]+.2382e-4*(c8*c7*c4-(-
si6*si8*c7+c6*si7)*si3+(-c6*si8*c7+si6*si7)*c3)*si4)*si5*q[16]-.2310e-4*(-
si6*si8*c7+c6*si7)*si3+(-c6*si8*c7+si6*si7)*c3)*si4*q[15]-.2382e-
4*((si6*si8*si7+c6*si7)*c3+(-c6*si8*c7+si6*si7)*si3)*c5*q[16]+.3186e-
4*((si6*si8*c7+c6*si7)*c3+(-c6*si8*c7+si6*si7)*si3)*si5*q[16]+.1527656e-1*((-
si6*si8*si7+c6*c7)*c3+(c6*si8*si7+si6*c7)*si3)*c5*q[16]+.3186e-4*(c8*c7*c4-(-
si6*si8*c7+c6*si7)*si3+(-c6*si8*c7+si6*si7)*c3)*si4)*c5*q[16]-.380196e-2*(si8*c4-
si6*c8*si3+c6*c8*c3)*si4)*c5*q[16]-.1527656e-1*(-c8*si7*c4-(-(si6*si8*si7+c6*c7)*c3+
(c6*si8*si7+si6*c7)*c3)*si4)*si5*q[16]-.2310e-4*si8*q[19]*c7*si4-
.1481480e-1*si8*q[19]*si7*si4+.1481480e-1*c8*c7*q[18]*si4+.1481480e-1*c8*si7*c4*q[15]-.2310e-
4*c8*si7*q[18]*si4+.2310e-4*c8*c7*c4*q[15]+.284252e-2*(c8*q[19]*c4-si8*si4*q[15]-
(c6*q[17]*c8*si3-si6*si8*q[19]*si3+si6*c8*c3*q[14]-si6*q[17]*c8*c3-c6*si8*q[19]*c3-
c6*c8*si3*q[14])*si4-(si6*c8*si3+c6*c8*c3)*c4*q[15])*c5+.1527656e-1*(si8*q[19]*si7*c4-
c8*c7*q[18])*c4+c8*si7*si4*q[15]-(-(c6*q[17]*si8*si7-si6*c8*q[19]*si7-si6*si8*c7*q[18]-
si6*q[17]*c7-c6*si7*q[18])*si3-(-si6*si8*si7+c6*c7)*c3*q[14]+(-
si6*q[17]*si8*si7+c6*c8*q[19]*si7+c6*si8*c7*q[18]+c6*q[17]*c7-si6*si7*q[18])*c3-
(c6*si8*si7+si6*c7)*si3*q[14])*si4-(-(si6*si8*si7+c6*c7)*c3+(c6*si8*si7+si6*c7)*c3)*c4*q[15])*c5-.380196e-2*(c8*q[19]*c4-
si8*si4*q[15]-c6*q[17]*c8*si3-si6*si8*q[19]*si3+si6*c8*c3*q[14]-si6*q[17]*c8*c3-
c6*si8*q[19]*c3-c6*c8*si3*q[14])*si4-(si6*c8*si3+c6*c8*c3)*c4*q[15])*si5-.1481480e-1*(-(-
c6*q[17]*si8*si7-si6*c8*q[19]*si7-si6*si8*c7*q[18]-si6*q[17]*c7-c6*si7*q[18])*si3-(-
si6*si8*si7+c6*c7)*c3*q[14]+(-si6*q[17]*si8*si7+c6*c8*q[19]*si7+c6*si8*c7*q[18]+c6*q[17]*c7-
si6*si7*q[18])*c3-(c6*si8*si7+si6*c7)*si3*q[14])*c4+.284252e-2*(-
c6*q[17]*c8*c3+si6*si8*q[19]*c3+si6*c8*si3*q[14]-si6*q[17]*c8*si3-
c6*si8*q[19]*si3+c6*c8*c3*q[14])*si5-.2382e-4*((c6*q[17]*si8*c7+si6*c8*q[19]*c7-
si6*si8*si7*q[18]-si6*q[17]*si7+c6*c7*q[18])*c3-
(si6*si8*c7+c6*si7)*si3*q[14]+(si6*q[17]*si8*c7-
c6*c8*q[19]*c7+c6*si8*si7*q[18]+c6*q[17]*si7+si6*c7*q[18])*si3+(-
c6*si8*c7+si6*si7)*c3*q[14])*si5-.275660e-2*(c6*q[17]*c8*si3-
si6*si8*q[19]*si3+si6*c8*c3*q[14]-si6*q[17]*c8*c3-c6*si8*q[19]*c3-c6*c8*si3*q[14])*c4-
.2043288e-1*(si8*q[19]*si7*c4-c8*c7*q[18])*c4+c8*si7*si4*q[15]-(-(c6*q[17]*si8*si7-
si6*c8*q[19]*si7-si6*si8*c7*q[18]-si6*q[17]*c7-c6*si7*q[18])*si3-(-
si6*si8*si7+c6*c7)*c3*q[14]+(-si6*q[17]*si8*si7+c6*c8*q[19]*si7+c6*si8*c7*q[18]+c6*q[17]*c7-
si6*si7*q[18])*c3-(c6*si8*si7+si6*c7)*si3*q[14])*si4-(-(si6*si8*si7+c6*c7)*c3+(c6*si8*si7+si6*c7)*c3)*c4*q[15])*si5+.2043288e-1*((-c6*q[17]*si8*si7-
si6*c8*q[19]*si7-si6*si8*c7*q[18]-si6*q[17]*c7-c6*si7*q[18])*c3-(-
si6*si8*si7+c6*c7)*si3*q[14]+(-si6*q[17]*si8*si7+c6*c8*q[19]*si7+c6*si8*c7*q[18]+c6*q[17]*c7-
si6*si7*q[18])*si3+(c6*si8*si7+si6*c7)*c3*q[14])*c5-.2382e-4*(-si8*q[19]*c7*c4-
c8*si7*q[18])*c4-c8*c7*si4*q[15]-(-(c6*q[17]*si8*c7+si6*c8*q[19]*c7-si6*si8*si7*q[18]-

```

```

si6*q[17]*si7+c6*c7*q[18])*si3-(si6*si8*c7+c6*si7)*c3*q[14]+(si6*q[17]*si8*c7-
c6*c8*q[19]*c7+c6*si8*si7*q[18]+c6*q[17]*si7+si6*c7*q[18])*c3-(-
c6*si8*c7+si6*si7)*si3*q[14])*si4-(-(si6*si8*c7+c6*si7)*si3+(-
c6*si8*c7+si6*si7)*c3)*c4*q[15])*c5+.1527656e-1*((-c6*q[17]*si8*si7-si6*c8*q[19]*si7-
si6*si8*c7*q[18]-si6*q[17]*c7-c6*si7*q[18])*c3-(-si6*si8*si7+c6*c7)*si3*q[14]+(-
si6*q[17]*si8*si7+c6*c8*q[19]*si7+c6*si8*c7*q[18]+c6*q[17]*c7-
si6*si7*q[18])*si3+(c6*si8*si7+si6*c7)*c3*q[14])*si5+.380196e-2*(-
c6*q[17]*c8*c3+si6*si8*q[19]*c3+si6*c8*si3*q[14]-si6*q[17]*c8*si3-
c6*si8*q[19]*si3+c6*c8*c3*q[14])*c5+.2310e-4*(-(c6*q[17]*si8*c7+si6*c8*q[19]*c7-
si6*si8*si7*q[18]-si6*q[17]*si7+c6*c7*q[18])*si3-
(si6*si8*c7+c6*si7)*c3*q[14]+(si6*q[17]*si8*c7-
c6*c8*q[19]*c7+c6*si8*si7*q[18]+c6*q[17]*si7+si6*c7*q[18])*c3-(-
c6*si8*c7+si6*si7)*si3*q[14])*c4-.3186e-4*((c6*q[17]*si8*c7+si6*c8*q[19]*c7-
si6*si8*si7*q[18]-si6*q[17]*si7+c6*c7*q[18])*c3-
(si6*si8*c7+c6*si7)*si3*q[14]+(si6*q[17]*si8*c7-
c6*c8*q[19]*c7+c6*si8*si7*q[18]+c6*q[17]*si7+si6*c7*q[18])*si3+(-
c6*si8*c7+si6*si7)*c3*q[14])*c5-.284252e-2*(si8*c4-
(si6*c8*si3+c6*c8*c3)*si4)*si5*q[16]+.1481480e-1*(-(-
si6*si8*si7+c6*c7)*si3+(c6*si8*si7+si6*c7)*c3)*si4*q[15]-.275660e-2*c8*q[19]*si4-.275660e-
2*si8*c4*q[15]+.284252e-2*(-si6*c8*c3+c6*c8*si3)*c5*q[16]-.380196e-2*(-
si6*c8*c3+c6*c8*si3)*si5*q[16]+.3186e-4*(-si8*q[19]*c7*c4-c8*si7*q[18]*c4-c8*c7*si4*q[15]-(-
c6*q[17]*si8*c7+si6*c8*q[19]*c7-si6*si8*si7*q[18]-si6*q[17]*si7+c6*c7*q[18])*si3-
(si6*si8*c7+c6*si7)*c3*q[14]+(si6*q[17]*si8*c7-
c6*c8*q[19]*c7+c6*si8*si7*q[18]+c6*q[17]*si7+si6*c7*q[18])*c3-(-
c6*si8*c7+si6*si7)*si3*q[14])*si4-(-(si6*si8*c7+c6*si7)*si3+(-
c6*si8*c7+si6*si7)*c3)*c4*q[15])*si5;
    f8_close=para[2789]*(pow((para[i+2277]*(t-para[i-1+156]))+para[i-
1+2277]*(para[i+156]-t))/(para[i+156]-para[i-1+156]),2)-Z2);
    f8_close_d=para[2801]*((para[i+3412]*(t-para[i-1+156]))+para[i-
1+3412]*(para[i+156]-t))/(para[i+156]-para[i-1+156])-dZ2);
    return (f8_open + f8_close + f8_close_d);
}
double fB(double t, double *q, double *para)
{
    double f9_open, f9_close, f9_close_d, B, dB;
    int i;
    for (i=0; i<=100 && t>=para[i+156]; i++);
    f9_open=(para[i+1065]*(t-para[i-1+156])+para[i-1+1065]*(para[i+156]-
t))/(para[i+156]-para[i-1+156]);
    B=-.40568e-3*si9*si8-.5918e-4*c9*si8-.40568e-3*c9*si6*c8+.564264e-2*c9*c6*si7-
.82314e-3*si9*c6*si7-.998528e-2*si9*c6*c7+.6844928e-1*c9*c6*c7+.6940963e-1-.82314e-
3*(c9*c8+si9*si6*si8)*c7+.564264e-2*(-si9*c8+c9*si6*si8)*c7+.998528e-
2*(c9*c8+si9*si6*si8)*si7+.5918e-4*si9*si6*c8-.6844928e-1*(-si9*c8+c9*si6*si8)*si7;
    dB=-.6844928e-1*(-c9*q[20]*c8+si9*si8*q[19]-
si9*q[20]*si6*si8+c9*c6*q[17]*si8+c9*si6*c8*q[19])*si7+.564264e-2*(-
c9*q[20]*c8+si9*si8*q[19]-si9*q[20]*si6*si8+c9*c6*q[17]*si8+c9*si6*c8*q[19])*c7+.998528e-2*(-
si9*q[20]*c8-c9*si8*q[19]+c9*q[20]*si6*si8+si9*c6*q[17]*si8+si9*si6*c8*q[19])*si7-.5918e-
4*c9*c8*q[19]-.40568e-3*c9*q[20]*si8+.5918e-4*si9*q[20]*si8-.82314e-3*(-si9*q[20]*c8-
c9*si8*q[19]+c9*q[20]*si6*si8+si9*c6*q[17]*si8+si9*si6*c8*q[19])*c7-.564264e-2*(-
si9*c8+c9*si6*si8)*si7*q[18]-.6844928e-1*(-si9*c8+c9*si6*si8)*c7*q[18]-.40568e-
3*si9*c8*q[19]+.998528e-2*(c9*c8+si9*si6*si8)*c7*q[18]+.82314e-
3*(c9*c8+si9*si6*si8)*si7*q[18]-.564264e-2*si9*q[20]*c6*si7-.564264e-
2*c9*si6*q[17]*si7+.564264e-2*c9*c6*c7*q[18]+.40568e-3*si9*q[20]*si6*c8-.40568e-
3*c9*c6*q[17]*c8+.40568e-3*c9*si6*si8*q[19]+.5918e-4*c9*q[20]*si6*c8+.5918e-
4*si9*c6*q[17]*c8-.5918e-4*si9*si6*si8*q[19]-.6844928e-1*si9*q[20]*c6*c7+.998528e-
2*si9*si6*q[17]*c7-.6844928e-1*c9*si6*q[17]*c7-.6844928e-1*c9*c6*si7*q[18]-.82314e-
3*c9*q[20]*c6*si7+.82314e-3*si9*si6*q[17]*si7-.82314e-3*si9*c6*c7*q[18]-.998528e-
2*c9*q[20]*c6*c7+.998528e-2*si9*c6*si7*q[18];
    f9_close=para[2790]*(pow((para[i+2378]*(t-para[i-1+156]))+para[i-
1+2378]*(para[i+156]-t))/(para[i+156]-para[i-1+156]),2)-B);
    f9_close_d=para[2802]*((para[i+3513]*(t-para[i-1+156]))+para[i-
1+3513]*(para[i+156]-t))/(para[i+156]-para[i-1+156])-dB);
    return (f9_open + f9_close + f9_close_d);
}
double fC(double t, double *q, double *para)
{
    double f10_open, f10_close, f10_close_d, C, dC;
    int i;
    for (i=0; i<=100 && t>=para[i+156]; i++);
    f10_open=(para[i+1166]*(t-para[i-1+156])+para[i-1+1166]*(para[i+156]-
t))/(para[i+156]-para[i-1+156]);

```

```

C=.11418115+.1114854e-1*c10*c9+.1114854e-1*si10*si9-.3190590e-
1*c10*si9+.3190590e-1*si10*c9;
dC=-.1114854e-1*si10*q[21]*c9-.1114854e-1*c10*si9*q[20]+.1114854e-
1*c10*q[21]*si9+.1114854e-1*si10*c9*q[20]+.3190590e-1*si10*q[21]*si9-.3190590e-
1*c10*c9*q[20]+.3190590e-1*c10*q[21]*c9-.3190590e-1*si10*si9*q[20];
f10_close=para[2791]*(pow((para[i+2479]*(t-para[i-1+156])+para[i-
1+2479]*(para[i+156]-t))/(para[i+156]-para[i-1+156]),2)-C);
f10_close_d=para[2803]*((para[i+3614]*(t-para[i-1+156])+para[i-
1+3614]*(para[i+156]-t))^(para[i+156]-para[i-1+156])-dC);
return (f10_open + f10_close + f10_close_d);
}
double fD(double t, double *q, double *para)
{
double f11_open, f11_close, f11_close_d, D, dD;
int i;
for (i=0; i<=100 && t>=para[i+156]; i++);
f11_open=(para[i+1267]*(t-para[i-1+156])+para[i-1+1267]*(para[i+156]-
t))/(para[i+156]-para[i-1+156]);
D=.11714106-.415000e-2*c11*si10+.415000e-2*si11*c10+.360000e-
2*c11*c10+.360000e-2*si11*si10+.2041520e-1*c11*c9+.2041520e-1*si11*si9-.3050970e-
1*c11*si9+.3050970e-1*si11*c9+.416000e-2*si10*c9-.416000e-2*c10*si9+.3315000e-
1*c10*c9+.3315000e-1*si10*si9;
dD=.415000e-2*si11*q[22]*si10-.415000e-2*c11*c10*q[21]+.415000e-
2*c11*q[22]*c10-.415000e-2*si11*si10*q[21]-.360000e-2*si11*q[22]*c10-.360000e-
2*c11*si10*q[21]+.360000e-2*c11*q[22]*si10+.360000e-2*si11*c10*q[21]-.2041520e-
1*si11*q[22]*c9-.2041520e-1*c11*si9*q[20]+.2041520e-1*c11*q[22]*si9+.2041520e-
1*si11*c9*q[20]+.3050970e-1*si11*q[22]*si9-.3050970e-1*c11*c9*q[20]+.3050970e-1*c11*q[22]*c9-
.3050970e-1*si11*si9*q[20]+.416000e-2*c10*q[21]*c9-.416000e-2*si10*si9*q[20]+.416000e-
2*si10*q[21]*si9-.416000e-2*c10*c9*q[20]-.3315000e-1*si10*q[21]*c9-.3315000e-
1*c10*si9*q[20]+.3315000e-1*c10*q[21]*si9+.3315000e-1*si10*c9*q[20];
f11_close=para[2792]*(pow((para[i+2580]*(t-para[i-1+156])+para[i-
1+2580]*(para[i+156]-t))/(para[i+156]-para[i-1+156]),2)-D);
f11_close_d=para[2804]*((para[i+3715]*(t-para[i-1+156])+para[i-
1+3715]*(para[i+156]-t))/(para[i+156]-para[i-1+156])-dD);
return (f11_open + f11_close + f11_close_d);
}
double fE(double t, double *q, double *para)
{
double f12_open, f12_close, f12_close_d, E, dE;
int i;
for (i=0; i<=100 && t>=para[i+156]; i++);
f12_open = (para[i+1368]*(t-para[i-1+156])+para[i-1+1368]*(para[i+156]-
t))/(para[i+156]-para[i-1+156]);
E=.7739006e-1-.226570e-2*c12*c11-.226570e-2*si12*si11-.3568860e-
1*c12*si11+.3568860e-1*si12*c11;
dE=.226570e-2*si12*q[23]*c11+.226570e-2*c12*si11*q[22]-.226570e-
2*c12*q[23]*si11-.226570e-2*si12*c11*q[22]+.3568860e-1*si12*q[23]*si11-.3568860e-
1*c12*c11*q[22]+.3568860e-1*c12*q[23]*c11-.3568860e-1*si12*si11*q[22];
f12_close=para[2793]*(pow((para[i+2681]*(t-para[i-1+156])+para[i-
1+2681]*(para[i+156]-t))/(para[i+156]-para[i-1+156]),2)-E);
f12_close_d=para[2805]*((para[i+3816]*(t-para[i-1+156])+para[i-
1+3816]*(para[i+156]-t))/(para[i+156]-para[i-1+156])-dE);
return (f12_open + f12_close + f12_close_d);
}
double fh(double t, double *q, double *para)
{
int i;
for (i=0; i<=100 && t>=para[i+156]; i++);
return ((para[i+1469]*(t-para[i-1+156])+para[i-1+1469]*(para[i+156]-t))/(para[i+156]-
para[i-1+156]));
}

```

Matlab code of the control system for demonstrating the motion of the replica.

```

clear all

% VALUES FOR PARAMETER LIST
P = [-0.0296,-0.0422, 0.0275, 0.0267,-0.1201,-0.0085, 0.0685,-0.1449, 0.0065,-0.0425,...
     -0.0726,-0.0024,-0.0522,-0.1765, 0.0329,-0.1899,-0.0016,-0.0252, 0.0016,-0.0248,...
     -0.0300,-0.1677, 0.0300,-0.1353,-0.0015,-0.0959, 0.0075,-0.0849, 0.2941, 0.0514,...
     0.0579,-0.2514,-0.1093, 0.0579, 0.3138,-0.1323, 0.0579, 0.0725,-0.0765,-0.0183,...
     -0.0566,-0.0601,-0.0191, 0.0575,-0.1220,-0.0134, 0.0539,-0.0094,-0.0190,-0.0397,...
     -0.0033,-0.00575,-0.0368, 0.1092, 0.0195,-0.0023, 0.0545,-0.0573,-0.0003, 0.1924,...
     0.0358, 0.0348, 0.1919,-0.0052,-0.0413, 0.0319,-0.0052,-0.0269, 0.1844, 0.0609,...
     0.0349,-0.0007, 0.3864, 0.0453, 0.0225, 0.0200, 0.0210, 0.0200, 0.0290, 0.0415,...
     0.0360,-0.0200,-0.0200, 0.0659, 0.0060, 0.0000, 0.0000, 0.0000, 0.0000, 0.0000,...
     0.0000];
A = [5.507, 0.04093, 0.00660, 0.00122, 0.00660, 0.02248,-0.00271, 0.00122,-0.00271, 0.05916];
B = [3.026, 0.01654,-0.00619,-0.00024,-0.00619, 0.00922, 0.00033,-0.00024, 0.00033, 0.02478];
C = [3.686, 0.03956, 0.00065,-0.00016, 0.00065, 0.00275, 0.00007,-0.00016, 0.00007, 0.03983];
D = [0.617, 0.00057, 0.00000, 0.00002, 0.00000, 0.00030, 0.00000, 0.00002, 0.00000, 0.00055];
E = [2.666, 0.02266,-0.00009, 0.00001,-0.00009, 0.00153, 0.00003, 0.00001, 0.00003, 0.02352];
F = [0.882, 0.00207,-0.00033, 0.00000,-0.00033, 0.00054, 0.00000, 0.00000, 0.00000, 0.00206];
O = [3.000, 0.03000, 0.03000, 0.03000];
G = 9.81;

for tj=1:101
    T(1,tj) = 0+(tj-1)*(0.67/100);
end

load Ft_t.txt Ft = Ft_t'; load Fh_t.txt Fh = Fh_t'; Ft=[Ft;Fh];

load length_t.txt lengths = length_t'; load dlength_t.txt dlength = dlength_t';

k1 = 100; k2 = 1000000; k3 =-75000000; k4 =-75000000; k5 =-75000000; k6 =-20000000;
k7 =-20000000; k8 =-20000000; k9 =-1000000; k10=-1000000; k11=-1000000; k12=-1000000;
dk1=10000; dk2=1000; dk3=-5000; dk4=-5000; dk5=-5000; dk6=-10000; dk7=-10000; dk8=-10000;
dk9=-2000; dk10=-4000; dk11=-3000; dk12=-6000;
K=[k1,k2,k3,k4,k5,k6,k7,k8,k9,k10,k11,k12,dk1,dk2,dk3,dk4,dk5,dk6,dk7,dk8,dk9,dk10,dk11,dk12];

% DEFINE THE PARAMETER LIST
% positions
parameters(1:91,1) = P(1,:);

% mass and inertia properties
parameters(92:101,1)=A(1,:); parameters(102:111,1)=B(1,:); parameters(112:121,1)=C(1,:);
parameters(122:131,1)=D(1,:); parameters(132:141,1)=E(1,:); parameters(142:151,1)=F(1,:);
parameters(152:155,1)=O(1,:);

% gravity
parameters(156,1) = G;

% time
parameters(157:257,1) = T(1,:);

% forces
for k=1:13
    parameters(258+(k-1)*101:358+(k-1)*101,1) = Ft(k,:);
end

% lengths of cylinders
for k=1:12
    parameters(1571+(k-1)*101:1671+(k-1)*101,1) = lengths(k,:);
end

% gains
parameters(2783:2806,1) = K(1,:);

% derivatives of lengths
for k=1:11
    parameters(2807+(k-1)*101:2907+(k-1)*101,1) = dlength(k,:);
end

```

```

% INITIAL CONDITIONS AT 0% OF STRIDE
theta_i = [0,0.0750,-0.2618,0,0.6629,0,-0.3402,0,0.5321,0.4797,0.4274,0.8286];
omega_i = [0,-0.483,0,0,0.994,0,-0.314,0,-3.285,-2.361,-1.439,4.115];
IC = [theta_i,omega_i];

% TIME
Ti = 0; Tf = .67;

% SET OPTIONS
figure(1)
options = odeset('RelTol',1e-8,'AbsTol',1e-8,'OutputFcn','odeplot','OutputSel',1);

% GAIT WITH CONTROL
[Time,QU] = ode45('equine_eq_forelimb_v5',[Ti:.01:Tf],IC,options,parameters);

% COLLECTED GAIT DATA TO BE MATCHED
x = -.067:.0335:0.737;
xx = -.067:0.737/110:0.737;
y_y =
[0.1398,0.1105,0.075,0.0926,0.1072,0.0974,0.1108,0.1059,0.0846,0.0645,0,0.0195,0.0229,0.0511,
0.0602,0.0548,0.0854,0.1339,0.1494,0.1464,0.1398,0.1105,0.075,0.0926,0.1072];
yy_y = spline(x,y_y,xx);
y_s =
[0.5757,0.6106,0.6629,0.6454,0.5757,0.5408,0.5059,0.4187,0.3489,0.3140,0.2617,0.2442,0.2791,0
.3489,0.4361,0.4884,0.5408,0.5669,0.5844,0.5757,0.5757,0.6106,0.6629,0.6454,0.5757];
yy_s = spline(x,y_s,xx);
y_h = [-0.4361,-0.3506,-0.3402,-0.3969,-0.5669,-0.6760,-0.6489,-0.7379,-0.8199,-0.8286,-
0.8443,-0.8548,-0.8304,-0.7641,-0.6768,-0.6210,-0.5268,-0.4762,-0.4588,-0.4832,-0.4361,-
0.3506,-0.3402,-0.3969,-0.5669];
yy_h = spline(x,y_h,xx);
y_r = [0.7327,0.6437,0.5321,0.4056,0.2181,0.1439,0.0488,-0.1099,-0.2442,-0.3751,-0.3733,-
0.2617,-0.0105,0.2826,0.5443,0.7222,0.9036,0.9891,0.9891,0.8426,0.7327,0.6437,0.5321,
0.4056,0.2181];
yy_r = spline(x,y_r,xx);
y_c = [0.5669,0.5390,0.4797,0.3620,0.2093,0.1352,0.0488,-0.1099,-0.2704,-0.4361,-0.5914,-
0.6106,-0.5512,-0.4152,-0.2058,-0.0192,0.2233,0.4222,0.5792,0.5983,0.5669,0.5390,0.4797,
0.3620,0.2093];
yy_c = spline(x,y_c,xx);
y_m = [0.4012,0.4344,0.4274,0.3184,0.2006,0.1265,0.0488,-0.1099,-0.2966,-0.4972,-0.8094,-
0.9594,-1.0920,-1.1130,-0.9560,-0.7606,-0.4570,-0.1448,0.1692,0.3541,0.4012,0.4344,0.4274,
0.3184,0.2006];
yy_m = spline(x,y_m,xx);
y_f = [0.4884,0.6437,0.8286,0.8940,0.9856,1.0336,1.0257,0.8495,0.5059,0.0436,-0.5303,-
1.2037,-1.2665,-1.1304,-1.0083,-1.0048,-0.8408,-0.5460,-0.0227,0.3890,0.4884,0.6437,0.8286,
0.8940,0.9856];
yy_f = spline(x,y_f,xx);
xx = 0:0.67/100:0.67; yy_y = yy_y(11:111); yy_s = yy_s(11:111); yy_h = yy_h(11:111);
yy_r = yy_r(11:111); yy_c = yy_c(11:111); yy_m = yy_m(11:111); yy_f = yy_f(11:111);

figure(2)
plot(Time,QU(:,1),'go',Time,QU(:,2),'ro',xx,yy_y,'b:')
ylabel('Position (m)'),xlabel('Time (sec)'),title('Thorax position')
figure(3)
plot(Time,QU(:,5),'r-',Time,QU(:,4),'g:',Time,QU(:,3),'g-',xx,yy_s,'b:')
ylabel('Absolute Angle (rad)'),xlabel('Time (sec)'),title('Scapula Angle')
figure(4)
plot(Time,QU(:,7),'r-',Time,QU(:,6),'g:',Time,QU(:,8),'g-',xx,yy_h,'b:')
ylabel('Absolute Angle (rad)'),xlabel('Time (sec)'),title('Humerus Angle')
figure(5)
plot(Time,QU(:,9),'r-',xx,yy_r,'b:')
ylabel('Absolute Angle (rad)'),xlabel('Time (sec)'),title('Radius Angle')
figure(6)
plot(Time,QU(:,10),'r-',xx,yy_c,'b:')
ylabel('Absolute Angle (rad)'),xlabel('Time (sec)'),title('Carpus Angle')
figure(7)
plot(Time,QU(:,11),'r-',xx,yy_m,'b:')
ylabel('Absolute Angle (rad)'),xlabel('Time (sec)'),title('Metacarpal Angle')
figure(8)
plot(Time,QU(:,12),'r-',xx,yy_f,'b:')
ylabel('Absolute Angle (rad)'),xlabel('Time (sec)'),title('Fetlock Angle')

```

Appendix B: Parts List

Table B- 1: List of required parts for a robotic replica of an equine forelimb.

Part #	Description/Part #	Manufacturer	Qty
101DSR	Shaft, Hinge Joint	ESM Machine Shop	4
102DSR	Bracket, Scapula Actuator	ESM Machine Shop	3
104DSR	Shaft, PII-PIII Joint	ESM Machine Shop	1
105DSR	Spring, PIII Return	ESM Machine Shop	1
109DSR	Pin, Actuator Retaining	ESM Machine Shop	1
110DSR	Pin, Actuator Retaining	ESM Machine Shop	1
111DSR	Pin, Actuator Retaining	ESM Machine Shop	1
112DSR	Pin, Actuator Retaining	ESM Machine Shop	1
113DSR	Pin, Actuator Retaining	ESM Machine Shop	2
203DSR	Radius	ESM Machine Shop	1
206DSR	Metacarpal	ESM Machine Shop	1
211DSR	Humerus	ESM Machine Shop	1
214DSR	Proximal Phalanx	ESM Machine Shop	1
215DSR	Middle Phalanx	ESM Machine Shop	1
216DSR	Distal Phalanx	ESM Machine Shop	1
217DSR	Thorax, Proximal	ESM Machine Shop	1
218DSR	Thorax, Intermediate	ESM Machine Shop	1
301DSR	Carpus	ESM Machine Shop	1
302DSR	Scapula	ESM Machine Shop	1
303DSR	Thorax, Distal	ESM Machine Shop	1
601DSR	Bearing, 2x Sealed, Grease Pkd, 203	BCA Bearings	10
602DSR	Snap Ring, VH-162-S02	Smalley Steel Ring Co.	10
603DSR	Bolt, M4x12mm	Havener Hardware	3
604DSR	Set Screw, M4x7mm	Havener Hardware	4
605DSR	Ball Joint, TBS12	THK America	2
606DSR	Ball Joint, TBS8	THK America	8
607DSR	Ball Joint, RBL8D	THK America	4
608DSR	Bearing,	McMaster Carr	2
609DSR	Shaft,	McMaster Carr	2
610DSR	Support,	McMaster Carr	4

Continued on next page...

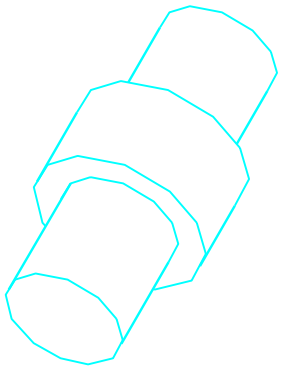
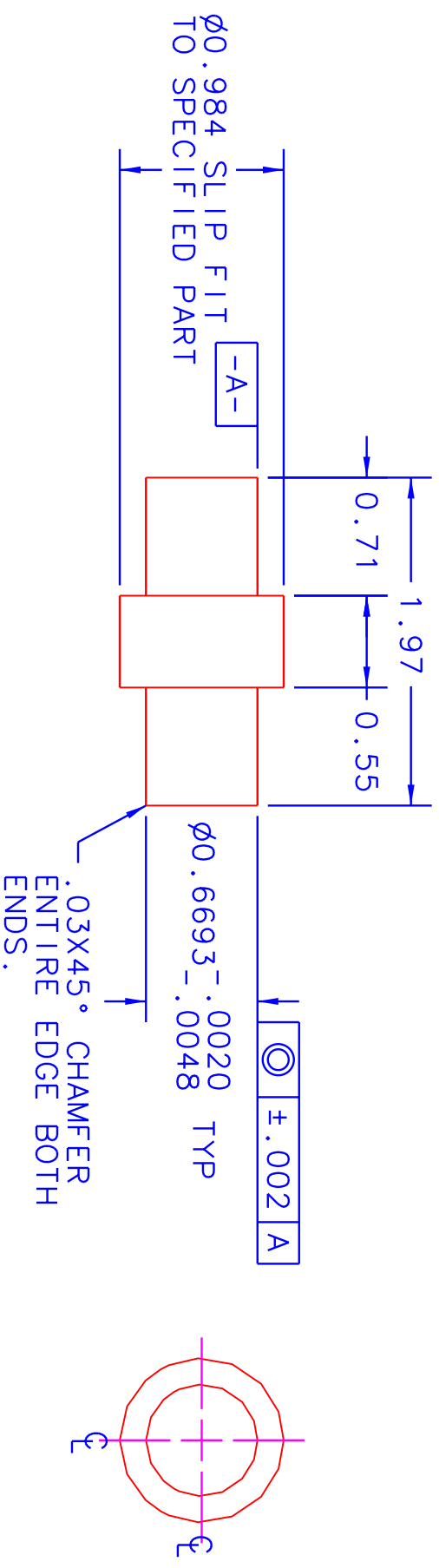
611DSR	Hydraulic Actuator	Custom built	2
612DSR	Hydraulic Actuator	Custom built	3
613DSR	Hydraulic Actuator	Custom built	1
614DSR	Hydraulic Actuator	Custom built	1
615DSR	Hydraulic Actuator	Custom built	1
616DSR	Hydraulic Actuator	Custom built	1
617DSR	Hydraulic Actuator	Custom built	1
618DSR	Linear Actuator, GL20S20+200	THK America	1
619DSR	Bolt, M5x25mm	Havener Hardware	6
620DSR	Bolt, M8x30mm	Havener Hardware	4
621DSR	Bolt, #10x0.75	Havener Hardware	12
622DSR	Spring, 72220	Century Spring	4
623DSR	Bolt, #8x0.75	Havener Hardware	8
624DSR	Nut Sleeve	Havener Hardware	4
625DSR	Bolt, M5x20mm	Havener Hardware	12
626DSR	Damper	To be determined	1

Appendix C: Engineering Drawings

Table C- 1: List of Detailed Drawings.

101DSR Shaft, Hinge Joint	217DSR Thorax, Proximal
102DSR Bracket, Scapula Actuator	218DSR Thorax, Intermediate
104DSR Shaft, PII-PIII Joint	220DSR Radius, Midpoint
105DSR Spring, PIII Return	301DSR Carpus
109DSR Pin, Actuator Retaining	302DSR Scapula
112DSR Pin, Actuator Retaining	303DSR Thorax, Distal
201DSR Radius to Humerus Joint	601DSR Bearing, 2x Sealed, Grease Pkd, 203
202DSR Radius to Carpus Joint	602DSR Snap Ring, VH-162-S02
203DSR Radius	608DSR Bearing, 5/8in Standard Length
204DSR Metacarpal to Carpal Joint	609DSR Shaft, 5/8in x 7in
205DSR Metacarpal to Fetlock Joint	610DSR Shaft Support, 5/8in
206DSR Metacarpal	612DSR Hydraulic Actuator
209DSR Humerus to Radius Joint	613DSR Hydraulic Actuator
210DSR Humerus to Scapula Joint	614DSR Hydraulic Actuator
211DSR Humerus	615DSR Hydraulic Actuator
212DSR Fetlock to Metacarpal Joint	616DSR Hydraulic Actuator
213DSR Fetlock to Hoof Joint	617DSR Hydraulic Actuator
214DSR Fetlock	622DSR Spring, 72220
215DSR Hoof to Fetlock Joint	
216DSR Hoof	

REVISIONS				
ZONE	REV	DESCRIPTION	DATE	APPROVED
	1	INITIAL ISSUE		



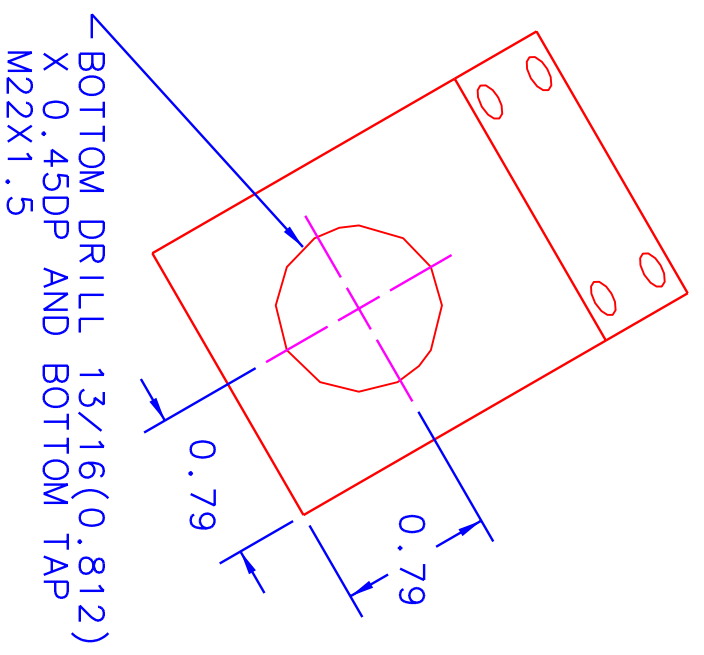
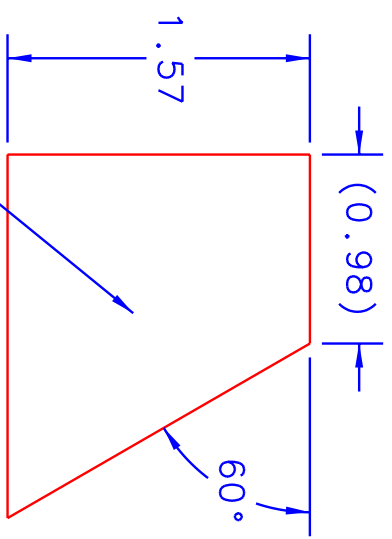
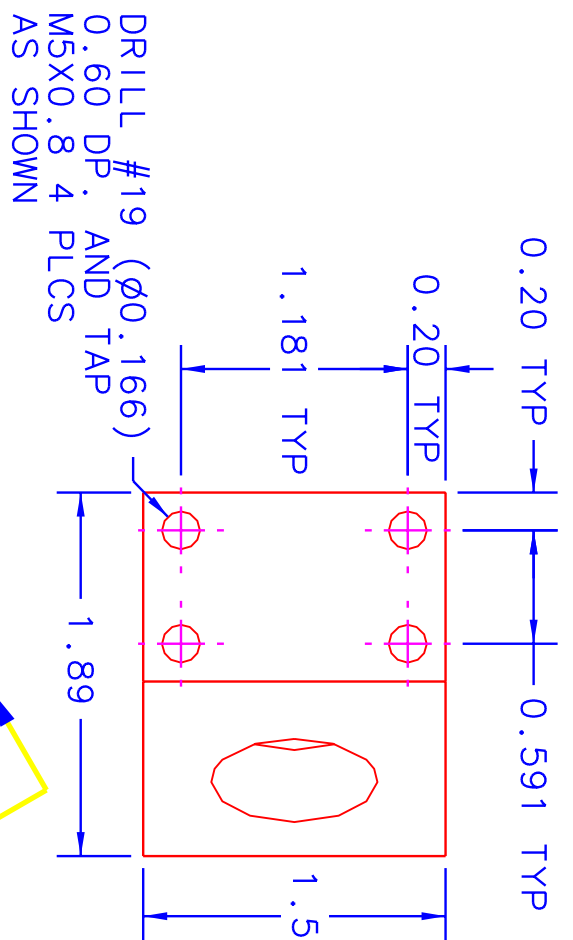
NOTES

- 1: BREAK ALL SHARP EDGES AND CORNERS W/ $.01 \times 45^\circ$ MIN CHAMFERS

UNLESS OTHERWISE SPECIFIED DIMENSIONS ARE IN INCHES		TOLERANCES ARE:	
FRACTIONS	DECIMALS	ANGLES	
$\pm .XX$	$\pm .01$	$\pm X^\circ \pm .5^\circ$	
DO NOT SCALE DRAWING			
MATERIAL	304SS		
FINISH	NONE		
SIMILAR TO	ACT. WT	CALC. WT	
APPROVALS		DATE	TITLE
DRAWN D.S. RUPPERT		7/24/01	SHAFT, JOINT
CHECKED			
ISSUED			
SIZE	FSCM NO.	DWG. NO.	
A		101DSR	
SCALE	NA	SHEET	1 OF 1

VIRGINIA POLYTECHNIC INSTITUTE AND STATE UNIVERSITY
DEPARTMENT OF ENGINEERING SCIENCE AND MECHANICS

REVISIONS				
ZONE	REV	DESCRIPTION	DATE	APPROVED
	1	INITIAL ISSUE		



VIEW A-A

- NOTES
- 1: BREAK ALL SHARP EDGES AND CORNERS
 - 2: STAMP DWG. # AND REV W/ 1/8 IN HIGH CHARACTERS HERE.

VIRGINIA POLYTECHNIC INSTITUTE AND STATE UNIVERSITY
DEPARTMENT OF ENGINEERING SCIENCE AND MECHANICS

UNLESS OTHERWISE SPECIFIED
DIMENSIONS ARE IN INCHES
TOLERANCES ARE:
FRACTIONS DECIMALS ANGLES
± .XX ±.01 X° ±.5°
DO NOT SCALE DRAWING

MATERIAL ALUMINUM

FINISH 6061

SIMILAR TO	ACT. WT	CALC WT
------------	---------	---------

APPROVALS

DRAWN D.S. RUPPERT 8/21/02

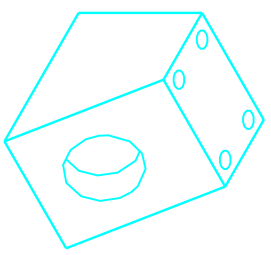
CHECKED

ISSUED

TITLE

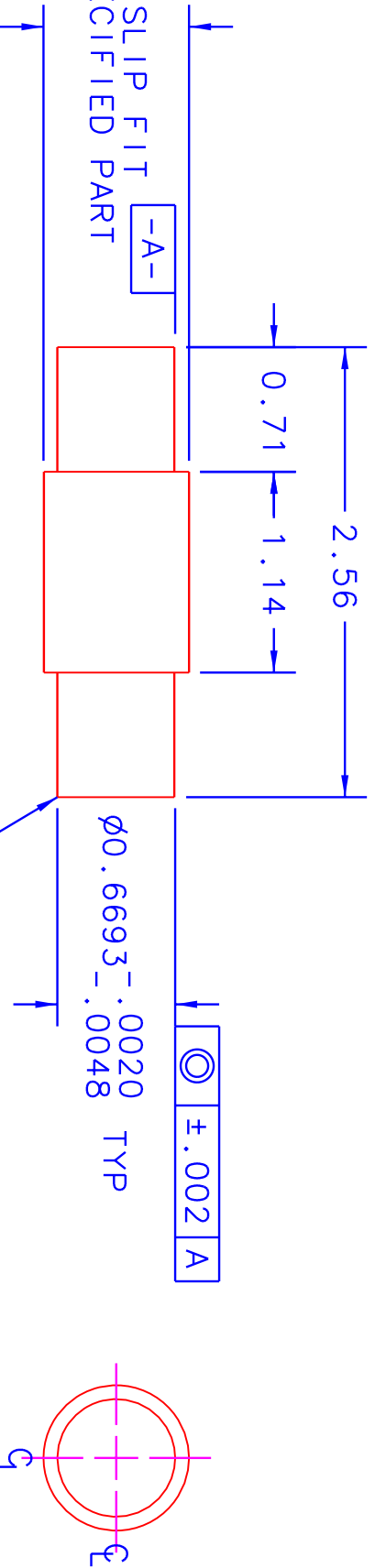
BRACKET, SCAPULA ACTUATOR

SIZE	FSCM NO.	DWG NO.	SHEET
A		102DSR	1 OF 1
SCALE	N/A		



REVISIONS				
ZONE	REV	DESCRIPTION	DATE	APPROVED
	1	INITIAL ISSUE		

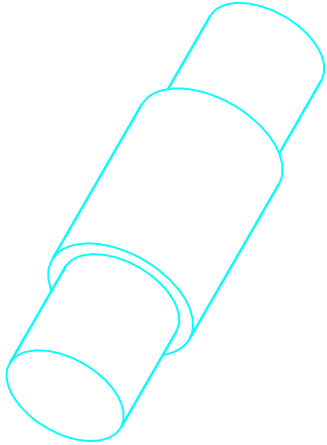
0.827 SLIP FIT
TO SPECIFIED PART



.03X45° CHAMFER
ENTIRE EDGE BOTH
ENDS.

NOTES

- 1: BREAK ALL SHARP EDGES AND CORNERS
W/ .01X45° MIN CHAMFERS UNLESS
OTHERWISE NOTED.



VIRGINIA POLYTECHNIC INSTITUTE AND STATE UNIVERSITY
DEPARTMENT OF ENGINEERING SCIENCE AND MECHANICS

UNLESS OTHERWISE SPECIFIED
DIMENSIONS ARE IN INCHES
TOLERANCES ARE:
FRACTIONS DECIMALS ANGLES
± .XX ±.01 X°.±.5°
DO NOT SCALE DRAWING

MATERIAL 304SS

FINISH NONE

SIMILAR TO 101DSR

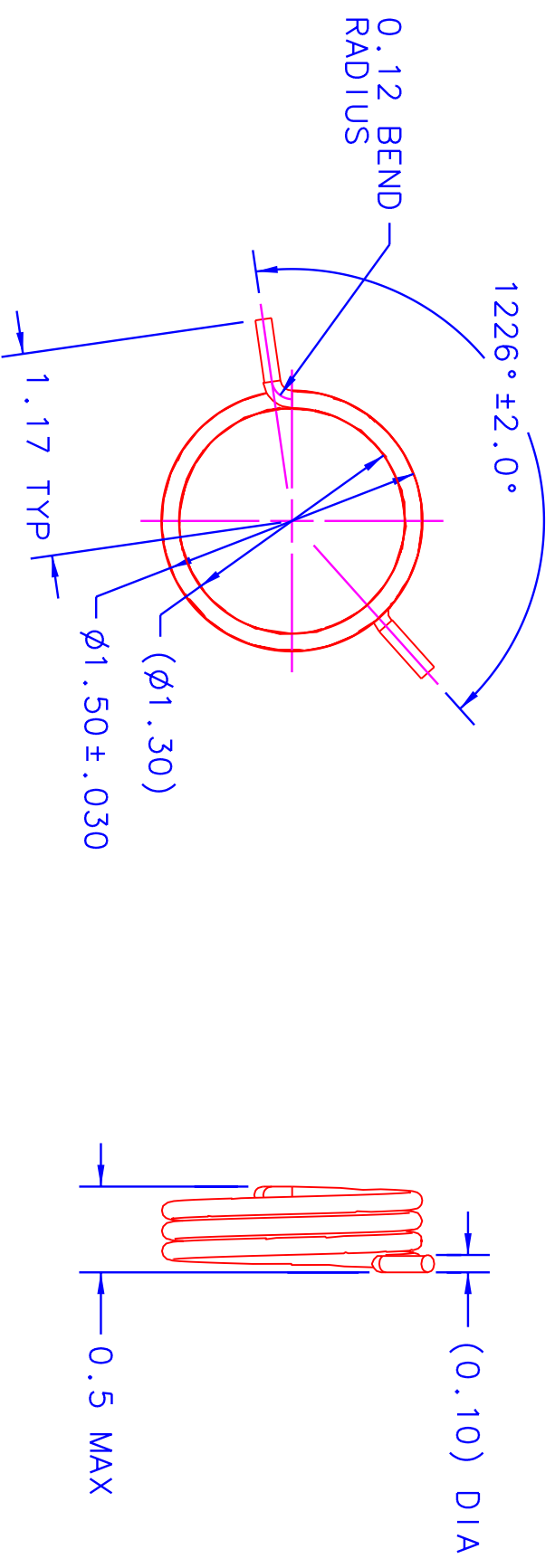
APPROVALS	DATE
DRAWN D.S. RUPPERT	10/11/01
CHECKED	
ISSUED	

TITLE
SHAFT 2, JOINT

SIZE A FSCM NO. 104DSR

SCALE NA SHEET 1 OF 1

REVISIONS				
ZONE	REV	DESCRIPTION	DATE	APPROVED
	1	INITIAL ISSUE		



NOTES

- 1: BREAK ALL SHARP EDGES AND CORNERS.
- 2: USE 0.10 DIAMETER MUSIC WIRE.



UNLESS OTHERWISE SPECIFIED DIMENSIONS ARE IN INCHES TOLERANCES ARE:		VIRGINIA POLYTECHNIC INSTITUTE AND STATE UNIVERSITY DEPARTMENT OF ENGINEERING SCIENCE AND MECHANICS	
FRACTIONS	DECIMALS	ANGLES	
± .XX±.01	± .XXX±.005	X°±.5°	
DO NOT SCALE DRAWING			
MATERIAL	SEE NOTE 2	DRAWN	D.S. RUPPERT
FINISH		CHECKED	
SIMILAR TO		ISSUED	
ACT. WT	CALC. WT	DATE	11/01/01
		TITLE	SPRING, TORSION
		SIZE	A
		FSCM NO.	
		DWG NO.	105DSR
		SCALE	NA
		SHEET	1 OF 1

NOTE
 BREAK ALL SHARP EDGES AND CORNERS
 W/ 0.01X45° MIN CHAMFERS.

REVISIONS				
ZONE	REV	DESCRIPTION	DATE	APPROVED
	1	INITIAL ISSUE		



PART	D	L
109DSR	0.236	1.18
110DSR	0.236	2.17
111DSR	0.177	1.06
113DSR	0.236	0.98

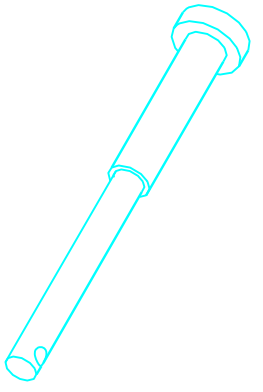
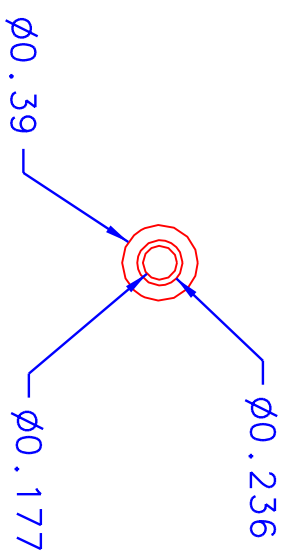
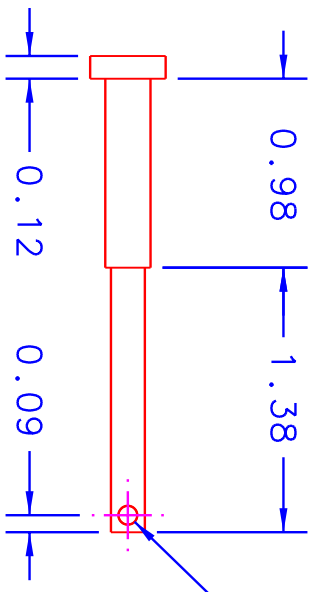


UNLESS OTHERWISE SPECIFIED DIMENSIONS ARE IN INCHES TOLERANCES ARE: FRACTIONS DECIMALS ANGLES ± .XX -±.01 X°-±.5° DO NOT SCALE DRAWING		VIRGINIA POLYTECHNIC INSTITUTE AND STATE UNIVERSITY DEPARTMENT OF ENGINEERING SCIENCE AND MECHANICS	
MATERIAL 304SS	DRAWN D.S. RUPPERT	DATE 8/21/02	TITLE PIN, ACTUATOR RETAINING
FINISH	CHECKED		SIZE A
SIMILAR TO	ISSUED		FSGM NO.
ACT. WT	CALC WT		DWG NO. 109DSR
			SCALE NA
			SHEET 1 OF 1

NOTE

BREAK ALL SHARP EDGES AND CORNERS
W/ 0.01X45° MIN CHAMFERS

REVISIONS				
ZONE	REV	DESCRIPTION	DATE	APPROVED
	1	INITIAL ISSUE		



UNLESS OTHERWISE SPECIFIED DIMENSIONS ARE IN INCHES TOLERANCES ARE: FRACTIONS DECIMALS ANGLES ± .XX = ±.01 X° = ±.5° DO NOT SCALE DRAWING		VIRGINIA POLYTECHNIC INSTITUTE AND STATE UNIVERSITY DEPARTMENT OF ENGINEERING SCIENCE AND MECHANICS	
MATERIAL 304SS	DRAWN D. S. RUPPERT	DATE 8/21/02	TITLE PIN, MULTI-ACTUATOR RETAINING
FINISH	CHECKED		SIZE FSCM NO. DWG NO.
SIMILAR TO	ISSUED		A 112DSR
ACT. WT			SCALE NA
CALC. WT			SHEET 1 OF 1

1

2

3

4

DWG. NO. 201DSR SH 1 REV. 1

REVISIONS				
ZONE	REV	DESCRIPTION	DATE	APPROVED
1	1	INITIAL ISSUE		

CHAMFER BOTH SIDES:
ENTIRE EDGE .03X45°

Ø0.984 SLIP FIT
TO SHAFT 101DSR

Ø1.57

0.79

0.787 ±.010

1.18

0.25

65°

2.76

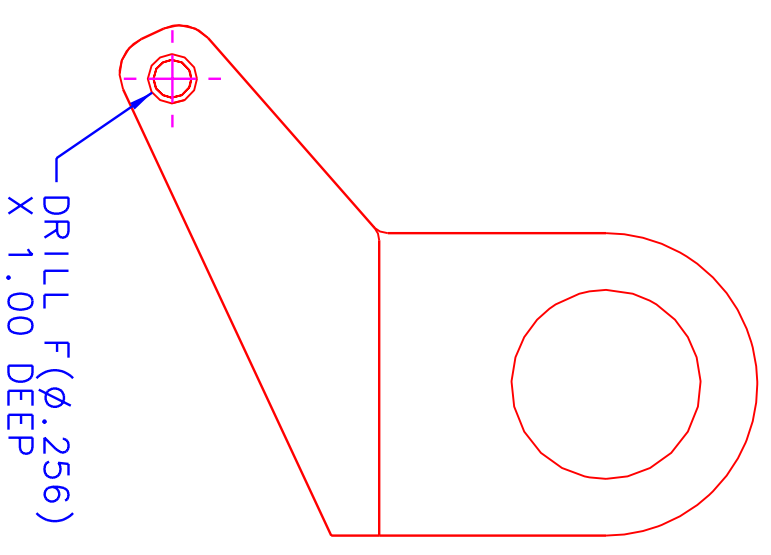
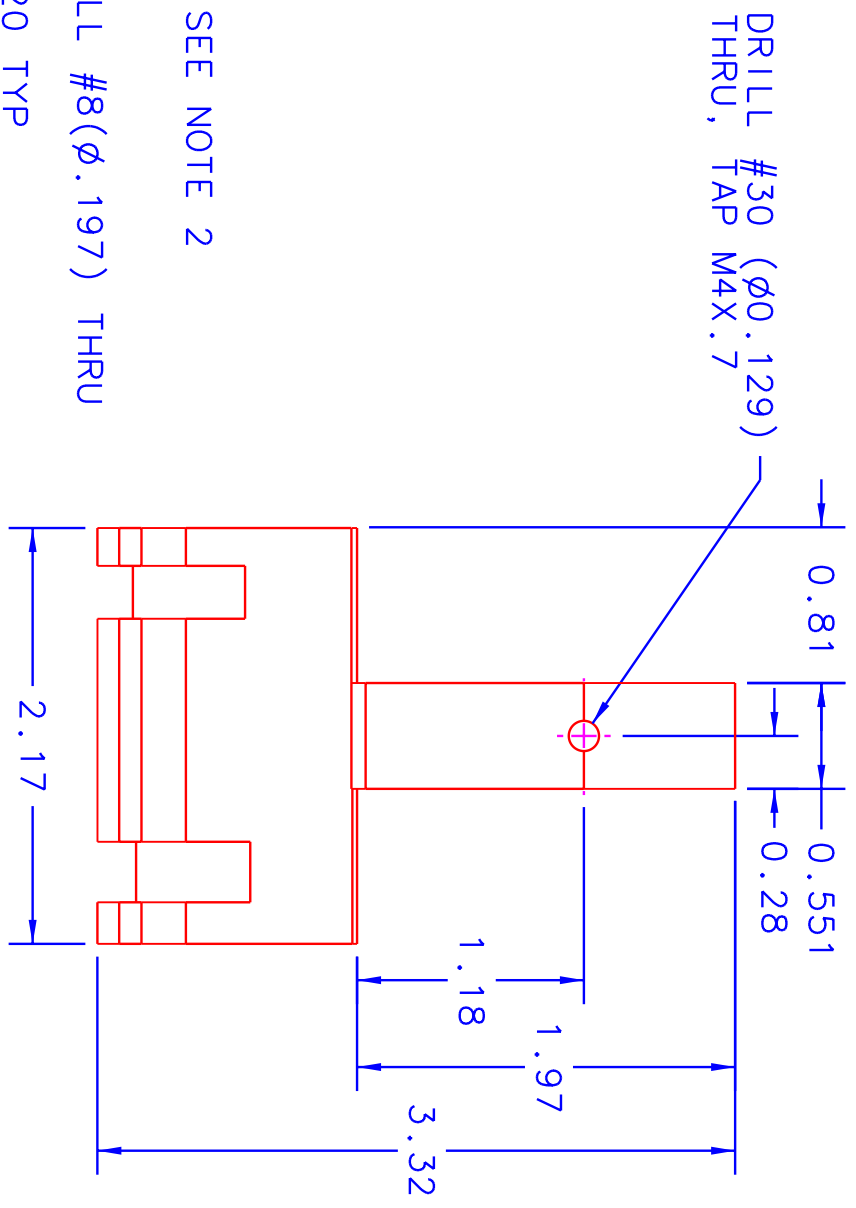
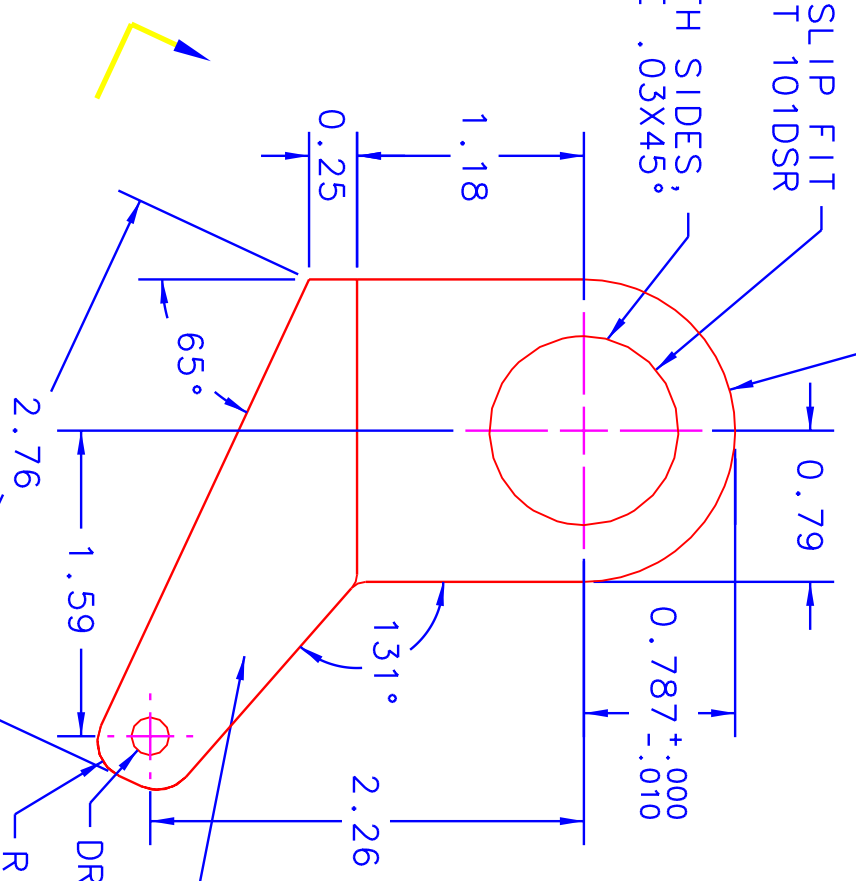
1.59

131°

2.26

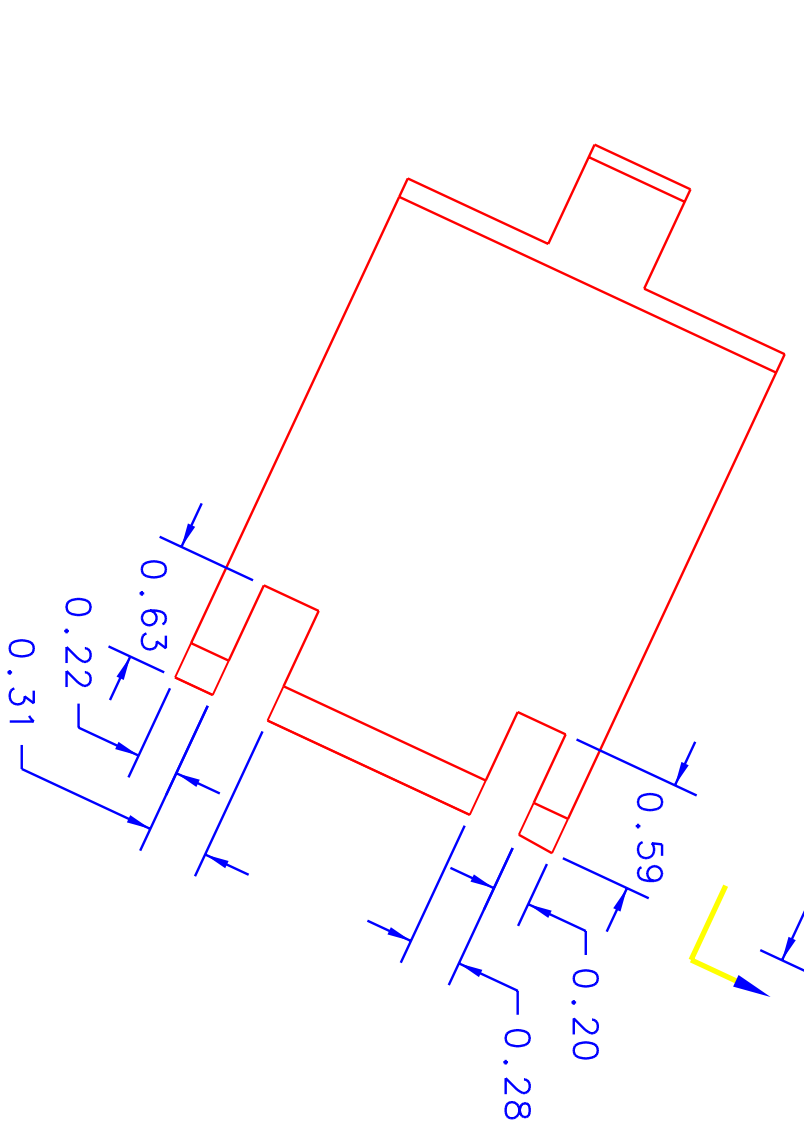
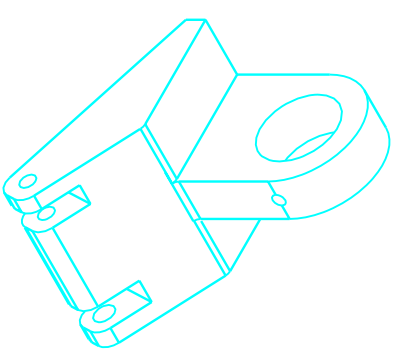
SEE NOTE 2

DRILL #30 (Ø0.129)
THRU, TAP M4X.7



NOTES

- 1: BREAK ALL SHARP EDGES AND CORNERS W/ .01X45° MIN CHAMFERS UNLESS OTHERWISE NOTED
- 2: STAMP DWG. # AND REV W 1/8 IN HIGH CHARACTERS HERE.



UNLESS OTHERWISE SPECIFIED DIMENSIONS ARE IN INCHES TOLERANCES ARE:

FRACTIONS DECIMALS ANGLES

± .XX ±.01 ± X°±.5°

DO NOT SCALE DRAWING

MATERIAL ALUMINUM

FINISH 6061 T-6

SIMILAR TO 204DSR

VIRGINIA POLYTECHNIC INSTITUTE AND STATE UNIVERSITY
DEPARTMENT OF ENGINEERING SCIENCE AND MECHANICS

RADIUS TO HUMERUS JOINT

APPROVALS		DATE		TITLE	
DRAWN	D.S. RUPPERT	CHECKED	4/28/02	SIZE	B
ISSUED				FSQM NO.	
				DWG NO.	201DSR
				SCALE	NA
				SHEET	1 OF 1

1

2

3

4

204DSR

RADIUS TO HUMERUS JOINT

1

2

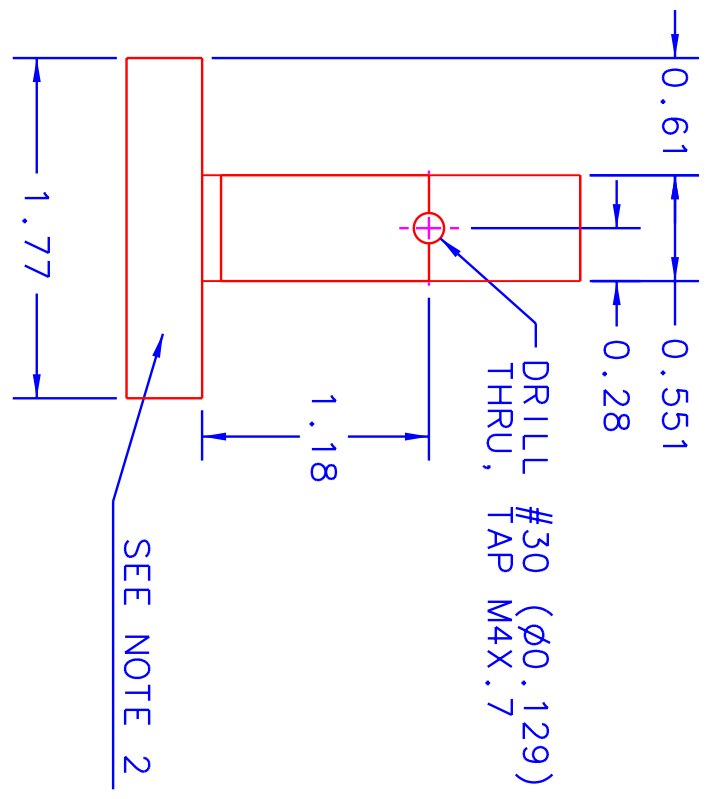
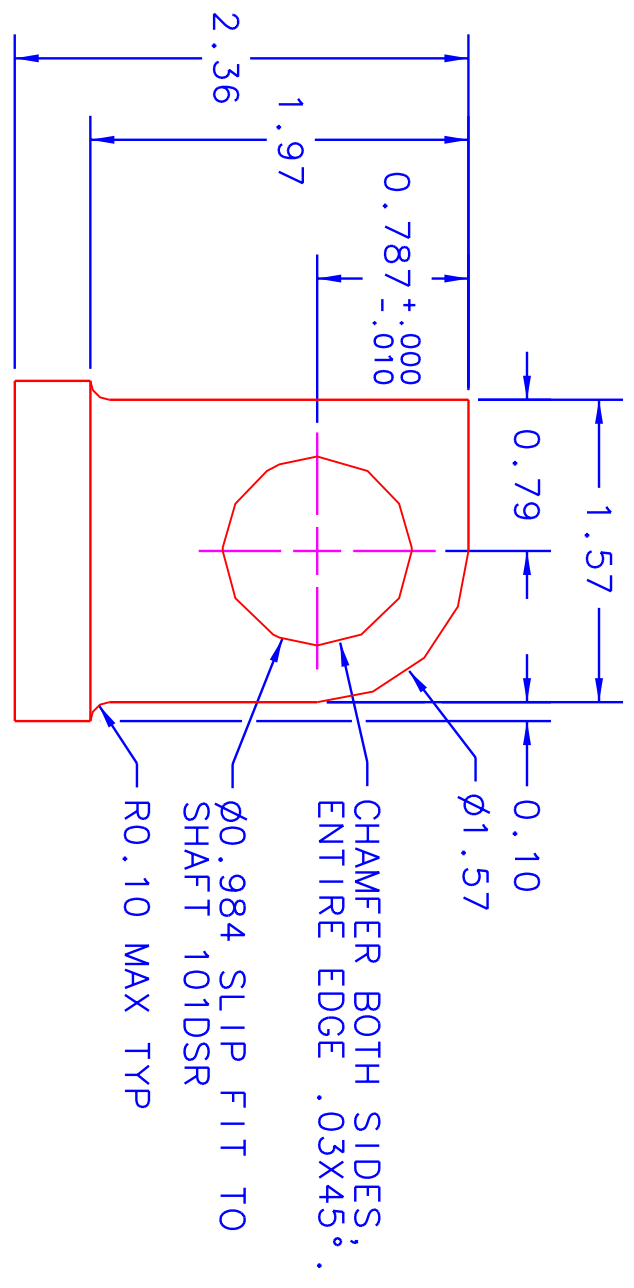
DWG. NO. 2020DSR

SH 1

REV. 1

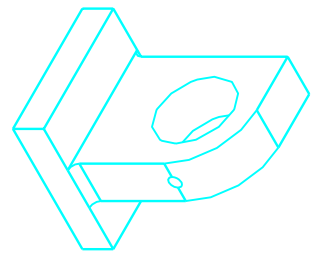
4

REVISIONS				
ZONE	REV	DESCRIPTION	DATE	APPROVED
1	1	INITIAL ISSUE		



NOTES

- 1: BREAK ALL SHARP EDGES AND CORNERS W/ 0.01X45° MIN CHAMFERS UNLESS OTHERWISE NOTED.
- 2: STAMP DWG. # AND REV W/ 1/8 IN HIGH CHARACTERS HERE.



A

B

C

D

A

B

C

D

UNLESS OTHERWISE SPECIFIED DIMENSIONS ARE IN INCHES TOLERANCES ARE:
 FRACTIONS DECIMALS ANGLES
 ± .XX ±.01 X° ±.5°
 ± .XXX ±.001
 DO NOT SCALE DRAWING

VIRGINIA POLYTECHNIC INSTITUTE AND STATE UNIVERSITY
 DEPARTMENT OF ENGINEERING SCIENCE AND MECHANICS

MATERIAL		ALUMINUM	
FINISH		6061 T-6	
SIMILAR TO		201DSR	
APPROVALS		DATE	
DRAWN		4/28/02	
CHECKED			
ISSUED			
TITLE		RADIUS TO CARPUS JOINT	
SIZE		FSQM NO.	
SCALE		NA	
DWG NO.		2020DSR	
SHEET		1/1	

1

2

3

4

1

2

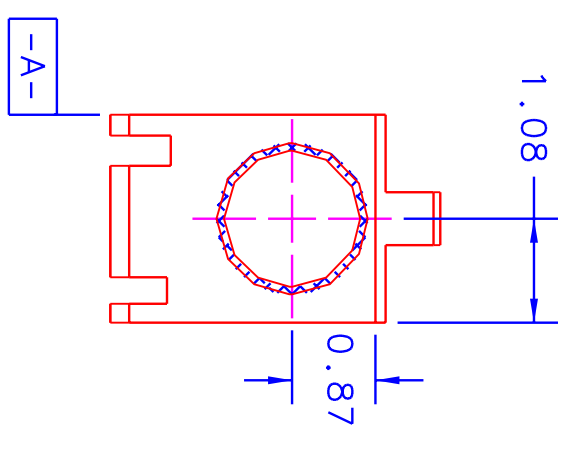
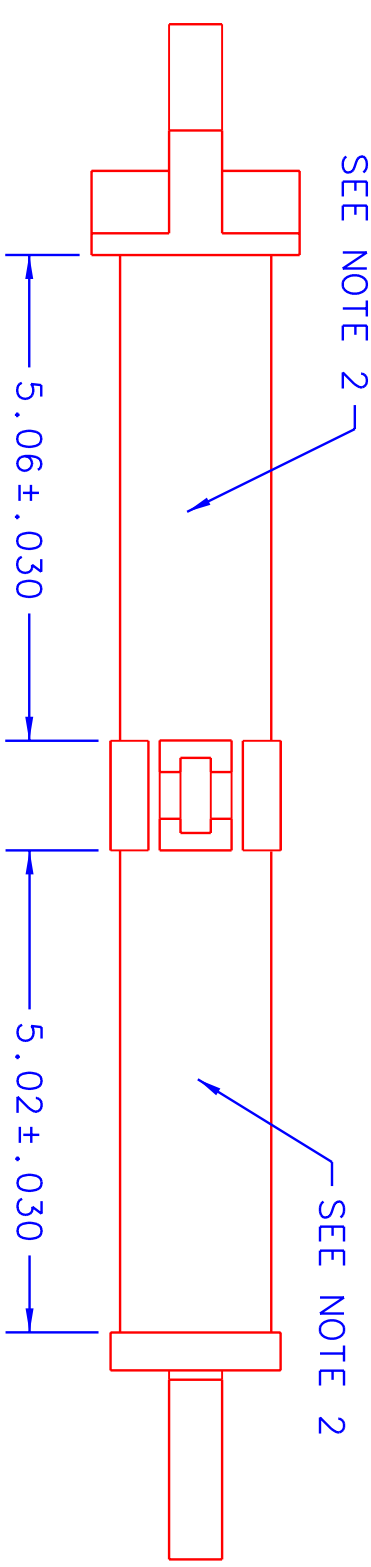
3

4

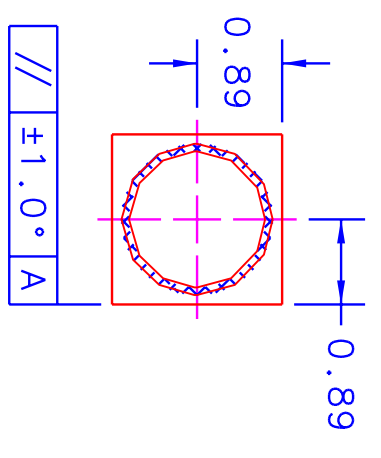
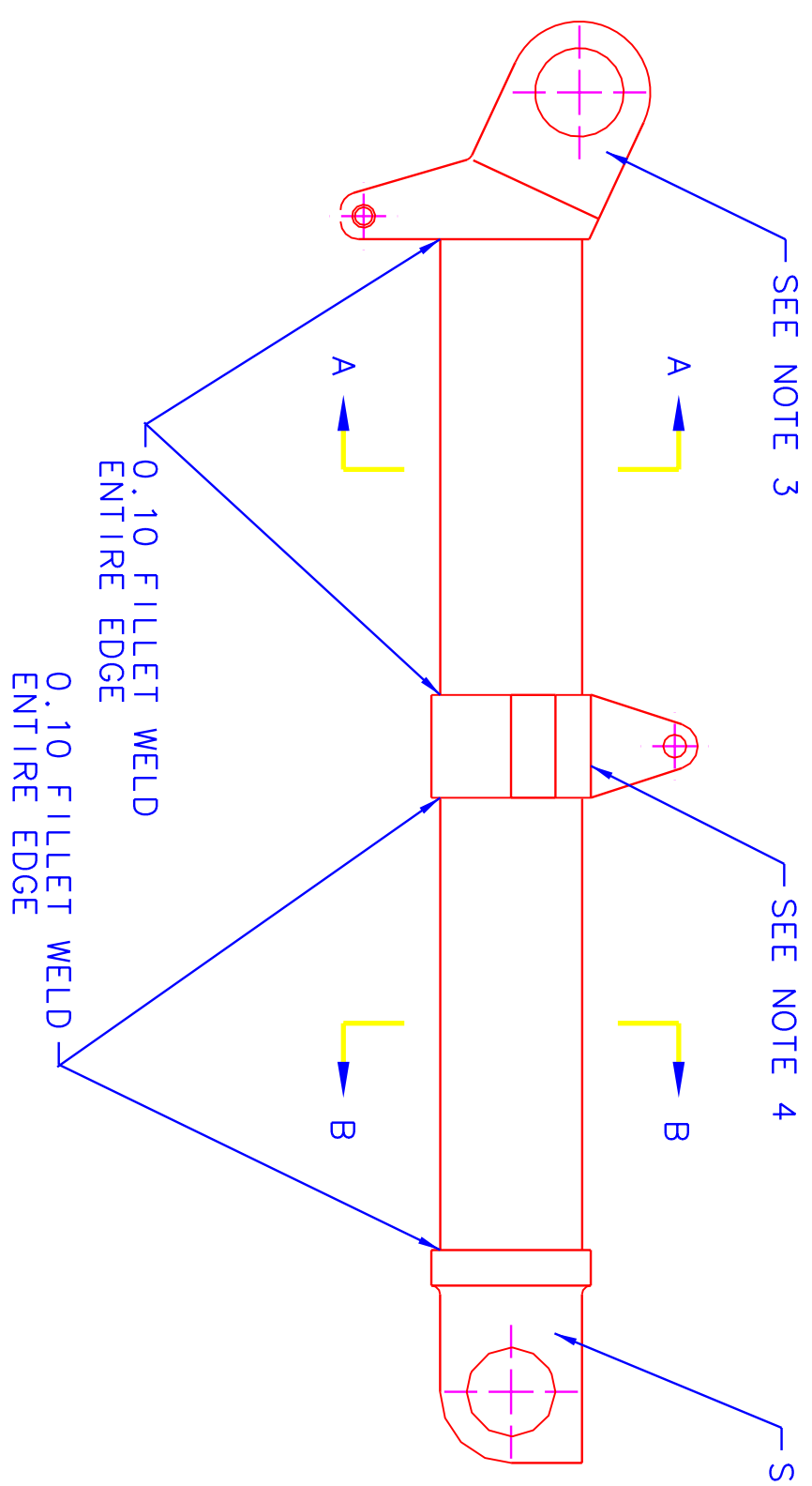
DWG. NO. 203DSR SH 1 REV. 1

REVISIONS

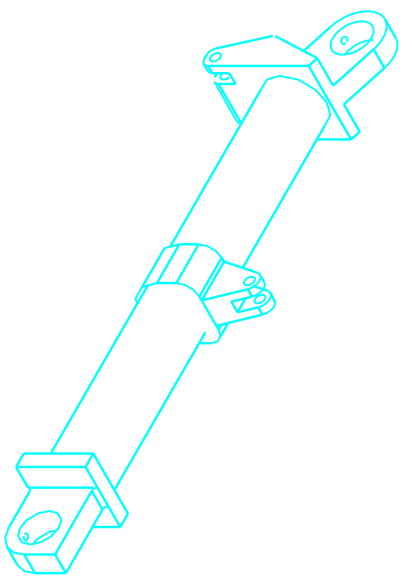
ZONE	REV	DESCRIPTION	DATE	APPROVED
1	1	INITIAL ISSUE		



SECTION A-A



SECTION B-B



A

B

C

D

A

B

C

D

UNLESS OTHERWISE SPECIFIED DIMENSIONS ARE IN INCHES TOLERANCES ARE:

FRACTIONS DECIMALS ANGLES
 ± .XX ±.01 X°±.5°
 ± .XXX±.005

DO NOT SCALE DRAWING

VIRGINIA POLYTECHNIC INSTITUTE AND STATE UNIVERSITY
 DEPARTMENT OF ENGINEERING SCIENCE AND MECHANICS

MATERIAL	ALUMINUM	DRAWN	D.S. RUPPERT	DATE	4/29/02	TITLE	RADIUS		
FINISH	6061 T-6	CHECKED				SIZE	FSCM NO.	DWG NO.	203DSR
SIMILAR TO	206DSR	ISSUED				SCALE	NA	SHEET	1 OF 1

1

2

3

4

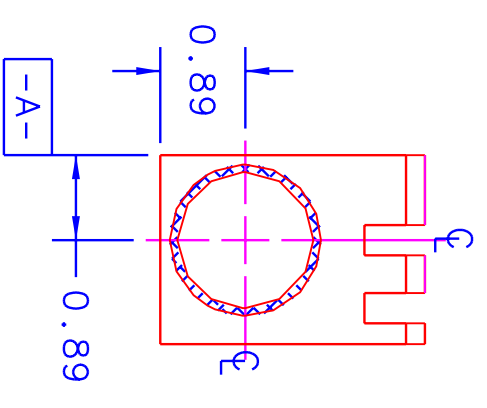
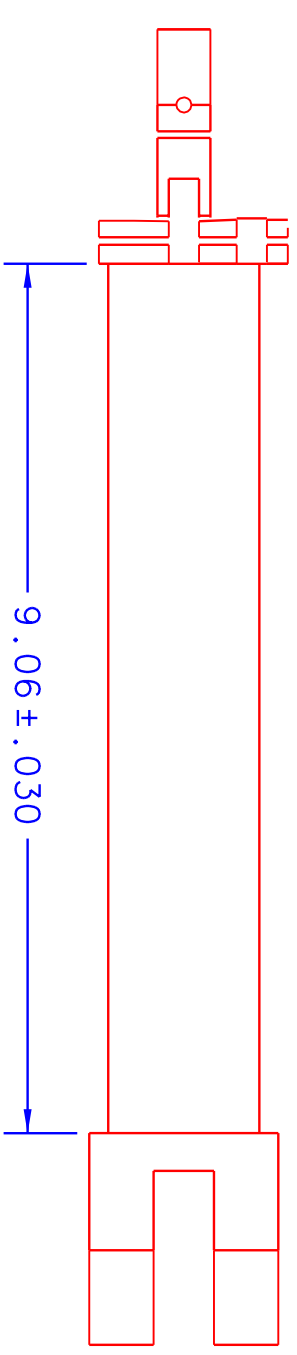
1

2

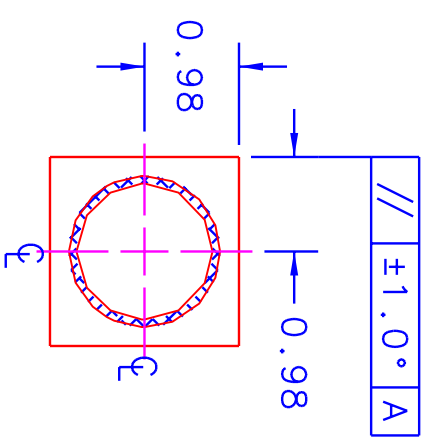
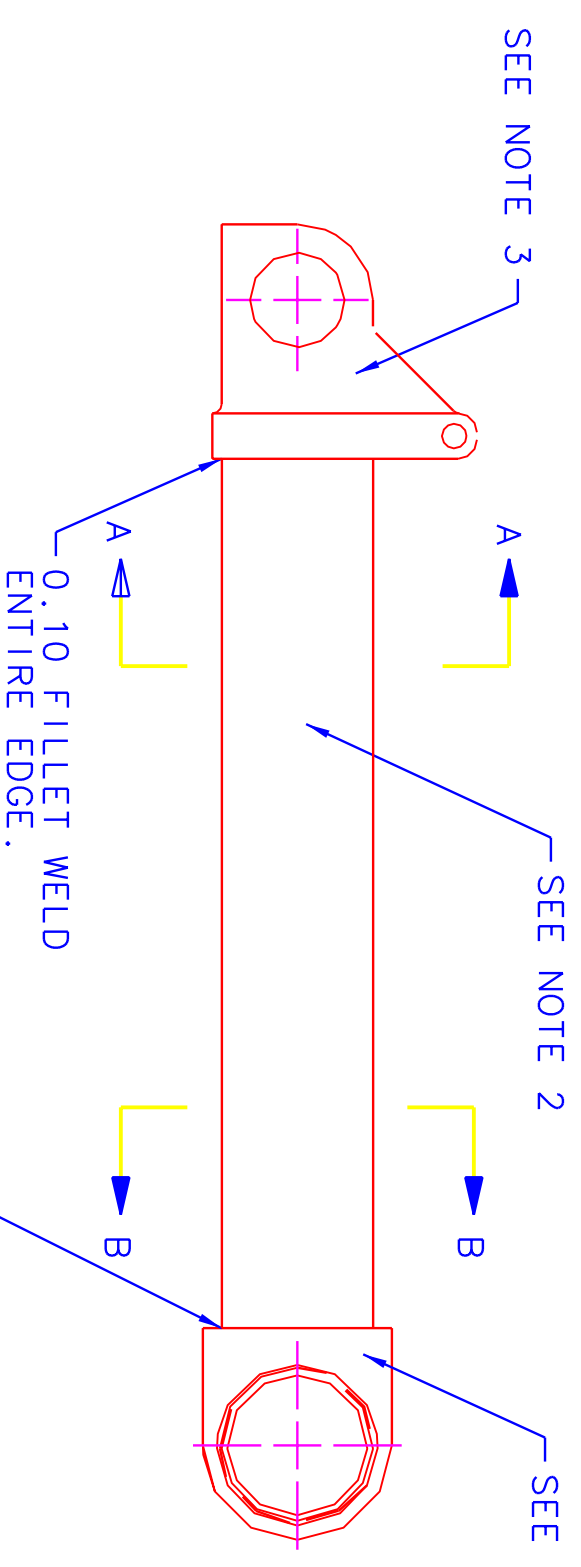
4

NOTES

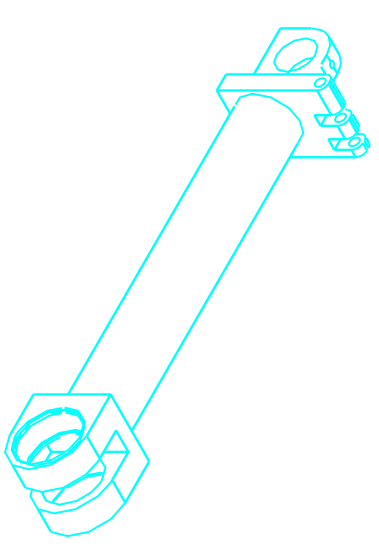
- 1: REMOVE ALL SHARP EDGES AND CORNERS FROM WELD.
- 2: ALUMINUM TUBE 45mm OD, 41mm I.D.
- 3: USE PART 204DSR.
- 4: USE PART 205DSR.



SECTION A-A



SECTION B-B



DWG. NO. 206DSR SH 1 REV. 1

REVISIONS				
ZONE	REV	DESCRIPTION	DATE	APPROVED
	1	INITIAL ISSUE		

UNLESS OTHERWISE SPECIFIED DIMENSIONS ARE IN INCHES TOLERANCES ARE:

FRACTIONS	DECIMALS	ANGLES
±	.XX ±.01	X° ±.5°
DO NOT SCALE DRAWING	.XXX ±.005	X° ±.5°

MATERIAL		DRAWN		CHECKED		ISSUED		TITLE	
ALUMINUM		D. S. RUPPERT		3/02/02				METACARPAL	
FINISH		APPROVALS		DATE		SCALE		SIZE	
6061 T-6						NA		B	
SIMILAR TO		ACT. WT.		CALC WT.		SCALE		FSQM NO.	
203DSR						NA		206DSR	
						SHEET		1 OF 1	

VIRGINIA POLYTECHNIC INSTITUTE AND STATE UNIVERSITY
DEPARTMENT OF ENGINEERING SCIENCE AND MECHANICS

1

2

3

4

A

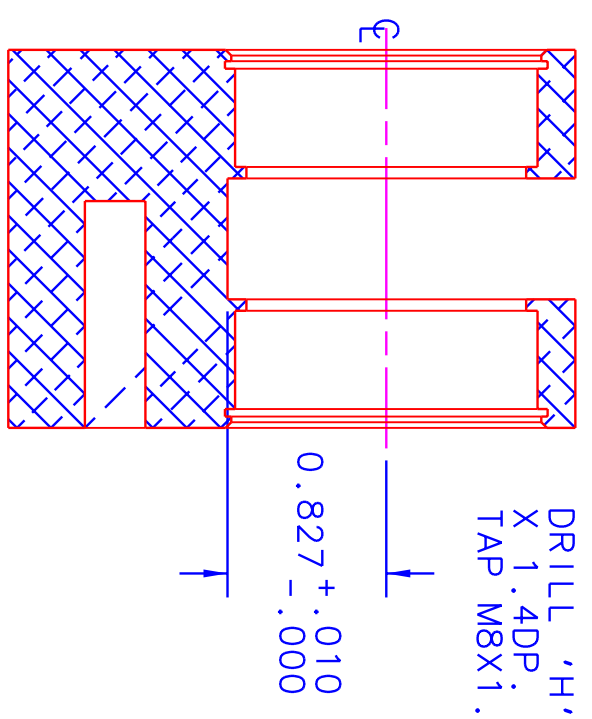
B

C

D

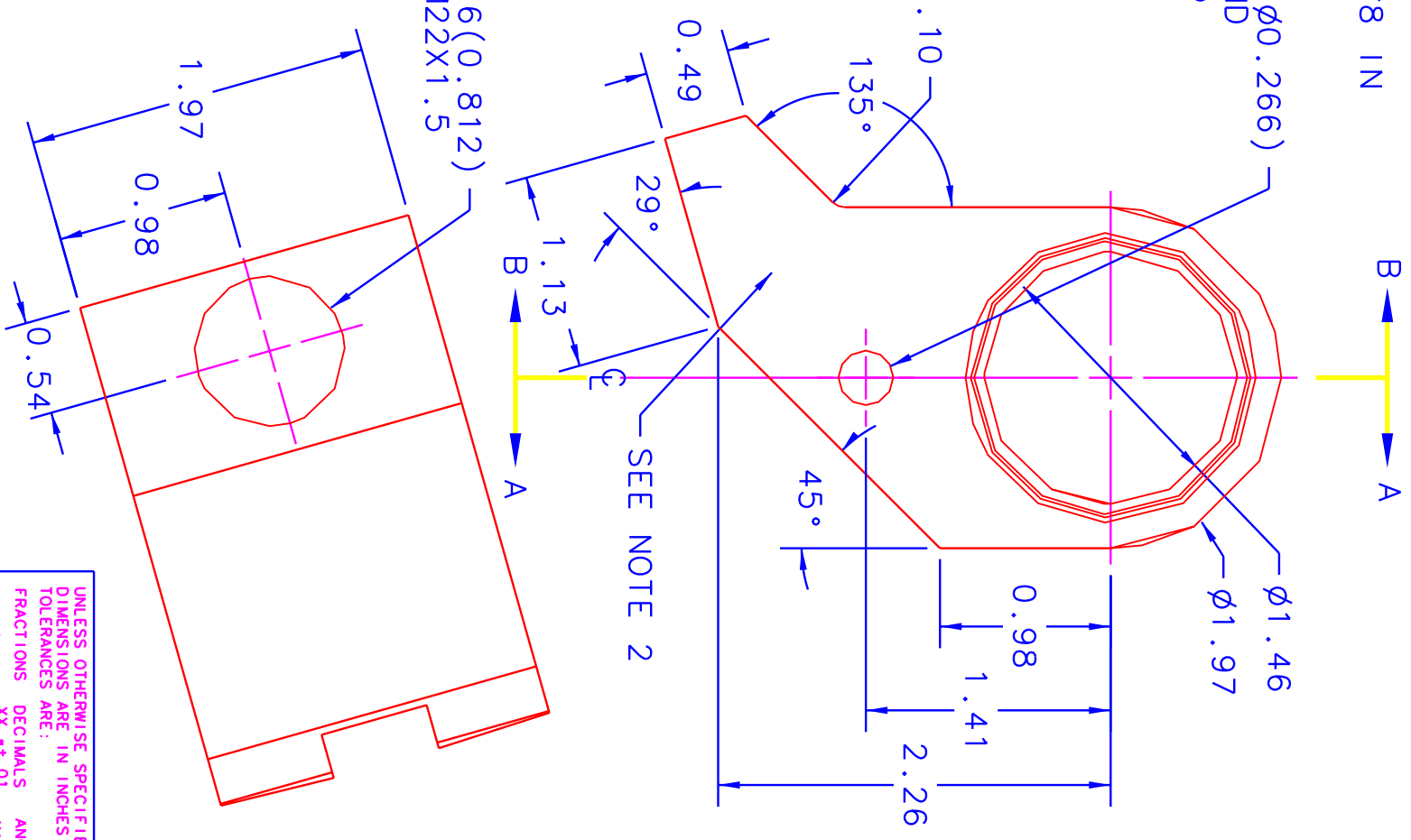
NOTES

- 1: BREAK ALL SHARP EDGES AND CORNERS W/ 0.01X45° MIN CHAMFERS UNLESS OTHERWISE NOTED.
- 2: STAMP DWG. # AND REV W/ 1/8 IN HIGH CHARACTERS HERE.

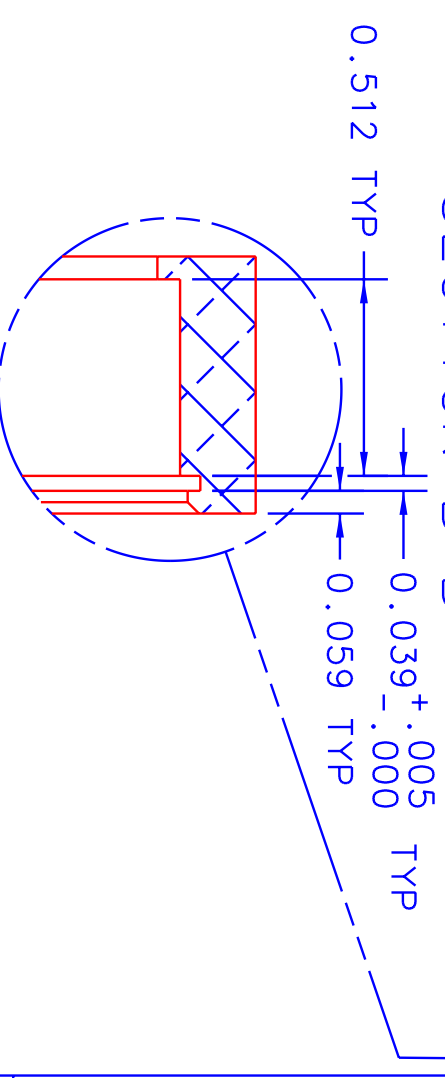
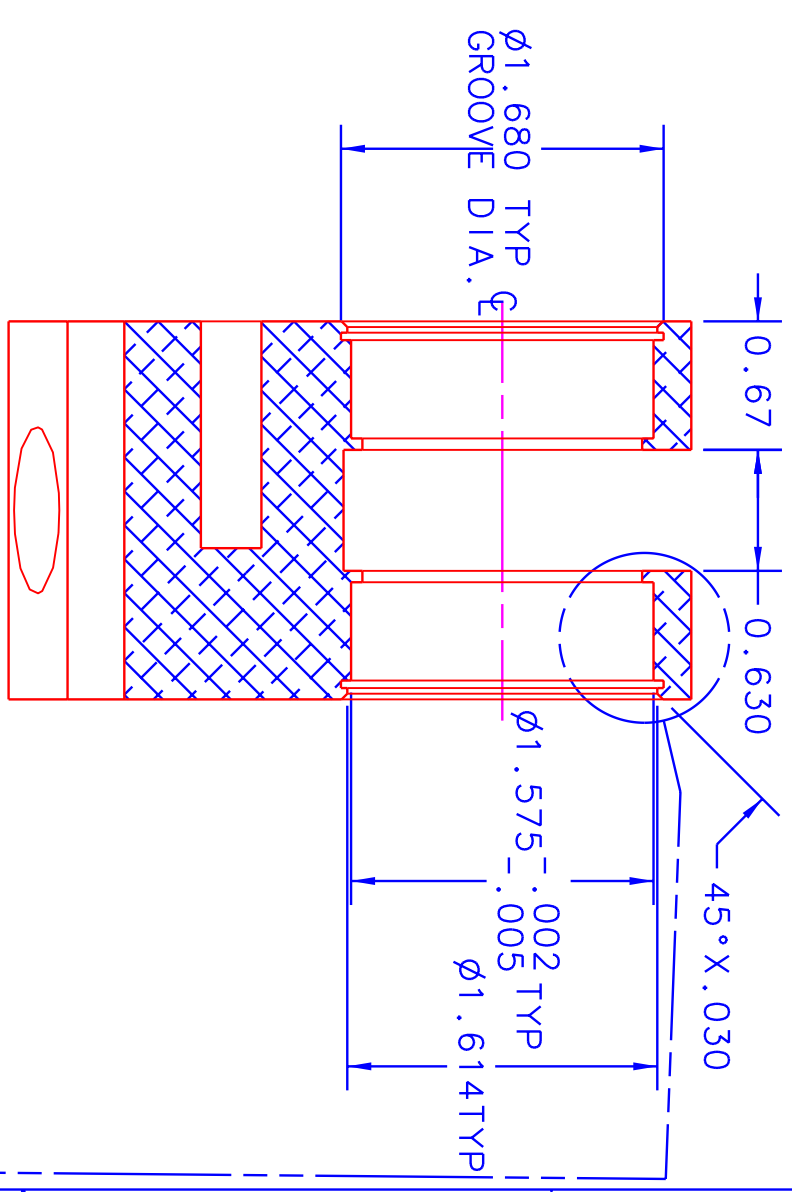


SECTION A-A

FLAT BOTTOM DRILL 13/16(0.812) 0.45 DP., BOTTOM TAP M22X1.5

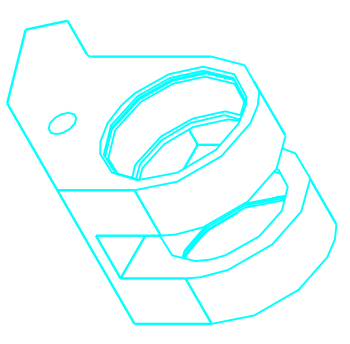


SECTION B-B



DETAIL

SCALE 2:1



VIRGINIA POLYTECHNIC INSTITUTE AND STATE UNIVERSITY
DEPARTMENT OF ENGINEERING SCIENCE AND MECHANICS

UNLESS OTHERWISE SPECIFIED DIMENSIONS ARE IN INCHES TOLERANCES ARE:			
FRACTIONS	DECIMALS	ANGLES	
\pm	.XX \pm .01	X° \pm .5°	
DO NOT SCALE DRAWING			
MATERIAL	ALUMINUM		
FINISH	6061 T-6		
SIMILAR TO	ACT. WT	CALC WT	
205DSR			

APPROVALS		DATE		TITLE	
DRAWN	D.S. RUPPERT	5/17/02		HUMERUS TO RADIUS JOINT	
CHECKED				SIZE	FSCM NO.
ISSUED				B	
			SCALE	NA	DWG NO.
					209DSR
			SHEET	1 OF 1	

REVISIONS				
ZONE	REV	DESCRIPTION	DATE	APPROVED
	1	INITIAL ISSUE		

1

2

3

4

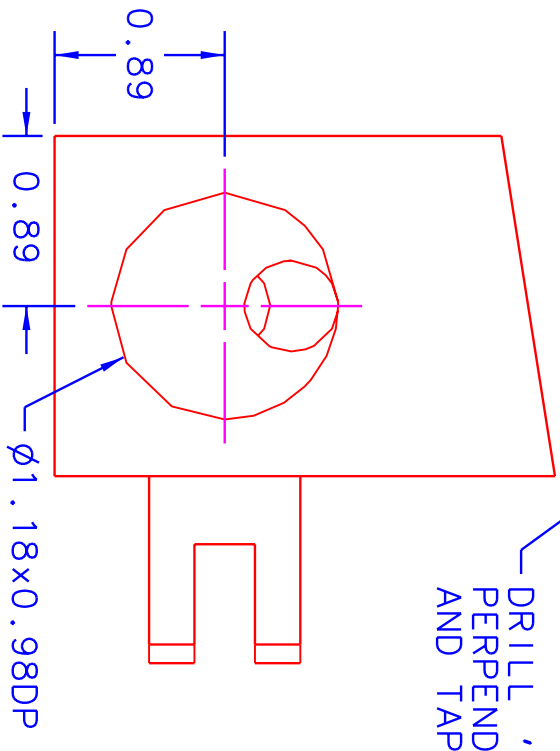
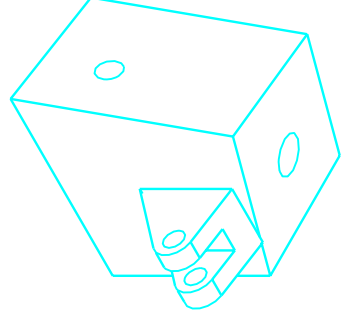
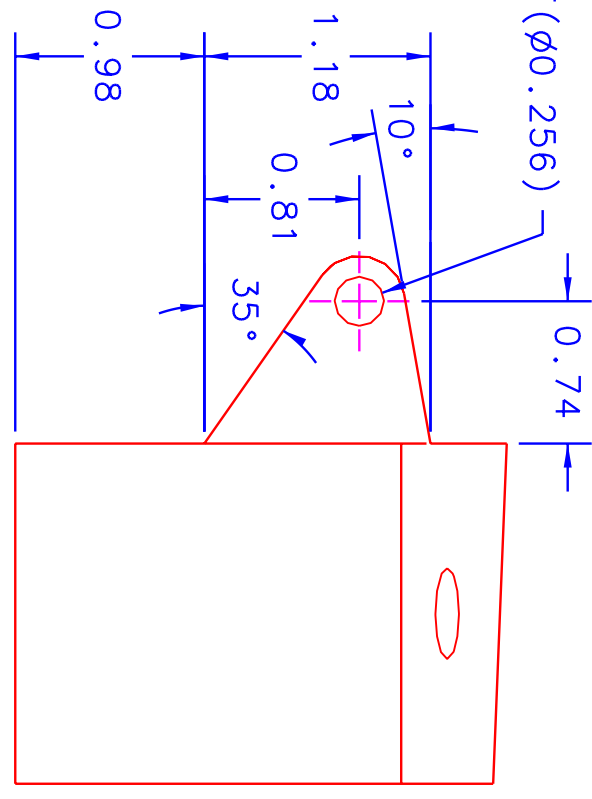
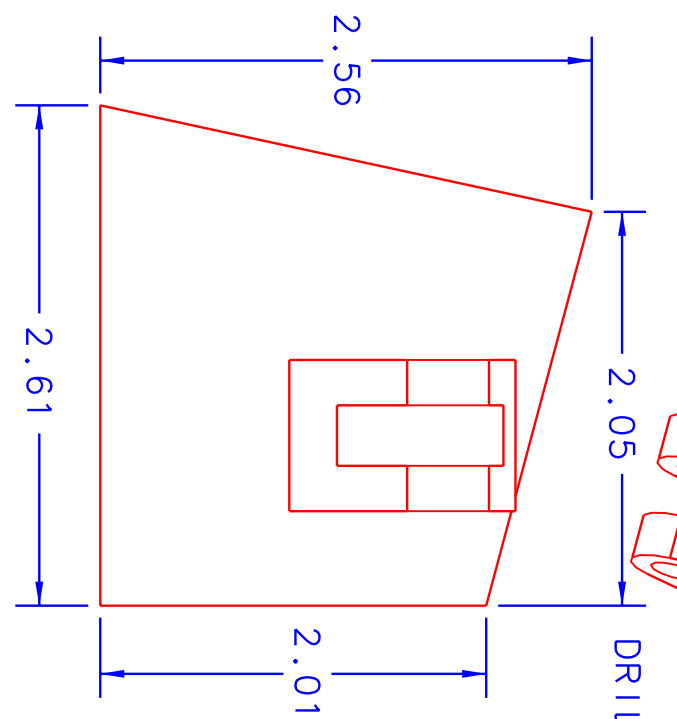
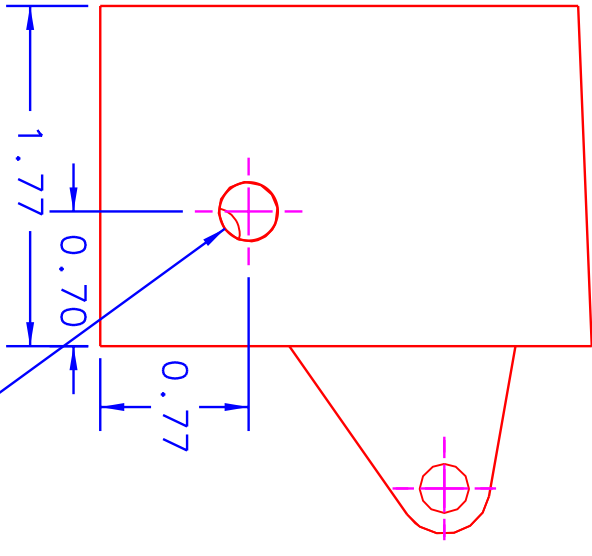
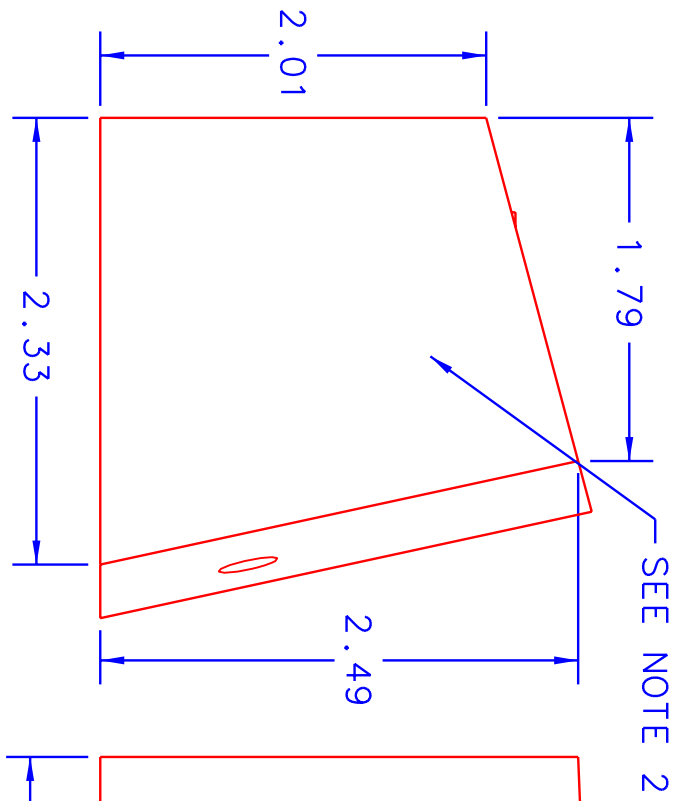
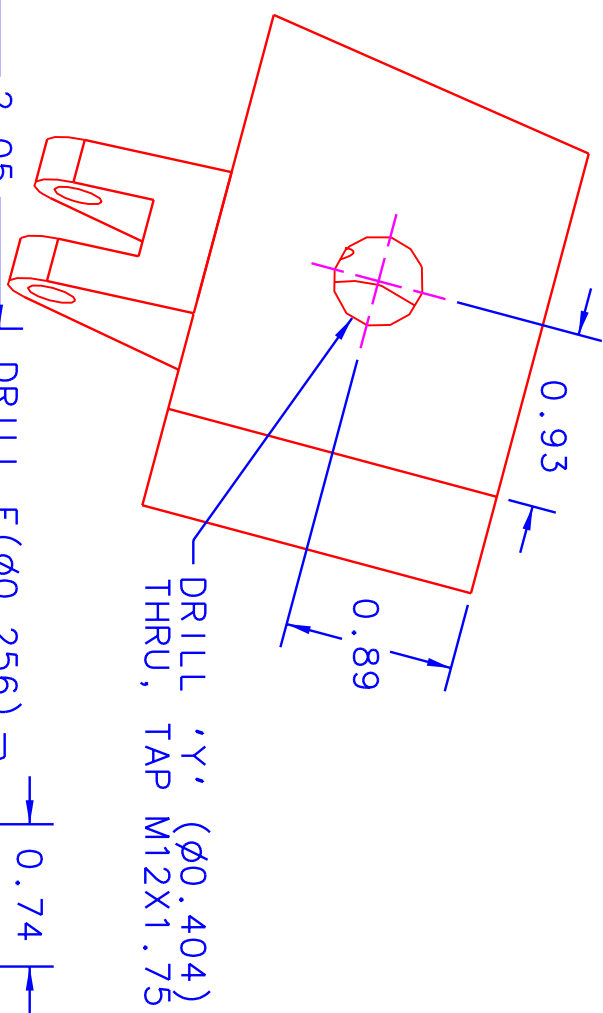
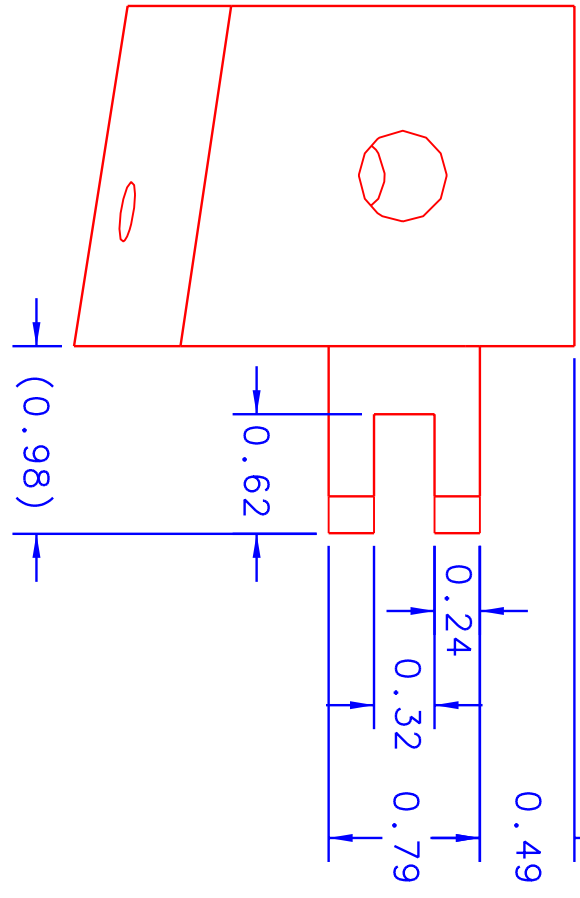
DWG. NO. 210DSR SH 1 REV.1

REVISIONS

ZONE	REV	DESCRIPTION	DATE	APPROVED
1	1	INITIAL ISSUE		

NOTES

- 1: BREAK ALL SHARP EDGES AND CORNERS W/ .01X45° MIN CHAMFERS UNLESS OTHERWISE NOTED.
- 2: STAMP DWG. # AND REV W/ 1/8" IN HIGH CHARACTERS HERE.



UNLESS OTHERWISE SPECIFIED DIMENSIONS ARE IN INCHES TOLERANCES ARE:

FRACTIONS DECIMALS ANGLES
± .XX ±.01 X°.±.5°
DO NOT SCALE DRAWING

MATERIAL
ALUMINUM

FINISH
6061 T-6

SIMILAR TO

VIRGINIA POLYTECHNIC INSTITUTE AND STATE UNIVERSITY
DEPARTMENT OF ENGINEERING SCIENCE AND MECHANICS

APPROVALS
DRAWN D.S. RUPPERT 5/16/02

TITLE
HUMERUS TO SCAPULA JOINT

SIZE FSQM NO. B
SCALE NA
DWG NO. 210DSR
SHEET 1 OF 1

1

2

3

4

▶

▶

1

2

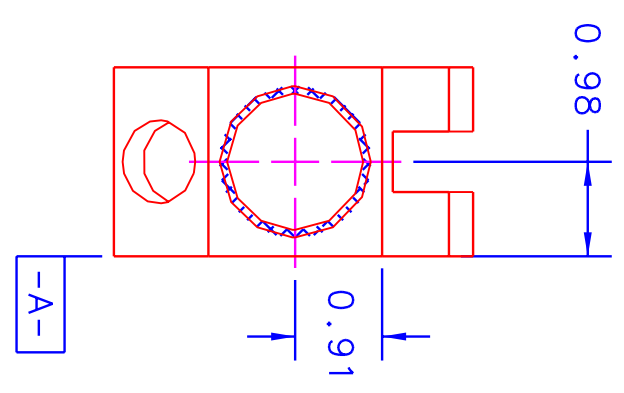
DWG. NO. 211DSR SH 1 REV. 1

4

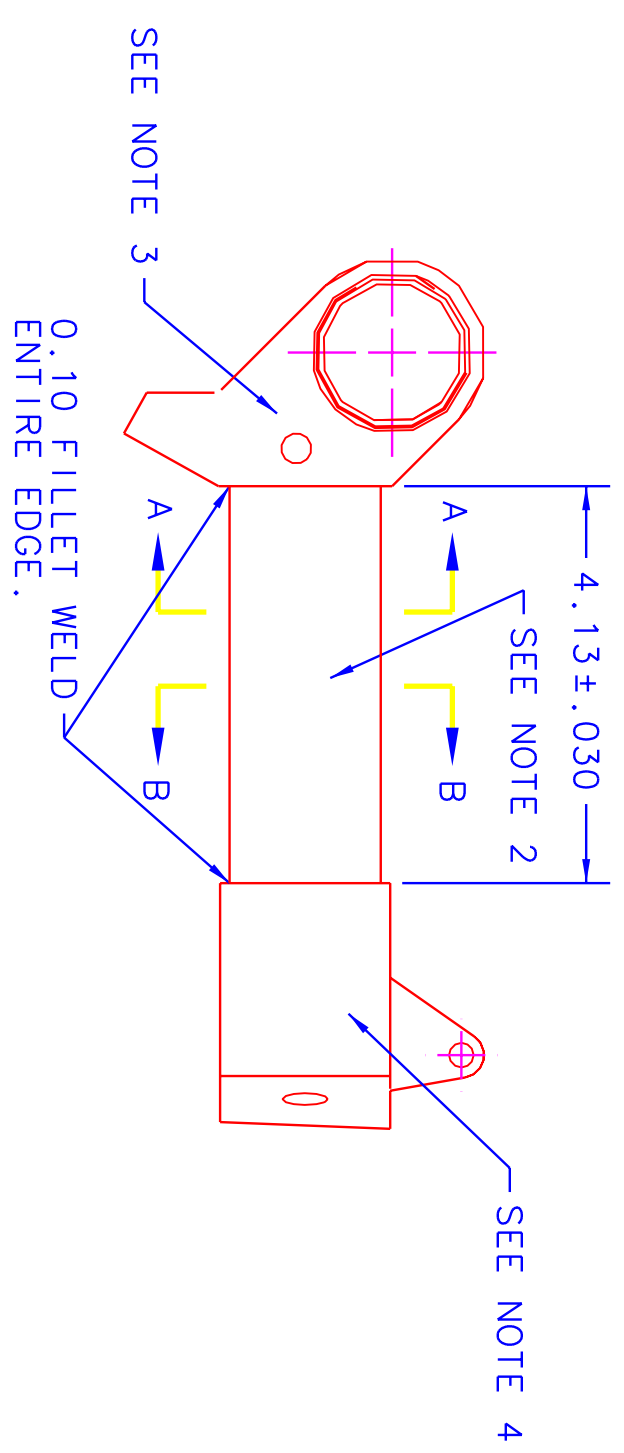
NOTES

- 1: REMOVE ALL SHARP EDGES AND CORNERS FROM WELD.
- 2: ALUMINUM TUBE 45mm OD, 41mm ID.
- 3: USE PART 209DSR.
- 4: USE PART 210DSR.

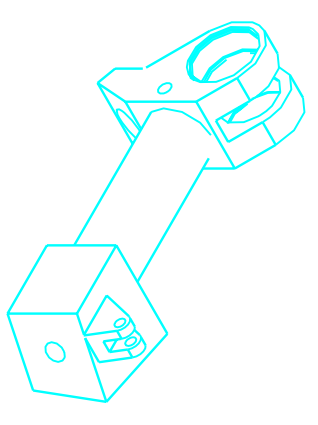
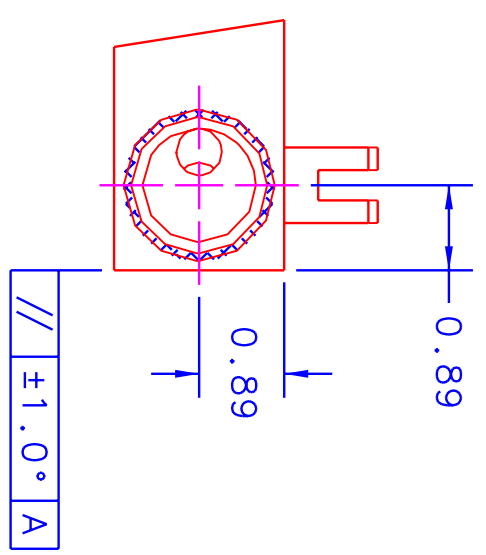
REVISIONS				
ZONE	REV	DESCRIPTION	DATE	APPROVED
	1	INITIAL ISSUE		



SECTION A-A



SECTION B-B



1

2

3

4

UNLESS OTHERWISE SPECIFIED DIMENSIONS ARE IN INCHES TOLERANCES ARE:

FRACTIONS DECIMALS ANGLES
 ± .XX ±.01 X° ±.5°
 ± .XXX ±.005

DO NOT SCALE DRAWING

VIRGINIA POLYTECHNIC INSTITUTE AND STATE UNIVERSITY
 DEPARTMENT OF ENGINEERING SCIENCE AND MECHANICS

MATERIAL	ALUMINUM	DRAWN	D.S. RUPPERT	DATE	5/17/02	TITLE	HUMERUS		
FINISH	6061 T-6	CHECKED				SIZE	FSCM NO.	DWG NO.	211DSR
SIMILAR TO	206DSR	ISSUED				SCALE	NA		SHEET 1 OF 1

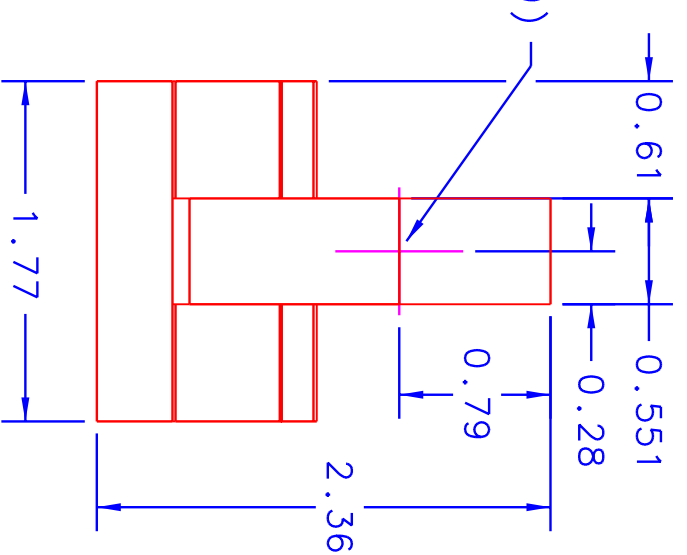
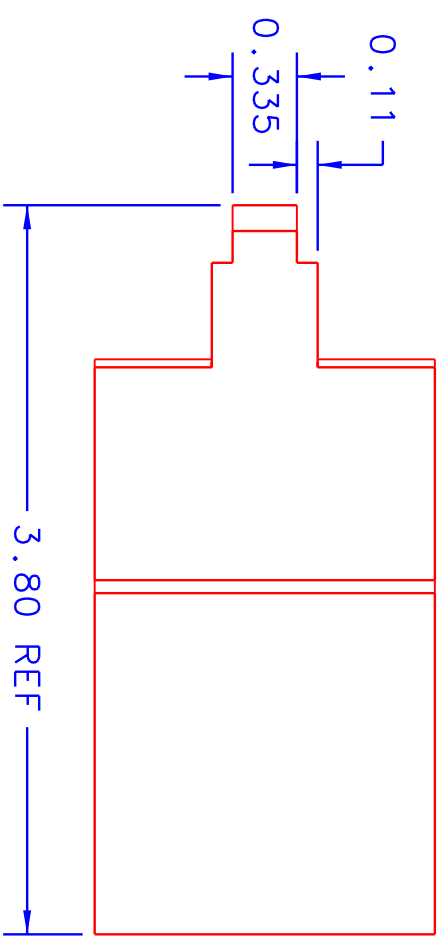
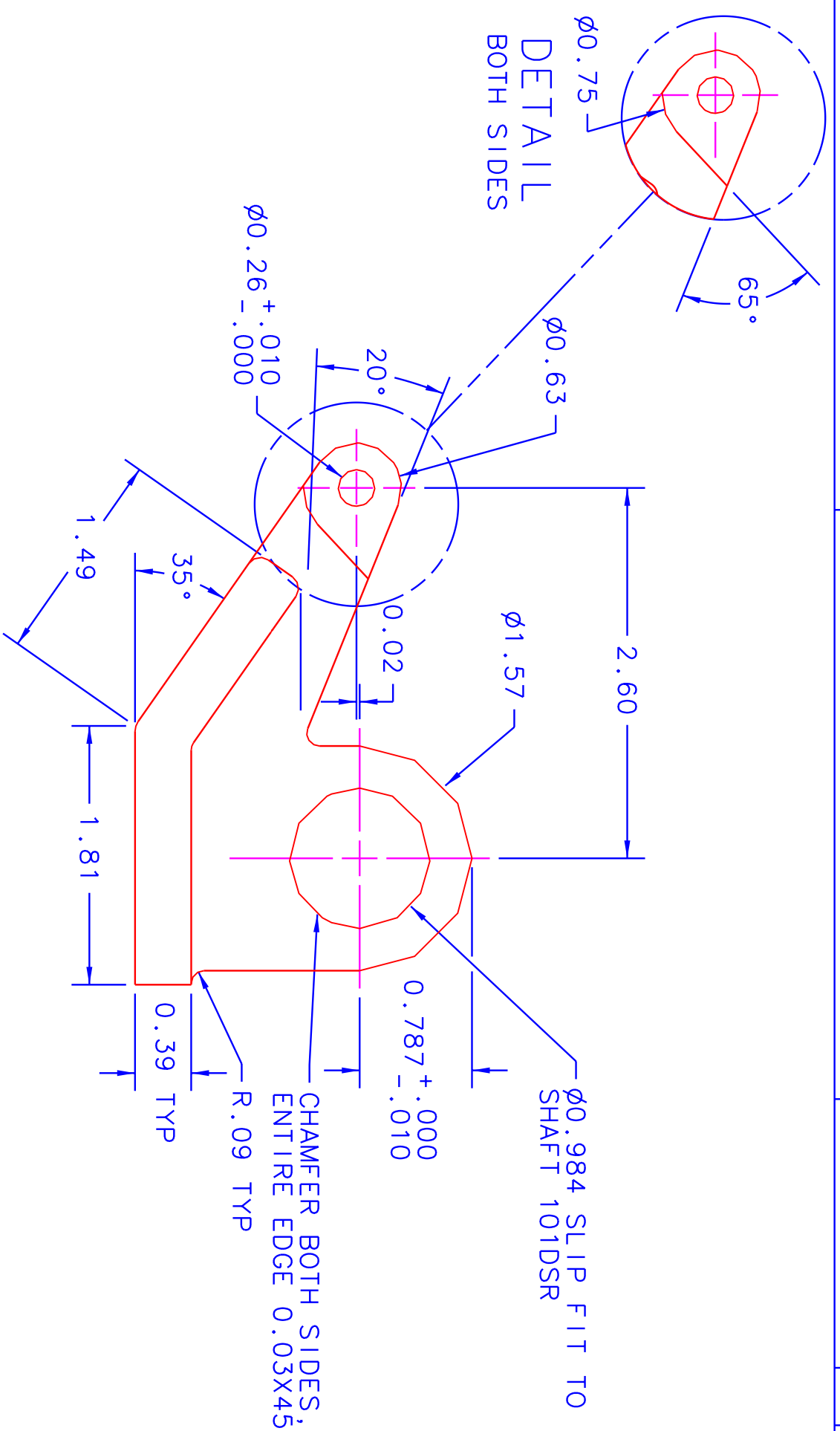
A

B

C

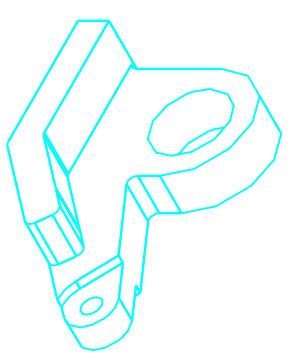
D

REVISIONS				
ZONE	REV	DESCRIPTION	DATE	APPROVED
	1	INITIAL ISSUE		



NOTES

- BREAK ALL SHARP EDGES AND CORNERS W/ .01X45° MIN SHAMFERS UNLESS OTHERWISE NOTED.
- STAMP DWG. # AND REV. W/ 1/8 IN HIGH CHARACTERS HERE.



UNLESS OTHERWISE SPECIFIED DIMENSIONS ARE IN INCHES TOLERANCES ARE:

FRACTIONS DECIMALS ANGLES
 \pm .XX \pm .01 \pm X° \pm .5
 DO NOT SCALE DRAWING

VIRGINIA POLYTECHNIC INSTITUTE AND STATE UNIVERSITY
 DEPARTMENT OF ENGINEERING SCIENCE AND MECHANICS

MATERIAL	ALUMINUM	DRAWN	D.S. RUPPERT	DATE	3/01/02	TITLE	FETLOCK TO METACARPAL JOINT		
FINISH	6061 T-6	CHECKED				SIZE	FSCM NO.	DWG NO.	212DSR
SIMILAR TO		ISSUED				SCALE	NA		SHEET 1 OF 1

A B C D 1 2 3 4

1

2

DWG. NO. 213DSR

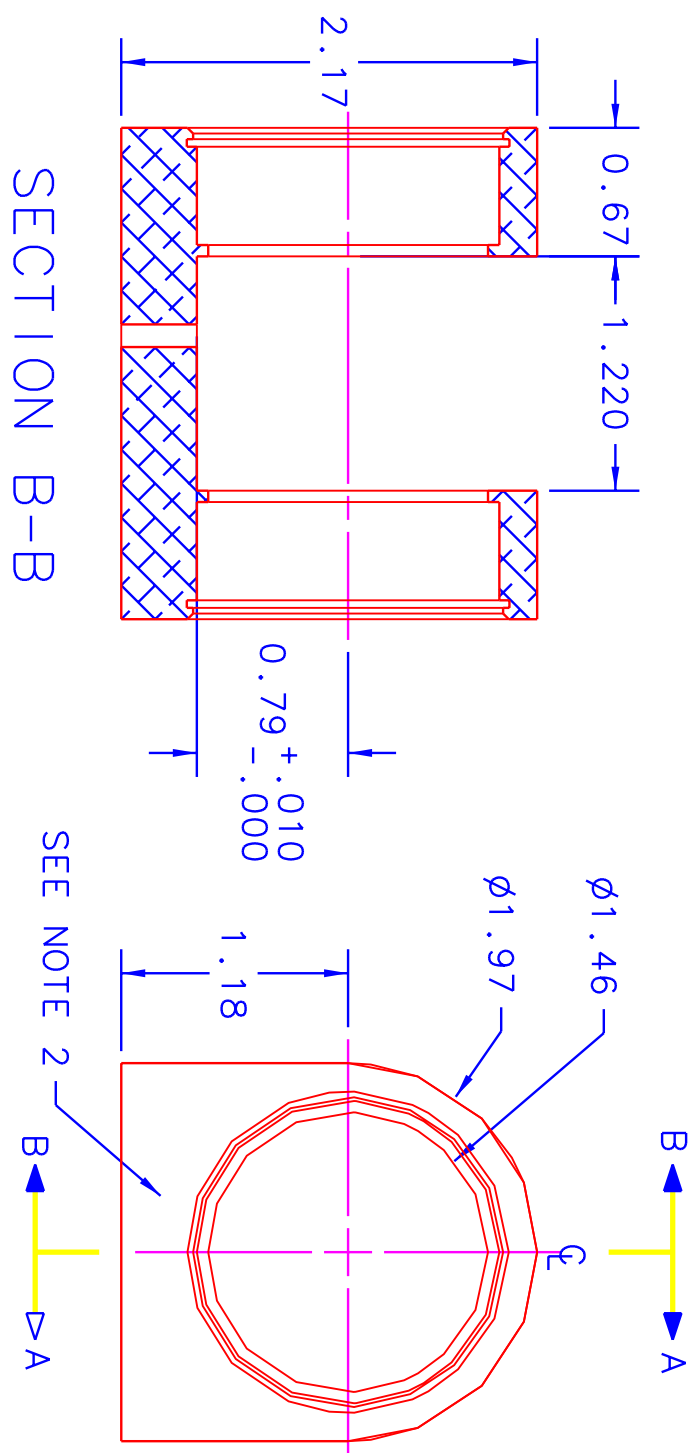
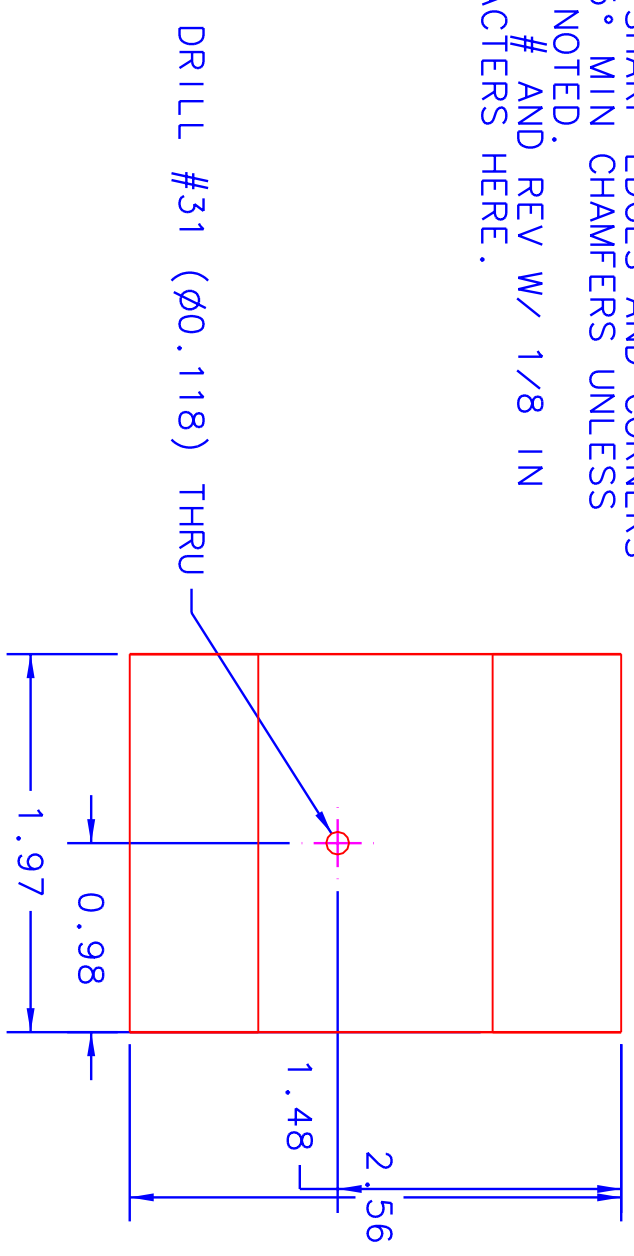
SH 1 REV. 1

REVISIONS

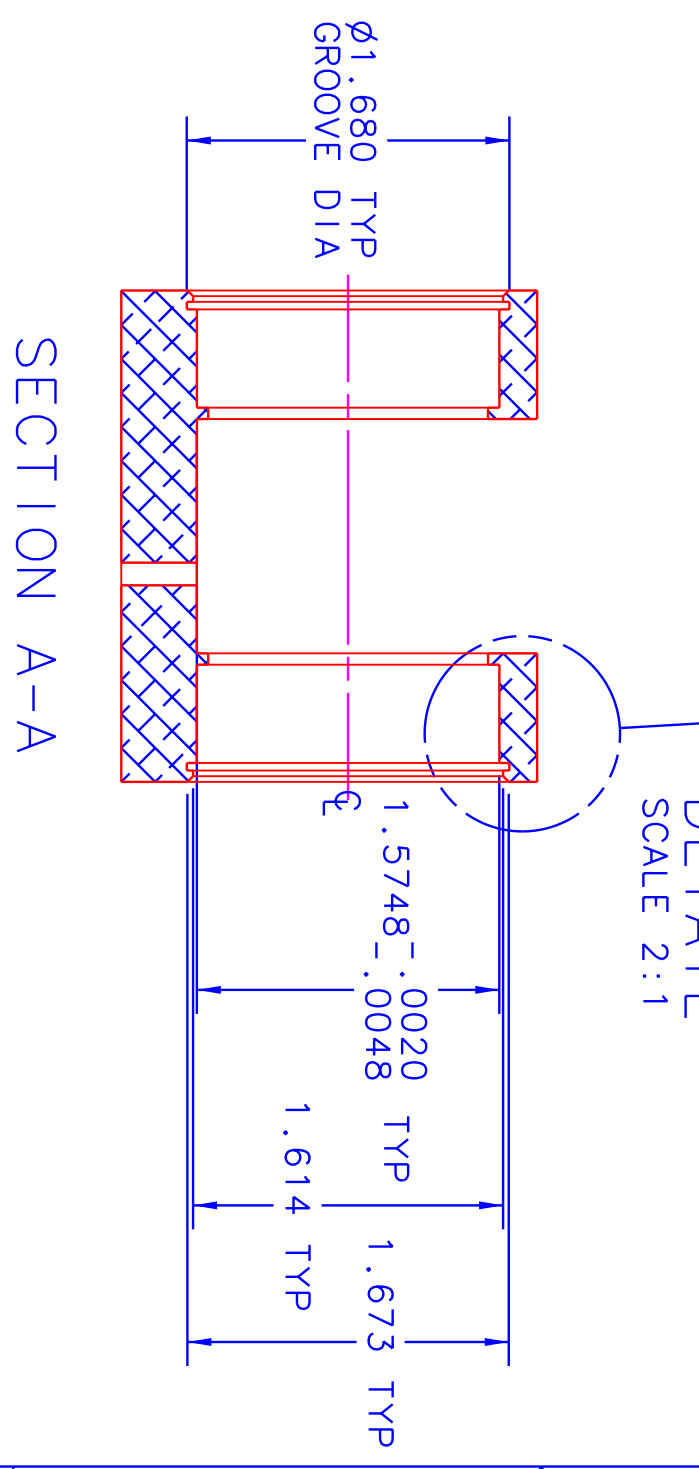
4

NOTES

- 1: BREAK ALL SHARP EDGES AND CORNERS W/ 0.01X45° MIN CHAMFERS UNLESS OTHERWISE NOTED.
- 2: STAMP DWG. # AND REV W/ 1/8 IN HIGH CHARACTERS AND HERE.



SECTION B-B



SECTION A-A

DETAIL SCALE 2:1

ZONE	REV	DESCRIPTION	DATE	APPROVED
1	1	INITIAL ISSUE		

UNLESS OTHERWISE SPECIFIED DIMENSIONS ARE IN INCHES TOLERANCES ARE:

FRACTIONS DECIMALS ANGLES
 \pm .XX \pm .01 \times \pm .5°
 DO NOT SCALE DRAWING

VIRGINIA POLYTECHNIC INSTITUTE AND STATE UNIVERSITY
 DEPARTMENT OF ENGINEERING SCIENCE AND MECHANICS

MATERIAL: ALUMINUM
 FINISH: 6061 T-6
 SIMILAR TO: 205DSR

DRAWN: D.S. RUPPERT
 CHECKED: 10/11/01

FETLOCK TO HOOF JOINT
 SCALE: NA

ACT. WT. CALC WT.

ISSUED

SIZE: B
 FSQM NO.: 213DSR

SCALE: NA

SHEET 1 OF 1

DWG NO.: 213DSR

1

2

3

4

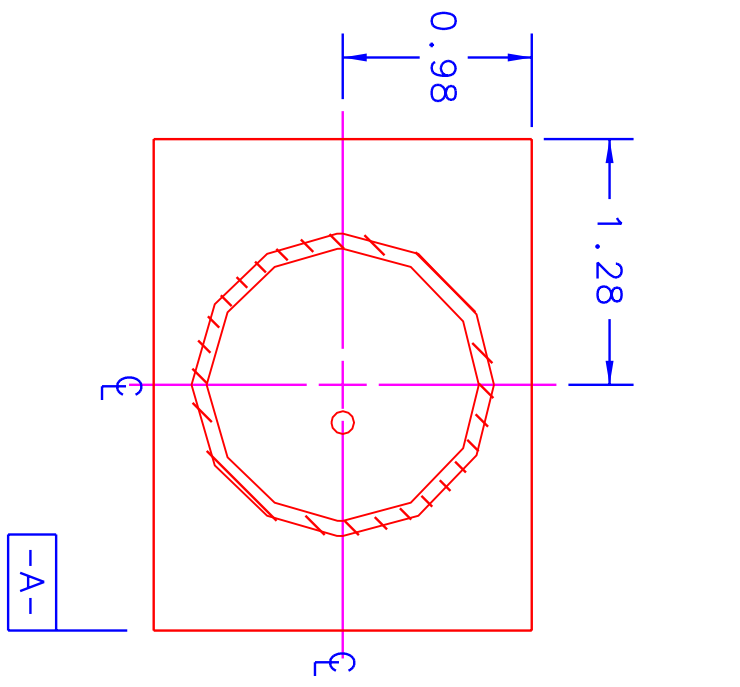
A

B

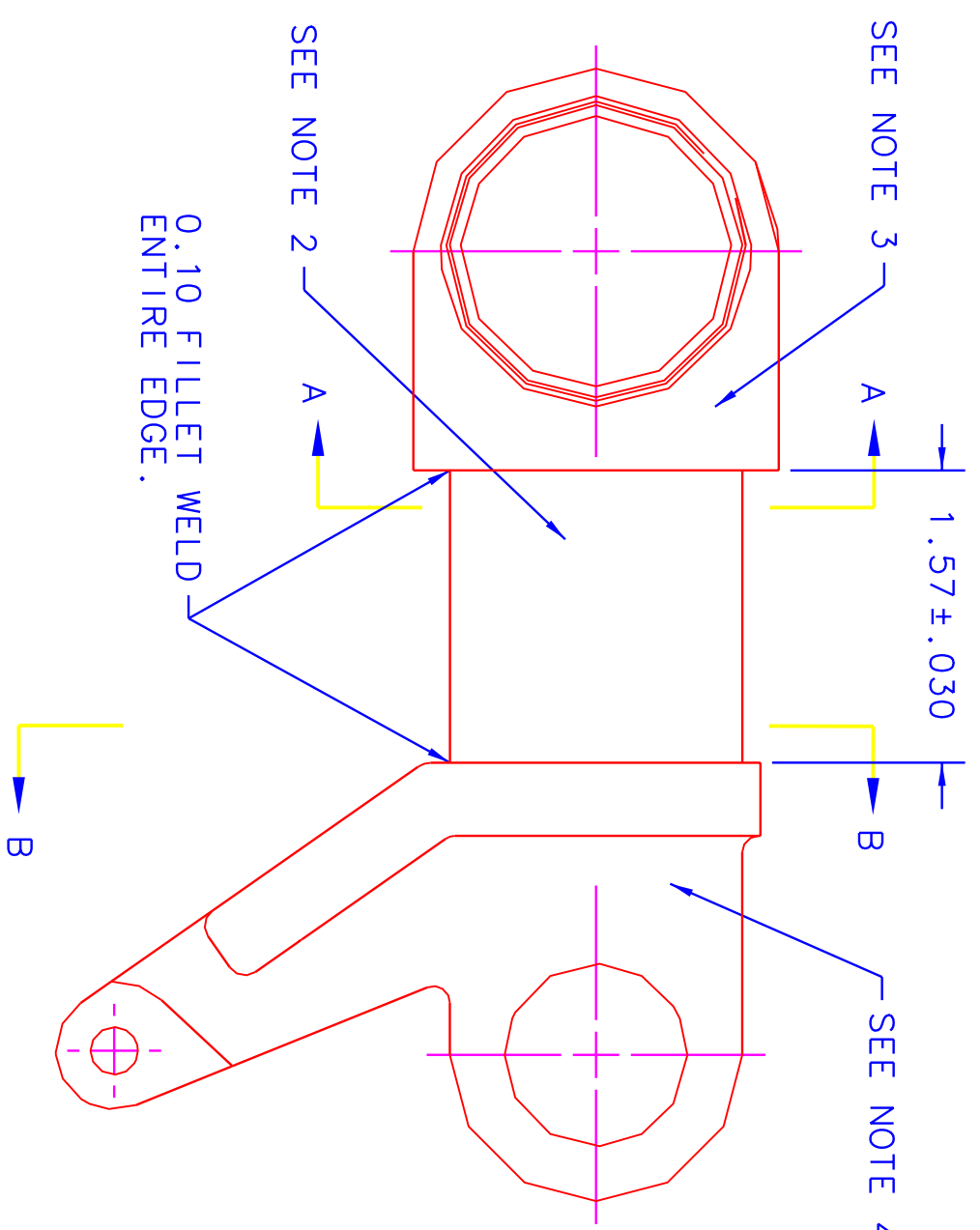
C

D

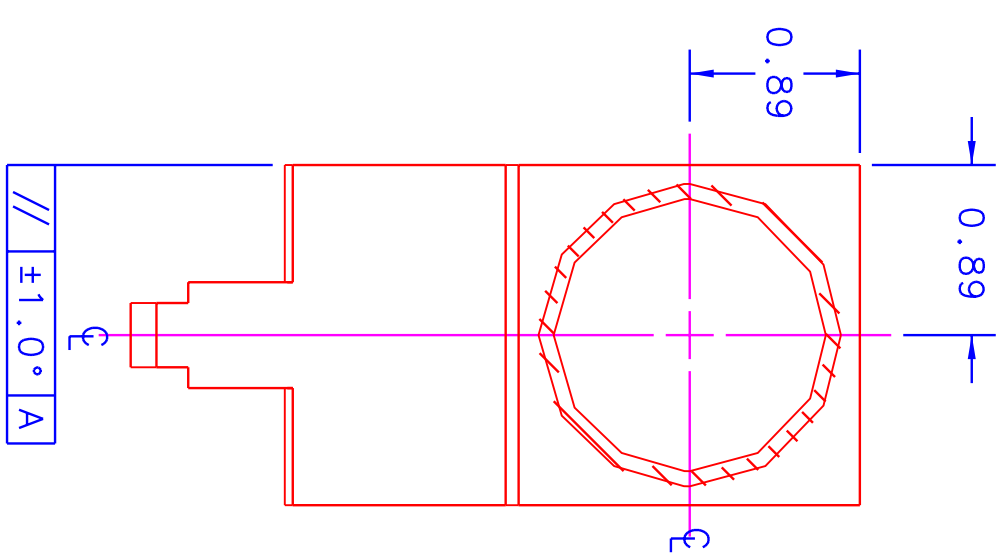
REVISIONS				
ZONE	REV	DESCRIPTION	DATE	APPROVED
	1	INITIAL ISSUE		



SECTION A-A



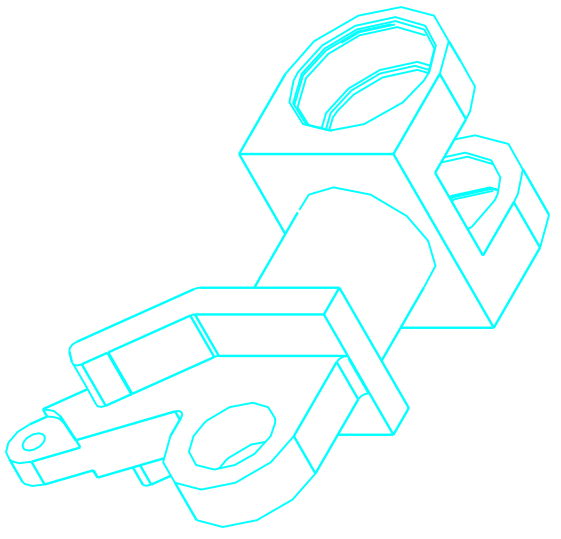
0.10 FILLET WELD ENTIRE EDGE.



SECTION B-B

NOTES

- 1: REMOVE ALL SHARP EDGES AND CORNERS FROM WELDS.
- 2: ALUMINUM TUBE 45mm OD, 41mm ID.
- 3: USE PART 213DSR.
- 4: USE PART 212DSR.



UNLESS OTHERWISE SPECIFIED DIMENSIONS ARE IN INCHES TOLERANCES ARE:				VIRGINIA POLYTECHNIC INSTITUTE AND STATE UNIVERSITY DEPARTMENT OF ENGINEERING SCIENCE AND MECHANICS			
FRACTIONS	DECIMALS	ANGLES		DRAWN APPROVALS DATE TITLE			
± .XX	± .01	± X° ± .5°					
DO NOT SCALE DRAWING				CHECKED D.S. RUPPERT 3/01/02			
MATERIAL ALUMINUM				FINISH 6061 T-6			
SIMILAR TO 211DSR				SCALE NA			
ACT. WT.				FSCM NO. 214DSR			
CALC. WT.				SHEET 1 OF 1			

1

2

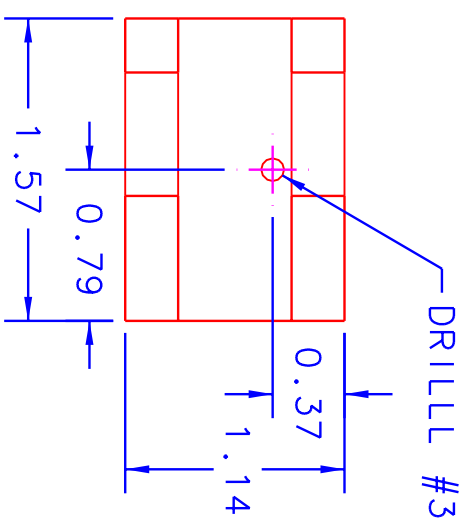
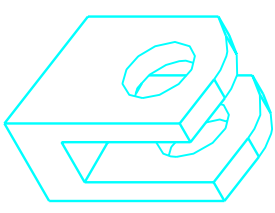
3

4

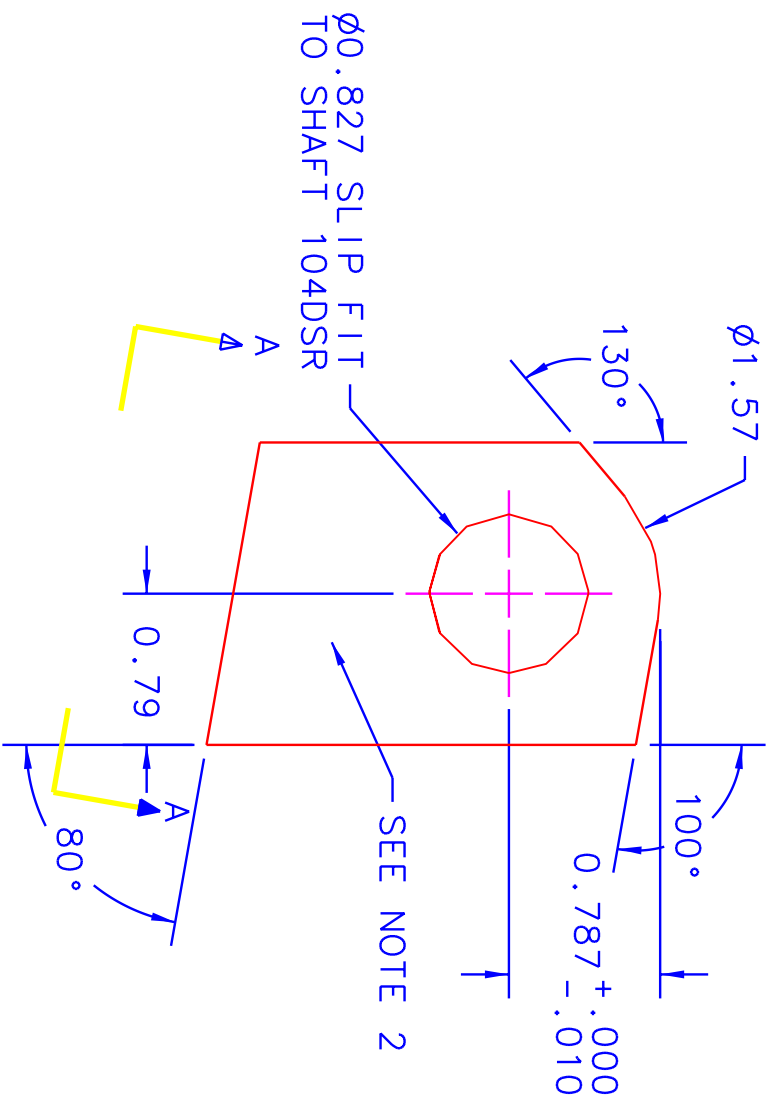
DWG. NO. 215DSR SH 1 REV.1

REVISIONS

ZONE	REV	DESCRIPTION	DATE	APPROVED
	1	INITIAL ISSUE		

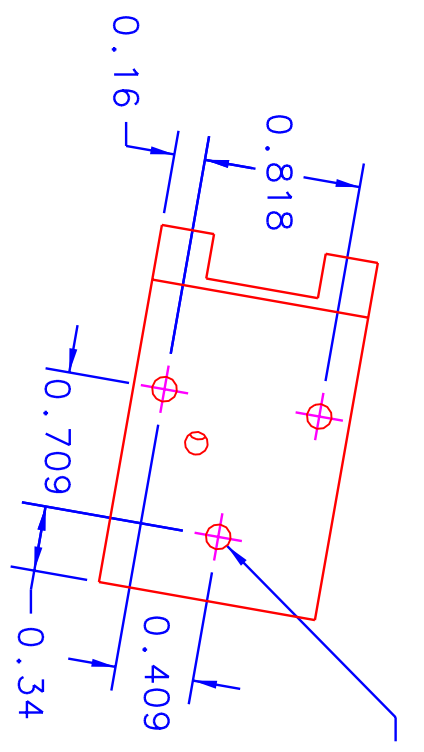
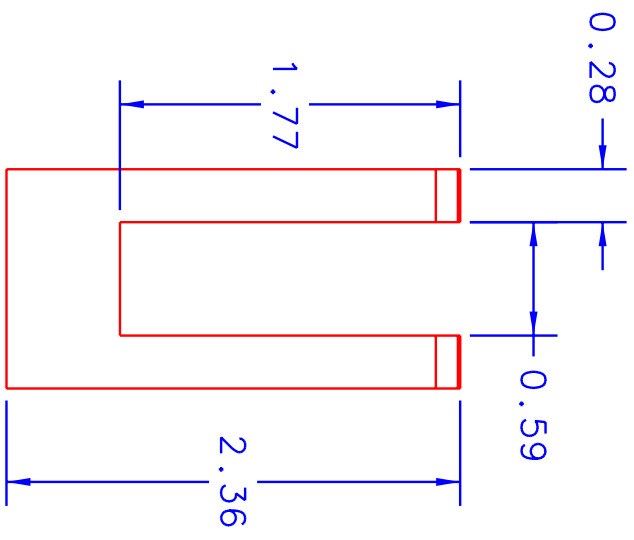


DRILL #31 (Ø0.118) THRU



Ø0.827 SLIP FIT TO SHAFT 104DSR

SEE NOTE 2



VIEW A-A

DRILL #30 (Ø0.130)
X0.49 DP, TAP MAX.7
3 PLC AS SHOWN

NOTES

- 1: BREAK ALL SHARP EDGES AND CORNERS W/ .01X45° MIN CHAMFERS UNLESS OTHERWISE NOTED.
- 2: STAMP DWG. # AND REV W/ 1/8 IN HUGH CHARACTERS HERE.

UNLESS OTHERWISE SPECIFIED DIMENSIONS ARE IN INCHES TOLERANCES ARE:

FRACTIONS DECIMALS ANGLES
 ± .XX ±.01 X° ±.5°
 ± .XXX ±.005 X° ±.5°
 DO NOT SCALE DRAWING

VIRGINIA POLYTECHNIC INSTITUTE AND STATE UNIVERSITY
 DEPARTMENT OF ENGINEERING SCIENCE AND MECHANICS

MATERIAL ALUMINUM

FINISH 6061 T-6

SIMILAR TO ACT. WT. CALC WT.

APPROVALS	DATE	TITLE
DRAWN D.S. RUPPERT	10/12/01	HOOF TO FETLOCK JOINT
CHECKED		
ISSUED		

SIZE FSQM NO. B
 SCALE NA

DWG NO. 215DSR

SHEET 1 OF 1

1

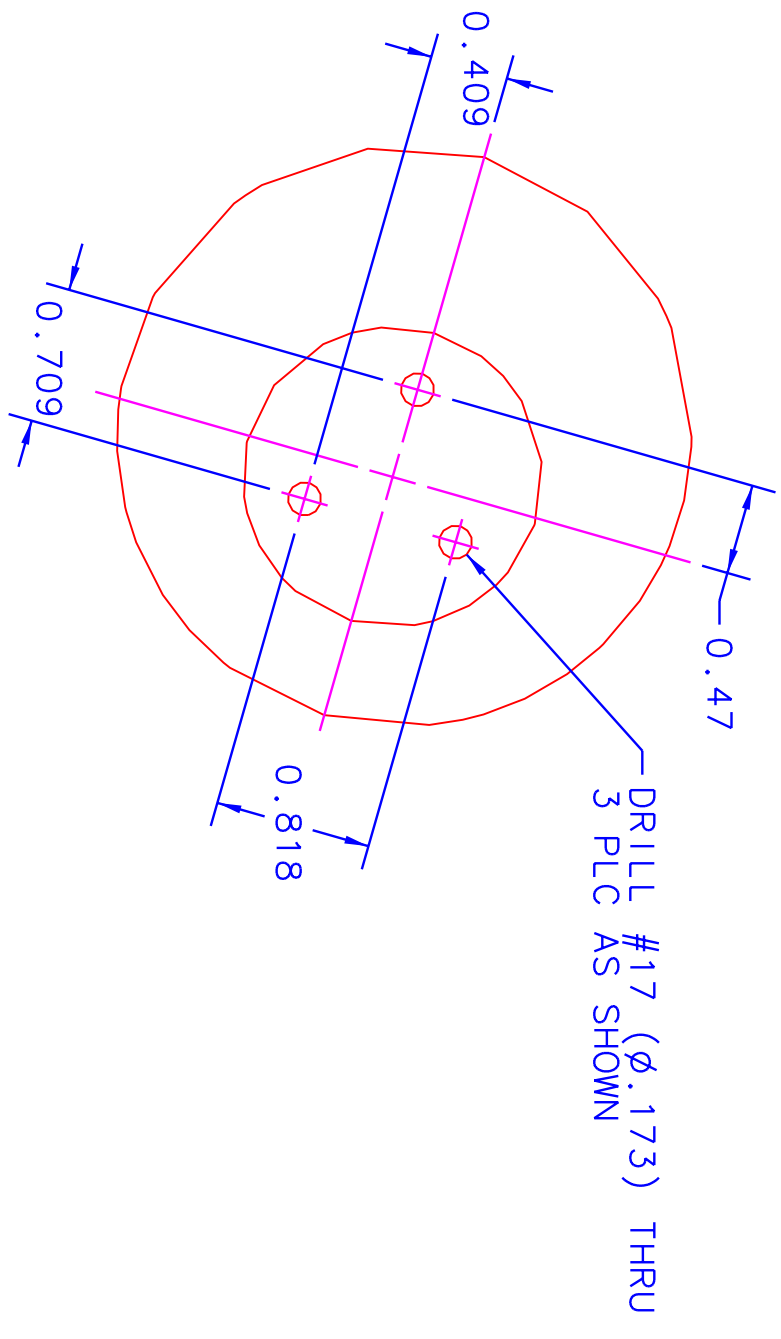
2

3

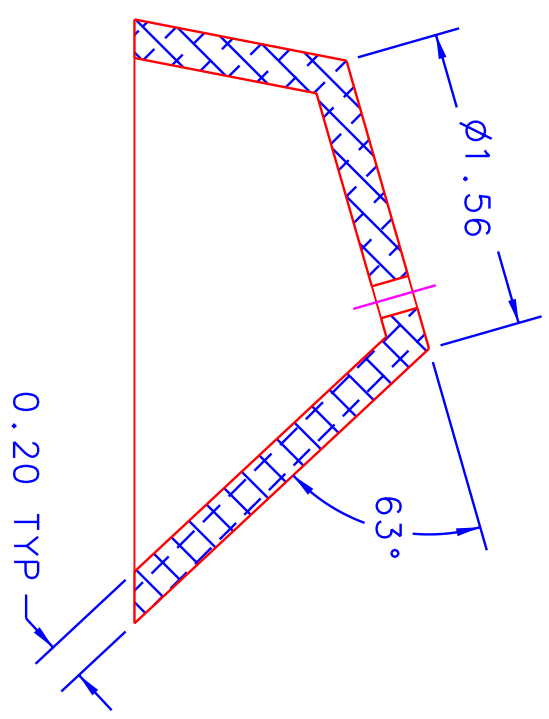
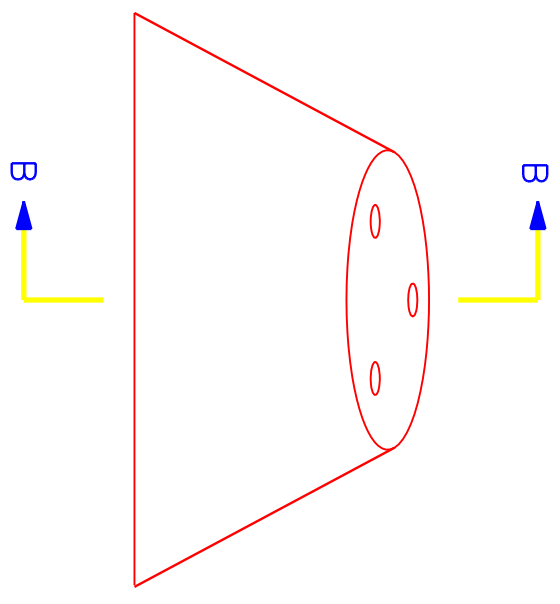
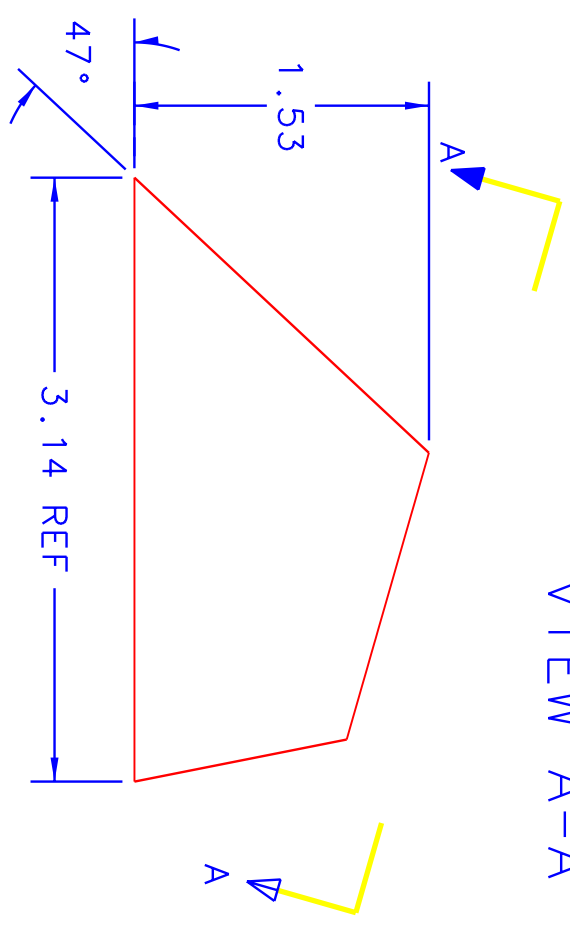
4



REVISIONS				
ZONE	REV	DESCRIPTION	DATE	APPROVED
	1	INITIAL ISSUE		



VIEW A-A



NOTES

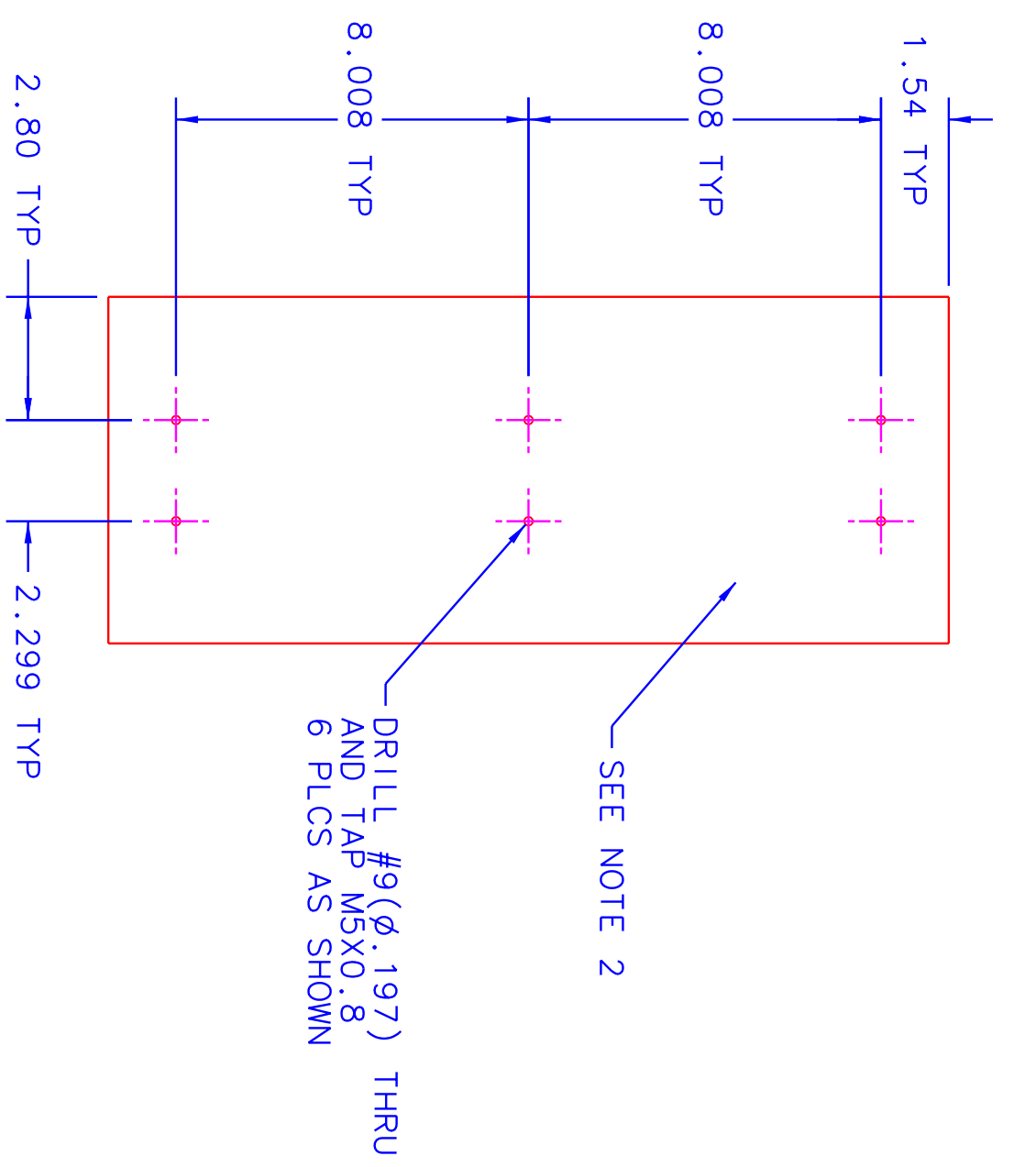
- BREAK ALL SHARP EDGES AND CORNERS W/ .01X45° MIN CHAMFERS UNLESS OTHERWISE NOTED.

VIRGINIA POLYTECHNIC INSTITUTE AND STATE UNIVERSITY
DEPARTMENT OF ENGINEERING SCIENCE AND MECHANICS

UNLESS OTHERWISE SPECIFIED DIMENSIONS ARE IN INCHES TOLERANCES ARE:		DRAWN		DATE		TITLE	
FRACTIONS	DECIMALS	ANGLES	D.S. RUPPERT	10/12/01	HOOF		
±	.XX ±.01	X°.±.5°	CHECKED		SIZE	FSQM NO.	DWG NO.
DO NOT SCALE DRAWING	.XXX±.005		ISSUED		B		216DSR
MATERIAL	ALUMINUM				SCALE	NA	SHEET 1 OF 1
FINISH	6061 T-6						
SIMILAR TO		ACT. WT	CALC WT				

1 2 3 4

REVISIONS				
ZONE	REV	DESCRIPTION	DATE	APPROVED
	1	INITIAL ISSUE		



NOTES

- 1: BREAK ALL SHARP EDGES AND CORNERS W/ 0.01X45° MIN CHAMFERS.
- 2: STAMP DWG. # AND REV W/ 1/8 IN HIGH CHARACTERS HERE.

UNLESS OTHERWISE SPECIFIED DIMENSIONS ARE IN INCHES TOLERANCES ARE:				VIRGINIA POLYTECHNIC INSTITUTE AND STATE UNIVERSITY DEPARTMENT OF ENGINEERING SCIENCE AND MECHANICS			
FRACTIONS		DECIMALS		ANGLES		TITLES	
±		.XX±		±		THORAX, PROXIMAL	
DO NOT SCALE DRAWING				DRAWN		CHECKED	
MATERIAL				D.S. RUPPERT		8/21/02	
ALUMINUM							
FINISH		ISSUED		SCALE		FSCM NO.	
6061 T-6				NA		217DSR	
SIMILAR TO		ACT. WT		CALC WT		DWG NO.	
						217DSR	
				SHEET		1 OF 1	
				1			

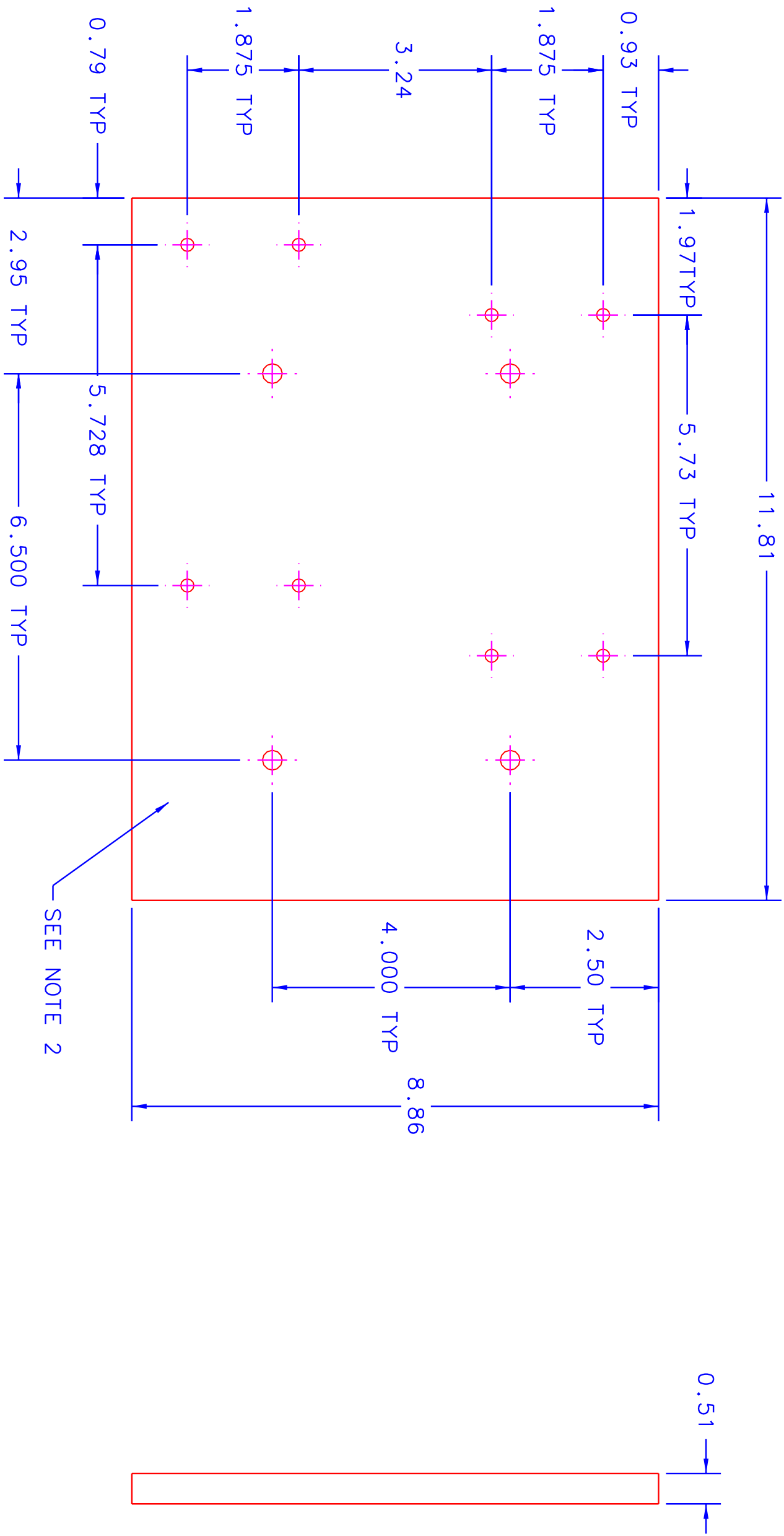
1

2

4

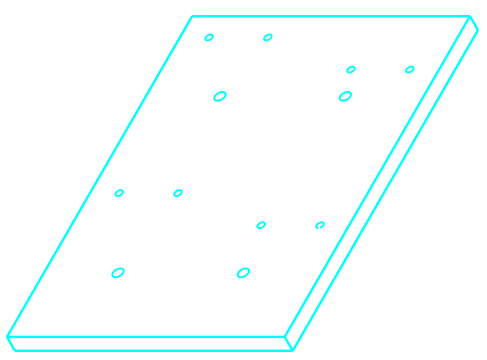
DWG. NO. 218DSR SH 1 REV. 1

REVISIONS			DATE	APPROVED
ZONE	REV	DESCRIPTION		
	1	INITIAL ISSUE		



NOTES

- 1: BREAK ALL SHARP EDGES AND CORNERS W/ 0.01X45° MIN CHAMFERS UNLESS OTHERWISE NOTED.
- 2: STAMP DWG. # AND REV W 1/8 IN HIGH CHARACTERS HERE.



UNLESS OTHERWISE SPECIFIED DIMENSIONS ARE IN INCHES TOLERANCES ARE:		DRAWN		DATE		TITLE	
FRACTIONS	DECIMALS	ANGLES	D.S. RUPPERT	8/21/02	THORAX, MIDDLE		
±	.XX ±.01	X° ±.5°	CHECKED		SIZE	FSQM NO.	DWG NO.
DO NOT SCALE DRAWING	.XXX ±.005		ISSUED		B		218DSR
MATERIAL	ALUMINUM				SCALE	NA	SHEET
FINISH	6061						1 OF 1
SIMILAR TO		ACT. WT	CALC WT				

VIRGINIA POLYTECHNIC INSTITUTE AND STATE UNIVERSITY
DEPARTMENT OF ENGINEERING SCIENCE AND MECHANICS

1

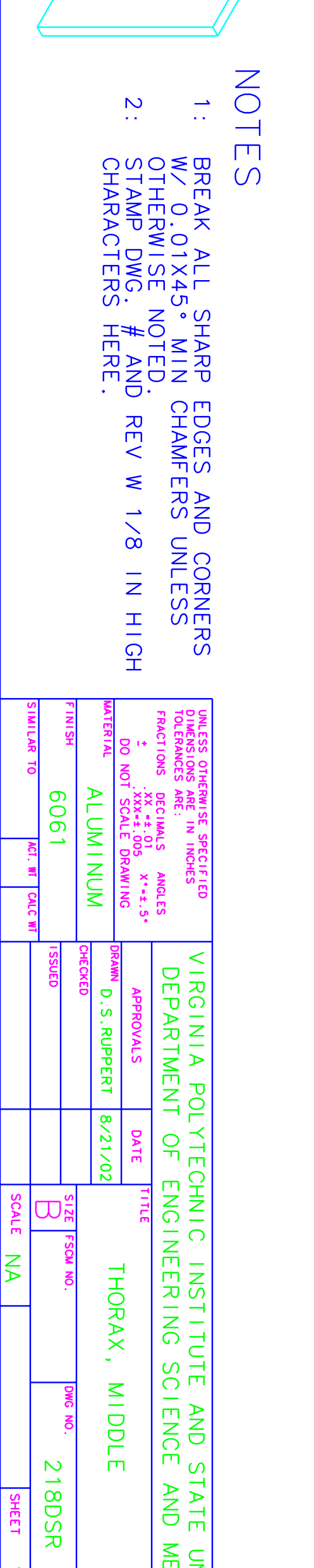
2

3

4

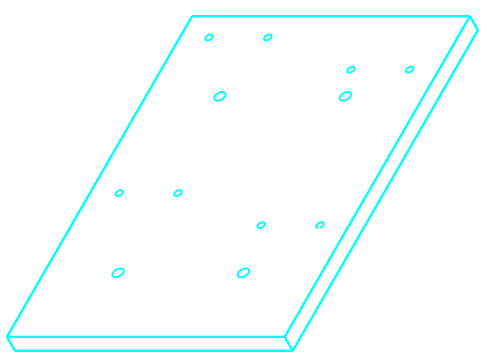
DWG. NO. 218DSR SH 1 REV. 1

REVISIONS			DATE	APPROVED
ZONE	REV	DESCRIPTION		
	1	INITIAL ISSUE		



NOTES

- 1: BREAK ALL SHARP EDGES AND CORNERS W/ 0.01X45° MIN CHAMFERS UNLESS OTHERWISE NOTED.
- 2: STAMP DWG. # AND REV W 1/8 IN HIGH CHARACTERS HERE.



UNLESS OTHERWISE SPECIFIED DIMENSIONS ARE IN INCHES TOLERANCES ARE:		DRAWN		DATE		TITLE	
FRACTIONS	DECIMALS	ANGLES	D.S. RUPPERT	8/21/02	THORAX, MIDDLE		
±	.XX ±.01	X° ±.5°	CHECKED		SIZE	FSQM NO.	DWG NO.
DO NOT SCALE DRAWING	.XXX ±.005		ISSUED		B		218DSR
MATERIAL	ALUMINUM				SCALE	NA	SHEET
FINISH	6061						1 OF 1
SIMILAR TO		ACT. WT	CALC WT				

VIRGINIA POLYTECHNIC INSTITUTE AND STATE UNIVERSITY
DEPARTMENT OF ENGINEERING SCIENCE AND MECHANICS

1

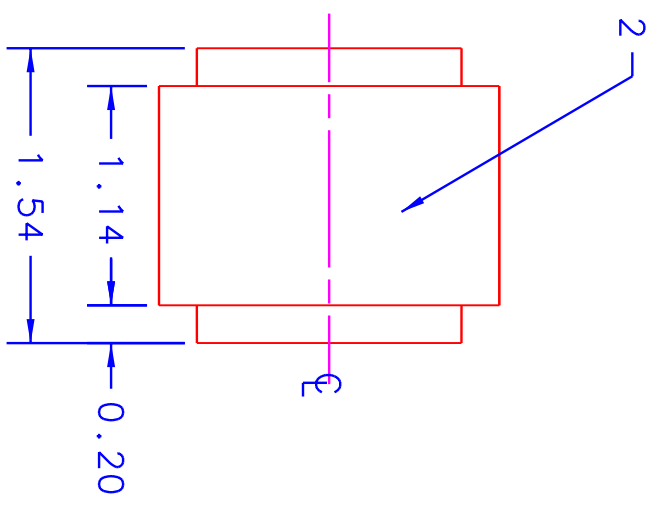
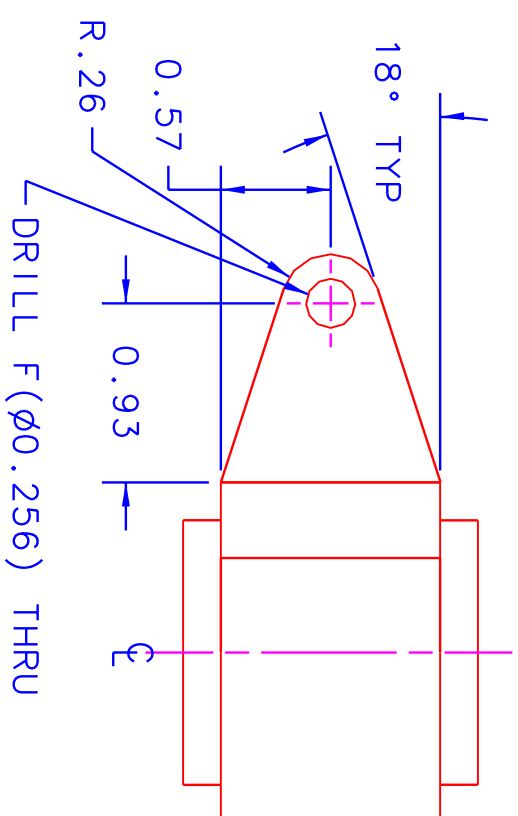
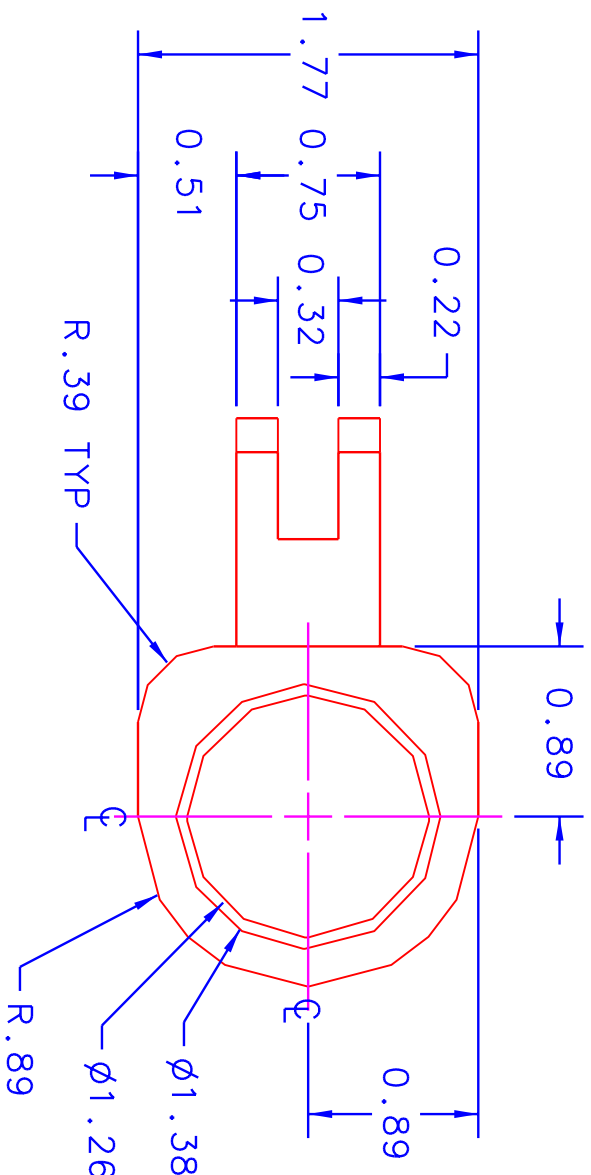
2

DWG. NO. 220DSR SH 1 REV. 1

SH 1 REV. 1

4

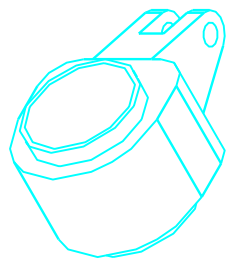
REVISIONS				
ZONE	REV	DESCRIPTION	DATE	APPROVED
	1	INITIAL ISSUE		



SEE NOTE 2

NOTES

- 1: BREAK ALL SHARP EDGES AND CORNERS W/ 0.01X45° MIN CHAMFERS UNLESS OTHERWISE NOTED.
- 2: STAMP DWG. # AND REV W/ 1/8 IN HIGH CHARACTERS HERE.



A

B

C

D

1

2

3

4

UNLESS OTHERWISE SPECIFIED DIMENSIONS ARE IN INCHES TOLERANCES ARE:

FRACTIONS	DECIMALS	ANGLES
$\pm .XX$	$\pm .01$	$1^\circ \pm .5^\circ$
DO NOT SCALE DRAWING	$\pm .XXX$	$\pm .005$

VIRGINIA POLYTECHNIC INSTITUTE AND STATE UNIVERSITY
DEPARTMENT OF ENGINEERING SCIENCE AND MECHANICS

MATERIAL	ALUMINIUM	DRAWN	D.S. RUPPERT	DATE	4/30/02	TITLE	RADIUS, MIDPOINT		
FINISH	6061 T-6	CHECKED				SIZE	FSCM NO.	DWG NO.	220DSR
SIMILAR TO		ISSUED				SCALE	NA		
									SHEET 1 OF 1

A

B

C

D

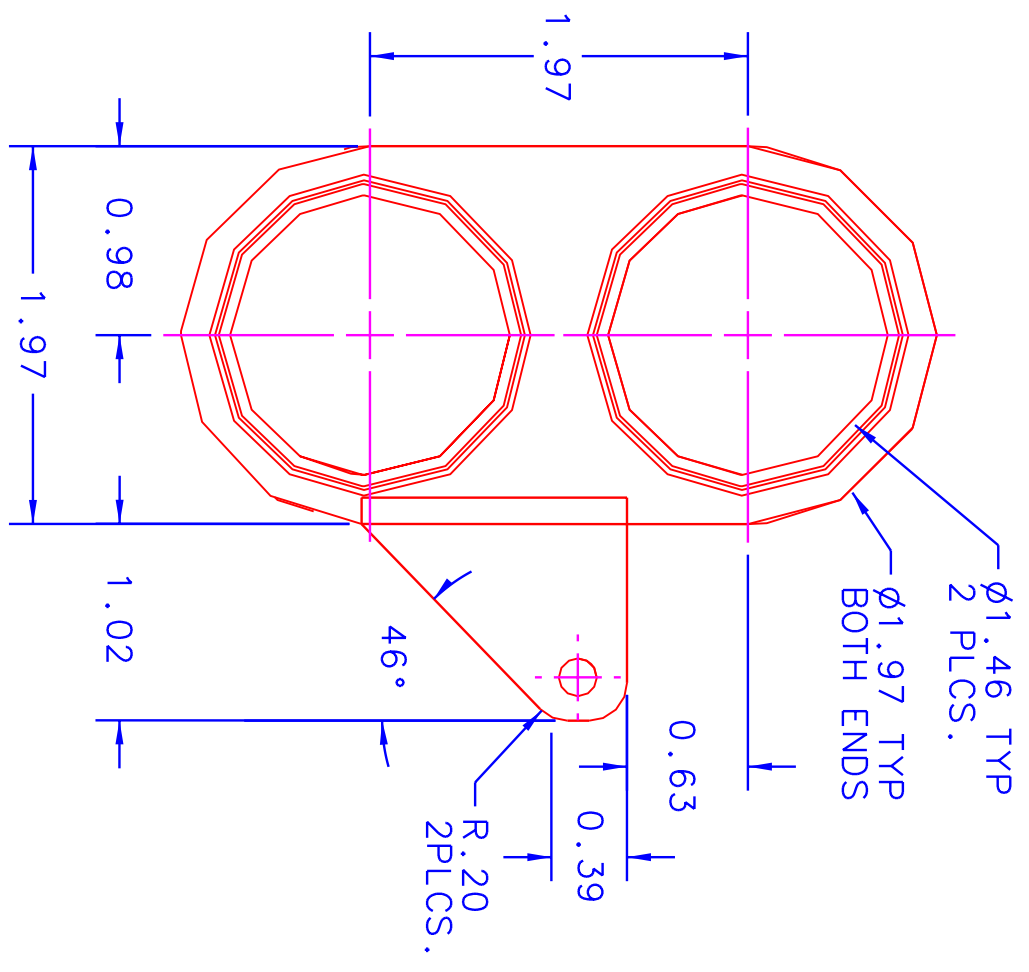
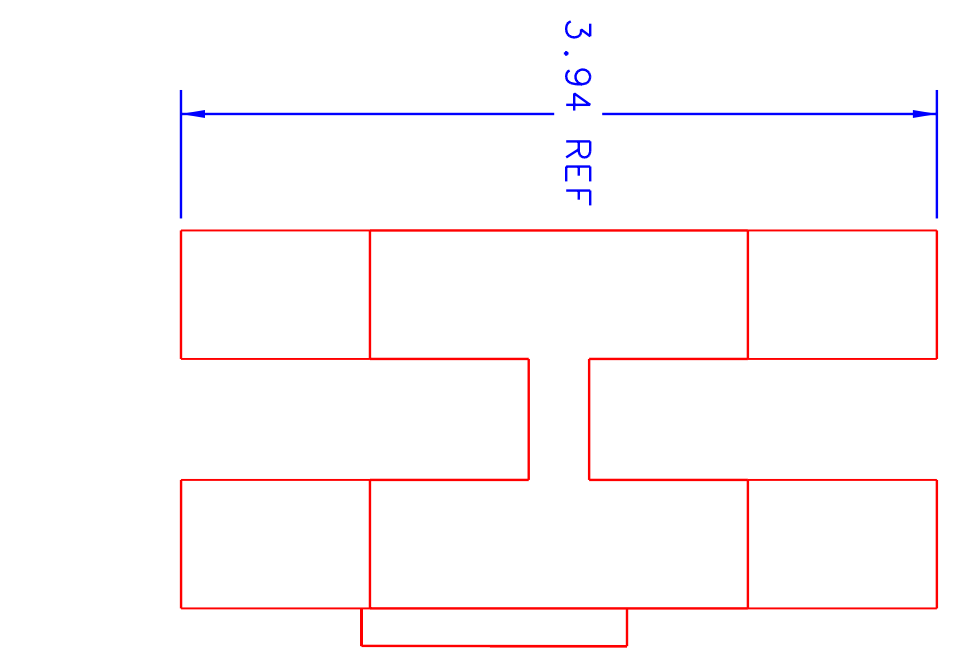
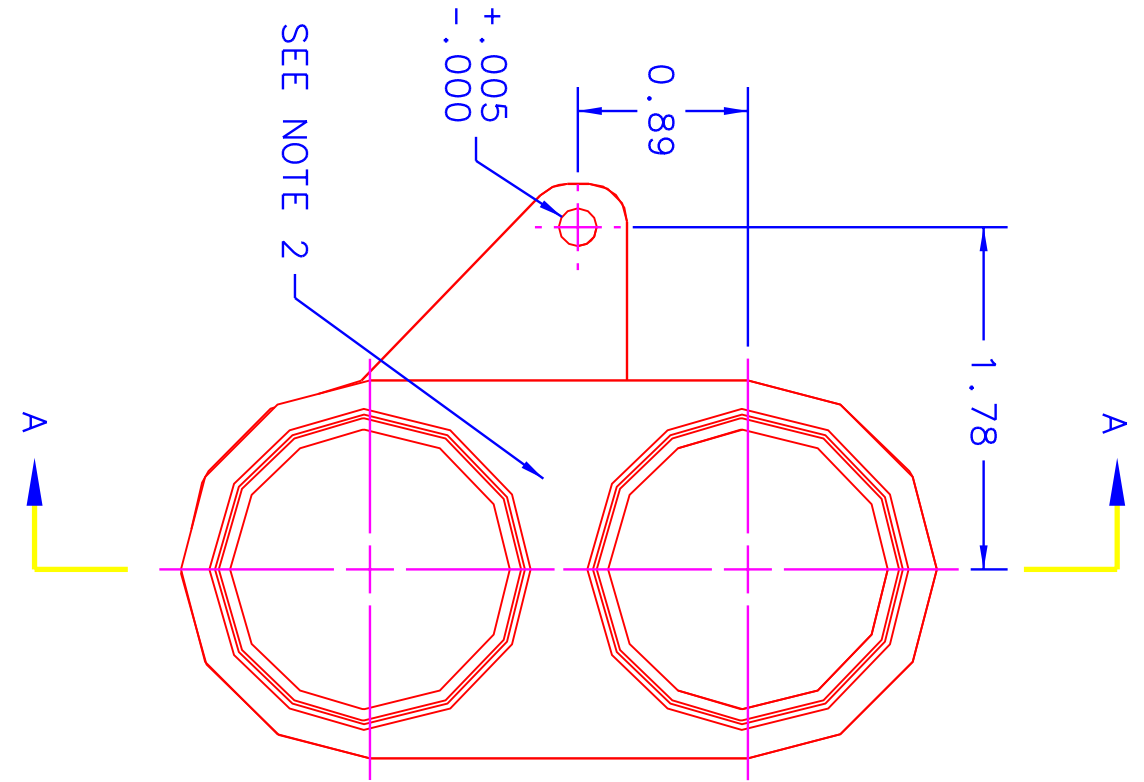
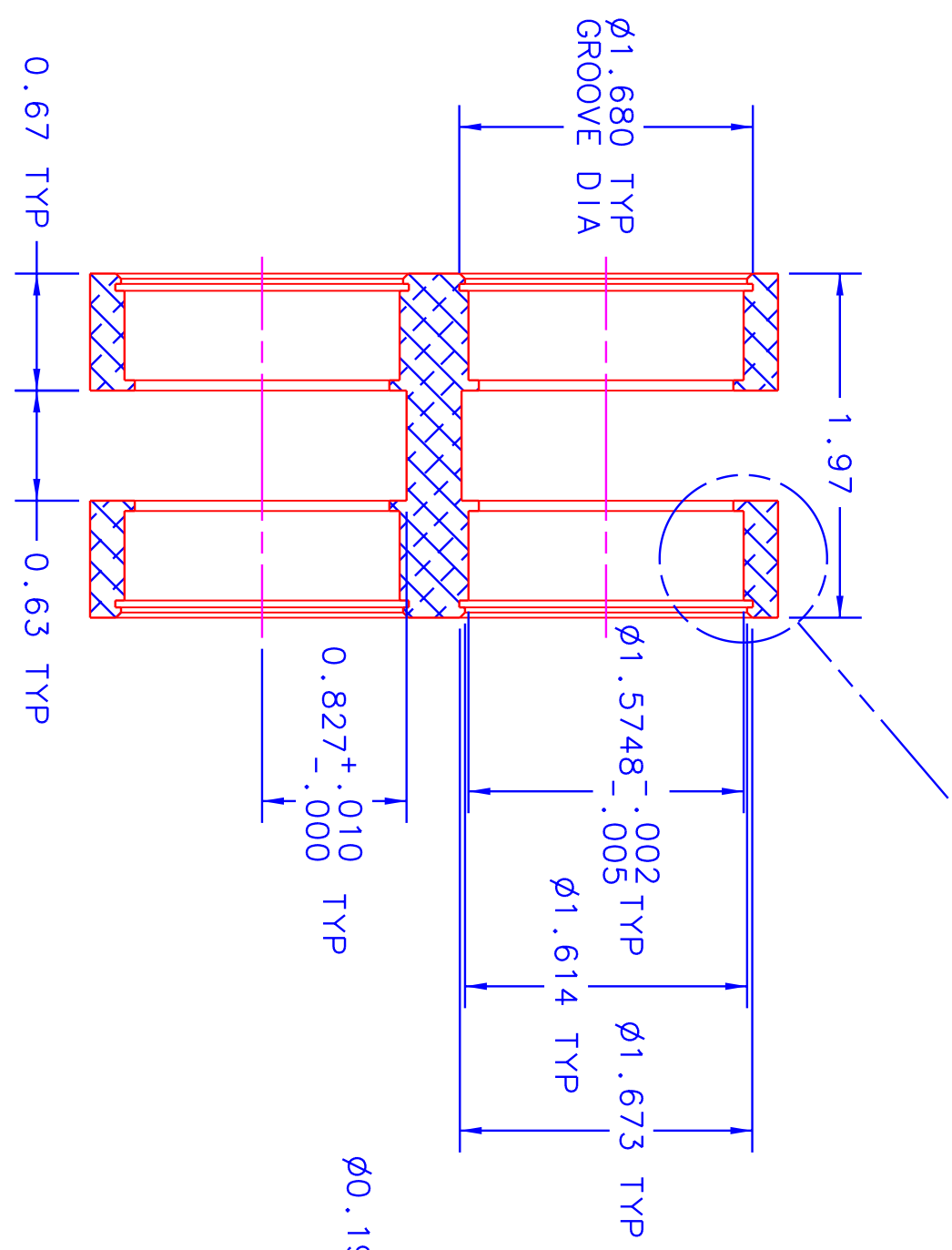
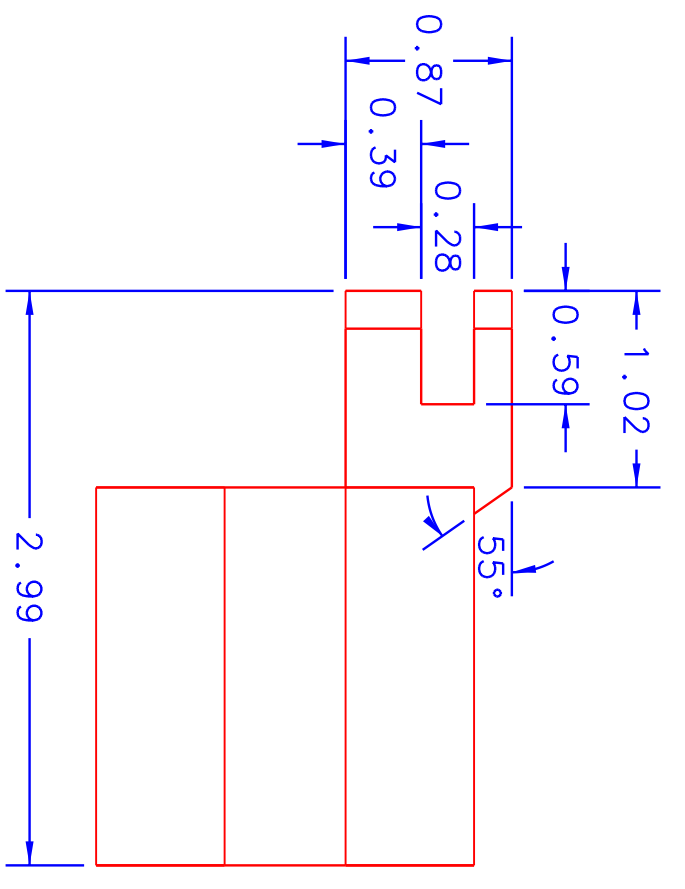
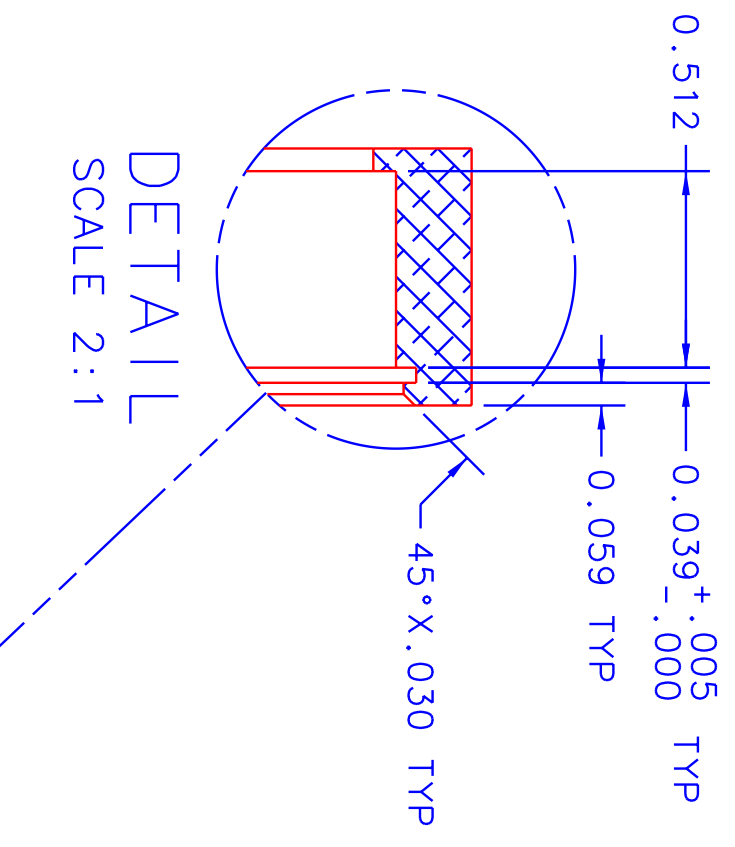
4

3

2

1

REVISIONS				
ZONE	REV	DESCRIPTION	DATE	APPROVED
	1	INITIAL ISSUE		



NOTES

- 1: BREAK ALL SHARP EDGES AND CORNERS W/ 0.01X45° MIN SHAMFERS UNLESS OTHERWISE NOTED.
- 2: STAMP DWG. # AND REV W/ 1/8 IN HIGH CHARACTERS HERE.

UNLESS OTHERWISE SPECIFIED DIMENSIONS ARE IN INCHES		TOLERANCES ARE:		ANGLES	
FRACTIONS	DECIMALS	XX+0.05	X+0.5	X+0.5°	X+0.5°
DO NOT SCALE DRAWING					
MATERIAL	ALUMINIUM	DRAWN	D. S. RUPPERT	DATE	3/04/02
FINISH	6061 T-6	CHECKED		TITLE	CARPUS, JOINT
SIMILAR TO	205DSR	ISSUED		SIZE	FSCM NO. C
				SCALE	NA
				DWG NO.	301DSR
				SHEET	1 OF 1

A

DWG. NO. 301DSR SH 1 REV. 1

C

D

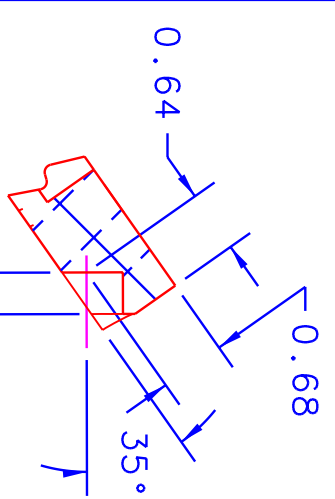
4

3

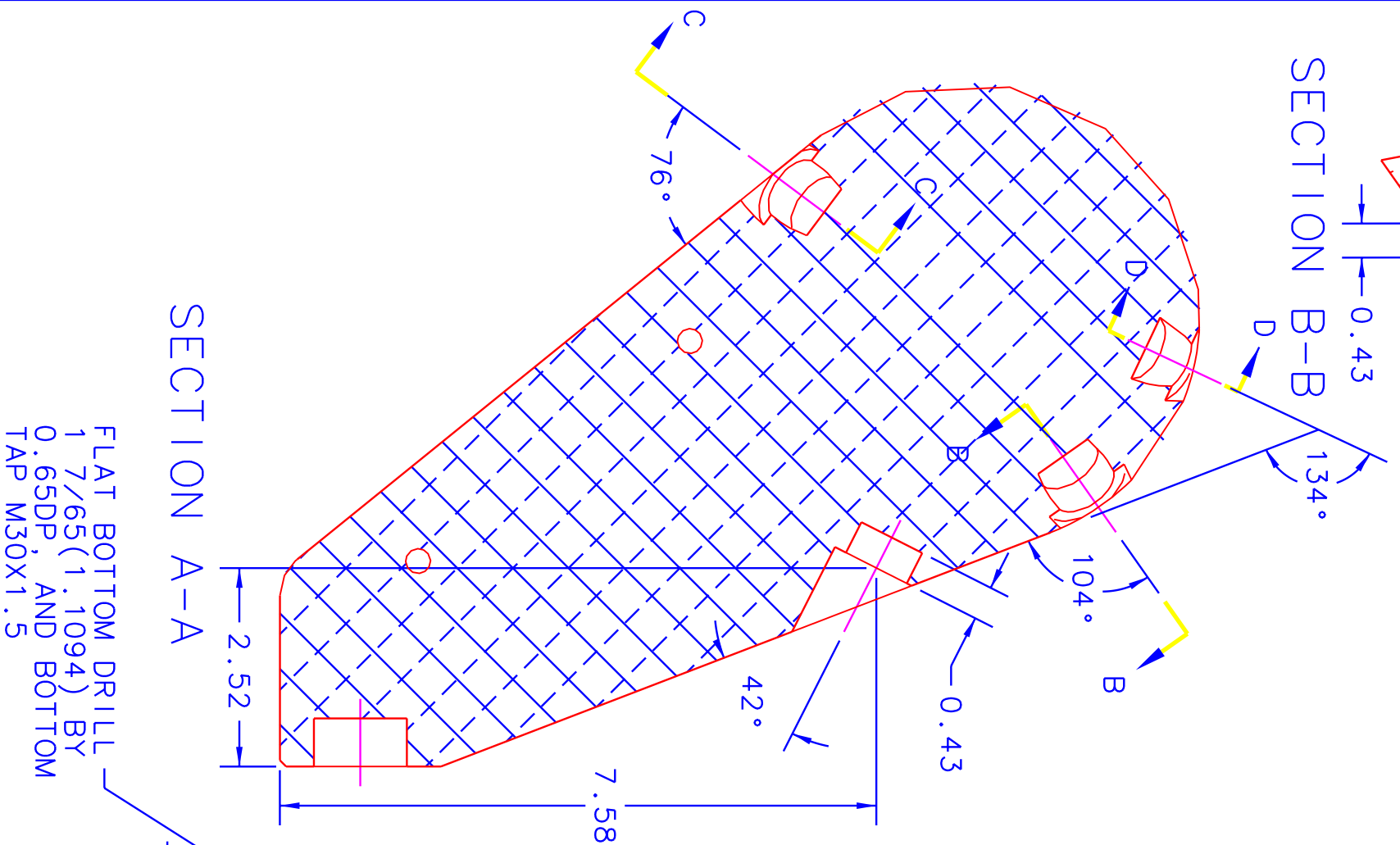
2

1

REVISIONS				
ZONE	REV	DESCRIPTION	DATE	APPROVED
	1	INITIAL ISSUE		



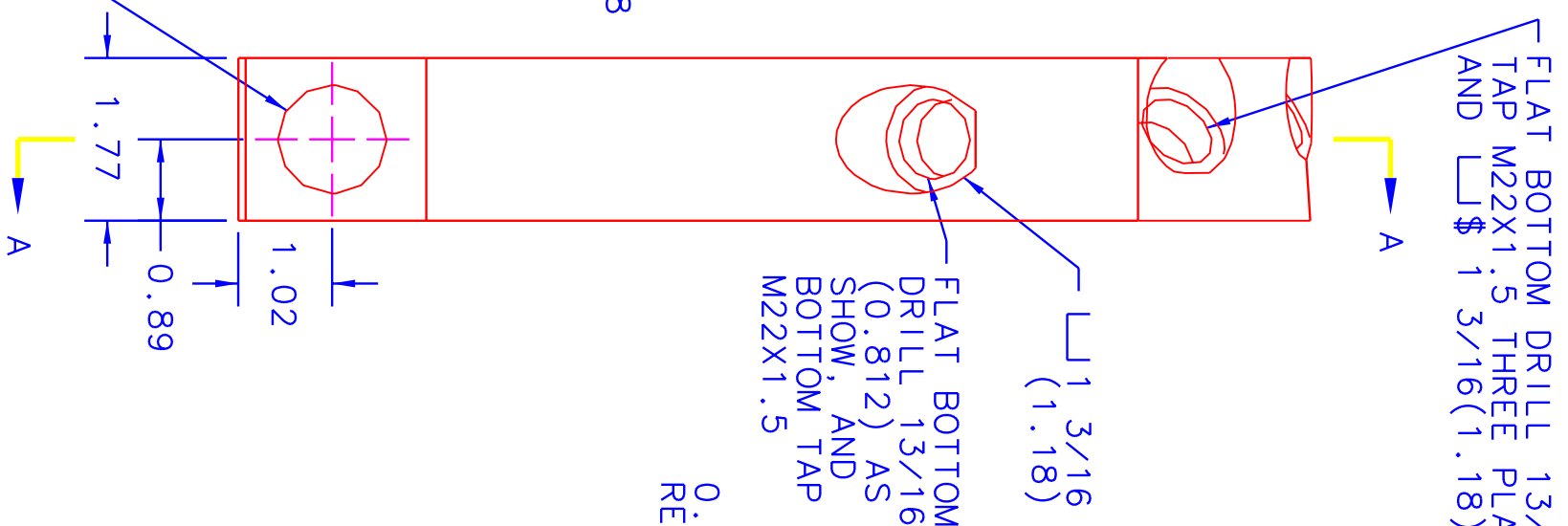
SECTION B-B



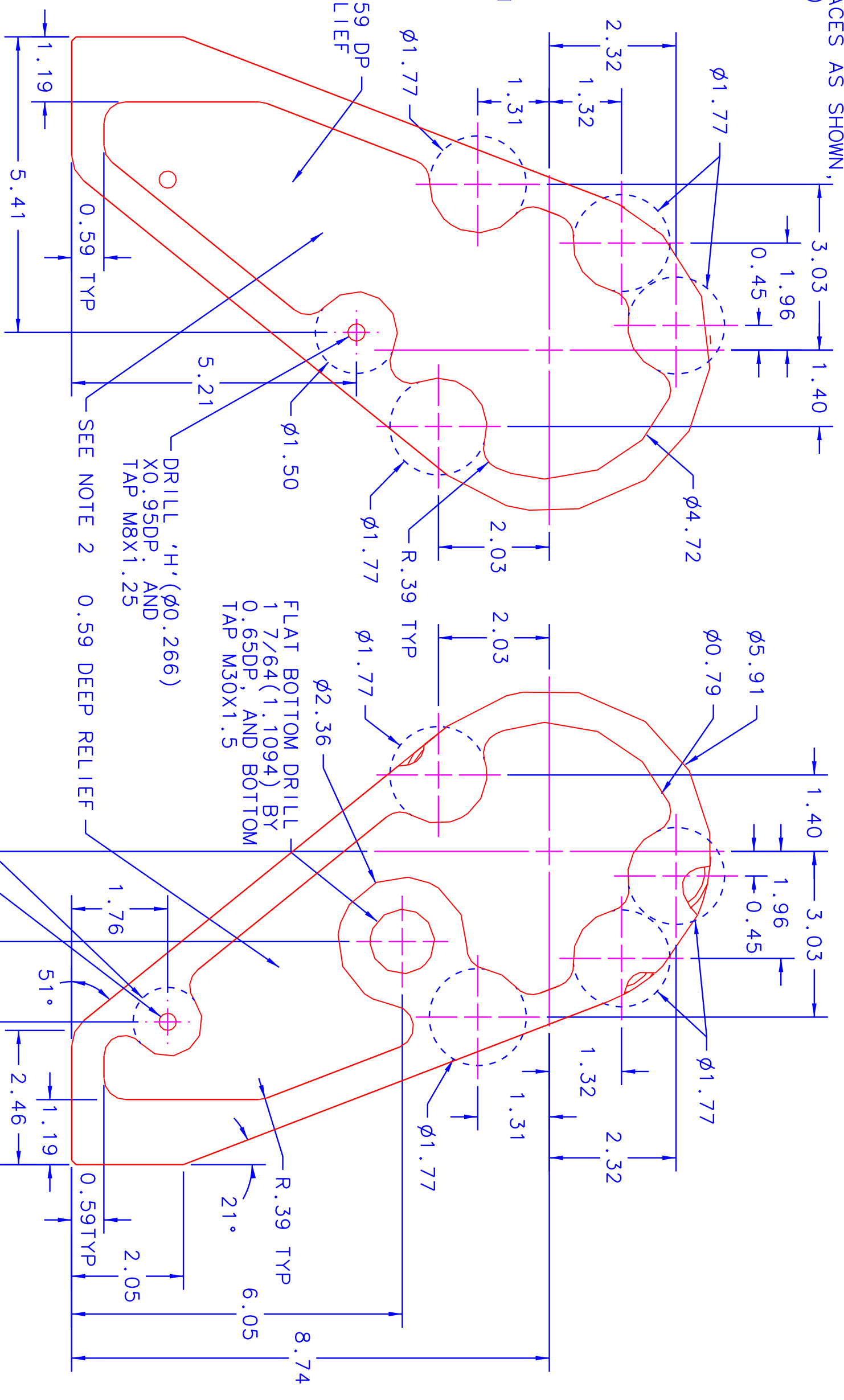
SECTION A-A

FLAT BOTTOM DRILL
1 7/65 (1.1094) BY
0.65DP, AND BOTTOM
TAP M30X1.5

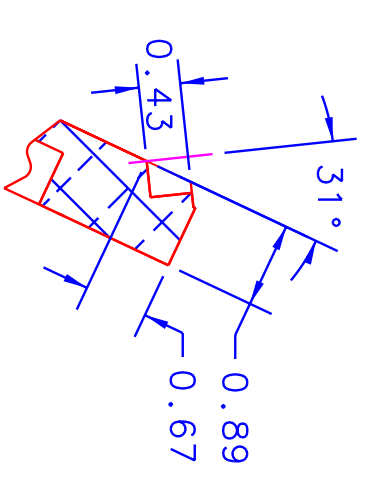
FLAT BOTTOM DRILL 1 3/16 (0.812) AND
TAP M22X1.5 THREE PLACES AS SHOWN,
AND 1 3/16 (1.18)



SECTION C-C



SECTION D-D



NOTES

- 1: BREAK ALL SHARP EDGES AND CORNERS W/ .01X45° MIN CHAMFERS UNLESS OTHERWISE NOTED.
- 2: STAMP DWG. # AND REV W/ 1/8 IN HIGH CHARACTERS HERE.

UNLESS OTHERWISE SPECIFIED DIMENSIONS ARE IN INCHES. TOLERANCES ARE:		VIRGINIA POLYTECHNIC INSTITUTE AND STATE UNIVERSITY DEPARTMENT OF ENGINEERING SCIENCE AND MECHANICS	
FRACTIONS	DECIMALS	ANGLES	
± .005	.XX ± .015		
DO NOT SCALE DRAWING		DRAWN BY: D.S. RUPPERT	
MATERIAL: ALUMINUM		DATE: 5/18/02	
FINISH: 6061 T-6		CHECKED: ISSUED:	
SIMILAR TO:		TITLE: SCAPULA	
SCALE: NA	DWG NO.: 302DSR	SHEET 1 OF 1	

NOTES

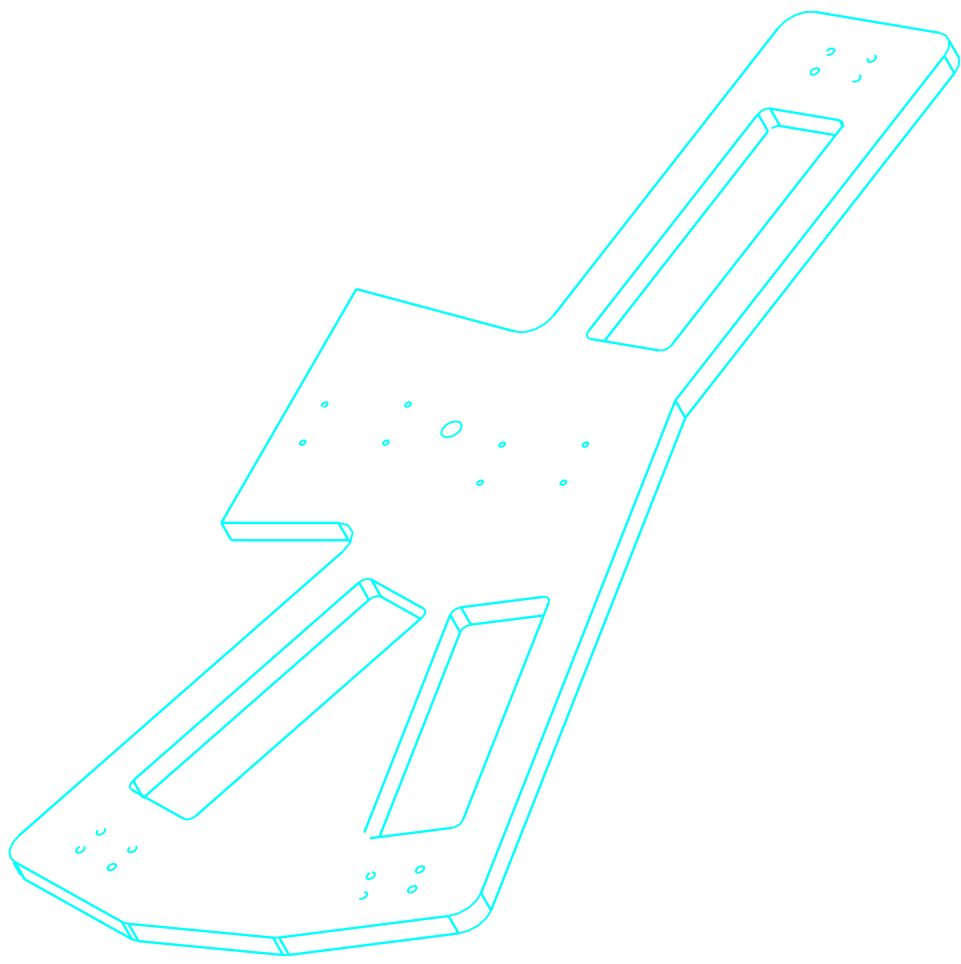
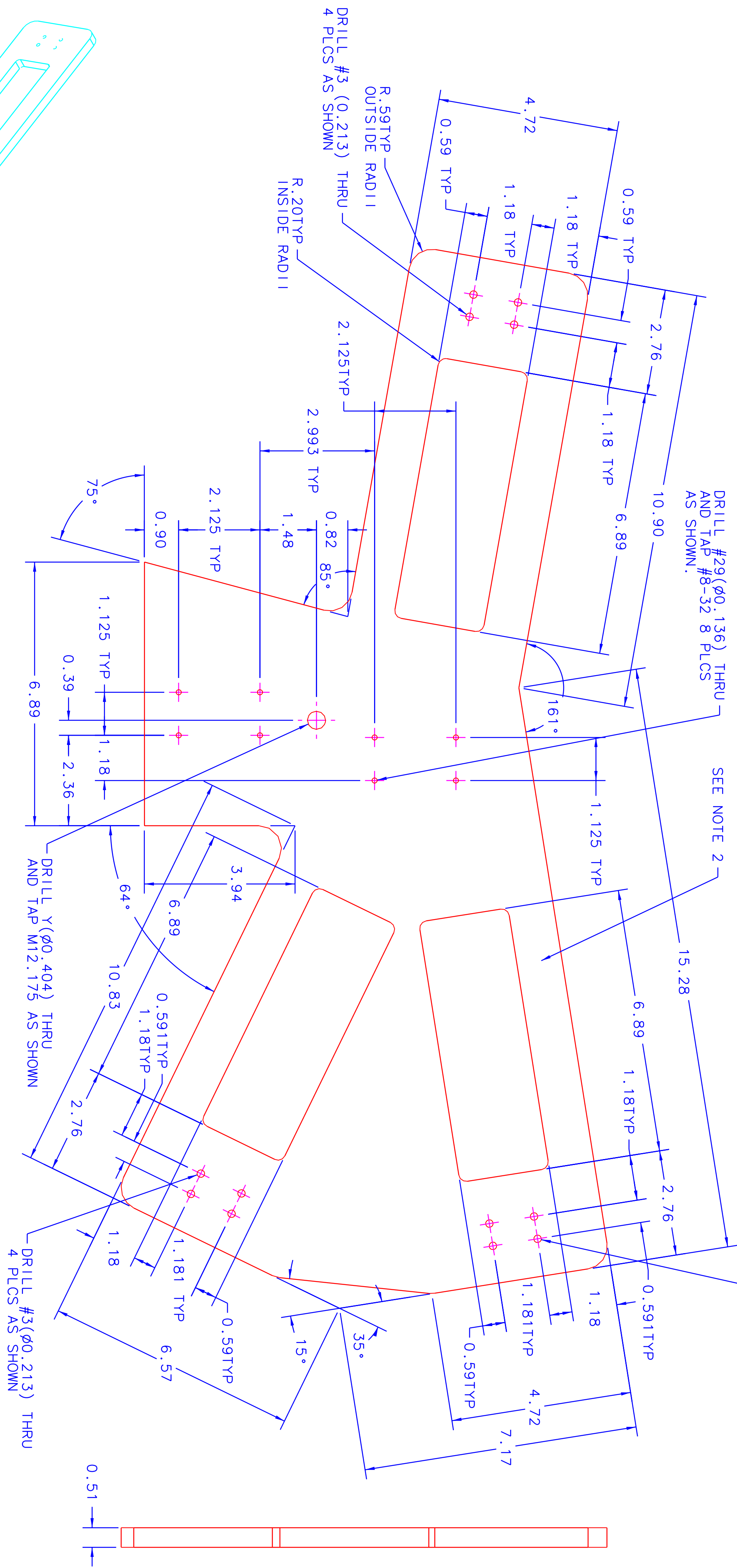
- 1: BREAK ALL SHARP EDGES AND CORNERS W/ .01X45° MIN CHAMFERS UNLESS OTHERWISE NOTED.
- 2: STAMP DWG. # AND REV W/ 1/8 IN HIGH CHARACTERS HERE.

DRILL #29(Ø.136) THRU AND TAP #8-32 8 PLCS AS SHOWN.

DRILL #3(Ø.213) Ø.197 THRU 4 PLCS AS SHOWN

DRILL #29(Ø.136) THRU AND TAP #8-32 8 PLCS AS SHOWN.

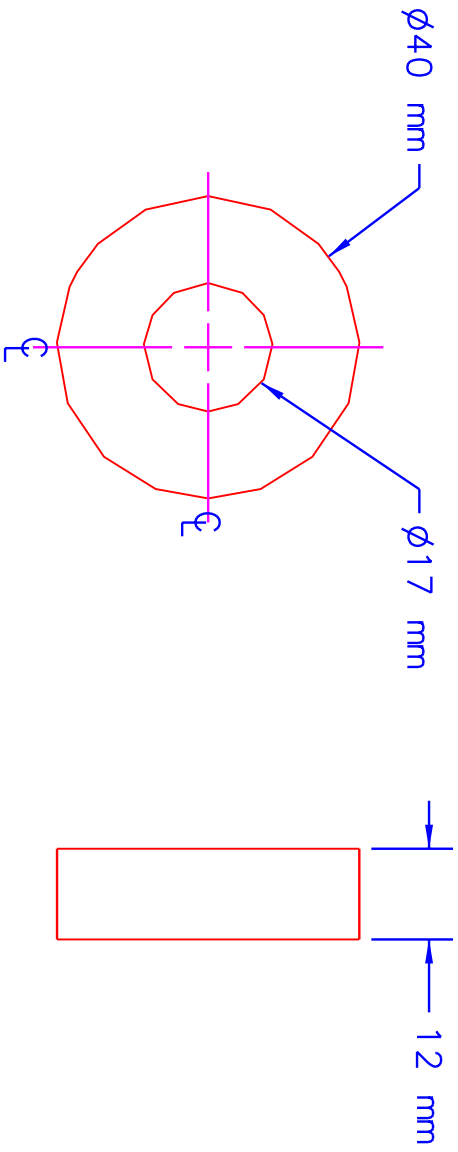
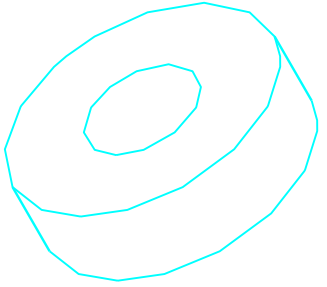
SEE NOTE 2



REVISIONS				
ZONE	REV	DESCRIPTION	DATE	APPROVED
1	1	INITIAL ISSUE		

UNLESS OTHERWISE SPECIFIED DIMENSIONS ARE IN INCHES FRACTIONS DECIMALS ANGLES		VIRGINIA POLYTECHNIC INSTITUTE AND STATE UNIVERSITY DEPARTMENT OF ENGINEERING SCIENCE AND MECHANICS	
±	.XX, .X, .015, X°.X, .5°	DRAWN	D. S. RUPPERT
±	DO NOT SCALE DRAWING	CHECKED	5/21/02
MATERIAL ALUMINIUM		TITLE THORAX, DISTAL	
FINISH	6061 T-6	SIZE	FSCAL NO. 303DSR
SIMILAR TO		SCALE	NA
		DWG NO.	303DSR
		SHEET	1 OF 1

REVISIONS				
ZONE	REV	DESCRIPTION	DATE	APPROVED
	1	INITIAL ISSUE		



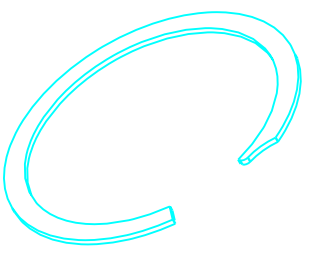
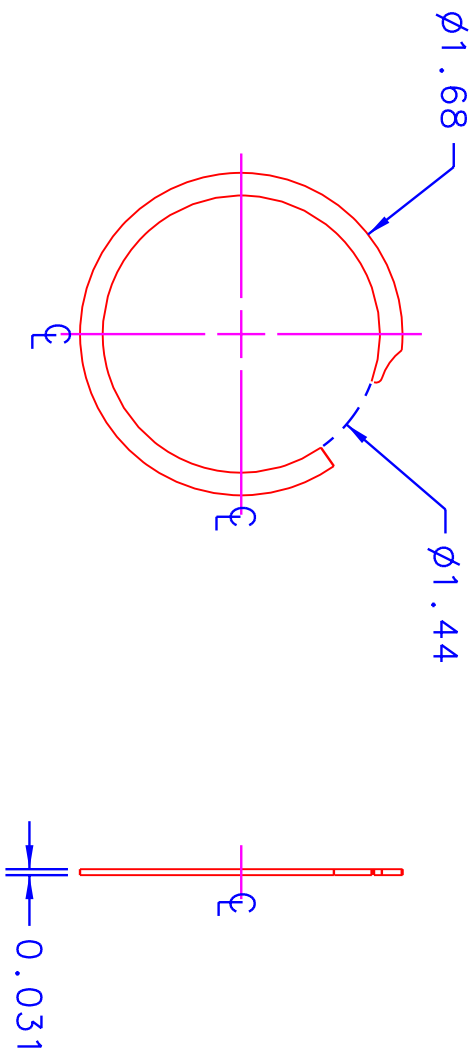
NOTE
 PURCHASE DOUBLE SEALED, GREASE PACKED,
 203 BEARING AT LOCAL AUTO-PARTS STORE.
 MANUFACTURE TO BE BCA BEARINGS.

UNLESS OTHERWISE SPECIFIED DIMENSIONS ARE IN INCHES TOLERANCES ARE:		VIRGINIA POLYTECHNIC INSTITUTE AND STATE UNIVERSITY DEPARTMENT OF ENGINEERING SCIENCE AND MECHANICS	
FRACTIONS	DECIMALS	ANGLES	
±	.XX ±.01	±X°±.5°	
DO NOT SCALE DRAWING	.XXX±.005	±X°±.5°	
MATERIAL	SEE NOTE		
FINISH			
SIMILAR TO	ACT. WT	CALC. WT	
APPROVALS		DATE	TITLE
DRAWN	D.S. RUPPERT	7/25/01	203 BEARING, DOUBLE SEALED, GREASE PACKED
CHECKED			
ISSUED			
SIZE	FSCM NO.	DWG NO.	
A		601DSR	
SCALE	NA	SHEET	1 OF 1

NOTE

PURCHASE PART VH-162-S02 FROM
 SMALLEY STEEL RING COMPANY
 385 GILMAN AVENUE,
 WHEELING, IL 60090
 1-800-537-7600

REVISIONS			DATE	APPROVED
ZONE	REV	DESCRIPTION		
	1	INITIAL ISSUE		

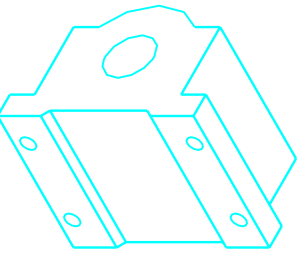
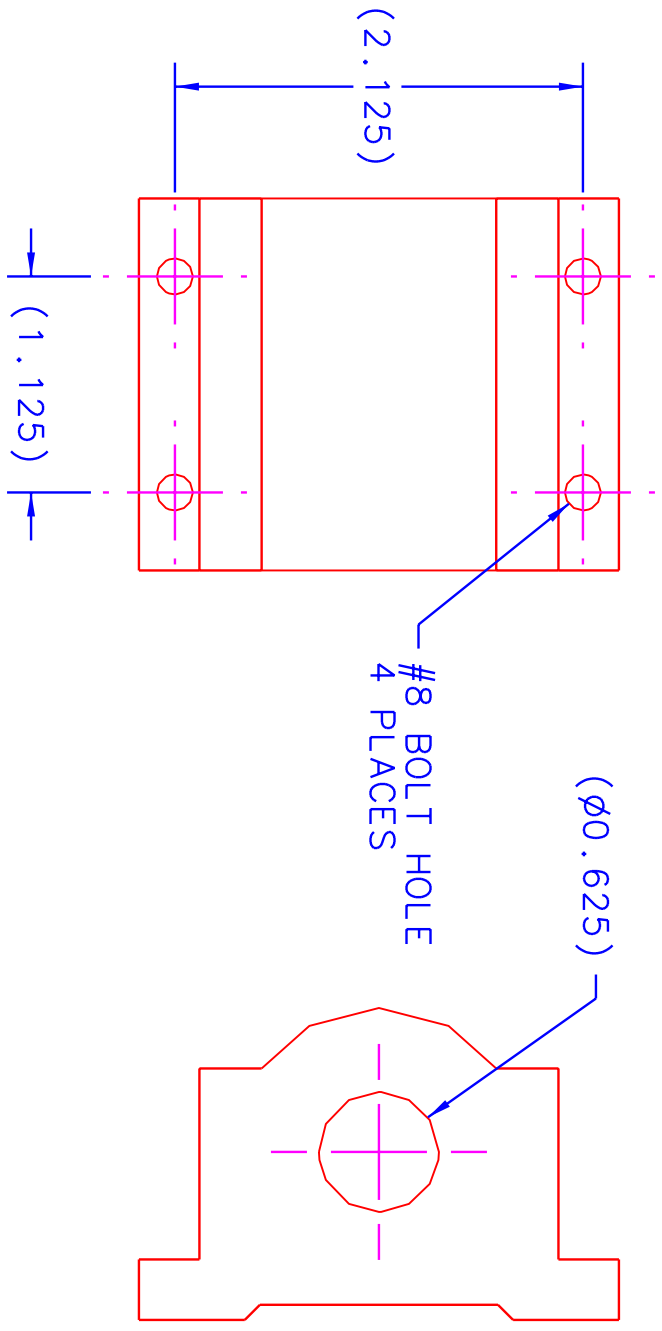


UNLESS OTHERWISE SPECIFIED DIMENSIONS ARE IN INCHES TOLERANCES ARE:		FRACTIONS		DECIMALS	ANGLES
+		.XX	±.01	X**	±.5°
DO NOT SCALE DRAWING					
MATERIAL	SEE NOTE				
FINISH					
SIMILAR TO	ACT. WT	CALC. WT			
DRAWN		DATE		TITLE	
D.S. RUPPERT		4/22/02		RETAINING RING	
CHECKED				SIZE	
ISSUED				FSCM NO.	
				DWG. NO.	
				602DSR	
SCALE		SHEET		1 OF 1	
NA		1		1	

VIRGINIA POLYTECHNIC INSTITUTE AND STATE UNIVERSITY
 DEPARTMENT OF ENGINEERING SCIENCE AND MECHANICS

REVISIONS				
ZONE	REV	DESCRIPTION	DATE	APPROVED
	1	INITIAL ISSUE	5/7/02	

NOTE:
 USE PART# 6374K4
 FROM MCMASTER CARR
 P.O. BOX 740100
 ATLANTA, GA 30374-0100
 (404) 346-7000

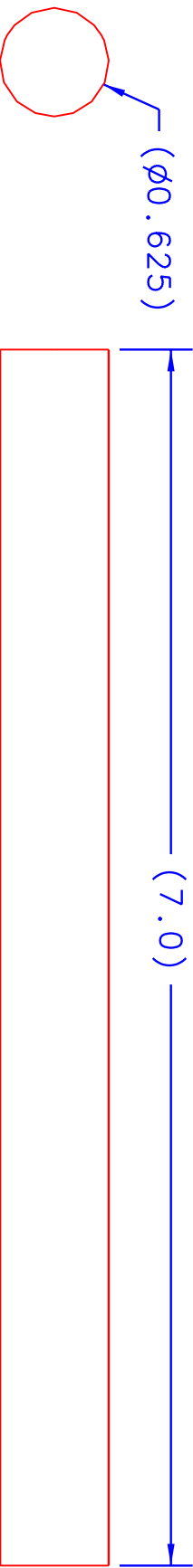


UNLESS OTHERWISE SPECIFIED DIMENSIONS ARE IN INCHES TOLERANCES ARE: FRACTIONS DECIMALS ANGLES ± .XX ±.01 X° ±.5° DO NOT SCALE DRAWING		VIRGINIA POLYTECHNIC INSTITUTE AND STATE UNIVERSITY DEPARTMENT OF ENGINEERING SCIENCE AND MECHANICS	
MATERIAL	SEE NOTE	DRAWN	D.S. RUPPERT
FINISH		CHECKED	
SIMILAR TO		ISSUED	
		DATE	5/7/02
		TITLE	BEARING, 5/8IN STANDARD LENGTH
		APPROVALS	
		SCALE	NA
		SIZE	A
		FSCM NO.	
		DWG NO.	608DSR
		SHEET	1 OF 1

REVISIONS				
ZONE	REV	DESCRIPTION	DATE	APPROVED
	1	INITIAL ISSUE	5/7/02	

NOTE:

USE PART # 6061K437
 FROM MCMASTER CARR
 P.O. BOX 740100
 ATLANTA, GA 30374-0100
 (404) 346-7000



UNLESS OTHERWISE SPECIFIED
 DIMENSIONS ARE IN INCHES
 TOLERANCES ARE:
 FRACTIONS DECIMALS ANGLES
 $\pm .XX$ $\pm .01$ $\pm X^{\circ}$ $\pm .5^{\circ}$
 $\pm .XXX$ $\pm .005$ $\pm X^{\circ}$ $\pm .5^{\circ}$
 DO NOT SCALE DRAWING

MATERIAL SEE NOTE

FINISH

SIMILAR TO

ACT. WT. CALC. WT.

VIRGINIA POLYTECHNIC INSTITUTE AND STATE UNIVERSITY
 DEPARTMENT OF ENGINEERING SCIENCE AND MECHANICS

APPROVALS

DRAWN D.S. RUPPERT 5/07/02

CHECKED

ISSUED

TITLE

SHAFT, 5/8 IN X 7 IN

SIZE FSCM NO.

A

DWG. NO.

609DSR

SCALE NA

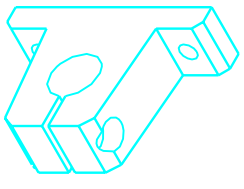
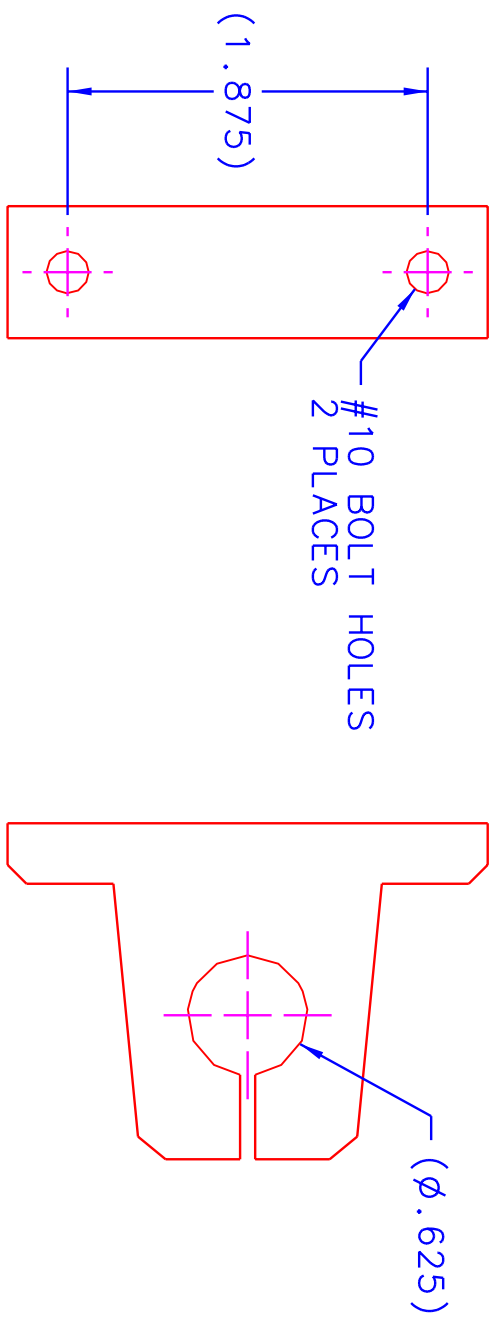
SHEET

1 OF 1

NOTE:

USE PART# 6068K24
 FROM MCMASTER CARR
 P.O. BOX 740100
 ATLANTA, GA 30374-0100
 (404) 346-7000

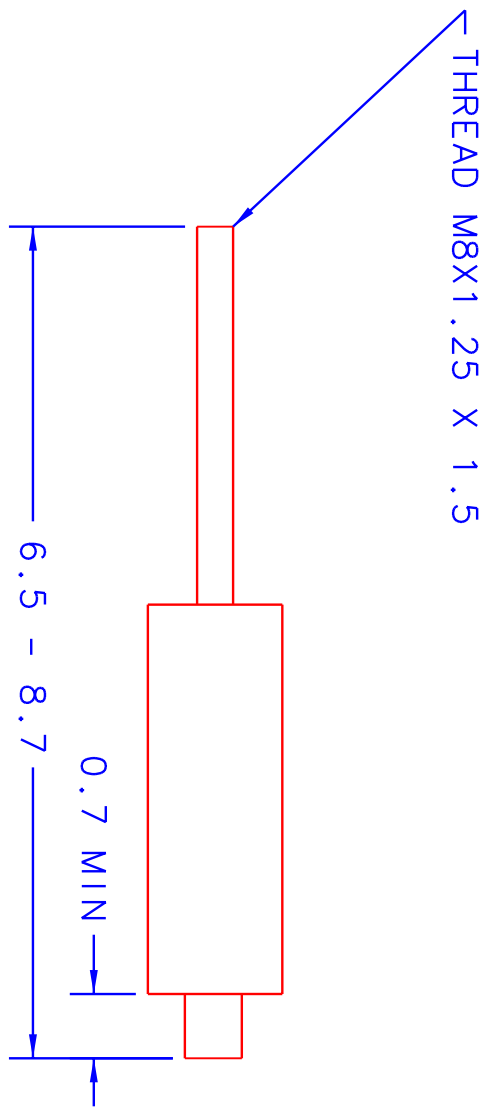
REVISIONS				
ZONE	REV	DESCRIPTION	DATE	APPROVED
	1	INITIAL ISSUE	5/7/02	



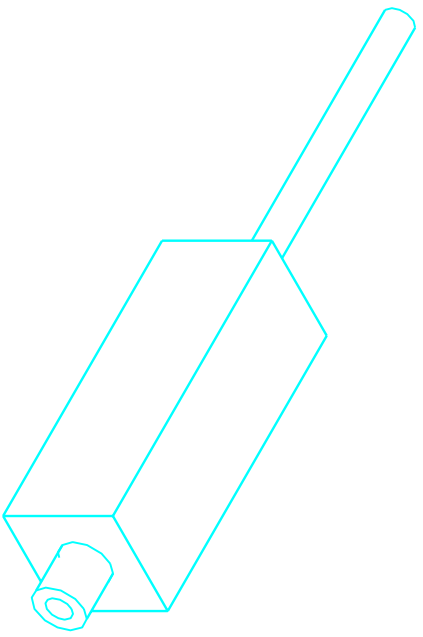
UNLESS OTHERWISE SPECIFIED DIMENSIONS ARE IN INCHES TOLERANCES ARE: FRACTIONS DECIMALS ANGLES $\pm .XX$ $\pm .01$ $X^{\circ} \pm .5^{\circ}$ DO NOT SCALE DRAWING		APPROVALS		DATE		TITLE	
MATERIAL SEE NOTE		DRAWN D.S. RUPPERT		5/7/02		SHAFT SUPPORT, 5/8IN	
FINISH		CHECKED				SIZE FSCM NO.	
SIMILAR TO		ISSUED				A	
ACT. WT		CALC WT				DWG. NO. 610DSR	
						SCALE NA SHEET 1 OF 1	

VIRGINIA POLYTECHNIC INSTITUTE AND STATE UNIVERSITY
 DEPARTMENT OF ENGINEERING SCIENCE AND MECHANICS

REVISIONS				
ZONE	REV	DESCRIPTION	DATE	APPROVED
	1	INITIAL ISSUE		



BOTTOM DRILL "H" ($\phi 0.267$) X 1.4 AND BOTTOM TAP M8X1.25



A

B

C

D

1

1

2

2

3

1

4

4

VIRGINIA POLYTECHNIC INSTITUTE AND STATE UNIVERSITY
DEPARTMENT OF ENGINEERING SCIENCE AND MECHANICS

HYDRAULIC ACTUATOR

DRAWN D.S. RUPPERT 8/22/02

UNLESS OTHERWISE SPECIFIED
DIMENSIONS ARE IN INCHES
TOLERANCES ARE:
FRACTIONS DECIMALS ANGLES
± .XX ±.01 X ±.5°
± .XXX ±.005
DO NOT SCALE DRAWING

FINISH

SIMILAR TO 613DSR

TITLE

SIZE

FSCM NO.

DWG NO.

612DSR

SHEET 1 OF 1

A

B

C

D

1

2

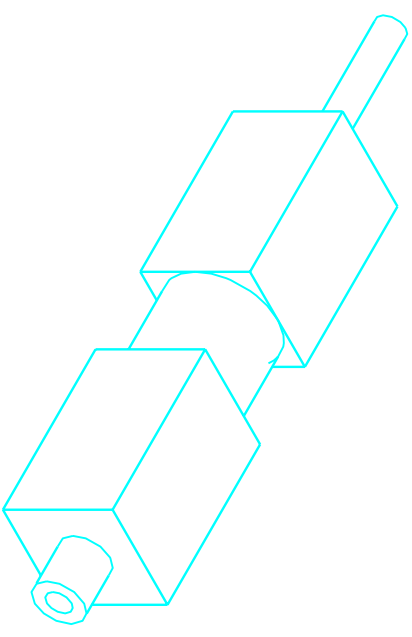
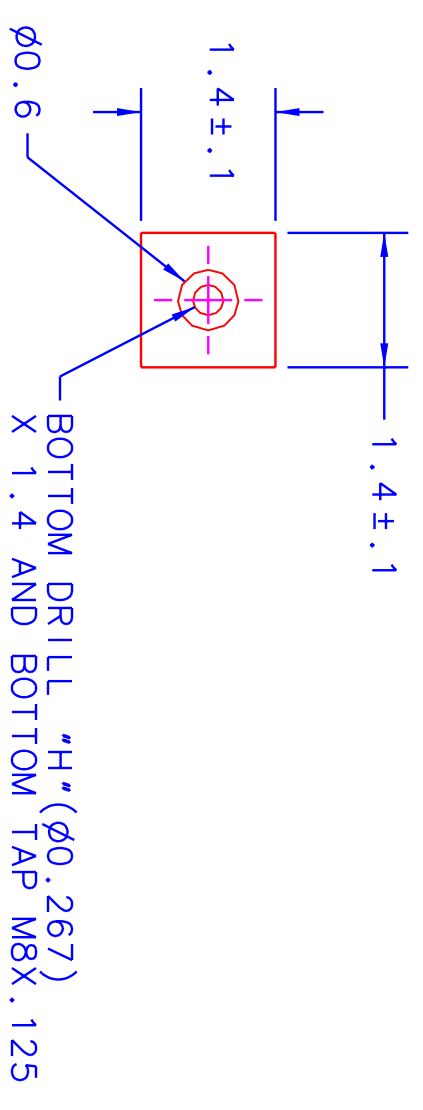
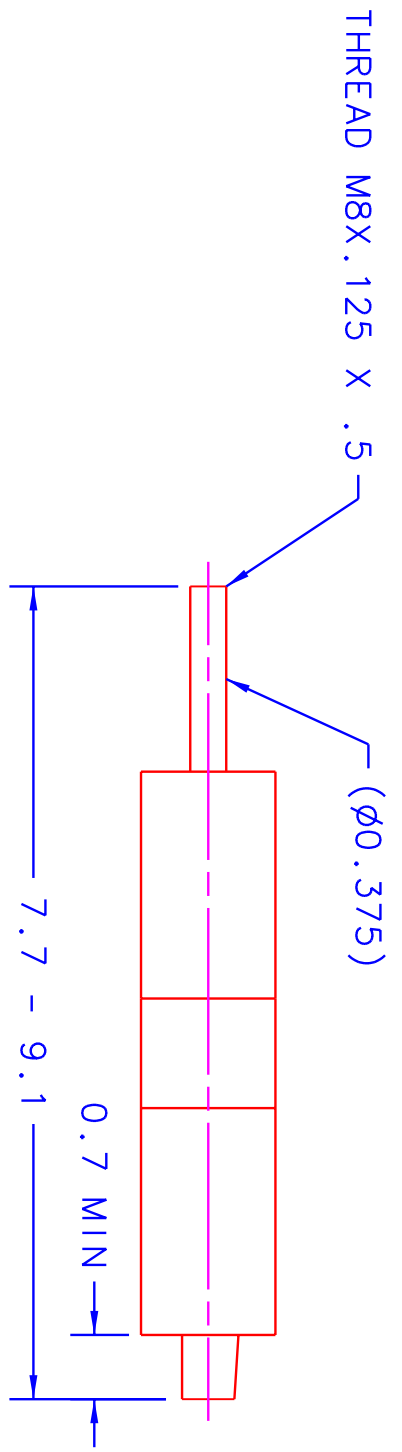
DWG. NO. 613DSR SH 1 REV. 1

4

NOTES

- 1: MAXIMUM LENGTH OF CYLINDER MUST BE AT LEAST 9.1 INCHES.
- 2: MINIMUM LENGTH OF CYLINDER MUST BE AT LEAST 7.7 INCHES.
- 3: ATTAINABLE FORCE MUST BE AT LEAST 2070 LBF.

REVISIONS				
ZONE	REV	DESCRIPTION	DATE	APPROVED
1	1	INITIAL ISSUE		



1

2

3

4

UNLESS OTHERWISE SPECIFIED DIMENSIONS ARE IN INCHES TOLERANCES ARE:				VIRGINIA POLYTECHNIC INSTITUTE AND STATE UNIVERSITY DEPARTMENT OF ENGINEERING SCIENCE AND MECHANICS			
FRACTIONS	DECIMALS	ANGLES		DRAWN	DATE	TITLE	
$\frac{XX}{YY}$	$\pm .01$	$X^{\circ}\pm .5^{\circ}$		D.S. RUPPERT	8/22/02	HYDRAULIC ACTUATOR	
DO NOT SCALE DRAWING				CHECKED		SIZE	FSCM NO.
				ISSUED		B	613DSR
MATERIAL				DWG NO.			
FINISH				SHEET 1 OF 1			
SIMILAR TO 612DSR				ACT. WT.			
				CALC. WT.			

1

2

3

4

1

2

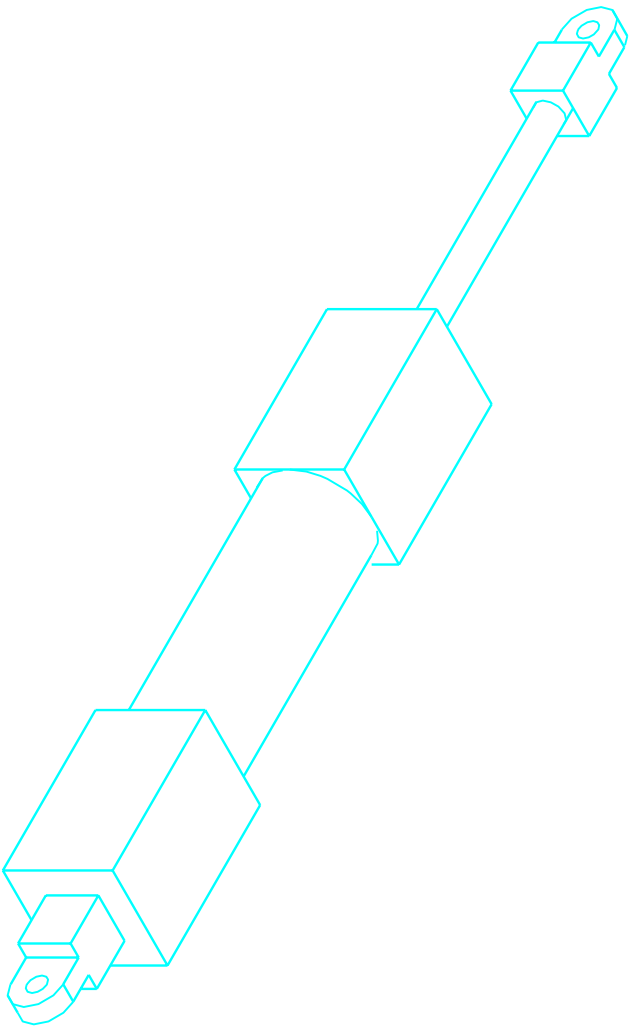
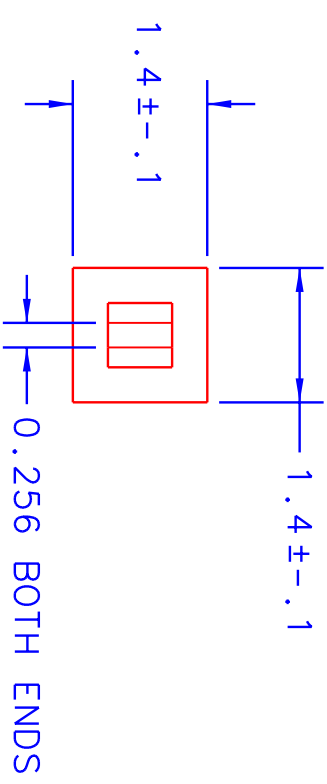
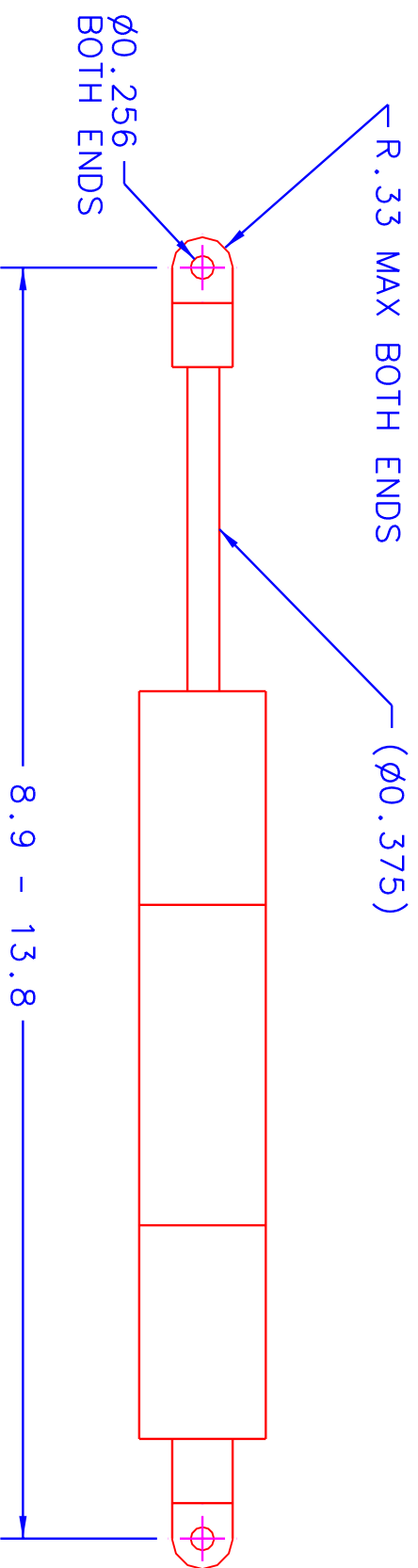
3

4

DWG. NO. 614DSR SH 1 REV. 1

NOTES

- 1: MAXIMUM LENGTH OF CYLINDER MUST BE AT LEAST 13.8 INCHES.
- 2: MINIMUM LENGTH OF CYLINDER MUST BE AT LEAST 8.9 INCHES.
- 3: ATTAINABLE FORCE MUST BE AT LEAST 2204 LBF.



REVISIONS				
ZONE	REV	DESCRIPTION	DATE	APPROVED
	1	INITIAL ISSUE		

A

B

C

D

A

B

C

D

UNLESS OTHERWISE SPECIFIED DIMENSIONS ARE IN INCHES TOLERANCES ARE:

FRACTIONS DECIMALS ANGLES
 $\pm .XX$ $\pm .01$ $X^{\circ}\pm .5^{\circ}$
 $\pm .XXX$ $\pm .005$ DO NOT SCALE DRAWING

MATERIAL

FINISH

SIMILAR TO 615DSR

VIRGINIA POLYTECHNIC INSTITUTE AND STATE UNIVERSITY
 DEPARTMENT OF ENGINEERING SCIENCE AND MECHANICS

APPROVALS

DRAWN D.S. RUPPERT 8/22/02

CHECKED

ISSUED

TITLE
 HYDRAULIC ACTUATOR

SIZE B FSQM NO. NA

DWG NO. 614DSR

SHEET 1 OF 1

1

2

3

4

1

2

3

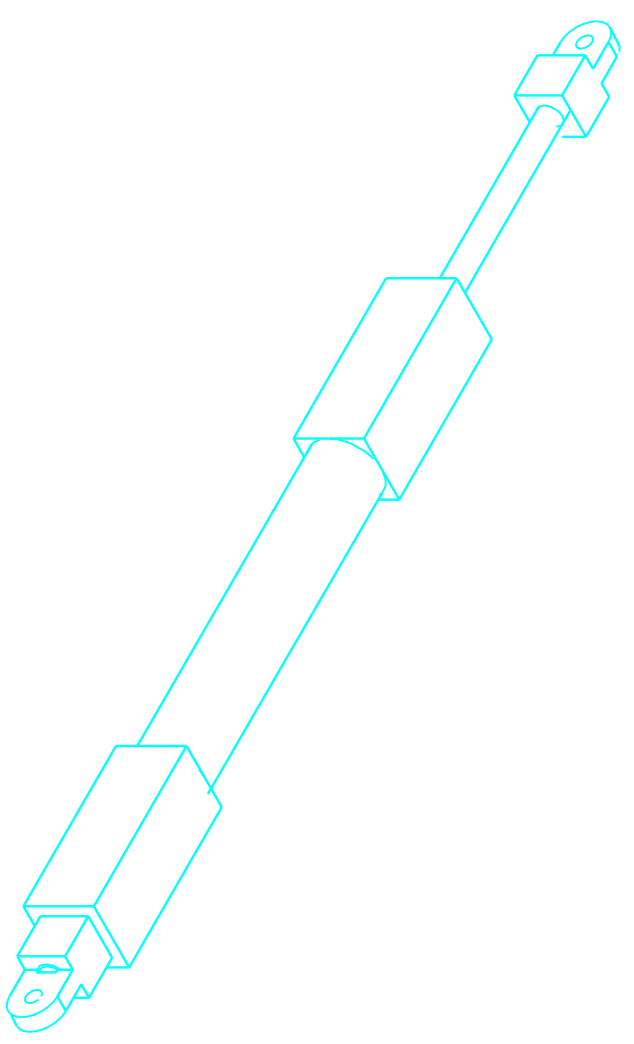
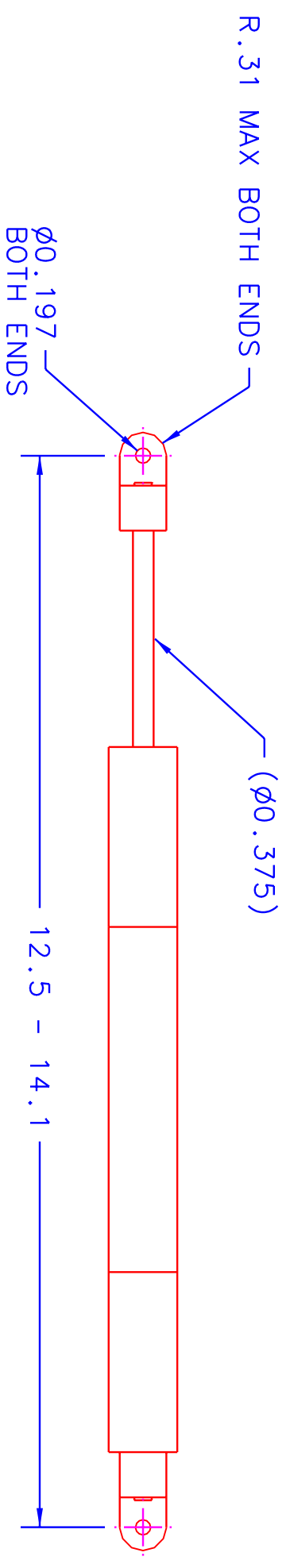
4

DWG. NO. 615DSR SH 1 REV. 1

NOTES

- 1: MAXIMUM LENGTH OF CYLINDER MUST BE AT LEAST 14.0 INCHES.
- 2: MINIMUM LENGTH OF CYLINDER MUST BE AT LEAST 12.4 INCHES.
- 3: ATTAINABLE FORCE MUST BE AT LEAST 600 LBF.

REVISIONS				
ZONE	REV	DESCRIPTION	DATE	APPROVED
1	1	INITIAL ISSUE		



A

B

C

D

A

B

C

D

VIRGINIA POLY TECHNIC INSTITUTE AND STATE UNIVERSITY
DEPARTMENT OF ENGINEERING SCIENCE AND MECHANICS

TITLE
HYDRAULIC ACTUATOR

APPROVALS
DRAWN D.S. RUPPERT 8/22/02

UNLESS OTHERWISE SPECIFIED
DIMENSIONS ARE IN INCHES
TOLERANCES ARE:
FRACTIONS DECIMALS ANGLES
± .XX ±.01 ±
± .XXX ±.005 ±
DO NOT SCALE DRAWING

MATERIAL

FINISH

SIMILAR TO 614DSR

ACT. WT. CALC WT.

CHECKED

ISSUED

SIZE B

FSQM NO.

SCALE NA

DWG NO. 615DSR

SHEET 1 OF 1

1

2

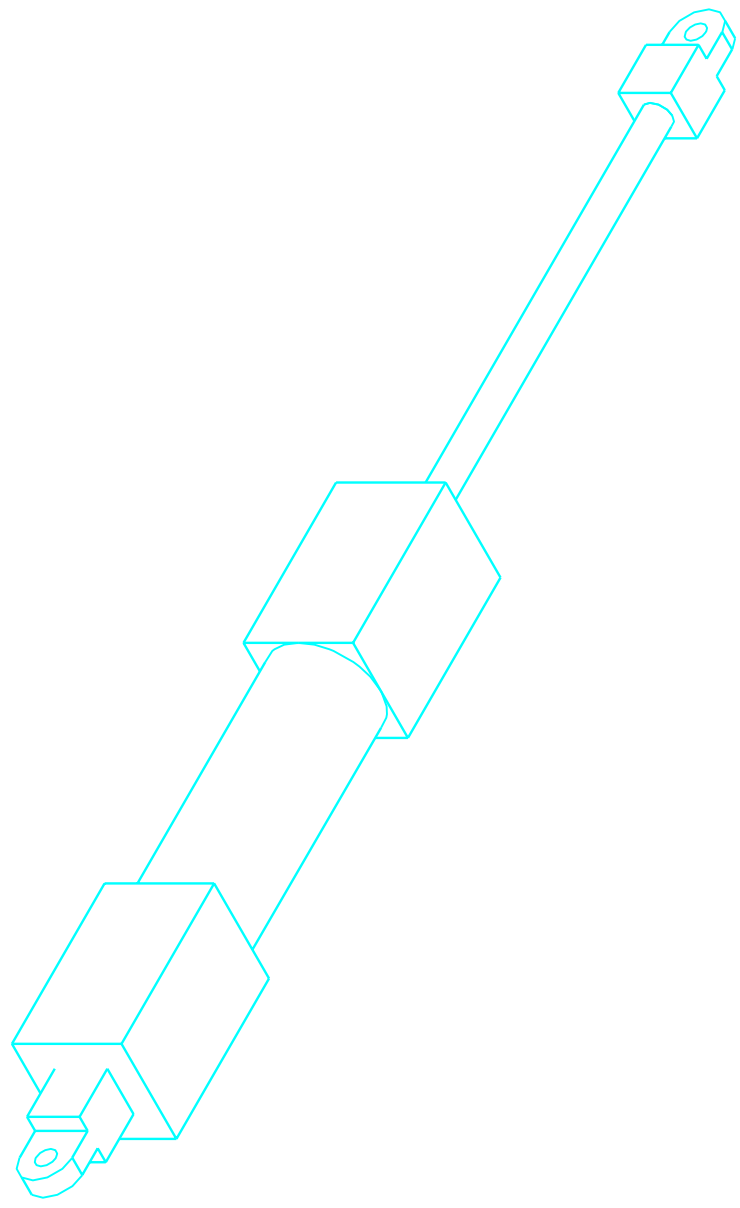
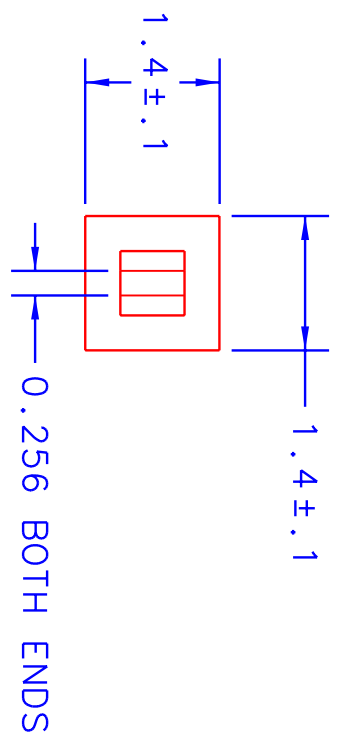
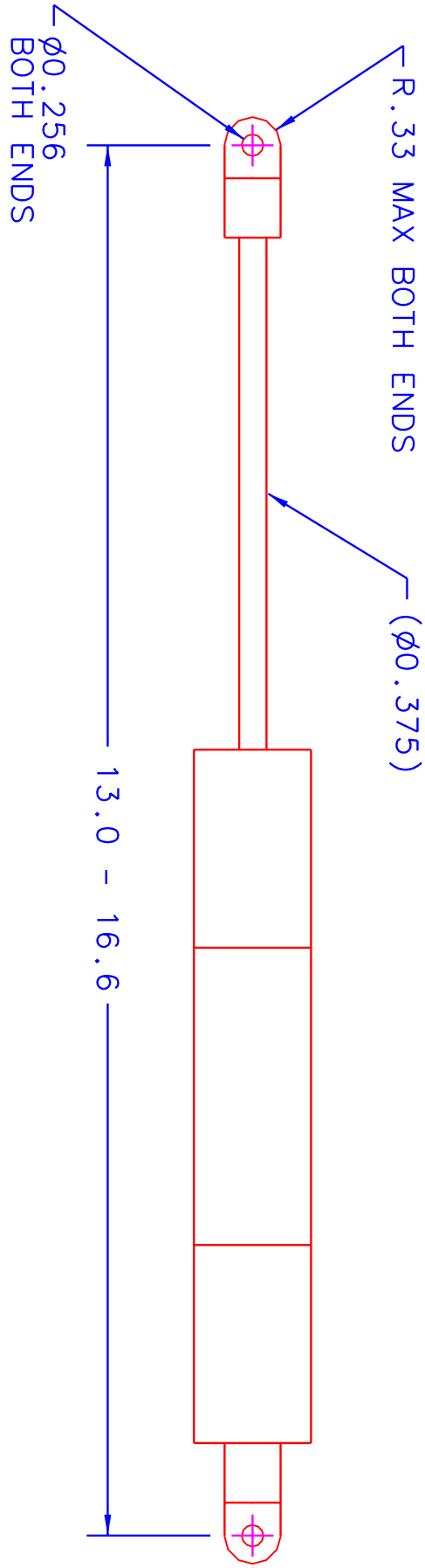
DWG. NO. 616DSR SH 1 REV. 1

4

NOTES

- 1: MAXIMUM LENGTH OF CYLINDER MUST BE AT LEAST 16.6 INCHES.
- 2: MINIMUM LENGTH OF CYLINDER MUST BE AT LEAST 13.0 INCHES.
- 3: ATTAINABLE FORCE MUST BE AT LEAST 1500 LBF.

REVISIONS				
ZONE	REV	DESCRIPTION	DATE	APPROVED
	1	INITIAL ISSUE		



UNLESS OTHERWISE SPECIFIED DIMENSIONS ARE IN INCHES
TOLERANCES ARE:

FRACTIONS	DECIMALS	ANGLES
±	.XX ±.01	X° ±.5°
DO NOT SCALE DRAWING	.XXX ±.005	X° ±.5°

MATERIAL

FINISH

SIMILAR TO 614DSR

ACT. WT

CALC WT

DEPARTMENT OF ENGINEERING SCIENCE AND MECHANICS

APPROVALS

DRAWN	D.S. RUPPERT	DATE	8/22/02
CHECKED			
ISSUED			

TITLE

HYDRAULIC ACTUATOR

SIZE B

FSQM NO.

DWG NO. 616DSR

SCALE NA

SHEET 1 OF 1

1

2

3

4

1

2

3

4

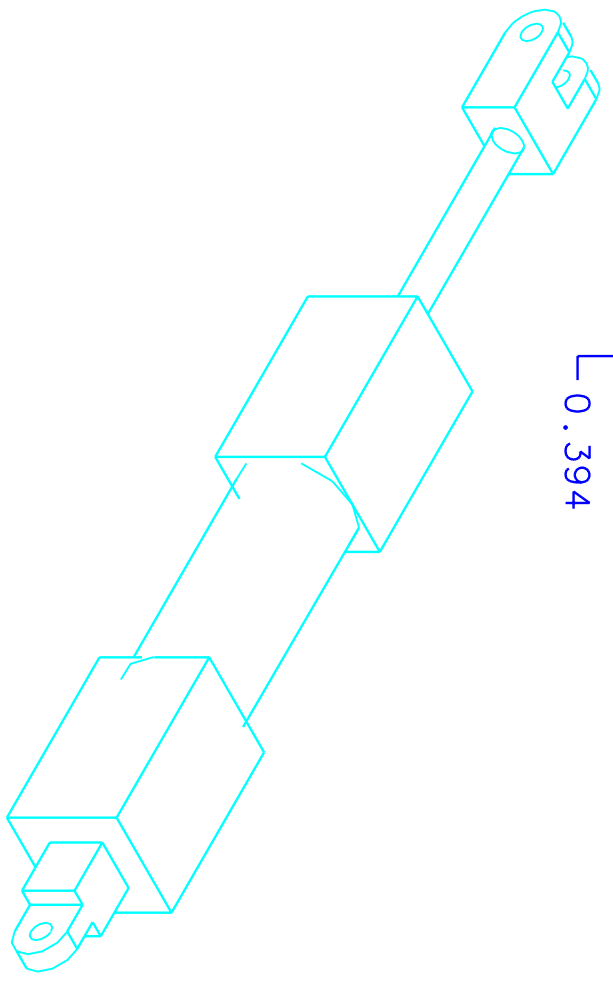
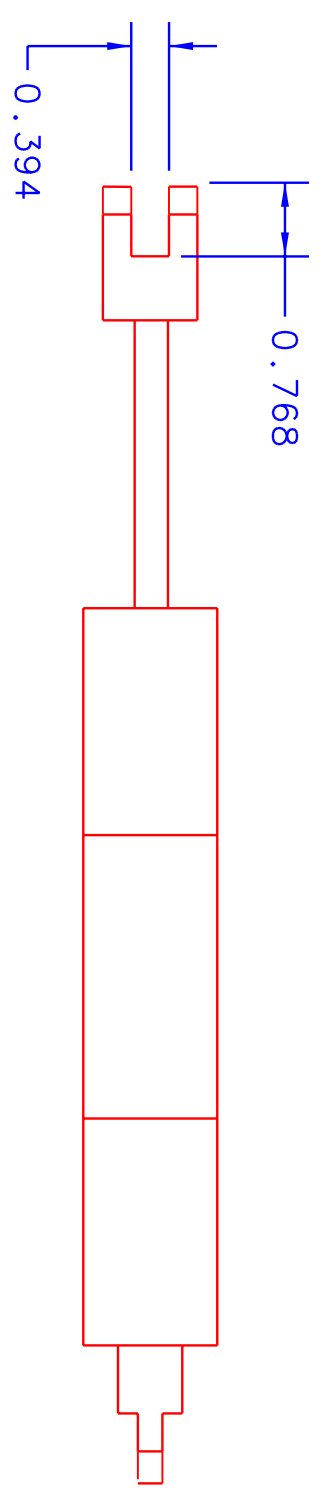
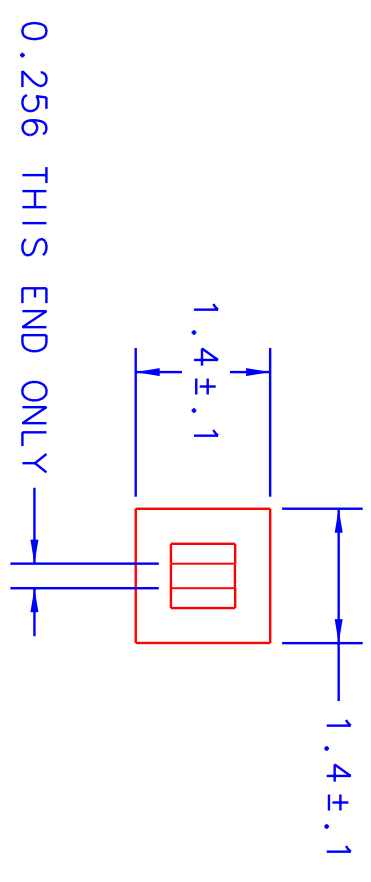
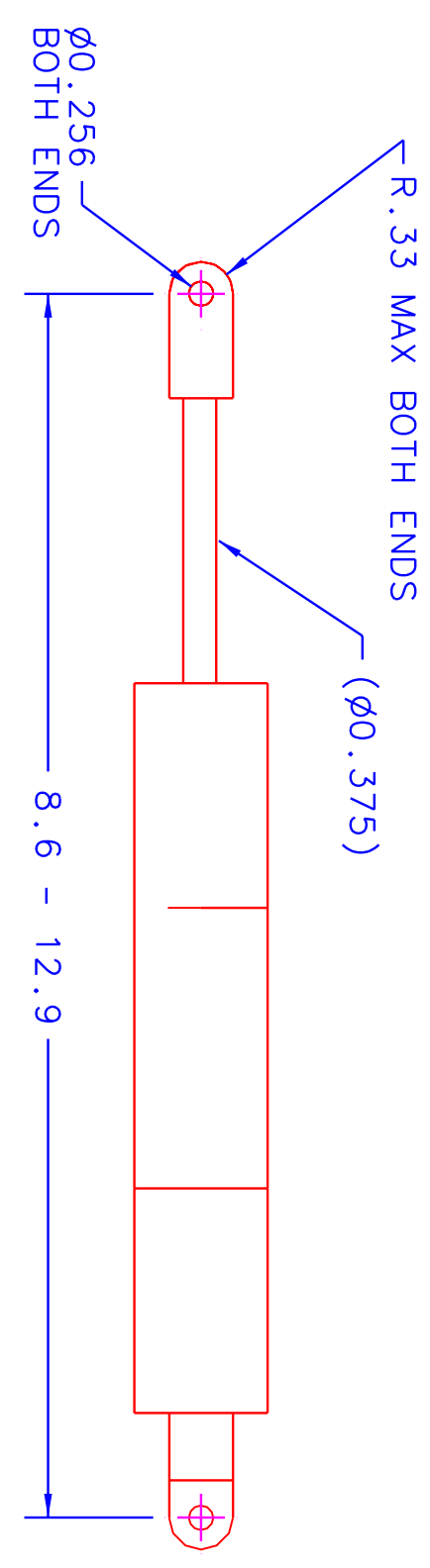
DWG. NO. 617DSR SH 1 REV. 1

REVISIONS

ZONE	REV	DESCRIPTION	DATE	APPROVED
	1	INITIAL ISSUE		

NOTES

- 1: MAXIMUM LENGTH OF CYLINDER MUST BE AT LEAST 16.6 INCHES.
- 2: MINIMUM LENGTH OF CYLINDER MUST BE AT LEAST 8.6 INCHES.
- 3: ATTAINABLE FORCE MUST BE AT LEAST 1800 LBF.



A

B

C

D

A

B

C

D

VIRGINIA POLYTECHNIC INSTITUTE AND STATE UNIVERSITY
DEPARTMENT OF ENGINEERING SCIENCE AND MECHANICS

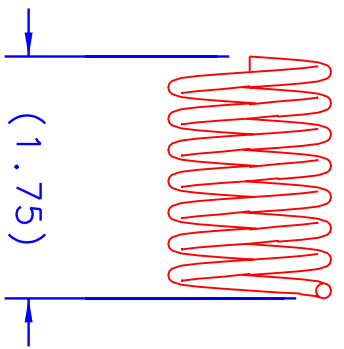
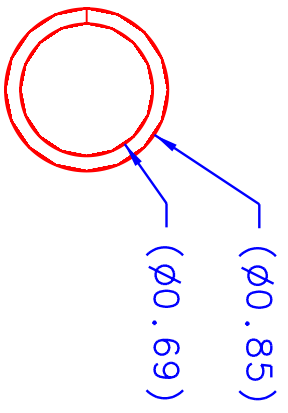
UNLESS OTHERWISE SPECIFIED
DIMENSIONS ARE IN INCHES
TOLERANCES ARE:
FRACTIONS DECIMALS ANGLES
± .005 ± .01 X ± .5°
DO NOT SCALE DRAWING

DRAWN D.S. RUPPERT 8/22/02
CHECKED
ISSUED

TITLE
HYDRAULIC CYLINDER

FINISH	ACT. WT.	CALC. WT.	SIZE	FSQM NO.	DWG. NO.	SHEET
SIMILAR TO 614DSR			B	NA	617DSR	1 OF 1

REVISIONS				
ZONE	REV	DESCRIPTION	DATE	APPROVED
	1	INITIAL ISSUE		



NOTES

1 : CENTURY SPRING PART # 72220
 222 EAST 16th STREET
 LOS ANGELES, CA 90015
 1-800-237-5225



UNLESS OTHERWISE SPECIFIED DIMENSIONS ARE IN INCHES TOLERANCES ARE :		VIRGINIA POLYTECHNIC INSTITUTE AND STATE UNIVERSITY DEPARTMENT OF ENGINEERING SCIENCE AND MECHANICS	
FRACTIONS	DECIMALS		
± .XX±.01	.XXX±.005	X**±.5°	
DO NOT SCALE DRAWING			
MATERIAL	SEE NOTE 1	DRAWN	D.S. RUPPERT
FINISH		CHECKED	5/06/02
SIMILAR TO		ISSUED	
ACT. WT	CALC. WT	TITLE	
		SPRING, 72220	
APPROVALS		DATE	
SIZE		FSCM NO.	DWG NO.
A			622DSR
SCALE		NA	SHEET
			1 OF 1

Vita

David S. Ruppert was born of David Farrell Ruppert and Nanette Strater in Sandford, Maine on October 16th, 1974. York High School of York, Maine is where he finished his primary education. He went on to earn a Bachelor of Science in Mechanical Engineering at the University of Maine (UMO). While at UMO, he was inducted into the national honors society for engineers, Tau Beta Pi, and the national honors society for mechanical engineers, Pi Tau Sigma. He graduated cum laude in 1997 from UMO. Next, he went on to work at Steag Hamatech in Saco Maine as a certified engineer in training. He worked supporting designers through analytical calculations, FEA, and experimentation. Also while at Steag Hamatech, he worked as a process engineer designing and completing research projects for various processes to improve yields and/or robustness of their machines. After approximately three years, he returned to academia to pursue a Masters of Science in Mechanical Engineering at Virginia Tech focusing in Biomechanics. Upon graduation from Virginia Tech (January 2003), he intends to rejoin the engineering work force.